

Bangor University

DOCTOR OF PHILOSOPHY

The post-glacial evolution and present-day sedimentary processes of the Mawddach Estuary

Larcombe, Piers

Award date:
1992

Awarding institution:
Bangor University

[Link to publication](#)

General rights

Copyright and moral rights for the publications made accessible in the public portal are retained by the authors and/or other copyright owners and it is a condition of accessing publications that users recognise and abide by the legal requirements associated with these rights.

- Users may download and print one copy of any publication from the public portal for the purpose of private study or research.
- You may not further distribute the material or use it for any profit-making activity or commercial gain
- You may freely distribute the URL identifying the publication in the public portal ?

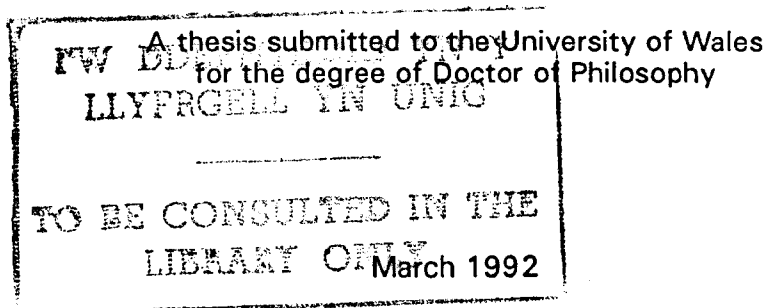
Take down policy

If you believe that this document breaches copyright please contact us providing details, and we will remove access to the work immediately and investigate your claim.

**The Post-Glacial Evolution
and Present-Day Sedimentary Processes
of the Mawddach Estuary**

by

Piers Larcombe B.Sc., M.Sc.



School of Ocean Sciences
University College of North Wales
Menai Bridge
Anglesey



VOLUME 1

Acknowledgements

Thanks to :

- Prof. Denzil Taylor-Smith for providing facilities at the School of Ocean Sciences
- my supervisor Colin Jago, for advice and discussion, and good humour in face of all !
- all the technicians who helped brilliantly in the fieldwork, Dave Boon, John Moore, Alan Nield and Geraint Williams, all who make mean cups of tea !
- Philip Allen and Colin Jago for stimulating my interest in sediments and geology .
- all the staff and students who have helped in the estuary, over long hours and in various states of weather : Colin Jago, Sarah Jones (+ Amy), Tony Jones, Jeremy Lowe, Tricia Murray, Pete Hepton, Gary Reid, Yusuff Mahamod, Bill Austin, Ian McDermott, and Duncan Lloyd, Barry Philips and Dai Thomas for diving.
- the Captain and crew of the Prince Madog
- Jim Bennell for magic fingers on the boomer amplifiers
- I.O.S. Bidston for the loan of the Sand Pebbler
- the Harbourmaster, Barmouth, for much local advice and information
- British Geological Survey, Aberystwyth, for making borehole data available
- Gwynedd Archives Department, Dolgellau, for supply of archive data
- Sally and Brian White, Ben and Flash, of Fegla Fach Farm, for hospitality and a warm caravan
- Tony Page, master of of 'The Boy Nick'
- The George at Penmaenpool for delicious pizzas
- Snowdonia National Park for allowing access to the track on the south side of the estuary
- various residents of Barmouth and Fairbourne, for allowing trisponder stations to sit on their roofs

- Gay and Nick Jacobs for allowing me to occupy a bed during those hilarious last few days of the write-up
- Tricia Murray, Ron Haynes and Dave Boon for lifts and cups of Pentraeth tea
- the Larcombe clan, Angela, Bernard, Fraser, Simon, Alison, and Kirstie for various amounts of manual labour and amusement !
- the weather and the tides
- the Mawddach Estuary for being so beautiful and intriguing, especially at daybreak. Long may it be so.
- Ruth, for very similar reasons.

Abstract

The Post-glacial evolution and present-day sedimentary processes of the Mawddach Estuary.

The Mawddach Estuary and Barmouth Bay now occupy what was a deeply incised glaciated valley at the last ice maximum. This valley is now filled by a complex suite of sediments, up to 75m thick at the present estuary mouth, which record increasing marine influence. A regressive coastline is also present today. In the Bay, Welsh glacial drifts were eroded to form deep depressions, infilled by complex cross- stratified Late- or Post-glacial sediments, overlain by a parallel-stratified sequence, perhaps formed behind a coast-parallel morainal barrier.

Net sediment transport of the fine sand in the Bay is shoreward, controlled by a strong mesotidal and wave regime. Calculated sediment transport rates infer long term sediment accumulation rates of 82mm per year for the estuary as a whole, but repeated surveys suggest much spatial variation within the estuary. Waves greatly enhance sediment transport in the bay, by approximately 30 times in storms, when coarse sand is mobilised. The estuarine sand fines landward, from medium- to very fine-grained. Grain size and petrological evidence suggest sediment is derived from erosion of glacial deposits in Cardigan Bay.

A highly skewed tidal wave creates strong flood currents and net flood sediment transport throughout the estuary and in the southwest portion of the bay. The estuary is generally well-mixed, and the tidal wave is a standing wave with a progressive component. The estuary comprises a two part hydrodynamic system, with decreased currents and sediment transport inland of a hard rock constriction.

Intertidal megaripples dominate large areas of the seaward portion of the estuary. They show very complex morphological and dynamic behaviour over a lunar cycle. Detailed velocity profile measurements over these megaripples, show complex relationships of bedform to flow. Flow parameters show considerable scatter, and have only weak correlations with bedform morphology or migration. Within each flood-ebb cycle, the relationship of shear velocity to roughness length appears related to the underlying bedforms. Natural variation of megaripple behaviour is a major factor in limiting palaeoflow estimates from deposits of intertidal megaripples.

A concluding chapter discusses the relationship between sea-level, sedimentation, and estuarine hydrodynamics, through the Holocene. Sea level rise brought drowning and erosion of coastal glacial complexes, leading to conditions allowing spit formation and growth, with, in the estuary, increased tidal asymmetry, salinity and low water elevation. Fine-grained estuarine sedimentation was initiated in the sheltered back-barrier region, intertidal flats and supratidal marshes prograded, and tidal channels were progressively restricted towards the northern side of the estuary mouth. Within the modern estuarine sand wedge, preserved estuarine sedimentary structures may exhibit an upwards-increasing expression of flood- directed sediment transport.

CONTENTS
VOLUME ONE

	PAGE
Acknowledgements	
Abstract	
Contents	1
List of Figures	9
List of Enclosures	19
List of Tables	20
Study Objectives	23

Chapter 1

Geology and Sediment Transport of the Nearshore Zone

Part A

1.1 Introduction	24
1.2 Geography	25
1.3 Geology of the Area	27
1.3.1 Pre-Quaternary Regional Geology	
1.3.1.2 Geological Succession	
1.3.1.3 Intrusive Rocks	
1.3.1.4 Structure	
1.3.1.5 Geophysical Studies	
1.3.1.6 Historical Seismic and Borehole Data	
1.3.1.7 Quaternary Geology	
1.3.1.8. Submerged Forests and Buried Peat Deposits	
1.3.1.9 Synthesis	
1.4 Sediment Transport in Northern Cardigan Bay	42
1.4.1 Regional Evidence - A Review	
1.4.2 Local Evidence - A Review	
1.5 Sub-Bottom Data Within the Estuary	48
1.5.1 The Estuary Mouth - Rail Bridge Section	
1.5.2 Boreholes east of Ro Wen	
1.5.3 Boreholes at Pont Glandwr	
1.5.4 The Estuary Head - Llanelltyd Section	
1.6 Offshore Boreholes	56
1.6.1 Boreholes 47 and 133	
1.6.2 Borehole 48	
1.6.3 Borehole 148	
1.7 Current Velocity Data in Barmouth Bay	57

	PAGE
1.8 Geophysical Surveying in Barmouth Bay - New Data	60
1.8.1 Purpose of Surveys	
1.8.2 Survey Details	
1.9 Bathymetry of Barmouth Bay	66
1.10 Acoustically Turbid Sediments	67
1.11 Construction of the Sub-Bottom Geology	68
1.12 Description of Seismic Sections	72
1.12.1 Section 1 - positions 522 - 529 - 534	
1.12.2 Section 2 - positions 552 - 542 - 535	
1.12.3 Section 3 - positions 555 - 566 - 569	
1.12.4 Section 4 - positions 586 - 590	
1.12.5 Section 5 - positions 597 - 603	
1.12.6 Section 6 - positions 608 - 605	
1.12.7 Section 7 - positions 638 - 641 - 644	
1.12.8 Section 8 - positions 570 - 575	
1.13 Sedimentary History, and Correlation with Boreholes, Exposure and other Seismic Facies Data	76
Part B	
1.14 Side-Scan Sonar	79
1.14.1 Description of Equipment	
1.14.2 Interpretation of Side-Scan Data	
1.14.3 Terminology of Shelf Bedforms	
1.14.4 Amos & King (1984) Shelf Bedform Terminology	
1.15 Sedimentary Facies of Barmouth Bay	86
1.15.1 The Outer Sand Sheet	
1.15.2 The 'Patchy' Sand Facies	
1.15.3 The Inner Sand Sheet	
1.16 Coastal Zone Ripple Bands	98
1.16.1 Hypotheses of Ripple Band Generation	
1.16.2 Ripple Bands in Barmouth Bay	
1.16.3 Ripple Generation	
1.17 Sediment Transport Rates	109
1.17.1 Bedload and Total-Load Sediment Transport Equations	
1.17.2 Suspended Load Equations	
1.17.3 Effects of Waves on Sediment Transport	
1.17.4 The Equation of Engelund & Hansen (1967)	
1.17.4.1 The Flow Data Used	
1.17.4.2 Results - In the Absence of Waves	
1.17.4.3 Results - in the Presence of Waves	
1.17.4.4 Discussion	
1.18 Summary and Conclusions	127

Chapter 2

Estuarine Circulation

	PAGE
2.1 Introduction	133
2.1.1 Long-Term Variable Factors	
2.1.1.1 Morphology	
2.1.1.2 Sea-Level Change	
2.1.2 Human Intervention	
2.1.3 Variable Non-Cyclical Factors	
2.1.4 Variable Cyclical Factors	
2.1.5 Spatial Variability	
2.1.6 Welsh Estuaries	
2.1.7 Previous Studies in the Mawddach	
2.1.8 Summary of Welsh Estuaries	
2.2 Methods	141
2.3 Results	143
2.3.1 Velocity Data	
2.3.1.1 Barmouth Bay, Station 1	
2.3.1.2 Penrhyn Point, Station 2	
2.3.1.3 Barmouth Bridge, Station 3	
2.3.1.4 Farchynys, Station 4	
2.3.1.5 Penmaenpool, Station 5	
2.3.2 Salinity Data	
2.3.2.1 Barmouth Bay	
2.3.2.2 Penrhyn Point	
2.3.2.3 Farchynys	
2.3.2.4 Penmaenpool	
2.3.3 Flow Direction Data	
2.3.3.1 Barmouth Bay	
2.3.3.2 Penrhyn Point	
2.3.3.3 Farchynys	
2.3.4 Summary of Results	
2.3.5 Data Interpolation/Extrapolation	
2.4 Discussion	149
2.4.1 Time-Averaged Parameters	
2.4.1.1 Flood Velocities	
2.4.1.2 Ebb Velocities	
2.4.1.3 Flood- and Ebb- Depth-Mean Velocities	
2.4.1.4 Tide-Averaged Velocities	
2.4.2 Tide-Averaged Salinities	
2.4.3 Flow Directions at Penrhyn Point	
2.4.4 Classification and Mixing Controls	
2.4.4.1 Qualitative Classification	
2.4.4.2 Quantitative Classification and Mixing Controls	
2.4.5 Tidal Wave Propagation and Flow Controls	
2.4.5.1 Tidal Height and Range	
2.4.5.2 Water Surface Slopes	
2.4.5.3 Tidal Wave Delays	
2.4.6 Fronts and Convergences	
2.4.7 Sources of Error and Notes on Unused Data	
2.5 Summary and Conclusions	175

VOLUME TWO

Chapter 3

Intertidal Bedform Behaviour

	PAGE
3.1 Introduction and Survey Objectives	177
3.1.1 Bedform Terminology	
3.1.2 Previous Studies of Modern Bedforms	
3.1.2.1 Recent Bed Sediment Transport	
3.1.2.2 Geological Significance	
3.2 Introduction and Survey Objectives	188
3.2.1 Surveying Megaripple Trains	
3.2.2 Survey Dates and Tides	
3.2.3 Megaripple Morphological Parameters	
3.3 Results - Bedform Dimensions - Line A	192
3.3.1 Variation with Time	
3.3.1.1 Mean Symmetry Index (b/a)	
3.3.1.2 Mean Height (h)	
3.3.1.3 Mean Wavelength (L)	
3.3.1.4 Mean Flatness (L/h)	
3.3.1.5 Mean Bed Level (B), Crest Level (C) and Trough Level (T)	
3.3.1.6 Qualitative Relationship between Morphometric Parameters	
3.3.2 Variation with Predicted Tidal Range	
3.3.2.1 Mean Symmetry Index (b/a)	
3.3.2.2 Mean Height (h)	
3.3.2.3 Mean Wavelength (L)	
3.3.2.4 Mean Flatness (L/h)	
3.3.2.5 Mean Bed Level (B), Crest Level (C) and Trough Level (T)	
3.4 Megaripple Populations	202
3.4.1 Introduction	
3.4.2 Modal Behaviour	
3.4.3 2D - 3D Megaripple Distinctions	
3.5 Bedform Migration	208
3.5.1 Definition of 'Migration Distance'	
3.5.2 Uses of Migration Data	
3.5.3 Results - Lag Cross-Correlation	
3.5.3.1 Discussion	
3.5.4 Migration Variation	
3.6 Comparison of Line A and Line B Data, and Interpretation	223
3.6.1 Height Comparison	
3.6.1.1 Interpretation and Conclusions	
3.6.2 Wavelength Comparison	
3.6.2.1 Interpretation and Conclusions	
3.6.3 Flatness Comparison	
3.6.3.1 Interpretation and Conclusions	
3.6.4 Symmetry Comparison	
3.6.4.1 Interpretation and Conclusions	
3.6.5 Migration Comparison	
3.6.5.1 Interpretation and Conclusions	

	PAGE
3.7 Palaeoflow Reconstruction from Megaripple Deposits	231
3.7.1 Introduction	
3.7.2 Geological Measures of Megaripple Migration	
3.7.3 Comparison of the Migration Measures	
3.7.4 Geological Implications	
3.7.5 Correlation of Flow with Sediment Transport and Megaripple Form	
3.7.5.1 Megaripple Migration as a Measure of Bed Material Sediment Transport	
3.7.6 Intra-Population Variation of Migration	
3.7.7 Megaripple Form and Sediment Transport: Palaeoflow Indicators ?	
3.7.7.1 Introduction	
3.7.7.2 Megaripple Morphological Threshold Conditions	
3.7.7.3 Conclusion	
3.8 Sediment Transport on Fegla Fach Shoal	247
3.8.1 Cyclical Accumulation of Sediment on the Shoal: Geological Implications	
3.9 Summary and Conclusions	251

Chapter 4

Bedform - Boundary Layer Interactions

4.1 Introduction	257
4.2 Tidal Current Velocity Profiles : General	259
4.2.1 The Logarithmic Profile	
4.2.2 Factors Influencing Velocity Profile Form	
4.3 Tidal Current Velocity Profiles : Measurements	268
4.3.1 The Velocity Gradient Unit (V.G.U.)	
4.3.2 Fegla Fach Site - V.G.U. Deployment	
4.3.2.1 Initial Data Processing	
4.3.2.2 Rotor Heights	
4.3.2.3 Description of Program, VGU.FOR	
4.3.3 The Data Obtained	
4.3.3.1 Number of Points on each Profile	
4.3.3.2 The 'Averaging Time'	
4.3.3.3 Were Velocity Profiles Logarithmic ?	
4.3.3.4 Summary Comparison of Neap and Spring Tidal Currents	
4.4 Relationship of Flow to Megaripple Form	278
4.4.1 Results	
4.4.2 Shear Velocity	
4.4.3 Roughness Lengths	
4.4.4 Comparison with Predicted Roughness	
4.5 Intra-Tidal Relationship of Roughness Length with Shear Velocity	285
4.5.1 Results	
4.5.2 Interpretation and Discussion	
4.5.3 Conclusions	
4.6 Spring-Neap Variation of Tidal Flow Parameters	296
4.6.1 Introduction	
4.6.2 Velocity at 1m above the Bed	

	PAGE
4.6.3 Shear Velocity	
4.6.4 Roughness Length	
4.7 Summary and Conclusions	303
Chapter 5	
Grain Size Investigations - The Fall Tower	
5.1 Introduction	306
5.2 Grain Size - Definitions	308
5.3 The Grain Settling Method - The Fall Tower	310
5.3.1 Apparatus	
5.4 Previous Work on Grain Settling	312
5.5 Factors Other Than Size Which Control Grain Settling	314
5.5.1 Concentration	
5.5.2 Sample Weight	
5.5.3 Grain Shape - Sphericity and Roundness	
5.5.4 Grain Density	
5.5.5 Fluid Temperature	
5.5.6 Fluid Movement	
5.5.7 Wall Effects	
5.6 Data Manipulation - Conversion of Grain Fall Velocity to Sieve Diameter	324
5.6.1 The Program, FTOWER1	
5.6.1.1 The Conversion Process	
5.6.2 The Measure of Grain Size Obtained	
5.6.3 Precision of Grain Size Parameters	
5.7 Framework for Presentation and Discussion of Grain Size	334
5.7.1 Statistical Parameters	
Chapter 6	
Grain Size Investigations - Review and Results	
6.1 Introduction	337
6.2 Interpretation of Grain Size Distributions	338
6.2.1 Moments Analysis	
6.2.2 Other Statistical Work	
6.2.3 Simpler Measures	
6.2.4 Transport Effects on Grain Size	
6.2.5 Hydrodynamic Interpretation and Modes of Transport	
6.3 Barmouth Bay - a Heterogeneous Sea Bed	346
6.4 Barmouth Bay - Grain Size Analysis	349
6.4.1 Gravel Fraction	
6.4.2 Sand Fraction	

	PAGE
6.4.3 Fine Fraction	
6.4.4 The Sand Fraction - Detailed Grain Size Analysis	
6.4.4.1 Mode Distribution	
6.4.4.2 Mean Distribution	
6.4.4.3 Sorting Distribution	
6.4.4.4 Skewness Distribution	
6.4.4.5 Kurtosis Distribution	
6.4.4.6 Initial Interpretation	
6.5 Sediment Petrology	355
6.5.1 Gravel Fractions	
6.5.2 Grain Types	
6.5.3 Conclusion	
6.6 Modal Behaviour	358
6.6.1 2.05phi Mode	
6.6.2 2.55phi Mode	
6.6.3 3.35phi Mode	
6.7 Dowling Plots	362
6.7.1 Results	
6.7.2 Fairbourne Spit and Barmouth Beach	
6.8 Estuarine Sediment Samples	365
6.8.1 Survey Lines and Survey Techniques	
6.8.2 Morphology of Estuarine Transects	
6.8.3 Grain Size Results	
6.8.3.1 Proportion of Fines and Gravel	
6.8.3.2 Sand Fraction	
6.8.4 Dowling Plots along the Estuary	
6.8.5 Estuarine Samples - General Points	
6.9 Conclusions	377

Chapter 7

Sediment Transport Paths and Estuarine Morphological Change

7.1 Introduction	379
7.2 Sediment Transport Pathways	380
7.2.1 Use of Surficial Bedforms	
7.2.2 Use of Grain Size Data	
7.2.2.1 McLaren & Bowles (1985)	
7.2.2.2 Skewness Trends	
7.2.3 Discussion	
7.3 Estuarine Accumulation and Erosion	388
7.3.1 Implications for Estuarine Transport and Deposition	
7.4 Estuarine Cross-Sectional Areas	394
7.4.1 Introduction	
7.4.2 Cross-Sections in the Mawddach	
7.4.3 Discussion	
7.5 Summary and Conclusions	401

Chapter 8**Concluding Remarks**

403

References

411

Appendix 2.1

430

List of Figures

DIAGRAM
FOLLOWS
PAGE

Chapter 1

Fig. 1.1	Geography and sea-floor topography in Cardigan Bay.	25
Fig. 1.2	The Mawddach Estuary.	25
Fig. 1.3	Simplified Geology of part of North Wales.	27
Fig. 1.4	Sub-Pleistocene geology of Cardigan and Tremadoc Bays. (After Dobson et al, 1973)	30
Fig. 1.5	E - W cross section through Cardigan Bay. (After Allen + Jackson, 1985).	32
Fig. 1.6	Distribution of Late Glacial/Early Flandrian sediment in Cardigan Bay. (After Garrard, 1977).	34
Fig. 1.7	Print of Barmouth Bay and Bars, dated 1748. (After Lloyd, 1974).	42
Fig. 1.8	Part of the one-inch map of the Fishery District of the Dyfi, Mawddach and Glasyn, dated 1866. (Courtesy of the Gwynedd Archives Service, Dolgellau).	42
Fig. 1.9	Chart showing dispersal vectors for each of the petrologically determined grain types (After Moore, 1968).	46
Fig. 1.10	Stratigraphy beneath Barmouth Railbridge. (Sources: British Rail, 1980/82; McMullen, 1964).	48
Fig. 1.11	Borehole data east of Ro Wen. (Data of Chettleburgh, 1988).	52
Fig. 1.12	Borehole data at Pont Glandwr. (Data supplied by B.G.S., Aberystwyth).	52
Fig. 1.13	Location of boreholes at Llanelltyd.	53
Fig. 1.14	(a) Position of B.G.S. offshore boreholes near Barmouth Bay; (b) Borehole data in Barmouth Bay and the Mawddach Estuary.	56
Fig. 1.15	(a)-(d) Barmouth Bay - Spring tide surface currents.	57
Fig. 1.16	Assumed tidal curve at Barmouth Bar for 7-8/7/87 and 26-28/5/87.	61
Fig. 1.17	Gas blanking of sub-bottom reflectors on Pinger record.	67
Fig. 1.18	Raypath geometry of seismic reflections - Boomer system.	69
Fig. 1.19	Depth - Time scales for water depths 8m and 13m.	69

	PAGE
Fig. 1.20 Block diagram of the main lower flow regime bedforms made by tidal currents on the continental shelf, with the corresponding mean spring near-surface tidal currents in m/s. (After Belderson, Johnson & Kenyon, 1982).	84
Fig. 1.21 Side-scan sonar record showing common sedimentary features.	86
Fig. 1.22 Echo sounder trace across trough and levee feature at the south of the outer Sand Sheet.	88
Fig. 1.23 Pinger record across Barmouth Bar, part of the ebb tidal delta.	94
Fig. 1.24 Contours of the base of the Inner Sand Sheet.	94
Fig. 1.25 Isopach map of the Inner Sand Sheet.	94
Fig. 1.26 Ripple Bands in the Patchy Sand Facies.	102
Fig. 1.27 Diagrammatic representation of the interaction of waves with a steady current (After Dyer, 1986)	113
Fig. 1.28 The ratio of the bed shear stress due to waves and currents (T_{wc}) to the bed shear stress due to currents alone (T), calculated using Bijker's (1967) equation. (After Heathershaw & Hammond, 1980)	113
Fig. 1.29 Penrhyn Point - Neap tide. Total load transport calculated by equation of Engelund & Hansen, 1967	118
Fig. 1.30 Penrhyn Point - Spring tide. Total load transport calculated by equation of Engelund & Hansen, 1967	118
Fig. 1.31 Farchynys - Neap tide. Total load transport calculated by equation of Engelund & Hansen, 1967	118
Fig. 1.32 Farchynys - Spring tide. Total load transport calculated by equation of Engelund & Hansen, 1967	118
Fig. 1.33 Penmaenpool - Neap tide. Total load transport calculated by equation of Engelund & Hansen, 1967	118
Fig. 1.34 Penmaenpool - Spring tide. Total load transport calculated by equation of Engelund & Hansen, 1967	118

Chapter 2

Fig. 2.1 Location of C.T.D. and tidal height stations in the Bay and Estuary.	134
Fig. 2.2 Time - depth distribution of tidal velocity in Barmouth Bay (Station 1), Spring tide.	143

	PAGE
Fig. 2.3 Time - depth distribution of velocity at Penrhyn Point (Station 2), Spring tide.	144
Fig. 2.4 Time - depth distribution of velocity at Penrhyn Point (Station 2), Neap tide.	144
Fig. 2.5 Time - depth distribution of tidal velocity at Farchynys (Station 4), Spring tide.	144
Fig. 2.6 Time - depth distribution of tidal velocity at Farchynys (Station 4), Neap tide.	144
Fig. 2.7 Time - depth distribution of tidal velocity at Penmaenpool (Station 5), Spring tide.	145
Fig. 2.8 Time - depth distribution of tidal velocity at Penmaenpool (Station 5), Neap tide.	145
Fig. 2.9 Time - depth distribution of salinity at Station 1, (Barmouth Bay), Spring tide.	145
Fig. 2.10 Time - depth distribution of salinity at Penrhyn Point (Station 2), Spring tide.	145
Fig. 2.11 Time - depth distribution of salinity at Penrhyn Point (Station 2), Neap tide.	145
Fig. 2.12 Time - depth distribution of salinity at Farchynys (Station 4), Spring tide.	145
Fig. 2.13 Time - depth distribution of salinity at Farchynys (Station 4), Neap tide.	145
Fig. 2.14 Time - depth distribution of salinity at Penmaenpool (Station 5), Spring tide.	146
Fig. 2.15 Time - depth distribution of current direction at Station 1, (Barmouth Bay), Spring tide.	146
Fig. 2.16 Time - depth distribution of current direction at Penrhyn Point (Station 2), Spring tide.	146
Fig. 2.17 Time - depth distribution of current direction at Penrhyn Point (Station 2), Neap tide.	146
Fig. 2.18 Flood-averaged velocity profiles - Stations 2,4,5.	149
Fig. 2.19 Ebb-averaged velocity profiles - Stations 2,4,5.	150
Fig. 2.20 'Ebb'-averaged profiles - Two definitions of 'Ebb' - Stations 2,4,5.	152
Fig. 2.21 Tide-averaged depth-mean velocity - Stations 2,4,5.	152
Fig. 2.22 Tide-averaged velocity profiles - Stations 2,4,5.	153
Fig. 2.23 Tide-averaged salinity profiles - Stations 2,4,5.	154

	PAGE
Fig. 2.24 Depth-averaged salinity at HW and LW - Stations 2,4,5.	156
Fig. 2.25 Tidal excursion directions over a tidal cycle at Penrhyn Point (Station 2).	157
Fig. 2.26 Estuary Classification of Stations 2,4 and 5, in the diagram of Hansen + Rattray (1966).	164
Fig. 2.27 Spring tidal curves measured at Stations X,Y, and Z (for an ordinary Spring Tide).	164
Fig. 2.28 Neap tidal curves measured at Stations X,Y, and Z (for a High Neap Tide).	164
Fig. 2.29 Tidal curves measured at Fegla Fach Shoal, 18/7/86 and 21/7/86.	164
Fig. 2.30 Limits of (a) tidal height; and (b) tidal range, along the Mawddach.	165
Fig. 2.31 (a) tidal delay; and (b) tidal flow duration, along the Mawddach.	165
Fig. 2.32 Spring tidal water slopes between Stations X,Y and Z.	165
Fig. 2.33 Neap tidal water slopes between Stations X,Y and Z.	165

Appendix 2.1

Time - depth distribution of temperature at Barmouth Bay (Station 1), Spring tide.	430
Time - depth distribution of temperature at Penrhyn Point (Station 2), Spring tide.	430
Time - depth distribution of temperature at Penrhyn Point (Station 2), Neap tide.	430
Time - depth distribution of temperature at Farchynys (Station 4), Spring tide.	430
Time - depth distribution of temperature at Farchynys (Station 4), Neap tide.	430

Chapter 3

Fig. 3.0 Map of Mawddach Estuary, showing study site, and extent of tidal megaripples in the lower estuary.	177
Fig. 3.1 Location of Fegla Fach Shoal.	188
Fig. 3.2 Predicted tidal heights - July 1986.	188

	PAGE
Fig. 3.3 Megaripple features and nomenclature.	190
Fig. 3.4 Migration of megaripple showing form of tidal bundle (schematic).	190
Fig. 3.5 Shoal profiles - Line A	191
Fig. 3.6 Shoal profiles - Line B	191
Fig. 3.7 Number of bedforms - Line A	191
Fig. 3.8 Number of bedforms - Line B	191
Fig. 3.9 Mean bedform symmetry index - Line A	192
Fig. 3.10 Mean bedform height - Line A	192
Fig. 3.11 Mean bedform wavelength - Line A	192
Fig. 3.12 Mean bedform flatness - Line A	192
Fig. 3.13 Mean crest, trough and bed elevation - Line A	193
Fig. 3.14 Bedform symmetry index v tidal range - Line A	193
Fig. 3.15 Mean bedform height v tidal range - Line A	198
Fig. 3.16 Mean bedform wavelength v tidal range - Line A	198
Fig. 3.17 Mean bedform flatness v tidal range - Line A	199
Fig. 3.18 Mean bed elevations v tidal range - Line A	199
Fig. 3.19 Range of bedform symmetry index - Line A	202
Fig. 3.20 Range of bedform wavelengths - Line A	202
Fig. 3.21 Range of bedform heights - Line A	204
Fig. 3.22 Range of bedform flatness - Line A	204
Fig. 3.23 Histogram of bedform wavelengths - Line A (n = 170)	204
Fig. 3.24 Histogram of bedform heights - Line A (n = 170)	204
Fig. 3.25 Histogram of bedform flatness - Line A (n = 170)	204
Fig. 3.26 Skewness of wavelength and height - Line A	204
Fig. 3.27 Fegla Fach bedform and flow data plotted on the bedform stability diagram of Vanoni (1974). (Modified after Terwindt & Brouwer, 1986).	212
Fig. 3.28 Mean bedform migration - Lines A and B.	212
Fig. 3.29 Correlation coefficients - Lines A and B.	213
Fig. 3.30 Mean migration v tidal range - Lines A and B.	213

	PAGE
Fig. 3.31 Correlation coefficient v tidal range - Lines A and B.	213
Fig. 3.32 Shoal profiles - Line A	221
Fig. 3.33 Shoal profiles - Line B	221
Fig. 3.34 Lag migration of 10m long sections - Line A	221
Fig. 3.35 Correlation coefficient of 10m long sections - Line A	221
Fig. 3.36 Mean crest, trough and bed elevations - Line B	223
Fig. 3.37 Histogram of bedform heights - Line B (n = 219)	223
Fig. 3.38 Mean bedform height - Line B	225
Fig. 3.39 Skewness of wavelength and height - Line B	225
Fig. 3.40 Mean bed elevations v tidal range - Line B	225
Fig. 3.41 Mean bedform height v tidal range - Line B	225
Fig. 3.42 Histogram of bedform wavelengths - Line B (n = 219)	226
Fig. 3.43 Mean bedform wavelength - Line B	226
Fig. 3.44 Mean bedform wavelength v tidal range - Line B	226
Fig. 3.45 Histogram of bedform flatness - Line B (n = 219)	226
Fig. 3.46 Mean bedform flatness - Line B	226
Fig. 3.47 Mean bedform flatness v tidal range - Line B	227
Fig. 3.48 Mean bedform symmetry index - Line B	227
Fig. 3.49 (a) Line A - Three measures of megaripple migration; (b) Line B - Three measures of megaripple migration	232
Fig. 3.50 Relationships between sediment transport and the three measures of migration. (Data points shown for lag migration data M only).	235
Fig. 3.51 (a)(i) Line A migration measure Mct, showing +/- 1 standard deviation: (a)(ii) same for Line A migration measure Msf; (b)(i) same for Line B migration measure Mct; (b)(ii) same for Line B migration measure Msf	241
Fig. 3.52 (a) Sediment transport j ($m^3/m/tide$) along Line A over the study period; (b) Same for Line B over the study period	247
Fig. 3.53 Bed level change, Accumulation minus Erosion - Lines A and B	249

	PAGE
Fig. 4.0 Location map of V.G.U. site.	258
Fig. 4.1 Flow separation over a megaripple.	260
Fig. 4.2 Spatially - averaged velocity profiles over a sandwave field : measurements where flow did, and did not, separate. (After Smith + McLean, 1977a).	260
Fig. 4.3 The four groups of velocity profiles over gravel megaripples. (After Dyer, 1970).	262
Fig. 4.4 Curvature of the log-profile produced by acceleration, and deceleration. (After Soulsby & Dyer, 1981).	262
Fig. 4.5 Tidal currents - Fegla Fach Shoal. Neap flood tide (NT, or T02).	274
Fig. 4.6 Tidal currents - Fegla Fach Shoal. Neap ebb tide (NT + 2, or T04).	274
Fig. 4.7 Tidal currents - Fegla Fach Shoal. Spring flood tide (ST, or T15).	274
Fig. 4.8 Tidal currents - Fegla Fach Shoal. Spring ebb tide (ST + 2, or T17).	274
Fig. 4.9 Velocity parameters for flood neap tide (NT).	276
Fig. 4.10 Velocity parameters for ebb neap tide (NT + 2).	276
Fig. 4.11 Velocity parameters for flood spring tide (ST).	276
Fig. 4.12 Velocity parameters for ebb spring tide (ST + 2).	276
Fig. 4.13 Flow roughness lengths at peak velocities for the study period. (C = flow measured at megaripple crest, F = at megaripple flank, T = at megaripple trough. Capitals denote flood tide data; lower case denote ebb tide data; dots denote predictions using Smith & McLean (1977a).	283
Fig. 4.14 Relationship of Z_o to U^* - Flood tide, NT + 3	288
Fig. 4.15 Relationship of Z_o to U^* - Flood tide, NT + 4	288
Fig. 4.16 Relationship of Z_o to U^* - Flood tide, NT + 7	288
Fig. 4.17 Relationship of Z_o to U^* - Flood tide, ST + 5	288
Fig. 4.18 Relationship of Z_o to U^* - Flood tide, ST + 4	288
Fig. 4.19 Relationship of Z_o to U^* - Ebb tide, NT + 1	288
Fig. 4.20 Relationship of Z_o to U^* - Ebb tide, NT + 2	288
Fig. 4.21 Relationship of Z_o to U^* - Ebb tide, NT + 6	288

	PAGE
Fig. 4.22 Relationship of Z_o to U^* - Ebb tide, NT + 10	288
Fig. 4.23 Relationship of Z_o to U^* - Ebb tide, ST + 3	288
Fig. 4.24 Effect of suspended sediment on the stratification of velocity profiles. (After Soulsby + Wainwright, 1987).	292
Fig. 4.25 Experimental existence fields for aqueous bedforms under equilibrium conditions, shown in the non-dimensional mean bed shear stress (wall-corrected) - grain size plane, at 25 degrees C. (After Allen, 1984).	292
Fig. 4.26 Relationship of Z_o to U^* - Ebb tide, NT + 9	294
Fig. 4.27 Relationship of Z_o to U^* - Ebb tide, ST + 2.	294
Fig. 4.28 Variation of U_{100max} over the lunar cycle. (. = flood, x = ebb).	296
Fig. 4.29 Variation of U_{100max} with maximum flow depth. (. = flood, x = ebb).	296
Fig. 4.30 Variation of U^*_{max} over the lunar cycle. (. = flood, x = ebb).	296
Fig. 4.31 Variation of U^*_{max} with maximum flow depth. (. = flood, x = ebb).	296
Fig. 4.32 Variation of $U_{100}^*_{max}$ with tidal range. (. = flood, x = ebb).	296
Fig. 4.33 Variation of U^*_{max} with tidal range. (. = flood, x = ebb).	296
Fig. 4.34 Roughness length plotted against mean megaripple height. C = flow measured at megaripple crest, F = at megaripple flank, T = at megaripple trough. Capitals denote flood tide, lower case denote ebb tide.	301
Fig. 4.35 Roughness length plotted against mean megaripple flatness. C = flow measured at megaripple crest, F = at megaripple flank, T = at megaripple trough. Capitals denote flood tide, lower case denote ebb tide.	301
Fig. 4.36 Roughness length v U_{100max} . C = flow measured at megaripple crest, F = at megaripple flank, T = at megaripple trough. Capitals denote flood tide, lower case denote ebb tide.	301

Chapter 5

Fig. 5.1 Fall tower calibration data - Correction curve for sediment weight collected on pan of Fall Tower, as a function of settling time. Error bars represent 68% confidence limits.	325
---	-----

	PAGE
Fig. 5.2 Fall velocity data. Shows the relationship between Grain Reynolds Number and Archimedes Buoyancy Index. (Data from Hallermeier, 1981).	328
Fig. 5.3 Standard deviation repeatability v mean grain size. 3 subsamples of each sample.	331
Fig. 5.4 Skewness repeatability v mean grain size. 3 subsamples of each sample.	331
Fig. 5.5 Kurtosis repeatability v mean grain size. 3 subsamples of each sample.	331

Chapter 6

Fig. 6.1 Location map of bay and estuarine sediment sample stations.	337
Fig. 6.2 Positions of survey lines across the Mawddach (and positions of sediment samples P303 and P304).	337
Fig. 6.3 Barmouth Bay - Sediment grab sample stations.	349
Fig. 6.4 Barmouth Bay - Sediment % weight > 2.0mm (gravel).	349
Fig. 6.5 Barmouth Bay - Sediment % weight 0.063 - 2.0mm (sand).	350
Fig. 6.6 Barmouth Bay - Sediment % weight < 0.063mm (silt & mud)	350
Fig. 6.7 Barmouth Bay - Mode grain size (phi)	351
Fig. 6.8 Barmouth Bay - Mean grain size (phi)	351
Fig. 6.9 Barmouth Bay - Sediment sorting (phi) - (moments)	351
Fig. 6.10 Barmouth Bay - Sediment sorting (phi) - (Folk)	351
Fig. 6.11 Barmouth Bay - Sediment skewness (phi) - (moments)	352
Fig. 6.12 Barmouth Bay - Sediment skewness (phi) - Folk	352
Fig. 6.13 Barmouth Bay - Sediment kurtosis (phi) - (moments)	353
Fig. 6.14 Barmouth Bay - Sediment kurtosis (phi) - (Folk)	353
Fig. 6.15 Barmouth Bay - % frequency of peak modal class	358
Fig. 6.16 Modal frequencies of the sand fraction	358
Fig. 6.17 Barmouth Bay - distribution of 2.05 phi mode (%)	360
Fig. 6.18 Barmouth Bay - distribution of 2.55 phi mode (%)	360
Fig. 6.19 Barmouth Bay - distribution of 3.35 phi mode (%)	362

	PAGE
Fig. 6.20 Dowling plots of transects between samples 448 and 412 (E-W), and 448 and 401 (NNE-SSW), in Barmouth Bay	362
Fig. 6.21 Dowling plots of transects between samples 443 and 402 (E-W), and 433 and 403 (E-W), in Barmouth Bay	362
Fig. 6.22 Dowling plot of a N-S transect between samples 446 and 434, in inner Barmouth Bay	362
Fig. 6.23 Dowling plot of a N-S transect between samples 413 and 420, in Barmouth Bay	362
Fig. 6.24 Dowling plot of a N-S transect between samples 412 and 404, in Barmouth Bay	362
Fig. 6.25 Dowling plot of a NE-SW transect between samples 440 and 404, in Barmouth Bay	362
Fig. 6.26 Location map and Dowling plot of sediment samples from near the tip of Ro Wen	364
Fig. 6.27 Bed profiles of Transect 1	367
Fig. 6.28 Bed profiles of Transect 2	367
Fig. 6.29 Bed profiles of Transect 3	367
Fig. 6.30 Bed profiles of Transect 4	367
Fig. 6.31 Bed profiles of Transect 5	367
Fig. 6.32 Bed profiles of Transect 7	367
Fig. 6.33 Sand fraction - Mode size along the estuarine transects	371
Fig. 6.34 Sand fraction - Mean size along the estuarine transects	371
Fig. 6.35 Sand fraction - Sorting along the estuarine transects	371
Fig. 6.36 Sand fraction - Skewness along the estuarine transects	371
Fig. 6.37 Sand fraction - Kurtosis along the estuarine transects	371
Fig. 6.38 Dowling plots of channel samples along the estuary	374
Fig. 6.39 Dowling plots of sandflat samples along the estuary	374

Chapter 7

Fig. 7.1 Block diagram of the main lower flow regime bedforms made by tidal currents on the continental shelf, with the corresponding mean spring near-surface tidal currents in m/s. (After Belderson, Johnson & Kenyon, 1982). Implied net sediment transport is towards the upper right	380
--	-----

	PAGE
Fig. 7.2 Chart of Barmouth Bay showing dispersal vectors for different grain types (After Moore, 1968)	382
Fig. 7.3 Implied sediment transport pathways in Barmouth Bay, using the method of McLaren + Bowles (1985)	383
Fig. 7.4 Implied sediment transport pathways in Barmouth Bay, using skewness of sand fraction distribution.	383
Fig. 7.5 Implied sediment transport pathways in Barmouth Bay, using bedform orientation suggested by side-scan sonar and echo-sounder data.	386
Fig 7.6 Estuarine cross-sectional areas at various tidal heights	396

Chapter 8

Fig. 8.1 Summary diagram of the sedimentary facies of Barmouth Bay. Arrows indicate inferred sediment transport directions of bed material. Also shown are zones of net sediment erosion and accumulation	403
Fig. 8.2 Summary diagram of outcrop and interpretation of seismic facies 1 - 4 in Barmouth Bay	405
Fig. 8.3 Environmental reconstruction of Barmouth Bay and the Mawddach Estuary for Early post-Glacial times. Arrows indicate observed onlap directions	405
Fig. 8.4 Environmental reconstruction of Barmouth Bay and the Mawddach Estuary for Late Post-Glacial times. Arrows indicate inferred sediment transport directions of bed material	406

List of Enclosures

- Enclosure 1 Facies interpretation of the stratigraphy at Llanelltyd, the estuary head. (Data supplied by B.G.S., Aberystwyth)
- Enclosure 2 Track plots of geophysical surveys conducted by R.V. 'Prince Madog', and 'Sand Pebbler', and positions of Shipek grab samples
- Enclosure 3 Bathymetric map of Barmouth Bay, drawn from echo-sounder and pinger records - contours in metres below Ordnance Datum Newlyn (Lowest astronomical tide at Barmouth i.e. chart datum, is -2.44m O.D.N).
- Enclosure 4 Interpreted seismic profiles across Barmouth Bay - from boomer and pinger data
- Enclosure 5 Distribution and orientation of sedimentary features in Barmouth Bay

List of Tables

TABLE
ON, OR
FOLLOWS
PAGE

Chapter 1

Table 1.1 Details of marine geophysical survey program - surveys 1 and 2	62
Table 1.2 Outer Sand Sheet - Summary of bedform morphologies	90
Table 1.3 Patchy Sand Facies - Summary of bedform morphologies	93
Table 1.4 Inner Sand Sheet - Summary of bedform morphologies	97
Table 1.5 Morphology of ripple bands in Barmouth Bay	101
Table 1.6 Wind and wave conditions during the storm of February 1988	109
Table 1.7 Calculated orbital velocities and diameters for storm conditions, plus 'normal' conditions for Barmouth Bay	110
Table 1.8 Total load sediment transport rates at Penrhyn Point, Farchynys, and Penmaenpool, in the absence of waves. (Equation of Engelund & Hansen, 1967)	119
Table 1.9 Calculated shear stress enhancement factors (T_{wc}/T) for storm conditions, plus 'normal' conditions for Barmouth Bay	121
Table 1.10 Calculated total load sediment transport rates under peak velocity flood tide currents and waves (jwc), for storm conditions, plus 'normal' waves conditions for Barmouth Bay. (Equation of Engelund & Hansen, 1967)	122
Table 1.11 Calculated net total load sediment fluxes at Stations 2,4, & 5	125

Chapter 2

Table 2.1 Summary of C.T.D. data collected	142
Table 2.2 Maximum currents measured at each station	142
Table 2.3 Summary of salinity data collected	145
Table 2.4 Near-surface (S) and near-bed (B) flow directions at Station 2 (degrees)	158
Table 2.5 Hansen & Rattray (1966) classification of some Welsh estuaries	162
Table 2.6 Some parameters derived from tidal curves	162

Table 2.7 HW and LW delay between Barmouth Quay (X) and Borthwnog (Z)	PAGE 168
--	-------------

Chapter 3

Table 3.1 Notation used to refer to surveys of Fegla Fach shoal	190
Table 3.2 Times of extreme bed levels	194
Table 3.3 Some published tidal bedform migration rates - modern and ancient examples	214
Table 3.4 Heights and migration rates around spring tide, Line A	219
Table 3.5 Four-tide mean lag migrations (metres) for 10m sections of Line A	221
Table 3.6 A comparison of some morphometric parameters - data from all simultaneous surveys of Lines A and B	224
Table 3.7 A comparison of three measurements of migration. Four-tide mean migrations (m) - Line A	233
Table 3.8 Comparison of predictive migration equations	238
Table 3.9 Four-tide standard deviations of megaripple migration (m)	242
Table 3.10 Velocity thresholds for intertidal megaripples - migration, shape change, ebb cap formation, partial and full reversal, 2-D to 3-D transition, and scour pit formation	244

Chapter 4

Table 4.1 Percentage of flow parameter data obtained by curve fits to 'n' rotors, 10 minute average profiles	273
Table 4.2 Categories of tidal flow measurements with respect to position of measurement over megaripples	279
Table 4.3 Peak shear velocities and associated roughness lengths measured over different parts of megaripples	281
Table 4.4 Roughness lengths over megaripples	300

Chapter 5

	PAGE
Table 5.1 Descriptive scales of grain size parameters. (After Folk & Ward, 1957)	330
Table 5.2 Grain size parameters of replicate samples	330
Table 5.3 Replicate fall tower data of Shagude (1989). Grain sizes in phi	330

Chapter 6

Table 6.1 Details of bed sediment samples taken by divers	346
Table 6.2 Petrological characteristics of the gravel fraction of sediments from the Mawddach Estuary and Barmouth Bay	355
Table 6.3 Details of bed sediment samples taken from Fairbourne Spit and Barmouth Beach	364
Table 6.4 Dates of survey of estuarine transects	367
Table 6.5 Grain size parameters from sandflat sediment samples	375

Chapter 7

Table 7.1 Dates of survey of estuarine transects	388
Table 7.2 Some parameters derived from the whole survey lines	389
Table 7.3 Some parameters derived from portions of the survey lines	389
Table 7.4 Cross-sectional areas of the Mawddach Estuary at different tidal heights	397

Study Objectives

This work addresses the sedimentary evolution of a coastal region during the last 10-12000 years, and the modern processes acting upon it. The original plan for the research, was to sample the buried sediments, analyse their structural and mineralogical character, and, through modern process studies, deduce the nature and magnitude of the sedimentary processes active during the deposition of the Holocene sequence.

However, this proved difficult to achieve, mainly because of the lack of coring equipment, land- or marine-based; this resulted in virtually no subbottom samples being collected. Thus, whilst much valuable and useful geophysical data were collected, little positive identification of seismic reflectors was possible, and mineralogical studies were severely curtailed. As a consequence, the study has concentrated on two main areas:

- 1 - a geophysical assessment of the sedimentary facies sequence of Barmouth Bay;
- 2 - a study of the hydrographic and sedimentary processes of the Mawddach Estuary, with, in particular, a detailed study of the dynamics of intertidal megaripples, which dominate large areas of the seaward portions of the estuary.

These areas are integrated through consideration of: the glacial and post-glacial history of Barmouth Bay; it's modern dynamic sedimentary regime; regional and local sediment transport paths; and the geological products of these processes.

Chapter 1

Bathymetry, Morphology and Stratigraphy of the Nearshore Zone

Part A

1.1 Introduction

Firstly, this chapter contains a review of the geological and sedimentological literature relevant to northern Cardigan Bay, Barmouth Bay, and the Mawddach Estuary. A synthesis of the literature describes the glacial and post-glacial evolution of the area. A review is presented of literature describing modern sediment transport processes and pathways.

The sub-bottom geology of the Mawddach is then summarised, using unpublished borehole data at the mouth and head of the estuary, and B.G.S. (British Geological Survey) boreholes in outer Barmouth Bay are described. Details of an extensive geophysical survey, using echo sounder, side-scan sonar, boomer and pinger, are given, from which are made interpretations of the sub-bottom and surface geology.

Estimates of sediment transport rates and wave effects on sediment transport, are presented; these aid understanding of the sedimentary regime in the Bay and Estuary, and the bedform suites developed.

1.2 Geography

The Mawddach Estuary and Barmouth Bay are located on the coast of Cardigan Bay, in Gwynedd, North Wales (Fig. 1.1). The Mawddach is the central of 3 estuaries in the northern part of Cardigan Bay, with in the extreme north the Dwyryd-Glaslyn which meets the sea at Porthmadog, and in the south the Dyfi, with Aberdyfi at its mouth. Each estuary is SW-NE elongate, and occupies a valley glaciated most recently during the late Devensian glacial episode.

The Mawddach Estuary lies within the Snowdonia National Park, and divides the high ground of the Rhinog mountain chain to the north from the Cader Idris range to the south. The ground either side of the estuary rises steeply, and NW of Glandwr it reaches an elevation of 461m in less than 2km from the estuary bank. In plan view, there are two constrictions; at the mouth the channel is less than 200m wide, and 5km upstream at Farchynys, it is less than 300m in width (Fig. 1.2). There are extensive saltmarshes present between Bonddu and Llanelltyd, on the northern bank at Glandwr, and north of Fairbourne behind the sand and shingle barrier Ro Wen.

The estuary is tidal up to Llanelltyd, ca. 11km from the mouth at Barmouth, and is 2km wide at its broadest point. At high water the estuary covers an area of ca. 9.5km². The estuary is fed by two main rivers, the Afon Mawddach which drains the high ground to the northeast, and the Afon Wnion which is fed from the east. Their combined catchment area is approximately 450km² and discharge of the Mawddach varies seasonally between 0.9 and 13.0 cumecs (pers. comm. Welsh Water Authority, data of 1970).

The coastline of northern Cardigan Bay has a number of long linear sections which broadly face the SW, such as Hells Mouth on the Lleyn Peninsular, Morfa Harlech north of Harlech, Morfa Dyffryn, between Llanaber and Llanbedr, and the coastline north from Aberdyfi to Morfa Gwylt

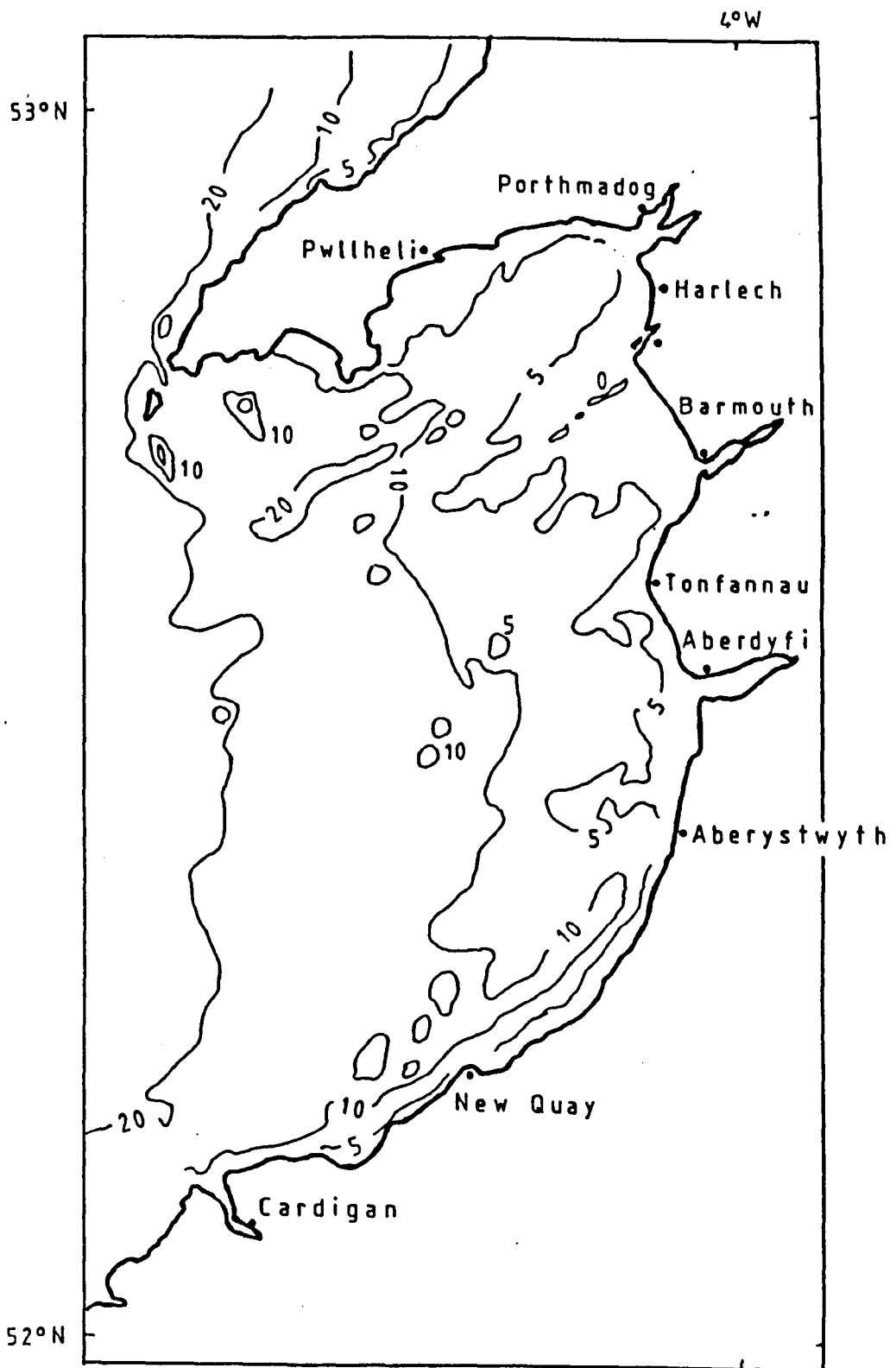


Fig. 1.1
 Geography and sea-floor topography
 in Cardigan Bay

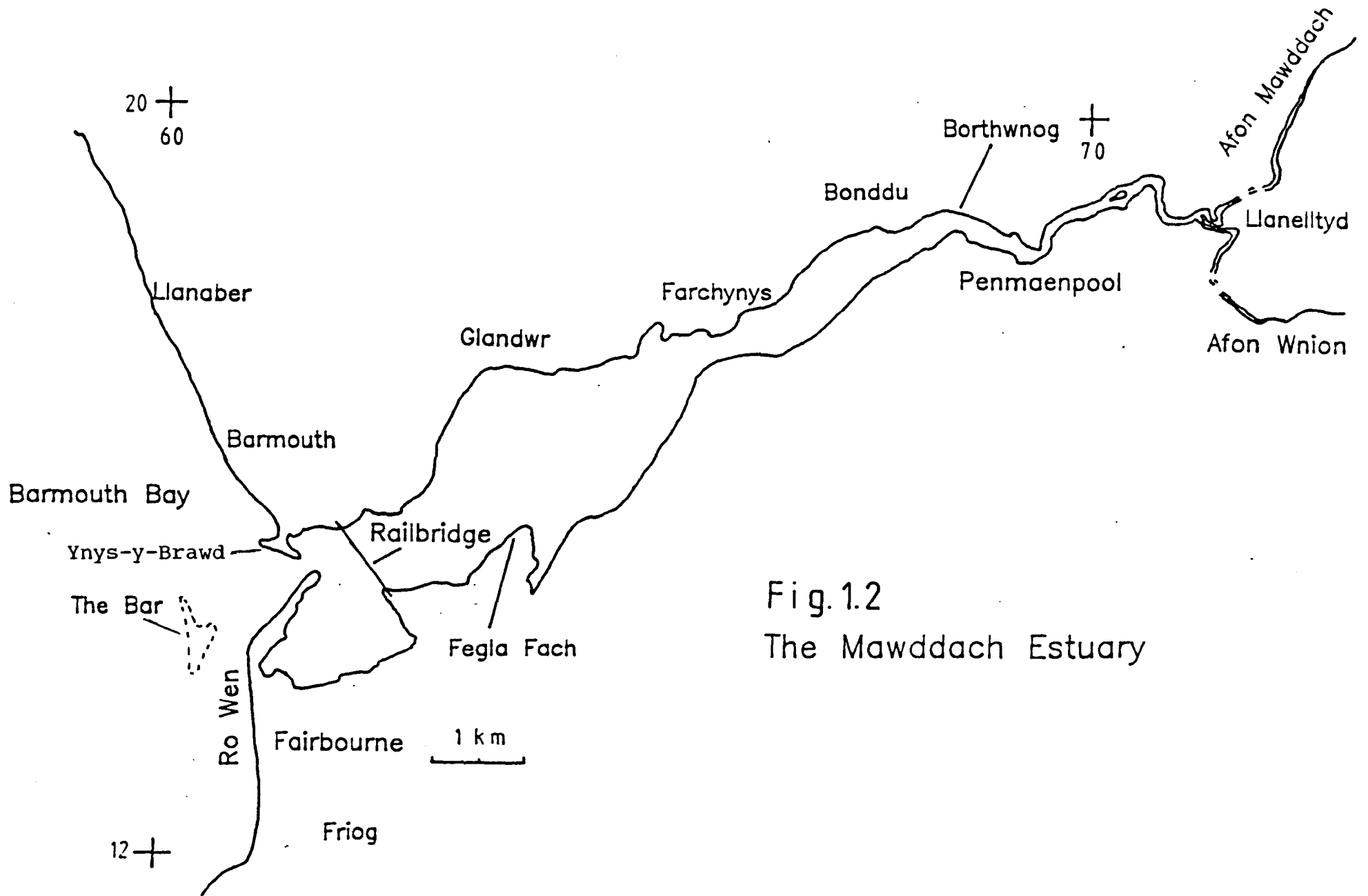


Fig.1.2
 The Mawddach Estuary

northwest of Tywyn. There is also a more southerly-facing section, east of Pwllheli. The Morfas Harlech, Dyffryn and Gwyllt form coastal terraces of up to 5km in width in front of steeply rising ground. The area of these coastal terraces increases in width northwards between Aberdyfi and Porthmadog.

1.3 Geology of the Area

1.3.1 Pre-Quaternary Regional Geology

The geology of North Wales has been discussed by Smith & George (1961), and more recently a memoir on the geology of the country around Harlech has been written by Allen & Jackson (1985); from these books, much of the following has been derived.

1.3.1.2 Geological Succession

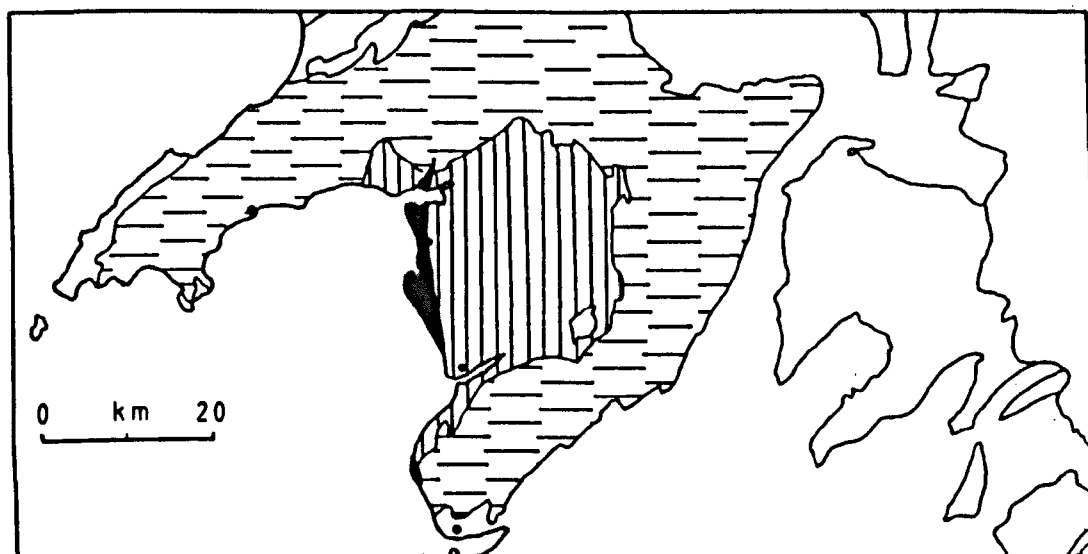
Northern Cardigan Bay is flanked by Palaeozoic rocks in the Lleyrn Peninsular and also south of Llanaber (Fig. 1.3). Between Llanaber and Porthmadog, Quaternary deposits cover Tertiary sediments which form the coastal platform (Woodland, 1971), behind which lie cliffs of Cambrian rocks of the Harlech Dome.

1) Cambrian - The oldest rocks exposed in the area are Lower Cambrian deltaic sediments of the Dolwen Formation, exposed extensively in the central area of the Harlech Dome. The Harlech Grits Group forms the base of the Cambrian succession, and is succeeded by the Mawddach Group. In total, the Cambrian sequence is about 4.5km thick, and is bounded by unconformities. The sequence as a whole records both basin formation and its subsequent infilling, with facies changing from deltaic through prodeltaic and basinal to open shelf. The Harlech Grits are dominated by sandstones, with increasing argillaceous beds towards the top, and the Mawddach Group is almost exclusively argillites.

To the south of the estuary, Cambrian rocks outcrop along the edge of the hills which rise southwards towards the Cader Idris range. They are open shelf siltstones and mudstones of the upper part of the Mawddach Group.

Fig. 1.3

Simplified geology of part of North Wales



-  Tertiary
-  Ordovician
-  Cambrian

2) Ordovician - The Ordovician rocks of the area are a complex mixture of volcanic and coarse clastic elements, representing the continuation of Late Cambrian tectonic and volcanic activity related to a southeasterly-dipping subduction zone at the south side of the Iapetus Ocean (Phillips et al, 1976). The regional metamorphism associated with this subduction nowhere in this area exceeds that of lower greenschist facies.

The Rhobell Volcanic Group is a remnant of a subaerially-erupted basaltic volcano, below which are more intermediate and acidic igneous rocks. The overlying Aran Volcanic Group comprises a suite of magmatic and interbedded sedimentary rocks, including tuffs, lavas and sandstones. The group is thickest in the south, at > 700m, and thickness decreases northwards due to thinning and disappearance of the lower formations.

3) Mesozoic and Tertiary - Woodland (1971) reported on the discovery of Mesozoic and Tertiary rocks beneath Morfa Dyffryn, found by the drilling of the Mochras Farm Borehole. The base of the borehole reached a depth of 1939m, and penetrated 77m of Recent and Pleistocene deposits, 524m of Tertiary strata, and 1338m of Mesozoic beds, not reaching its base. Neither Tertiary or Mesozoic deposits are today exposed at surface in the area, although they are implied to outcrop extensively beneath Cardigan Bay (see below).

1.3.1.3 Intrusive Rocks

There are many intrusive rocks associated with both the Cambrian and Ordovician sequences. Those occurring in Cambrian rocks include dolerite, microdiorite and microtonalite, forming sills, dykes and laccoliths. Dolerite, rhyolite and microdiorites in the Ordovician succession occur as sills, with few dolerite dykes. Cader Idris itself is formed of Ordovician rocks of both sedimentary and igneous origin.

1.3.1.4 Structure

The main fold elements of the Harlech Dome area are the Caerdon Syncline and the Dolwen Pericline, of large wavelength and with N-S trending fold axes. The latter is the main anticlinal feature, which gives the Harlech Dome its name. Neither are simple structures, being made up of a number of parallel en-echelon folds, giving a sinusoidal trace to the main fold axis. On the east side of the Harlech Dome large-scale folding is also present, with Rhobell Fawr (734m) forming part of a syncline, and further east the Cambrian Mawddach Group forming an anticline. The structural style is largely controlled by the competent horizons in the succession. Four main phases of folding have been recognised in the area, varying in age from pre-Rhobell Volcanic Group to the main broad, open, N-NE trending periclinal structures of end-Silurian age, marking progressive deformational phases in the Caledonian Orogeny.

There is a very complex pattern of faulting in the area. Allen & Jackson (1985) discussed them in terms of their recognised dominant trends; NNE faults, NNW faults and tension faults are most common. The Trawsfynydd valley follows the line of the Trawsfynydd Fault down to the confluence of the Afon Eden with the Afon Wen, which flows along the line of the Afon Wen - Derwas Fault. This fault crosses the upper-estuary at Llanelltyd.

The Bala Fault (which according to Challinor & Bates, 1973, is probably a series of closely-spaced parallel faults) extends for ca. 100km northeastwards from Tywyn through Bala towards Chester. It has two major splays to the northwest, one 8km south of Ruthin, and the second from 9km northeast of Dolgellau to the confluence of the Afon Mawddach and Afon Wnion at the estuary head (I.G.S., 1979). There is speculation (R. Whittington, pers. comm. 1986) that this splay continues beneath the estuary fill, and was responsible for the delineation of the valley and its subsequent glacial overdeepening. Dobson et al (1973, their fig. 6) show

the offshore existence of a SW-NE aligned, 18km long 'Mawddach Estuary Fault', which offsets the Mochras Fault (see below) west of Fairbourne by 6km (Fig. 1.4). At its landward end the Mawddach Fault bounded the Tertiary Tremadoc Bay - Barmouth Bay basin, and the throw of the fault decreased rapidly southwestwards. In their Fig. 11, they infer the landward continuation of the fault NE up the entire length of the estuary. However, there is no up-estuary continuation of the fault shown by Dobson & Whittington (1987, their fig. 1).

In the literature there is no direct evidence for the existence of a fault; it seems to be inferred by :

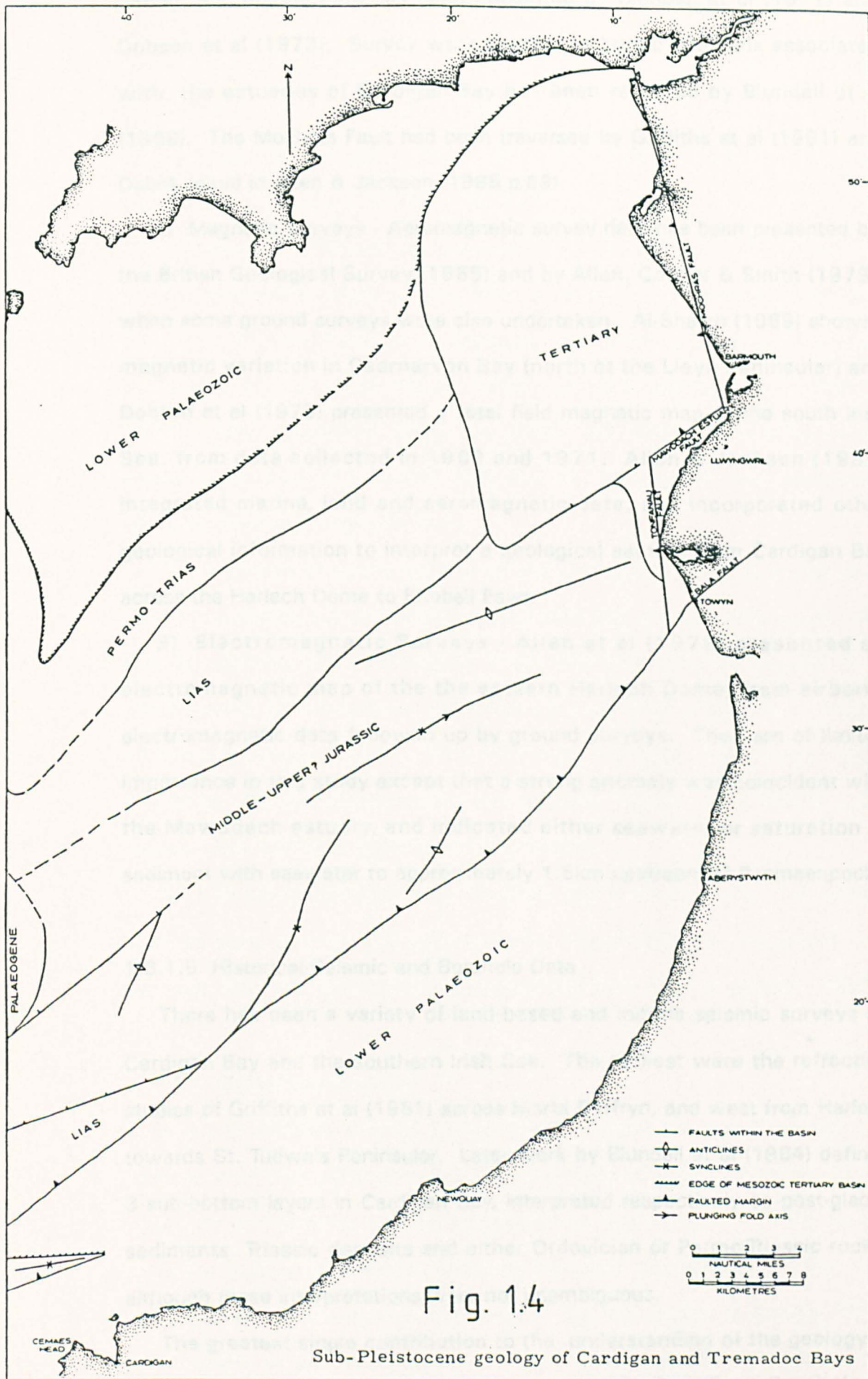
- a) - the apparent offshore westerly offset of the Mochras Fault
- b) - the presence of an deep infilled glacial valley (i.e. the Mawddach) with a trend consistent with a recognised splay of the Bala Fault.

The Mochras Fault truncates Cambrian rocks at the western edge of the Harlech Dome. However, the Llanegryn Fault, 5km east of Tonfanau, has a downthrow of 610m to the west (Jones, 1933), and this N-S trending fault matches the position of a potential southward extension of the Mochras Fault (if either the Mawddach fault did not exist or produced no E-W offset in the N-S fault). (Blundell et al (1971) consider the Llanegryn Fault may have increased the depth of the Tertiary Basin to the west). Thus, there remains speculation about the existence of a major fault beneath the Mawddach estuary.

1.3.1.5 Geophysical Studies

Previous regional geophysical studies have included gravity, magnetic, electromagnetic and seismic surveys :

- 1) Gravity surveys - The regional gravity field of the Harlech area was measured by Powell (1956) on about 50 land stations. Offshore measurements have been made by Griffiths, King & Wilson (1961) on Sarn



(After Dobson, Evans & Whittington, 1973)

Badrig, and marine data has been presented by Blundell et al (1971) and Dobson et al (1973). Survey work across the buried channels associated with the estuaries of Cardigan Bay has been reported by Blundell et al (1969). The Mochras Fault had been traversed by Griffiths et al (1961) and Dabek (cited in Allen & Jackson, 1985 p.69).

2) Magnetic Surveys - Aeromagnetic survey data has been presented by the British Geological Survey (1965) and by Allen, Cooper & Smith (1979), when some ground surveys were also undertaken. Al-Shaikh (1969) showed magnetic variation in Caernarvon Bay (north of the Lleyrn Peninsular) and Dobson et al (1973) presented a total field magnetic map of the south Irish Sea, from data collected in 1969 and 1971. Allen & Jackson (1985) integrated marine, land and aeromagnetic data, and incorporated other geological information to interpret a geological section from Cardigan Bay across the Harlech Dome to Rhobell Fawr.

3) Electromagnetic Surveys - Allen et al (1979) presented an electromagnetic map of the the eastern Harlech Dome, from airborne electromagnetic data followed up by ground surveys. They are of limited importance in this study except that a strong anomaly was coincident with the Mawddach estuary, and indicated either seawater or saturation of sediment with seawater to approximately 1.5km upstream of Penmaenpool.

1.3.1.6 Historical Seismic and Borehole Data

There has been a variety of land-based and marine seismic surveys in Cardigan Bay and the southern Irish Sea. The earliest were the refraction studies of Griffiths et al (1961) across Morfa Dyffryn, and west from Harlech towards St. Tudwals Peninsular. Later work by Blundell et al (1964) defined 3 sub-bottom layers in Cardigan Bay, interpreted respectively as post-glacial sediments, Triassic deposits and either Ordovician or Permo-Triassic rocks, although these interpretations were not unambiguous.

The greatest single contribution to the understanding of the geology of northern Cardigan Bay was the drilling of the Mochras Farm Borehole on

Morfa Dyffryn in a joint project by the University of Wales, Aberystwyth and the Institute of Geological Sciences (now called the British Geological Survey, B.G.S.). The results were published in Woodland (1971), and various aspects were dealt with in detail in related publications. Aspects included the Tertiary succession (O'Sullivan, 1979), forams (Copestake, 1978; Johnson, 1975) and the palynology (Herbert-Smith, 1971, 1979).

The Mochras borehole proved 77m of recent and Pleistocene deposits, 524m of Tertiary, 1305m of Jurassic, and drilling was ceased after penetrating 32m of Upper Triassic rocks. An I.G.S. borehole at Tonfanau in 1971 (10km southwest along the coast from Fairbourne) showed the presence of 37m of a pebbly drift and ca. 70m of Tertiary sediments overlying Cambro-Ordovician rocks.

The Mochras borehole confirmed the interpretation of Griffiths et al (1961) regarding the uppermost postglacial and Triassic sediments. The seismic refraction line extending for 12km NW from Tonfanau (Blundell et al, 1964) could be interpreted as Quaternary sediments (seismic velocity 1500m/s) overlying Triassic (1800-2000m/s) and lower Palaeozoics (2950-3740m/s). Further interpretation was made by Blundell et al (1971), using seismic data and other geophysical information.

An E-W cross section through Cardigan Bay is shown in Fig. 1.5, drawn from seismic, gravity and aeromagnetic interpretations, combined with borehole data, and surface exposure (modified from Allen & Jackson, 1985).

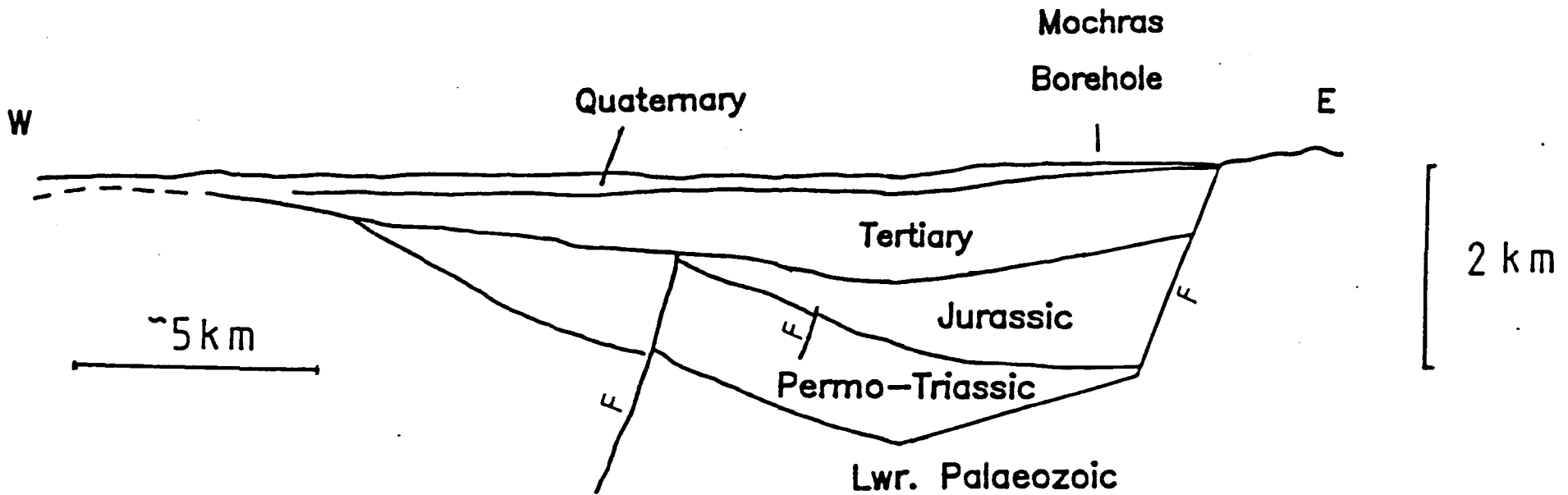
1.3.1.7 Quaternary Geology

It is only recently that the Quaternary geology of the Irish Sea Basin has been inferred from other than coastal information (Garrard & Dobson, 1974). Attempts to correlate coastal exposures on the Welsh coast and form a coherent picture of Quaternary history have not proved very fruitful. The large quantity of literature on the subject (eg. the review of Bowen, 1977) often relates to specific locations or topics, and unsatisfactory progress has

Fig. 1.5

E - W cross-section through Northern Cardigan Bay

(modified from Allen + Jackson, 1985)



been made towards a synthesis of data into an agreed general model. Referring specifically to the Holocene (i.e. the last 10,000 years) Bowen (1977) stated that present data allowed 'no detailed pattern of either sea-level change or isostatic movements' in Wales. Much speculation and uncertainty also exists about the nature of the Devensian and Pre-Ipswichian glacial events. Bowen argues that much of this ignorance stems from a lack of systematic sampling and dating.

The combined survey techniques of seismic surveying and coring have produced a wealth of information on the Quaternary of the Irish Sea as a whole, and of its parts, such as Cardigan Bay. Seismic definition of the sedimentary sequences was begun by Blundell and co-workers in the 1960's (see above) and was continued in the 1970's by co-operative work between the Continental Shelf Unit 1 of the Institute of Geological Sciences and the Department of Geology, U.C.W., Aberystwyth (eg. Al-Shaikh, 1970; Dobson et al, 1973; Garrard & Dobson, 1974; Garrard, 1977). Some research has also been undertaken by workers at U.C.N.W., Bangor. Fenemore (1976) presented data from over 600km of continuous seismic profiling, and developed ideas of Sommerville (1973) on the generation of the sequence in Tremadoc Bay area. Taylor-Smith (1987) reviewed geophysical and geotechnical measurements made by workers at Bangor in Tremadoc Bay.

Haynes et al (1977) used information from three boreholes in the south of Cardigan Bay to study the distribution of foraminifera, ostracods, diatoms and pollen in the sediments infilling Late Glacial age meltwater channels cut in Welsh and Irish Sea boulder clay. These channels represent the former extension of the modern river system (Jones, 1971). Muddy Hollow, south of the Lleyn Peninsular, and the Trawling Ground southwest of Aberystwyth are the partially filled remains of two such channels. Haynes et al (1977) showed the Holocene transgression represented by a sedimentary sequence changing in nature upwards from estuarine to marine. Estuarine deposits were found as deep as -51m O.D., suggesting Late Glacial sea levels as low as -60m O.D.. This also inferred Welsh ice retreated from the area before

14000 years B.P. In the borehole off Aberporth (borehole 73/42), at a depth of -39m O.D. there was a transition from brackish/marine deposits to marine sediments; a similar transition occurs in Tremadoc Bay at -28m O.D. (Spencer, 1976).

In the same volume, a major step in the understanding of the Irish Sea Quaternary is the paper by Garrard (1977), who by interpretation of seismic profiles and correlations with over 230 boreholes or shallow cores, was able to clarify many hypotheses on the subject (Kidson, 1977). His paper also complicated other issues, such as the interpreted ice limits at some coastal sites. Garrard (1977) shows the distribution of Late Glacial and Early Holocene sediments in Cardigan Bay (Fig. 1.6).

The whole of the area surveyed in this study (except perhaps the survey lines in the extreme southwest) lies within Garrard's (1977) area of 'Postglacial estuarine and lagoonal sediments'. This forms the north of a belt of such sediments which continues southwest around the west of Sarn Bwch and then spreads south and east into the bay offshore of the Dyfi estuary. These sediments fill a channel system at least 68km long following the same trend, i.e. parallel to today's coast but deflected westwards by Sarn Bwch. In Barmouth Bay (west of the limits of this study) glacial drift has been eroded to form a narrow, linear, steep-sided depression, with > 120m of recent sediment fill, and which closes both to the southwest and northeast. However, his conclusions on nearshore sub-bottom seismic and sedimentary facies in the area appear based on limited seismic coverage and from patterns in adjacent areas. Whittington (1987, pers. comm.) stated that very few seismic reflection profiles have been taken by Aberystwyth University in Barmouth Bay largely because of the problem of gassy sediments (see this chapter).

More recently, Hession & Whittington (1987) and Hession (1989) have correlated seismic data with boreholes in the Irish Sea both north and south of Anglesey. Eyles & McCabe (1989a,b) have recently proposed that during

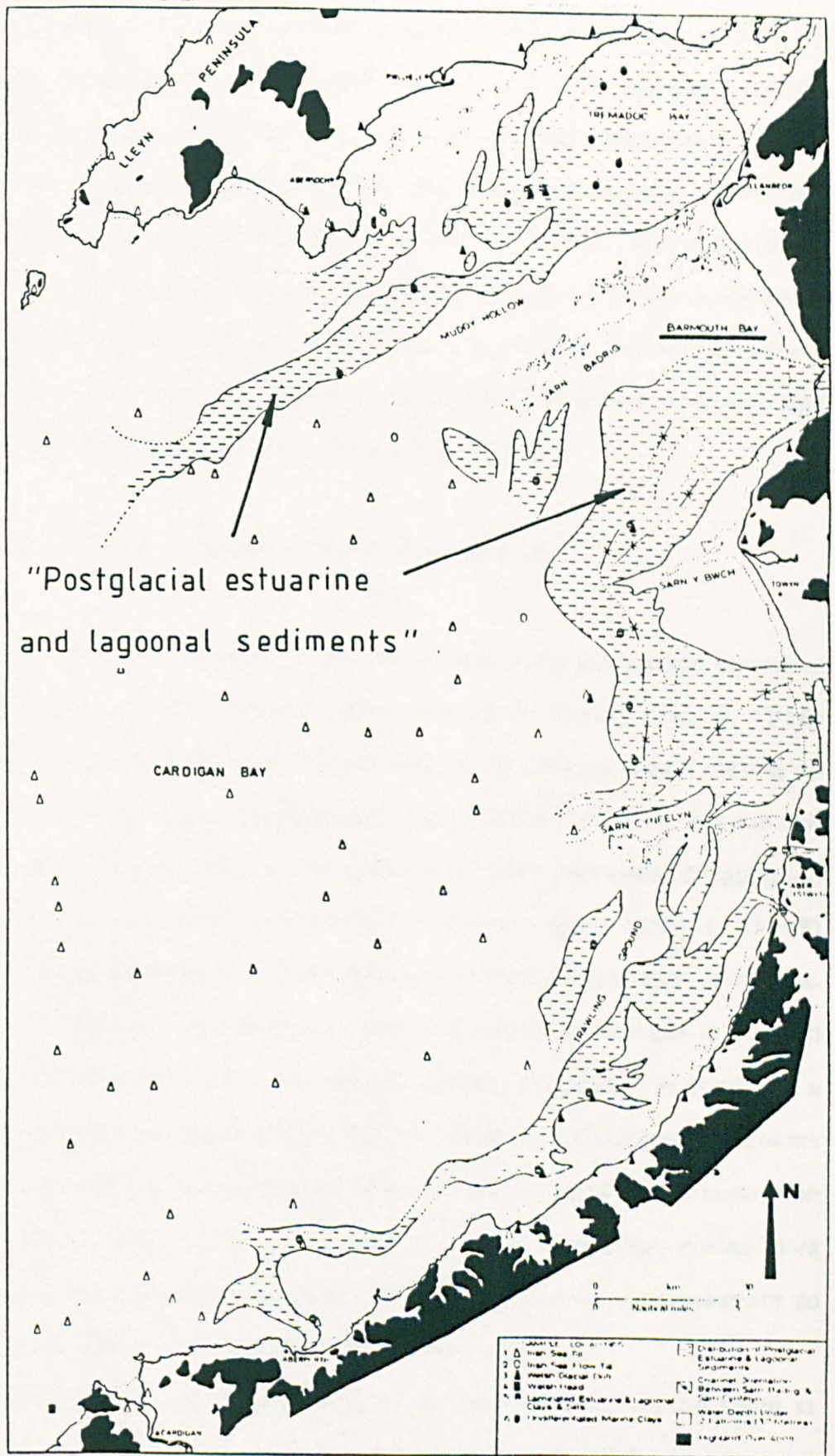


Fig.1.6

Distribution of Late Glacial/Early Flandrian sediments in Cardigan Bay.
After Garrard, 1977.

the last glaciation a major control on the nature of marginal glacial sedimentation in the Irish Sea Basin was high relative sea level, caused by crustal downwarping under the regional ice load. This created a rapidly retreating ice margin. From coastal exposures and interpreted seismic profiles, they recognised sub-glacially formed eroded topography, cut by fast-flowing ice streams (surges) associated with ice retreat. Rising sea-levels decoupled the ice sheet from the bed, allowing a glaciomarine infill stratigraphy to develop in the hollows. In shallow water, temporary stabilisation of ice margins occurred, recorded by set of large moraine ridge complexes (documented by Eyles & McCabe, 1989b).

1.3.1.8 Submerged Forests and Buried Peat Deposits

Wilks (1977) reviews the published reports of the submerged forests of Cardigan Bay and the adjacent Welsh coastline. Greenly (1919, 1928) reports ten sites on Anglesey where forests are present, some resting on boulder clay, others upon 'Scrobicularia clays', which often form the top unit of the intertidal sequence. A thin peaty clay, often containing Phragmites, lies between these clays and the overlying forest peat. McMillan (1949) found the Scrobicularia clay fauna represents sheltered, intertidal conditions. Yates (1832) was aware of the impact of possible changes in coastal geomorphology upon the preserved sedimentary sequence. In observing a submerged forest sequence along the Merioneth and Cardiganshire coasts (now parts of Gwynedd and Dyfed respectively) he noted that 'the position of its landward-bounding wall of shingle is liable to change, it may have enclosed the part which is now submarine, and it is not necessary to suppose a subsidence effected by subterranean agency'.

George (1933) recorded peat and clay units exposed on the shore at Llanaber (2km north of Barmouth). Below the beach shingle on the upper shore, and exposed lower down the beach, was a peat unit 1.7-1.8m thick, containing many Alder stools, many in a growth position. The unit was

3.95-4.25m above O.D. at its highest point. Beneath the peat was a blue-grey silty clay, 'sloping noticeably seawards'. The clay contained a 'considerable proportion' of organic matter, including vertical rootlet moulds, and the unit passed down imperceptibly into a coarser sandy deposit.

The peat consisted mainly of the remains of Phragmites and similar plants, and the clay contained a number of 'moulds of the shells of the bivalve Scrobicularia piperata in life position, and very occasional fragments of a Turritella-like gastropod'. Assessing the ecological distribution of Scrobicularia, George concluded that where there is a freshwater influx, it may occur at neap tide high water mark, or higher. He therefore speculated that 'the coast hereabouts was more sheltered during the accumulation of the Submerged Forest Series than it is at the present day', and that the relative fall of sea level resulting in Alder forest growth may have been smaller than previously thought.

George also noted that within the Mawddach Estuary at Arthog, the flats lying just above high water mark are good examples of the old land surface upon which the forest grew. There are fallen trunks and in situ tree stumps, the species represented indicative of a climate near identical to present day conditions.

Wilks (1977, 1979) discusses the stratigraphy of the extensive submerged forest under Borth Bog in the Dyfi Estuary, which has been dated at 6000-4700 years B.P.. He re-interprets the sequence in terms of the formation and development of a coastal barrier rather than a fall in sea level. At Borth, the surface of the intertidal 'Scrobicularia clay' is a few decimetres below O.D., and is overlain by a diachronous woody peat. Peat thickness, species composition and tree life-span all suggest that the forest was more developed towards the southern land margin.

Thus a clay-woody peat sequence is present near sea level in many areas of Cardigan Bay. Wilks (1979) considers that the interpretation of the causal factors for their production should incorporate a smooth, steadily rising sea

level and coastal geomorphic adjustments, rather than plausible but at present unresolvable sea level fluctuations.

1.3.1.9 Synthesis

The basic stratigraphy of the Cardigan Bay area can be summarised into a small number of sedimentary units (Garrard, 1977). In eastern Cardigan Bay, the succession is :

Recent (Holocene) - Marine sands.

Late Glacial / Early Holocene - Laminated clays and silts of marginal marine origin with locally developed peats.

Late Devensian Glaciation - Erosion of meltwater channels

Main Devensian Glaciation - Irish Sea Till terminating to the east, Welsh glacial drift terminating to the west.

Bedrock.

Lower units are found in Cardigan Bay. The Lower Irish Sea Till is considered to be pre-Devensian in age, and a deposit of an extensive ice sheet which reached the north of Devon and Cornwall, the Scilly Isles, and westwards to the southern coast of Eire. In the Cardigan Bay area, this material is only present at certain coastal sites, but in the majority of the bay the basal units are either of Irish Sea or Welsh till.

Welsh till is found in the east of Cardigan Bay, and in Tremadoc Bay. It is known to underlie the Irish Sea till along their contacts, and therefore is presumed to pre-date the Irish Sea drifts (Garrard & Dobson, 1974). The Welsh drifts occupy over four separate areas, divided by the Cardigan Bay Sarns, which are elongate mounds of Welsh-derived glacial sediment. These are now interpreted by most workers as terminal/lateral morainal complexes of each of the Welsh piedmont glaciers which fanned out from the mountains of north and mid-Cardigan Bay, prior to the arrival of the Irish Sea ice sheet. However, Wingfield (pers. comm. 1987), from seismic profiles over the Sarns, considers that the idea of a very late Weichselian glacial readvance,

producing these features, merits consideration.

Garrard (1977) considers that Welsh till remained in Tremadoc Bay only because of the sheltering effect of the Llyn Peninsula on the later southerly movement of the Irish Sea ice sheet. Further south, the sarns were truncated at their seaward end by the Irish Sea ice, which incorporated and removed Welsh morainic debris, so the sarns mark the westerly limit of outcrop of Welsh drift in the bay. Welsh drifts locally include tills, heads, varved clays and fluvioglacial outwash. From Garrard's work, the characteristics of the drifts may be summarised.

Welsh deposits :

- are more texturally immature than Irish Sea drifts;
- have a carbonate content of < 5%;
- have a sand fraction composed of mainly lithic fragments.
- Outside Tremadoc Bay the tills have gravel content of over 50%, whereas in Tremadoc Bay the till is characterised by having a rich clay matrix.

In contrast, Irish Sea tills have :

- a dark yellowish brown colour, or in the east, olive grey;
- a clay matrix forms 70-90% by weight of the total sediment, which contains up to 20% of marine sands and shell fragments;
- small and relatively few matrix-supported clasts, normally < 10% by weight. Distinctive erratics include Carboniferous limestones, Permo-Triassic sandstones, Middle Jurassic limestones (oolitic, bioclastic and hard compared to the Carboniferous), Cretaceous flints and Tertiary lignite;
- a high carbonate content (concentrated mainly in the clay fraction) of 12-27% of the total weight.

There are also differences in the seismic character of the two types of glacial drifts. Irish Sea till is typically seen as a single, acoustically

homogeneous unit, with no evidence of internal stratification except for occasional faint diffuse banding, possibly due to discontinuous bands of silt, sand or gravel. The Welsh glacial drifts are often acoustically opaque, because of their rubbly nature. Information is also limited by shallow water effects such as noise and multiple reflections.

In the nearshore areas of Cardigan Bay, both the Irish Sea and Welsh deposits are deeply incised by channels. In Tremadoc Bay these have been interpreted by Fenemore (1976) as the seaward extensions of a post-glacial drainage system feeding into a lake, dammed to the south and west by boulder clay. The lake base was interpreted as consisting of boulder clay, and was at ~80m below sea level at its deepest point. The southwest edge of the lake had a depression in it, interpreted as a possible deepened overspill channel.

The lake fill was subdivided into four acoustically defined units:

- A - a basal unit comprising sediments deposited in a (ice-dammed?) basin, possibly with remnant ice-lenses retained in the basin during sedimentation;
- B - a cross-stratified unit (dip of cross-strata ~2.5 degs.) formed by deposition of Welsh glacial outwash in the lake. This unit correlates with the sands found overlying Welsh till in the Mochras Borehole (Woodland, 1971). Its upper surface has an irregular topography, and is cut by a channel-like depression (1km long, 12m deep) - thought by Fenemore (1976) to be caused by the re-commencement of significant outwash after the short cold phase of the Loch Lomond Stadial (11-10000 yrs B.P, Lowe & Walker, 1984). This outwash increase may also have deepened the overspill channel, causing the lake to drain and subaerial erosion of the sand unit to occur. Using the ideas of Eyles & McCabe (1989a), this channel may now be interpreted in terms of the subglacial cutting of tunnel valleys;
- C - a unit containing some low-angle reflectors, and many minor reflectors. It is of ~5-10m thickness throughout, i.e. does not infill the channel structure in the top of unit B;

D - also with many minor internal reflectors, and thickens from 8m to ~30m towards the centre of the basin. Together with C, this is interpreted as the products of marine transgression into the post-glacial basin. Discontinuities are thought to be related to fluctuations in the trend of rising sea level. However, it is not clear what processes caused the topography of unit C to parallel that of the channelled unit B. Unit D would represent the glaciomarine infill stratigraphy of Eyles & McCabe (1989a).

One conclusion to be drawn from Fenimore's (1976) ideas is that for the lake to drain completely, the sea level at the time must have been lower than the elevation of the lowest part of unit B, i.e. 53m below O.D.. From the eustatic sea level curve of Fairbridge (1961), this would suggest that lake drainage occurred before ~12500 yrs ago, and from the curve of Jelgersma (1966) before 11500 yrs. BP and that unit C is younger than that. Fenimore's (1976) work suggests erosion of unit B at ~10000-10500 yrs.BP. Unfortunately, more recent sea-level curves which relate to the Welsh coastline (Devoy, 1977) do not extend beyond 9000 yrs.BP (before present) and 29m below O.D.. There is also current debate on the relative stability of the western British Isles during the Quaternary (Eyles & McCabe, 1989b). The evidence suggests the possibility that the lake did not drain completely, remaining partially-filled with seawater, and/or that the channel was eroded to well below sea-level. The latter case, with erosion by ice or by large volumes of poorly-sorted and coarse-grained debris, would be implied by Eyles & McCabe's (1989a) model.

In Barmouth Bay, ice-retreat may also have been associated with the production of sub-glacially cut tunnel valleys. The NE-SW elongate enclosed hollow, described by Garrard (1977), contains over 120m of sediment fill and may represent such a feature. The glaciomarine sediments may be similar in Barmouth Bay to those found by Haynes et al (1977) further south, i.e. showing an upwards-increasing marine influence. The lower sediments were likely to have been deposited by a combination of sediment gravity flows,

mud from suspended sediment plumes, and ice-rafted debris. These deposits would have passed upwards into estuarine deposits. Closer to shore, possibly in lagoonal environments enclosed by morainic banks, fine-grained material accumulated, possibly with some peat and forest development in the shallower areas.

With continued relative sea-level rise, the morainic material will have been eroded by the advancing surf zone, and coastal shingle barriers formed, behind which forests grew (Wilks, 1977,79). Further marine influence caused increased barrier size, and more sheltered estuarine conditions were formed in the flooded glacial valleys.

1.4 Sediment Transport in northern Cardigan Bay

1.4.1 Regional Evidence - A Review

A study of the sea-bed sediments of the South Irish Sea by Dobson, Evans and James (1971) included Cardigan Bay. They found that Cardigan Bay has restricted sandy sub-littoral zones, and diverse broad offshore areas, separated by a belt of exposed gravel. The inner zones are characterised by sand pools of low relief, which they considered to be merged sand patches. The sand pools become discontinuous further offshore, and are replaced by isolated sand patches and sand ribbons, above the gravel layer. The mineralogy of the Cardigan Bay sediments implies a source entirely of local origin, especially around the sarns.

In the north of Cardigan Bay sand patches are common; these are compared to a predominance in the south of sand ribbons. They related this trend to the northerly increase in the rotary nature of the tidal currents. They considered wave activity to be significant, in terms of sediment transport in the south Irish Sea; wave-induced current speeds are increased by 0.25m/s during bad weather in the south of the area (14 days/yr.) and by 0.5m/s during storms (2 days/yr.) (Draper, 1967).

Conclusions regarding sediment transport are :

- 1 - there is a nearshore zone of fine-medium sands with a net landward transport vector
- 2 - currents are sufficient to create bedforms indicative of high sediment transport rates, such as sandwaves and, where there is lower sand supply, sand ribbons.

1.4.2 Local Evidence - A Review

Historical Information

The town of Barmouth stands on a narrow coastal flat approximately 300m wide. Although no authentic records exist, it seems that erosion has taken place at the south end of the town for a very long time (Steers, 1948). A print dated 1748 (Fig. 1.7) published in Lloyd (1974), and held at

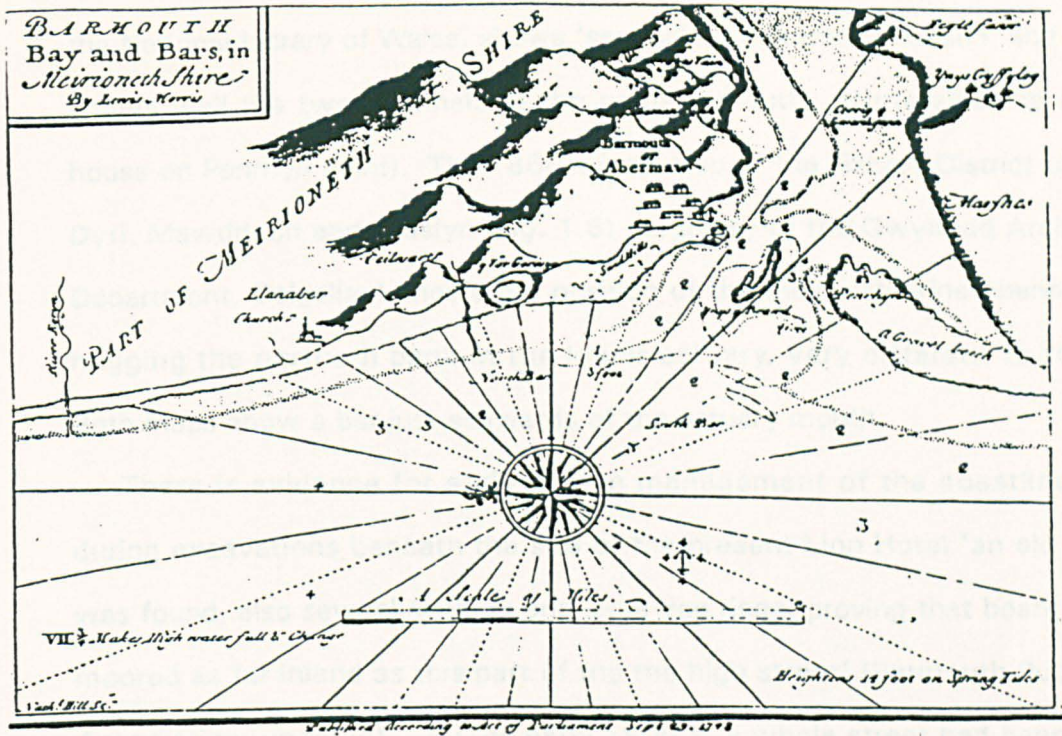


Fig. 1.7 Print of Barmouth Bay and Bars, dated 1748. (After Lloyd, 1974).



Fig. 1.8 Part of the one-inch map of the Fishery District of the Dyfi, Mawddach and Glasyn, dated 1866. (Courtesy of the Gwynedd Archives Service, Dolgellau).

the National Library of Wales, shows 'sandhills' on Barmouth beach, and also shows well the two channels at the estuary mouth. (Note also the ferry house on Penrhyn Point). The 1866 1 inch map of the Fishery District of the Dyfi, Mawddach and Glaslyn (Fig. 1.8) (courtesy of the Gwynedd Archives Department, Dolgellau) shows the position of the main estuarine channel as hugging the northern bank in the lower estuary, very different to today. Both maps show a bar just seawards of the estuary mouth.

There is evidence for early human management of the coastline, as during excavations beneath the site of the present Lion Hotel 'an old quay was found, also several anchors and large iron rings, proving that boats were moored as far inland as this part of the the high street' (Barmouth Publicity Association, undated). 'By the early 1800's, a whole street had been built on the flat sands, with shops, houses and hotels. The street, however, was still a bed of sand'. Around the year 1800, the present Barmouth Quay was constructed, at a cost of 1600 pounds (Morgan, 1948).

The dangerous nature of the estuary mouth for mariners prompted two attempts to build a lighthouse on Ynys-y-Brawd (Fig. 1.2), in 1839 and 1843. However, storms demolished the foundation walls (Barmouth Publicity Association, undated). Barmouth promenade, which protects over 2km of the shore north from Barmouth harbour, was opened in 1933. Tidal currents of over 8 knots (A.R.Allan [Posford Duvivier], 1988, pers. comm.) maintained a channel into the harbour from the north of Ynys-y-Brawd, and for both bathing safety reasons and as protection for the harbour, particularly from dangerous cross currents, a barrage linking the mainland with Ynys-y-Brawd was built in 1972/3, closing the northern channel and forcing the Mawddach to enter the sea over the bar.

There is much local speculation, though no actual data, that this barrage is responsible for high sedimentation rates within the estuary. The barrage has allegedly caused an increased duration of high water in the estuary (no data exists to confirm or deny this), because of the lower channel area

through which the ebb tide flows. This is held to increase the amount of sediment settling out of suspension at high water, and therefore increase siltation in the estuary (see below). Another possible cause is the increased quantity of the pioneer species Spartina over the last few decades. Steers (1948) states that 'on the bare mudflats near Barmouth Junction are 3 patches of Spartina townsendii'. Whether they were natural migrants or artificially introduced is unknown. Today Spartina is widespread on the lower and mid-estuary mudflats, such as behind Ro Wen, and particularly along the wide mudflats of the southern flank of the estuary between Fegla Fach and the mid-estuary constriction, Farchynys. There is also local speculation that the presence of the barrage has further increased the Spartina colonisation by raising the average salinity of the estuary, particularly in the mid-reaches. Unfortunately, no data is available.

Steers (1948, 1969)

Steers (1948, 1969) includes a discussion of sediment transport processes in the coastal zone in the Barmouth area. The largest single feature of the coastline is Ro Wen, a typical coarse pebble storm beach, with several minor recurved ridges near its northern end. Like the spit of the Dyfi estuary, it is set back from the general trend of the coast, and extends due north from its southern attachment with the coast. Ro Wen indicates a northerly transport of pebbles along the shore, driven by wave action. At Llwyngwriil (G.R. 59200950) there is a large gravel fan, 300m wide and > 1km long, which supplies shingle to the beach and presumably has contributed to the formation and/or maintenance of Ro Wen. Whether there are other sources of coarse sediment today, or were other significant sources in earlier stages of barrier development is unclear from this initial appraisal of the present coastal morphology. This aspect will be considered later.

Clearly, waves which are capable of transporting pebbles and cobbles would be capable of producing very large rates of sand transport, so the presence of the shingle spit is an indication of much potential active sand

transport in the coastal zone. Wind is also an agent of sand transport, not only via the waves it produces, but as a primary transport medium. Simple aeolian dunes occur on the north of Ro Wen, much eroded and patchy due to human activity. Sediment is blown mostly into the estuary by the prevailing westerly wind regime.

Caston (1965)

There have been very few scientific publications relevant to sediment transport within Barmouth Bay and the Mawddach estuary. Caston (1965) described a detailed echo-sounding survey of marine sandwaves in the southeastern corner of Tremadoc Bay, north of Barmouth Bay, and separated from it by Sarn Badrig. The sandwaves had typical wavelengths of 650-950m, and heights of 0.6-2m, though were up to 3 or 4m high in places. Occasional large ripples or megaripples were found superimposed on the large sandwaves. Sandwave asymmetry indicated mass sediment transport to the southeast, and inferred net water and sediment transport through the Mochras Channel (between Sarn Badrig and the mainland) and southwards into northern Barmouth Bay. Active erosion of the Mochras Channel by the sand-laden water was inferred. It was suggested that this transport pathway was caused by water 'ponded-up' in eastern Tremadoc Bay at high water by strong westerly or southwesterly winds, which could escape through the channel to the southeast. Spring tides would produce the largest 'overflow' effect and therefore greatest volumes of sediment transport. Caston's (1965) study therefore provides evidence for a possible source of sediment from the north of Barmouth Bay.

Moore (1968)

Moore (1968) presented a detailed study of the sediments of the central coastal portion of Cardigan Bay (between Harlech and Aberystwyth) bounded by Sarn Badrig in the north and Sarn Wallog in the south. He thus covered

an area approximately 36km long and 20km wide. With a database of 262 sediment samples he discussed in depth the sediment mineralogy, and inferred sediment transport pathways within the area by charting the dispersal patterns of various grain types (i.e. minerals). He inferred local coastal sediment sources as most important, and specified four sites :

1 - low glacial cliffs at Tywyn

2 - the shingle fan at Llwyngwriil, north of Sarn Bwch

3 - north of Sarn Badrig, i.e. from Tremadoc Bay through the Mochras Channel

4 - from deeper water west of the area.

Both the rivers Dyfi and Mawddach were found not to be active suppliers of sediment to Cardigan Bay, most bay sands were derived from coastal erosion sites, and Moore inferred that the estuaries were being infilled from the sea.

Moore considered that the distribution patterns of elements of accessory minerals defined zones of (strongest) tidal currents, which in Barmouth Bay were implied to be near the coast off Tywyn, and along the coast between Barmouth and the Mochras Channel. Strong currents were also inferred from the Mochras Channel southwestwards for over 15km in central Barmouth Bay. Moore proposed that the distribution patterns of elements of the aluminosilicate minerals largely indicated the locations of eroding coastal exposures supplying detritus to the bay.

Assuming that a positive dispersal vector is indicated by a decrease in the concentration of each grain type in a sample, Moore constructed a chart showing the implied dispersal vectors for different grain types (Fig. 1.9). This indicates a broad anticlockwise circulation of sediment within the bay. Inshore, net transport is northwards, but offshore the transport vectors have both southwards and seaward components, and the offshore area was considered a very active transport zone. Between approximately 3 and 7km west of the estuary mouth there is an area which has no marked

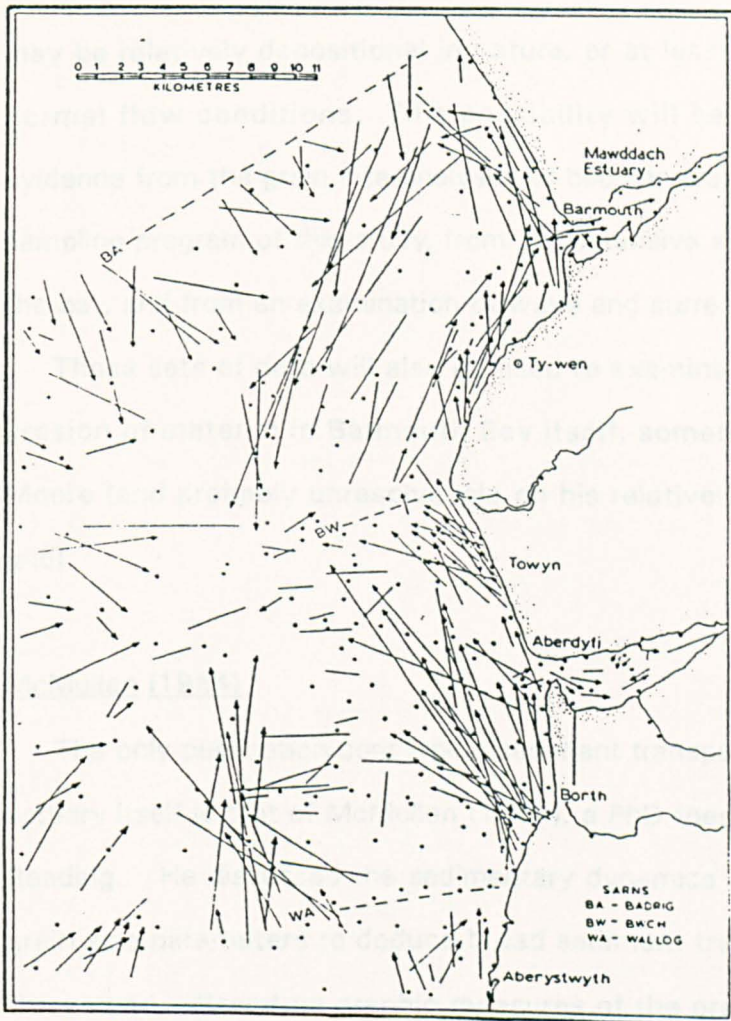


FIG. 33. Chart showing dispersal vectors for each of the petrographically determined grain types.

Fig. 1.9 Chart showing dispersal vectors for each of the petrologically determined grain types (After Moore, 1968).

compositional gradients across it. Thus a possible inference is that this area may be relatively depositional in nature, or at least relatively stable under normal flow conditions. This possibility will be discussed later using evidence from the grain size analyses of bed samples from the more detailed sampling program of this study, from the extensive side scan sonar survey of the bay, and from an examination of wave and current parameters.

These sets of data will also be used to examine whether there is active erosion of material in Barmouth Bay itself, something not considered by Moore (and probably unresolvable on his relatively widely-spaced sample grid).

McMullen (1964)

The only publication concerning sediment transport within the Mawddach estuary itself is that of McMullen (1964), a PhD thesis from the University of Reading. He discussed the sedimentary dynamics of the estuary, and used grain size parameters to deduce broad sediment transport pathways within the estuary. Based on graphic measures of the grain size distributions, he also delineated three subenvironments within the estuary, erosional, near-equilibrium and depositional. Combining data on the heavy mineral content of the sediments with the grain size data, he deduced (as did Moore, see above) that the long term net transport direction was into the estuary from the bay.

1.5 Sub-Bottom Data Within the Estuary

There have been a small number of published reports concerned with the nature and structure of the material beneath today's estuary bed. Synthesis of the presented data can add greatly in the reconstruction of Postglacial sedimentary environments.

1.5.1 The Estuary Mouth - Rail Bridge Section

In 1980, British Rail employed Wimpey Laboratories Ltd. to conduct a seismic refraction survey adjacent to the Barmouth rail bridge. This was to determine depth to bedrock and obtain information about the unconsolidated sediment sequence. The results were presented in a report published by British Rail (British Railways Board, B.R.B., 1980). Associated borehole data was also obtained by Wimpey, to confirm the geophysical findings. A geotechnical report (B.R.B., 1982) was written to collate previous information and the new findings.

A sedimentological interpretation of the data is presented in Fig. 1.10, in a cross section drawn along a line parallel to the bridge. Unfortunately, all samples taken during the surveys have since been discarded, so no examination of them by the author was possible. Hence, the correlations and interpretations are tentative. The 'seismic refractor' identified by Wimpey at depths up to 10m was interpreted by them as the boundary of loose sediment saturated with water.

The refraction survey showed 3 layers :

- 1 - The lowest layer (seismic velocity $V_p > 4000\text{m/s}$) proved to be Cambrian micaceous siltstones and sandstones.
- 2 - The intermediate layer ($V_p 1500\text{m/s}$) was interpreted as waterlogged unconsolidated sediments, mainly sand.
- 3 - A surface layer ($V_p 1200\text{m/s}$) was present for 300m in the northern part of the section, and was interpreted as loose pebbly sand.

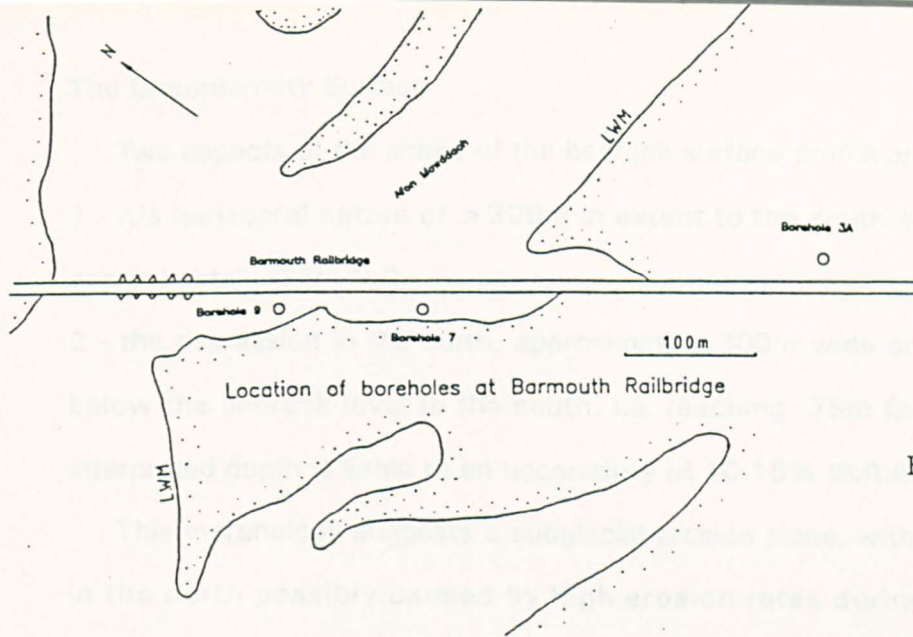
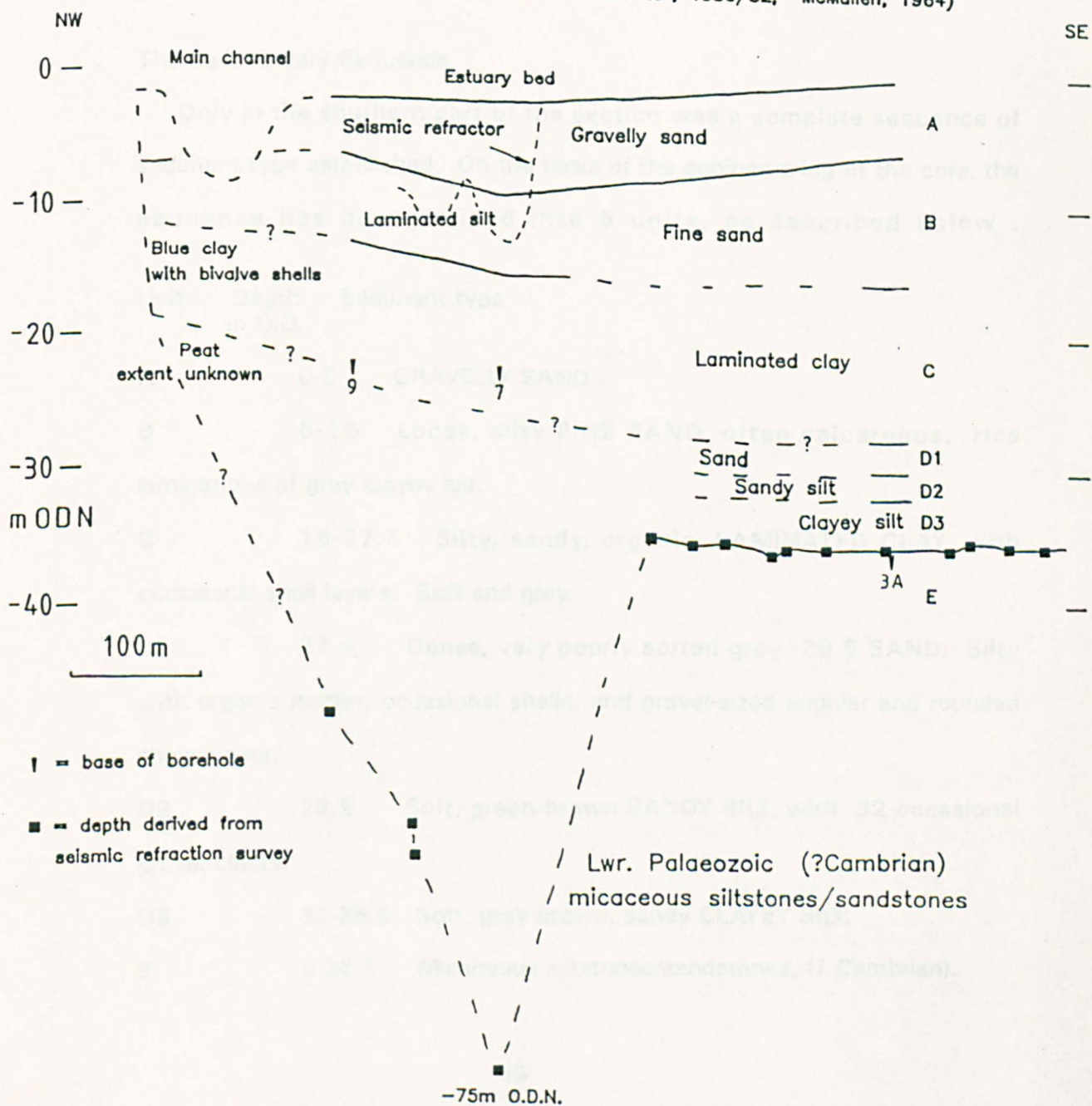


Fig. 1.10

Stratigraphy beneath Barmouth Railbridge

(Sources : British Rail, 1980/82; McMullen, 1964)



The Unconformity Surface

Two aspects of the shape of the bedrock surface profile are striking :

1 - it's horizontal nature of > 300m in extent to the south of the profile, at approximately -35m O.D.

2 - the depression in the north, approximately 300m wide and at least 40m below the bedrock level to the south, i.e. reaching -75m O.D. The quoted interpreted depth is liable to an uncertainty of 10-15% (B.R.B., 1980).

This morphology suggests a subglacial erosion plane, with overdeepening in the north possibly caused by high erosion rates during ice wastage. Erosion may have been locally enhanced by faults within the Lower Palaeozoic bedrock.

The Sedimentary Sequence

Only in the southern part of the section was a complete sequence of sediment type established. On the basis of the engineers log of the core, the sequence has been divided into 5 units, as described below :

Unit	Depth m O.D.	Sediment type
A	0-6	GRAVELLY SAND
B	6-16	Loose, silty FINE SAND, often calcareous. Has laminations of grey clayey silt.
C	16-27.5	Silty, sandy, organic, LAMINATED CLAY, with occasional shell layers. Soft and grey.
D	1 27.5	Dense, very poorly sorted grey -29.5 SAND. Silty with organic matter, occasional shells, and gravel-sized angular and rounded shale clasts.
D2	29.5	Soft, green-brown SANDY SILT, with -32 occasional gravel clasts.
D3	32-35.5	Soft, grey-brown, sandy CLAYEY SILT.
E	> 35.5	Micaceous siltstones/sandstones, (? Cambrian).

The sequence found at the north shore of the estuary has units A, B and C, below which is a peat layer of unknown extent (Conybeare, 1870). However, Miller (1946) describes the succession found when the bridge foundations were reconstructed in about 1900, and does not mention the peat bed, which apparently lies within a 'clayey mud' layer.

Interpretation

There are obvious problems in interpreting and correlating units from engineers descriptions of sediment type, and particularly from old publications. Taking into account the spatial variation in deposits, found in this and other alluvial and coastal environments, a first-order interpretation of the sequence is presented below.

Unit A - This is interpreted as material deposited in modern strongly tidal estuarine conditions, formed during migration, abandonment and infilling of of tidal channels in the lower estuary. There is much verbal evidence from local people that less than 10 years ago a substantial navigable tidal channel existed under the southern end of the rail bridge. Like today's main channel and the intertidal zone around the bridge, this channel would have been megarippled, and it is likely that the whole of unit A contains complex trough cross- stratification, i.e. a suite of channel fills with megaripple cross-beds within them.

Unit B - This unit is dominantly fine-grained, with laminae of silt and a calcareous content, and is tentatively interpreted as the deposits of tidal flats. The silt 'laminae' could represent deposition at neap tides of one (or a suite of) slack water fine sediment drapes, possibly enhanced by high suspended sediment concentrations in high land runoff. The calcareous matter is most likely to be shells, perhaps concentrated into layers as lag deposits during storms, or deposited in creek bottoms. It would originate from either within the estuary or from the immediate shallow shelf of

Barmouth Bay.

Unit C - The soft, organic, very fine grained nature of this unit suggests lower energy conditions of deposition with lower sediment transport rates. Possibilities include a partially-vegetated mudflat or saltmarsh environments. The laminated nature and shell layers are often observable in eroding saltmarshes of the present-day estuary, and respectively represent periodic low energy inundation, and more random high energy lag deposits or basal tidal creek markers. The 'peat' unit, below unit C at the north shore, cannot be placed into any sedimentary environment with any certainty, but does strongly suggest supratidal conditions.

Unit D - This unit was only penetrated in one core, so the following interpretations have a greater degree of uncertainty.

Unit D1 - This 2m thick unit is not easy to assign to a particular coastal or glacial depositional environment, especially considering the limited sedimentological data and the poor vertical resolution. It possibly represents a combination of saltmarsh and channel deposition, possibly a large tidal creek, which might explain the presence of the gravel-sized shale clasts. It could also be alluvial in origin, but the presence of shells (of assumed estuarine or marine origin) would tend to negate such an interpretation.

Units D2 and D3 - From the limited data available, they could be products of a similar depositional environment as unit D1, but the lack of shells increases the possibility of an alluvial interpretation.

The sequence as a whole is tentatively interpreted as consisting of sediments deposited under an increasing marine influence. The dominant source of the sediment is considered to be from reworking of glacial and glaciomarine sediments further seaward, though some fine sediment may have been derived from the land. There is insufficient evidence to deduce a relationship between the development of Ro Wen and the facies deposited behind it. Wilks (1977,79) suggested barrier growth enhanced

sedimentation rates behind the barrier at the Dyfi estuary. Sea levels of -35m occurred at ~ 10500yrs. BP (Jelgersma, 1966), however, with the errors involved in deducing sea-level curves, and particularly with the lack of data in Cardigan Bay, no deductions regarding the relative rates of sedimentation and sea-level rise above -35m O.D. can be made.

1.5.2 Boreholes east of Ro Wen

As part of initial survey work for a proposed marina development, four 7m deep boreholes were drilled in the intertidal zone behind the shingle spit Ro Wen (Fig. 1.11). The results were presented in Chettleburgh (1986). Boreholes 1,2 and 3 proved at least 7m of fine sand with some shell fragments, and borehole 4 at Penrhyn Point found 3.8m of sandy gravel overlying fine sand. The gravel represents a lag deposit in the very high tidal energy regime of this immediate area (see Chapter 2), and the fine sand is interpreted as having been deposited under conditions similar to the back-barrier intertidal flats of today.

Bulk sediment samples were kindly made available by the contractors, and sample grain size distributions have been measured using the same methods as for other samples taken for this study. Their grain size distributions and mineralogy shows no significant differences with the surface sediments of the area.

1.5.3 Boreholes at Pont Glandwr

In 1967, 3 boreholes were sunk down to -4m O.D. in relation to a roadbridge construction at Glandwr on the northern estuary bank (G.R. 63501730). The logs were kindly made available by the British Geological Survey at Aberystwyth, and here have been interpreted in a cross section (Fig. 1.12).

The section shows that the sedimentary sequence is capped by a peat/silt unit of up to 4.5m thick, extending down to below -3m O.D., which is interpreted as being estuarine saltmarsh deposits. This is underlain by a

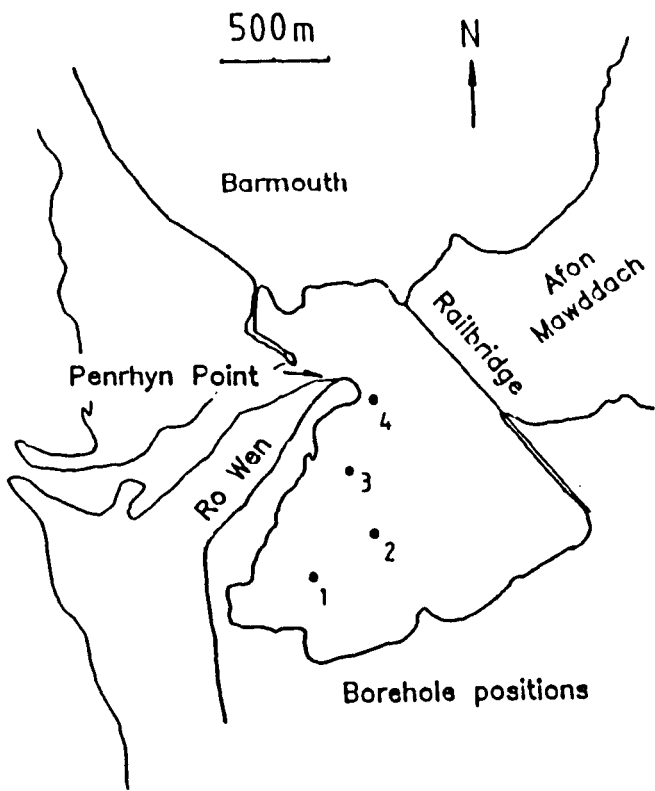
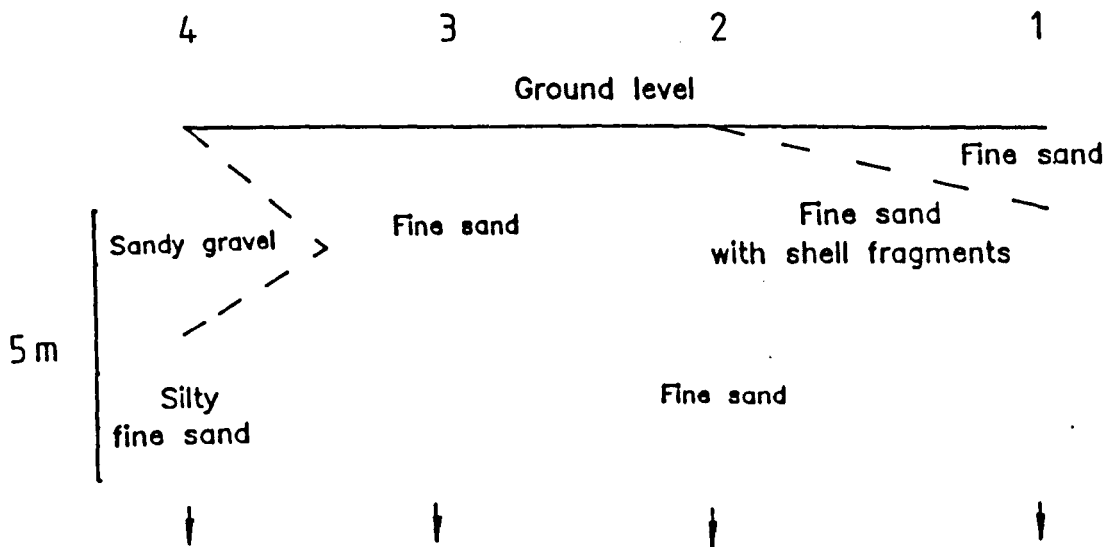


Fig. 1.11 Borehole data east of Ro Wen.
(Data of Chettleburgh, 1988).



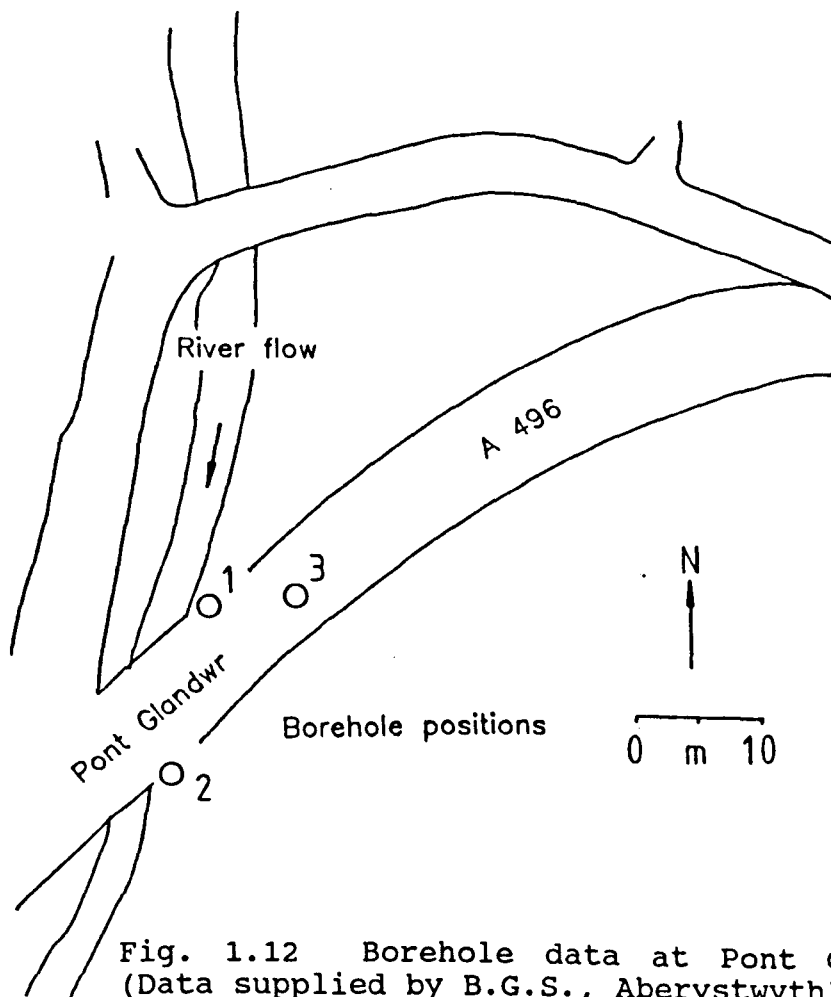
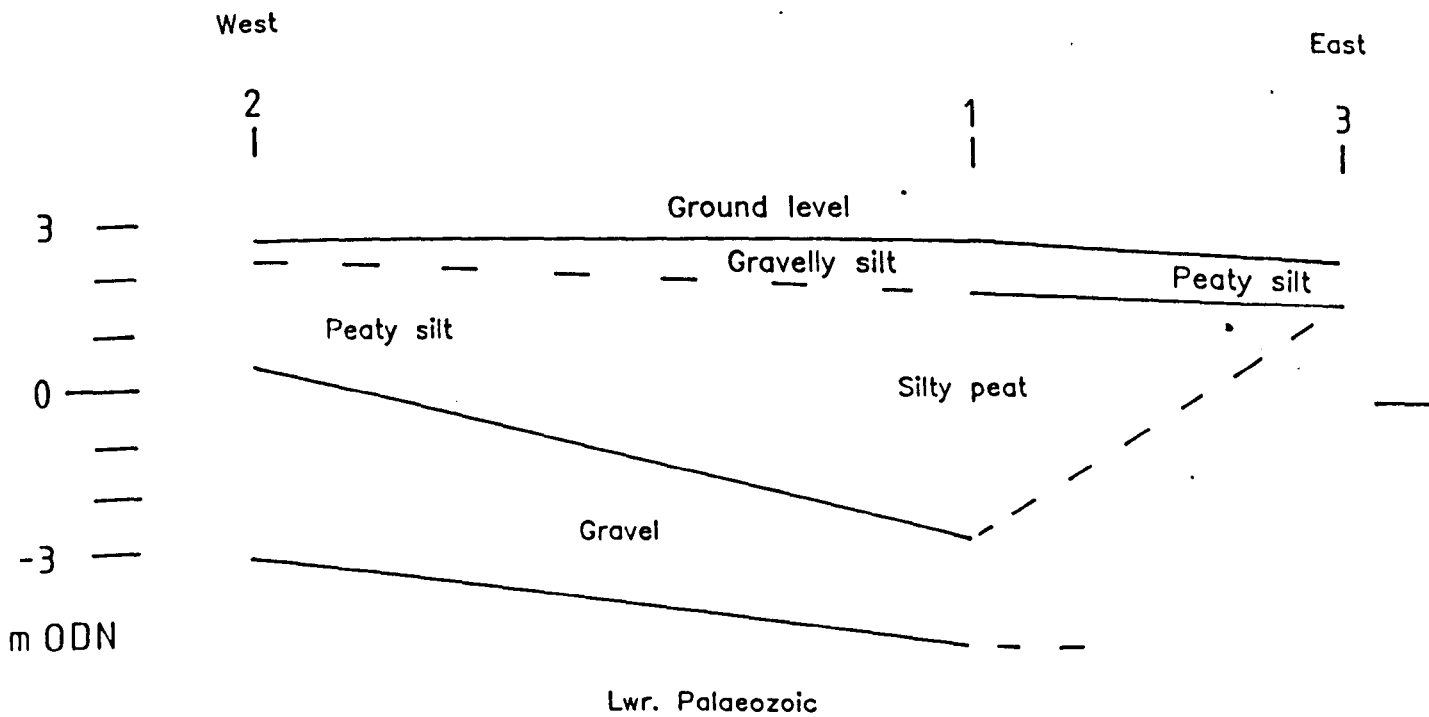


Fig. 1.12 Borehole data at Pont Glandwr.
 (Data supplied by B.G.S., Aberystwyth).



unit containing gravel-sized shale fragments, which reaches +1.8m O.D. at borehole 3, and which is interpreted as being essentially fluvial, eroded from the underlying shales of the Maentwrog Formation and deposited locally by the Afon Glandwr.

1.5.4 The Estuary Head - Llanelltyd Section

In 1970, a total of 61 shell and auger boreholes were drilled at the estuary head between Dolgellau and Llanelltyd, in relation to the building of the Dolgellau by-pass and the bridge over the river Mawddach for the A470 trunk road. The B.G.S at Aberystwyth also made the borehole logs available, and as in the above examples, from the engineers' soil descriptions a sedimentological interpretation of the data has been made (Fig. 1.13 and Enclosure 1). On Fig. 1.13, the figures at the side and bottom of the map are shortened grid references.

The section across the Mawddach clearly shows a sandy gravel channel body, over 120m wide and 7m thick, either side of which are finer grained and more organic deposits. The present day river is bounded by well-developed levees, best defined on the northern side, and composed of organic silty or sandy clay, the 'Upper Clay'. Below the topsoil, there is a clay rich brown bed, on average 0.8m thick. Close to the river channel, it overlies a grey clay which grades laterally away from the river axis into a peat.

Next down the sequence is another fine-grained unit, which is up to 3 or 4m thick adjacent to the channel body and thins to below 0.5m thick at 200m north and 300m south. Underlying the predominantly fine-grained sequence is a thick sandy gravel unit, which at borehole 10 was proved at -36m O.D. to be overlying a slightly metamorphosed mudstone, containing pyrite and mica.

A number of notes of organic clasts were taken by the engineers describing the sequence, such as 'decayed timber' or 'enclosures of peat';

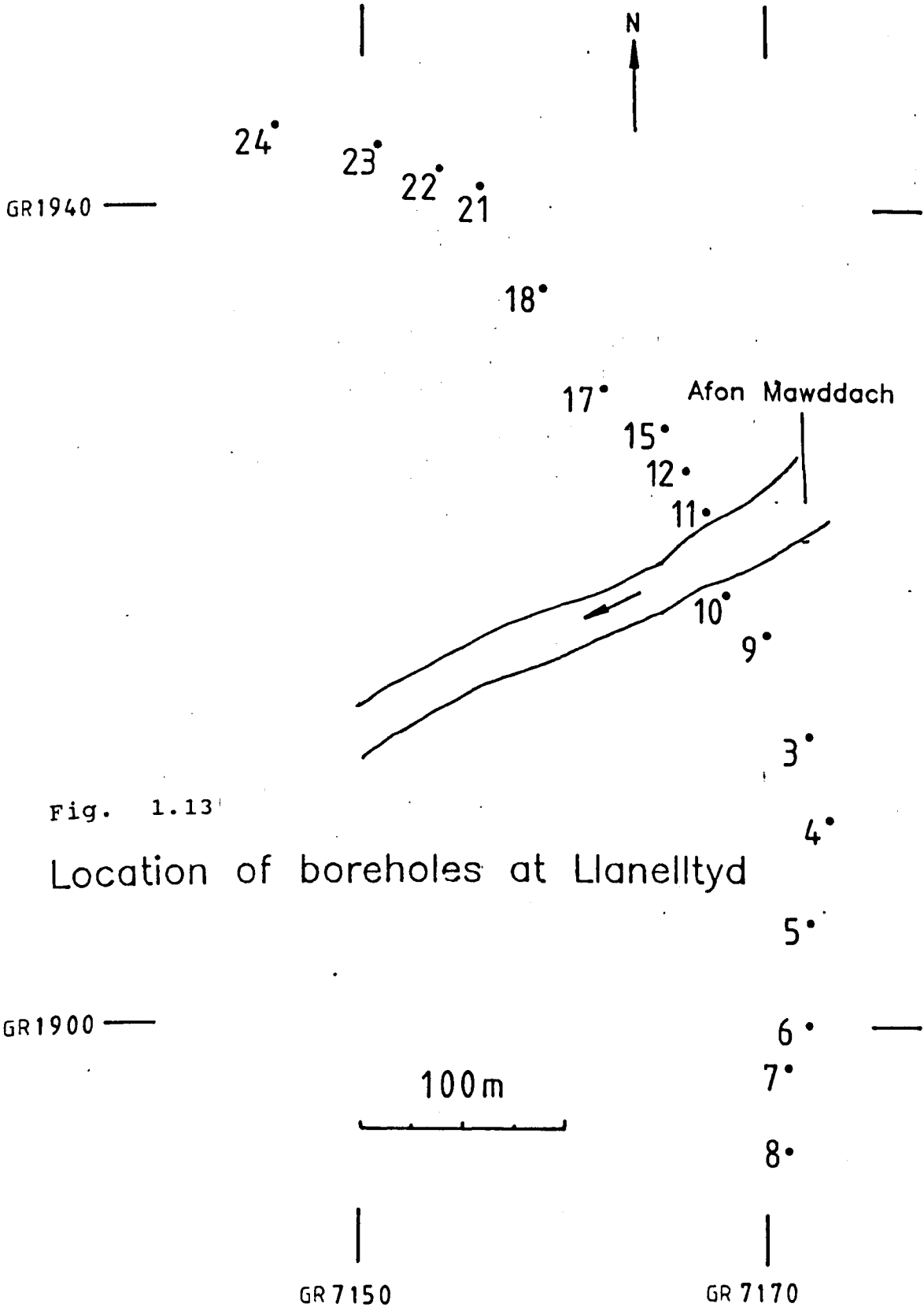


Fig. 1.13

Location of boreholes at Llanelltyd

unfortunately no material samples remain, all having since been discarded. As with the above interpretations and for the same reasons, the deductions made below are tentative.

Interpretation

Upper Clay - This is interpreted as a deposit of an alluvial floodplain, and it is considered that conditions now are near-identical to those of its deposition. It is unknown whether the clay is derived from marine or land sources.

Peat - The presence of this unit suggests deposition in a continuously wet marshy area rather than a periodically drying one, and therefore points to a deposit with a lower relative elevation to the groundwater level. The occurrence beneath of a (relatively impermeable) clay would probably have increased water table elevation across the floodplain.

Lower Clay - It is likely this was deposited on an alluvial floodplain similar to today's, although because of its relatively low elevation it is possible that a greater estuarine influence was present. There is a great similarity between the lithological gradation from silty clay to sandy gravel in the 'present day' Upper Clay deposits and the older Lower Clay sediments.

Upper Gravel - This is interpreted as the coarse-grained clastic body deposited by the 'proto-Mawddach' at its base and the present river at its top. It is certainly alluvial at the top but lower down may represent either pure alluvial or estuarine-influenced environments, depending on the relationship of sedimentation rate, sea level and coastal and estuarine morphology.

Lower Gravel - Allen & Jackson (1985) describe these thick deposits as 'alluvium', but this seems a simplification for the sake of brevity rather than a considered interpretation. There is no other data on these sediments known to the author, but possible environments of deposition for the gravel body should include glacially-related environments, such as subglacial channels or proglacial outwash fans.

It is interesting to consider the reason for the presence of the 'peat' unit. As mentioned above the underlying clay may have contributed to its formation by maintaining a high water table, but a reason is needed to explain why there was a period of organic- dominated deposition between apparently alluvial floodplain deposits. One possibility is sea-level. If part of the channel sand body is estuarine, then it is possible that the peat layer represents a stable period of sea-level, where sedimentation rates decreased and the estuarine margins developed into peat beds.

A further option in explaining the peat is that the sand body is glaciofluvial, and that the lower clay unit represents deposition by glacial outwash containing high concentrations of suspended sediment. During or subsequent to the post-glacial melt episode, the glacial basin (either local or extending along the valley) filled, and conditions allowed peat formation. At this point there are alternative explanations for the deposition of the Upper Clay. Either a rising sea- level brought fine sediment into the estuary from erosion of offshore glacial deposits, depositing clay above the peat, or the main channel decreased in size due to lower discharges after the melt event; thus overbank events in the river system may have become more common, and the clay represents accumulation from these flood events. This second possibility does not require any of the deposits to be estuarine in nature.

1.6 Offshore Boreholes

There are some vibrocore, gravity core and grab sample data held at B.G.S. Aberystwyth which is relevant to the Barmouth Bay area. Borehole numbers 52-05-47, -48, -133 and -148 are of most interest. Their positions and the logs respectively, are shown in Figs. 1.14a & b.

1.6.1 Boreholes 47 and 133

These were taken in 1971, close to each other at 52 deg. 39 min. N, 5 deg. 13 min. W, in 17m of water. Borehole 47 encountered Tertiary sediments at 55m below sea bed. Borehole 133 terminated within Holocene sediments at 70m below sea bed, and proved a (gravel and) sand dominated sequence, including, at 14m below bed 'sand, coarse with pebbles and lumps of brown clay', a 6m shelly sand unit at 44m below sea bed, and at 63m depth a unit of at least 7m thick of sandy gravel, with cobbles of Lower Palaeozoic origin. Microfauna within Lignite fragments at 60m below sea bed indicated a Holocene age and a marine environment.

1.6.2 Borehole 48

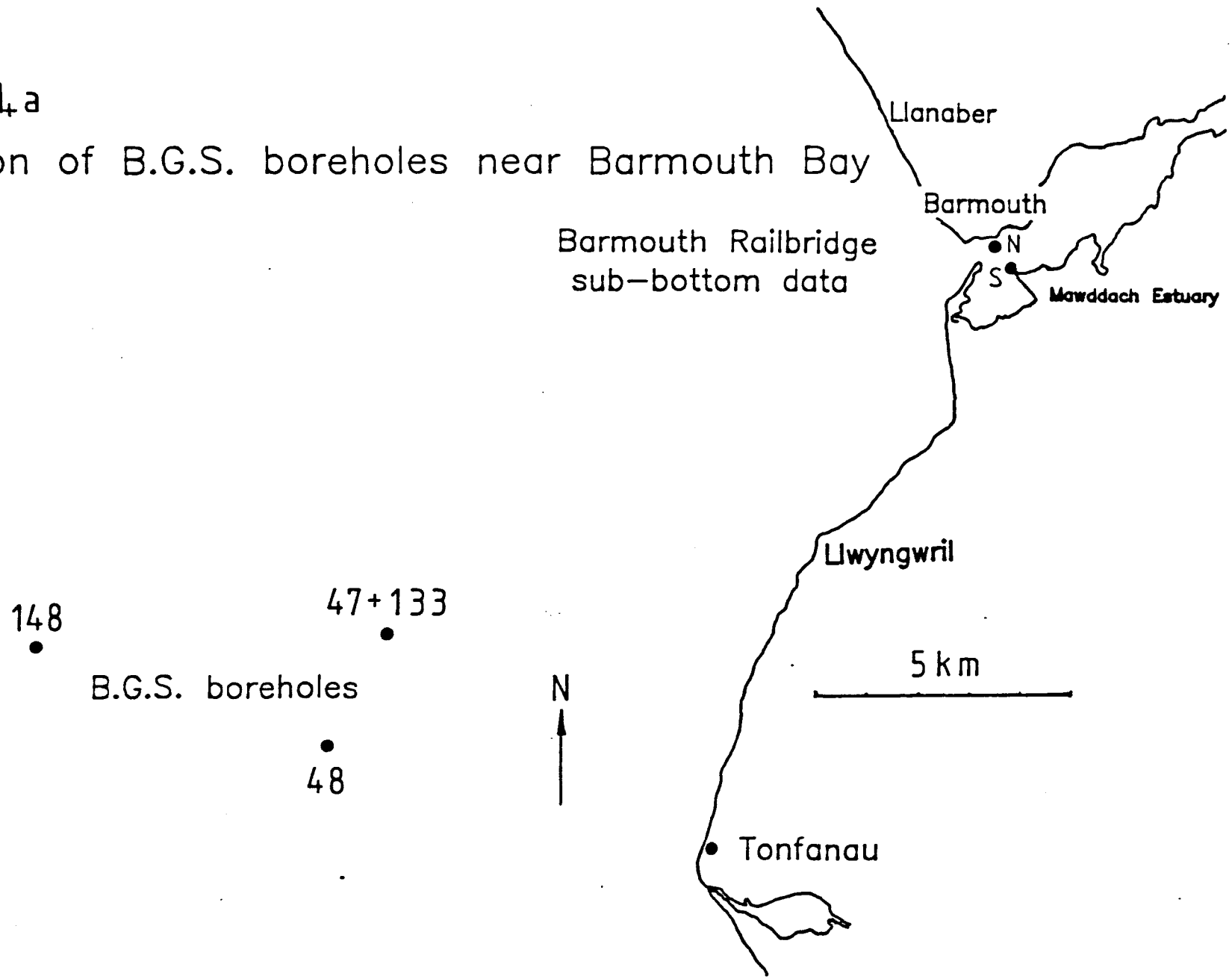
This was drilled (in 1974) in 20m of water, and reached Middle Jurassic limestone at 43m below sea bed. The overlying Quaternary sequence contains 22.5m of boulder clay at its base, above which is 1m of clayey peat (undated), 11.5m of a fining-up sand unit, and 7.7m of a sulphide rich grey clay. The sea bed is comprised of a sand and gravel lag. Microplankton analysis of a sample of the grey clay at 4m depth gave a Holocene age.

1.6.3 Borehole 148

This was drilled in 1974 in 27m of water, reaching a Tertiary rockhead at 30m below sea bed. The Quaternary succession includes lignitic sand at a depth of 20-28m. Above it are three clay units, with sand interbeds. The lower clay, at 20m depth, is pebbly, and the upper unit contains peat and is overlain by a pebbly sand lag forming the sea bed.

Fig. 114a

Position of B.G.S. boreholes near Barmouth Bay



Barmouth Railbridge
sub-bottom data

148

47+133

B.G.S. boreholes

48

N

5 km

Tonfanau

Llwyngwriil

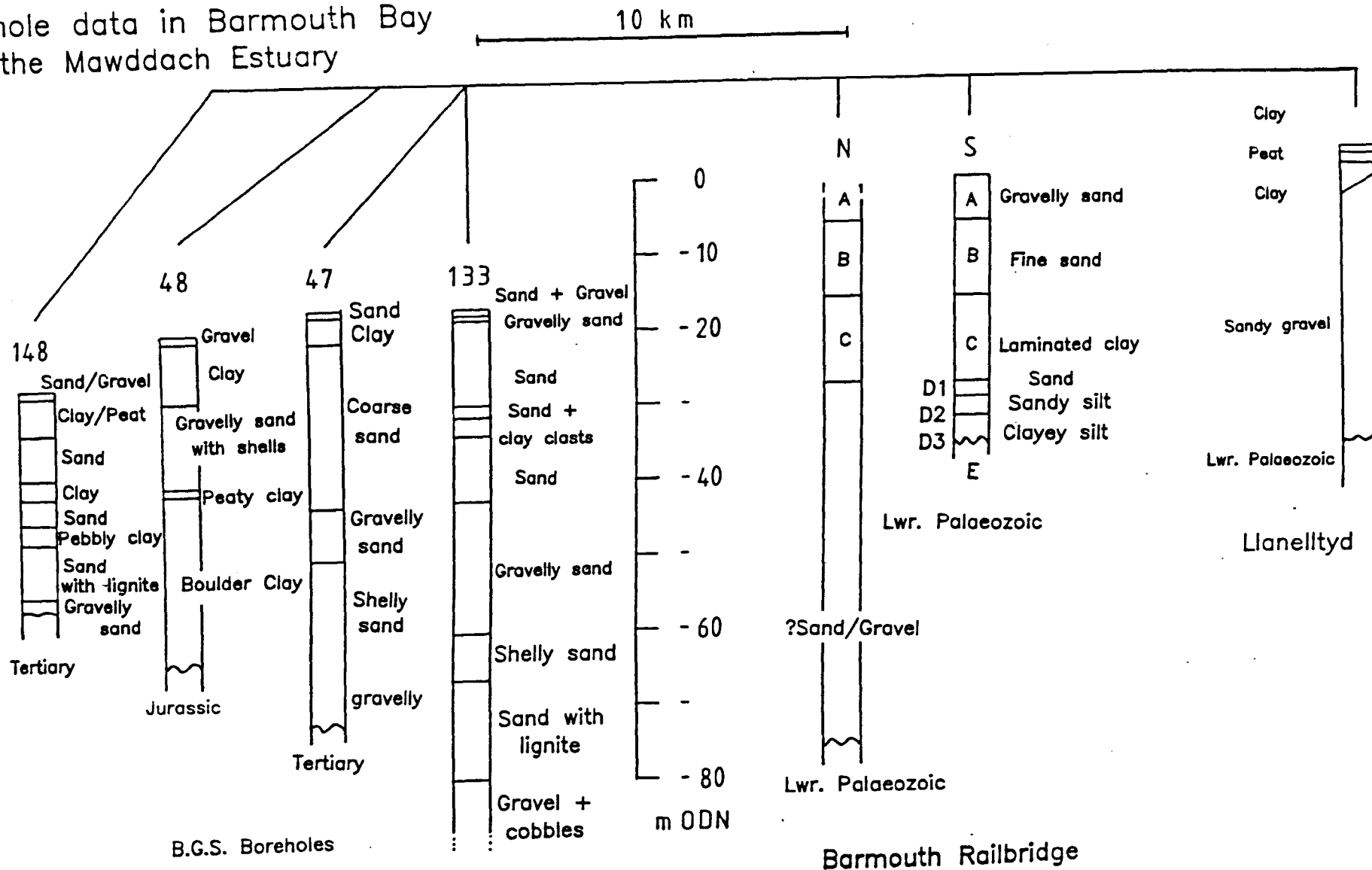
Barmouth

Mawddach Estuary

Llanaber

Fig. 1.14b

Borehole data in Barmouth Bay and the Mawddach Estuary



1.7 Current Velocity Data in Barmouth Bay

A brief section reviewing current data in Barmouth Bay is presented here, because knowledge of the currents within the Bay are useful for interpretation of the geophysical data presented below, and is particularly relevant for full understanding of the side-scan sonar data discussed later.

There are few published examples of directly measured currents in Barmouth Bay. The data available include information on the Admiralty Chart, and a set of float tests carried out in 1969 by Waters & Partners for Barmouth Council, in relation to a proposed sewage outfall. There was also a study by the Welsh Water Authority (1980) related to this proposal. This study (Chapter 2) has presented limited data taken at G.R 570120 during the largest spring tide of the year.

Below is a summary of the above data. On each part of Figure 1.15, the lines and arrows indicate the trend of the tidal flow, as derived from the studies cited above. Current speeds quoted are minimum surface currents (in m/s) averaged over 15-60 minutes, at that position. Data refer to mean spring tides of tidal range of $\sim 4.1\text{m}$. The data were concentrated within 3km of the bar and the Barmouth shoreline. Discussion is omitted on the weak variable currents around slack water.

Flood tide -

- HW-4 to -3 hrs. Flow at the bar and up to 1.5km westwards is to the NE at $\sim 0.17\text{m/s}$. Above 2km west of the bar currents are to the N; these change to a NW direction 1km north, attaining 0.23m/s .

-HW-3 to -2 hrs. Flow is northwards, at $\sim 0.25\text{m/s}$, but $> 2\text{km}$ offshore its direction tends NW and is $\sim 0.3\text{m/s}$. Immediately seaward of the bar flow is directed into the estuary.

-HW-2 to -1hrs. Data are limited, but flow appears similar to the previous hour.

Fig. 1.15.a

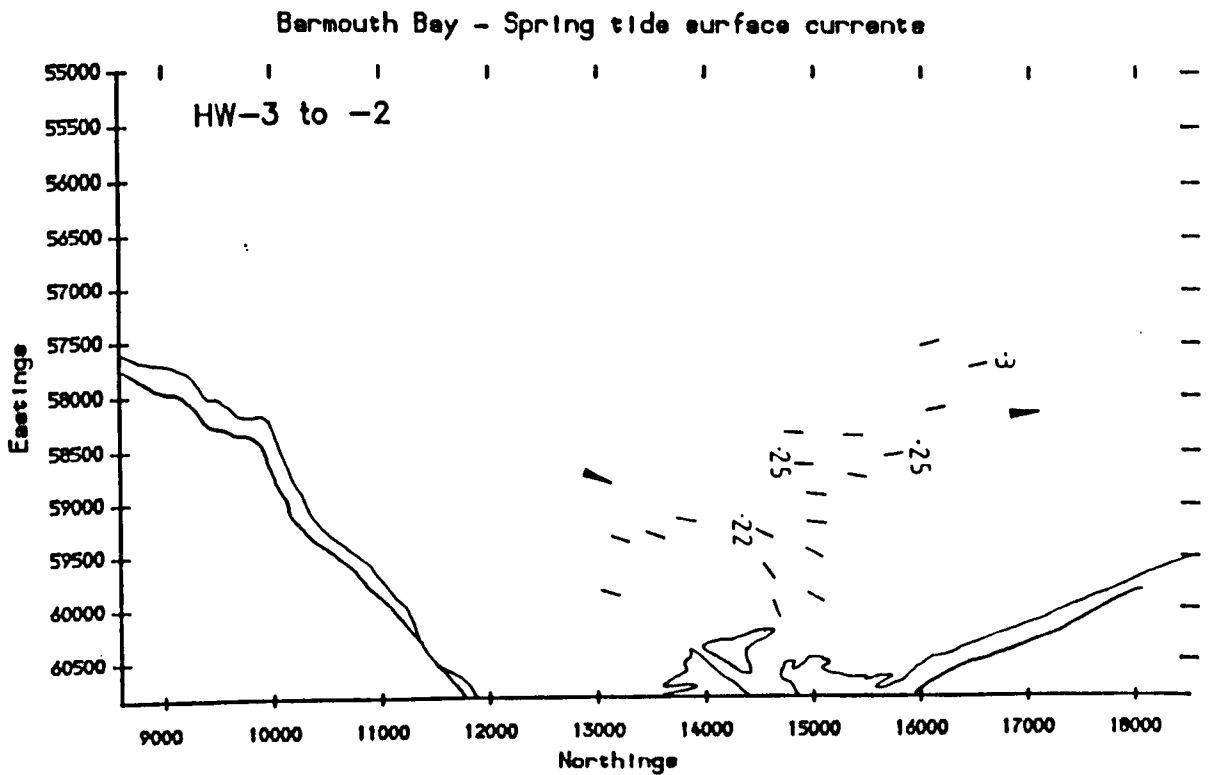
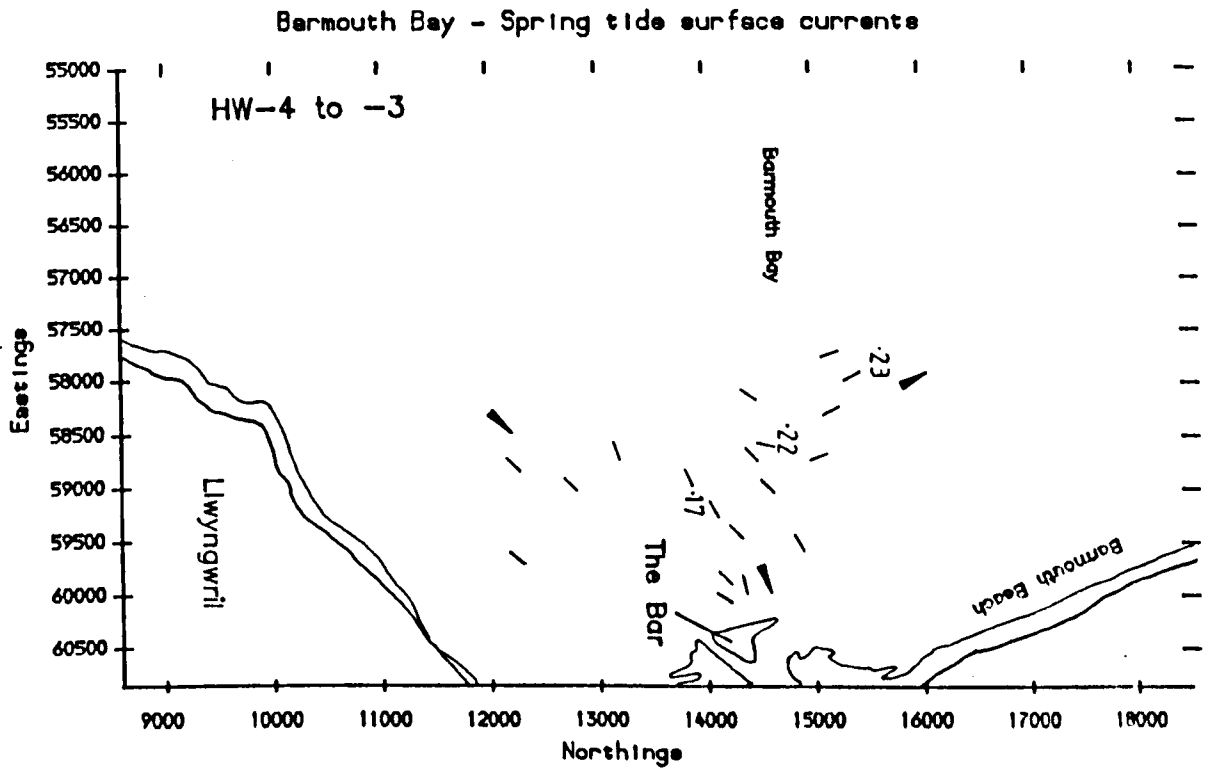
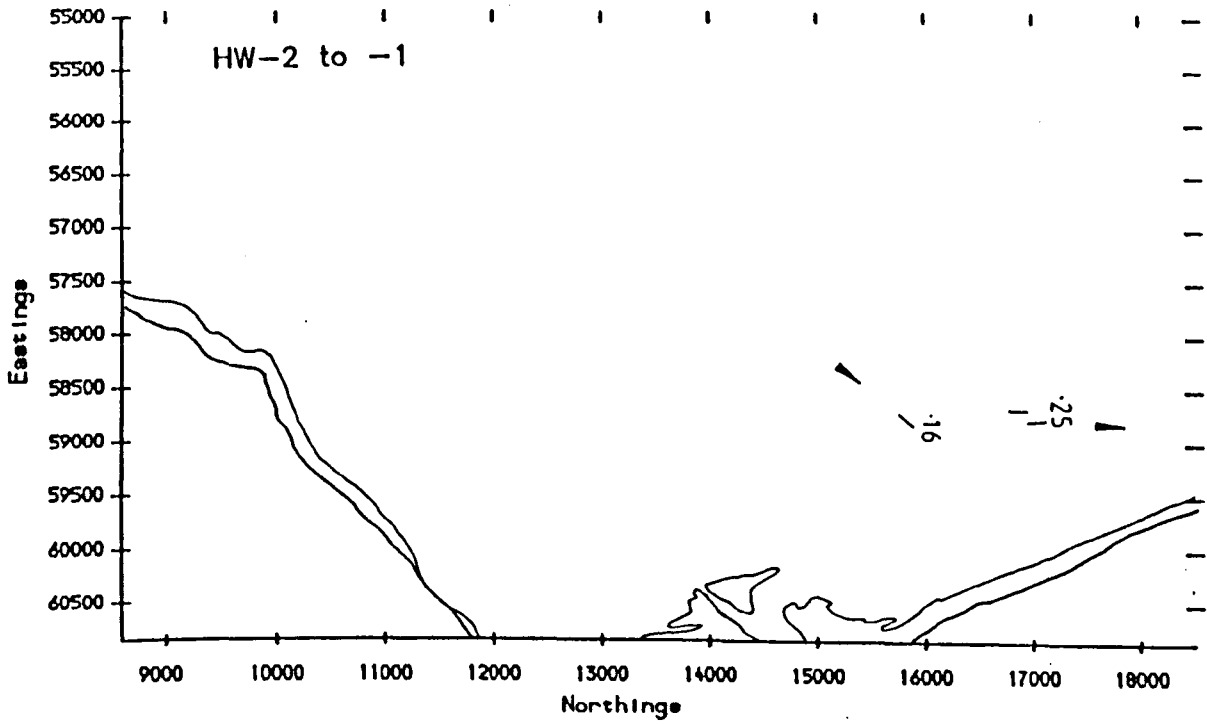


Fig. 1.15.b

Barmouth Bay - Spring tide surface currents



Barmouth Bay - Spring tide surface currents

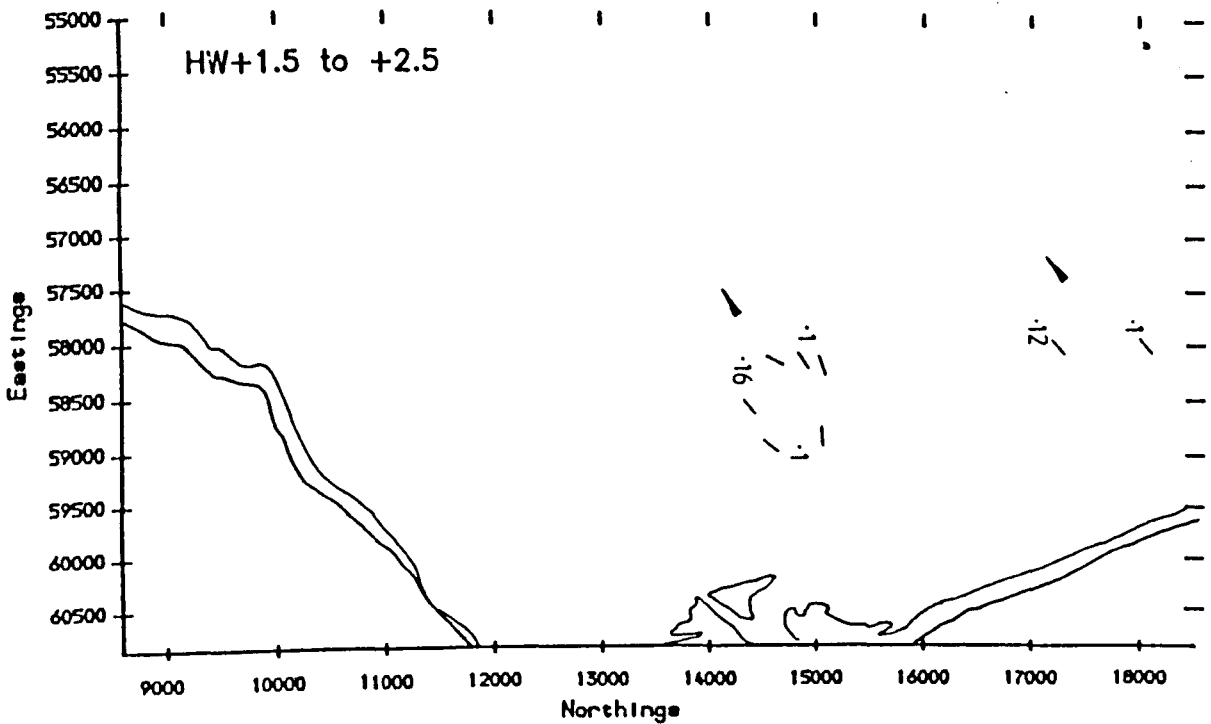


Fig. 1.15.c

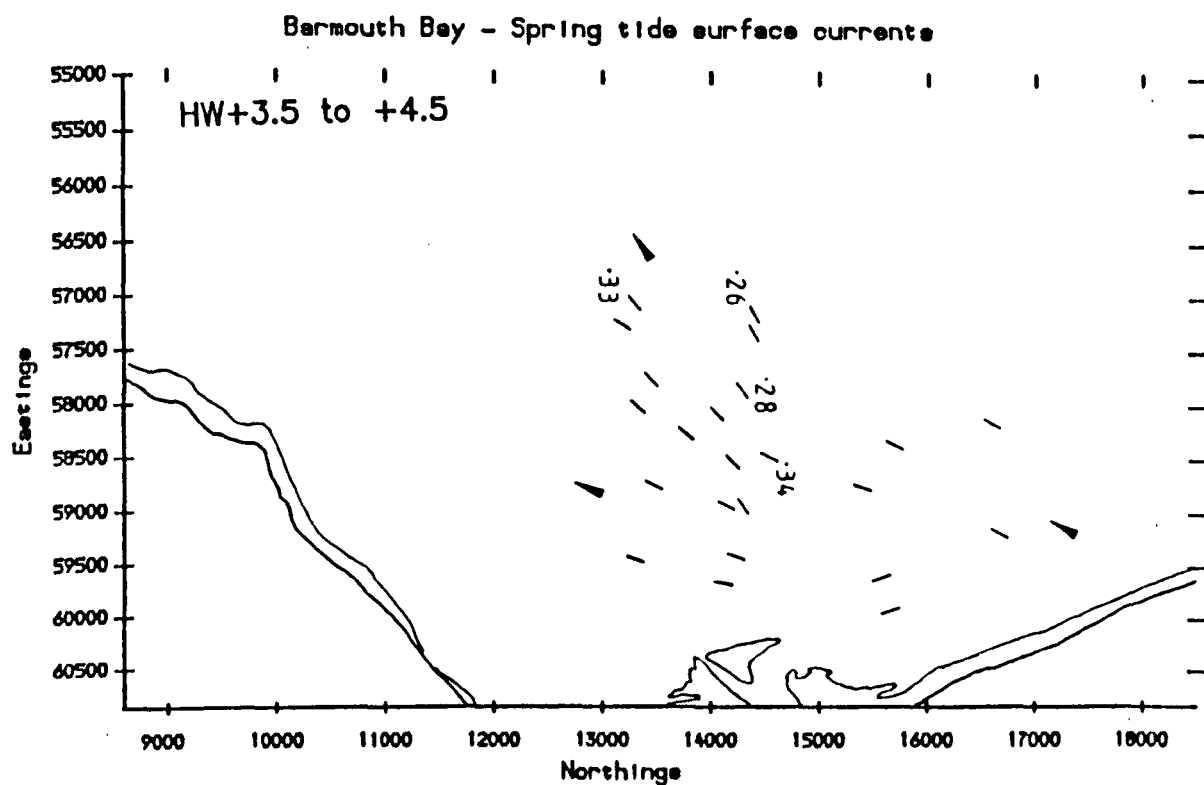
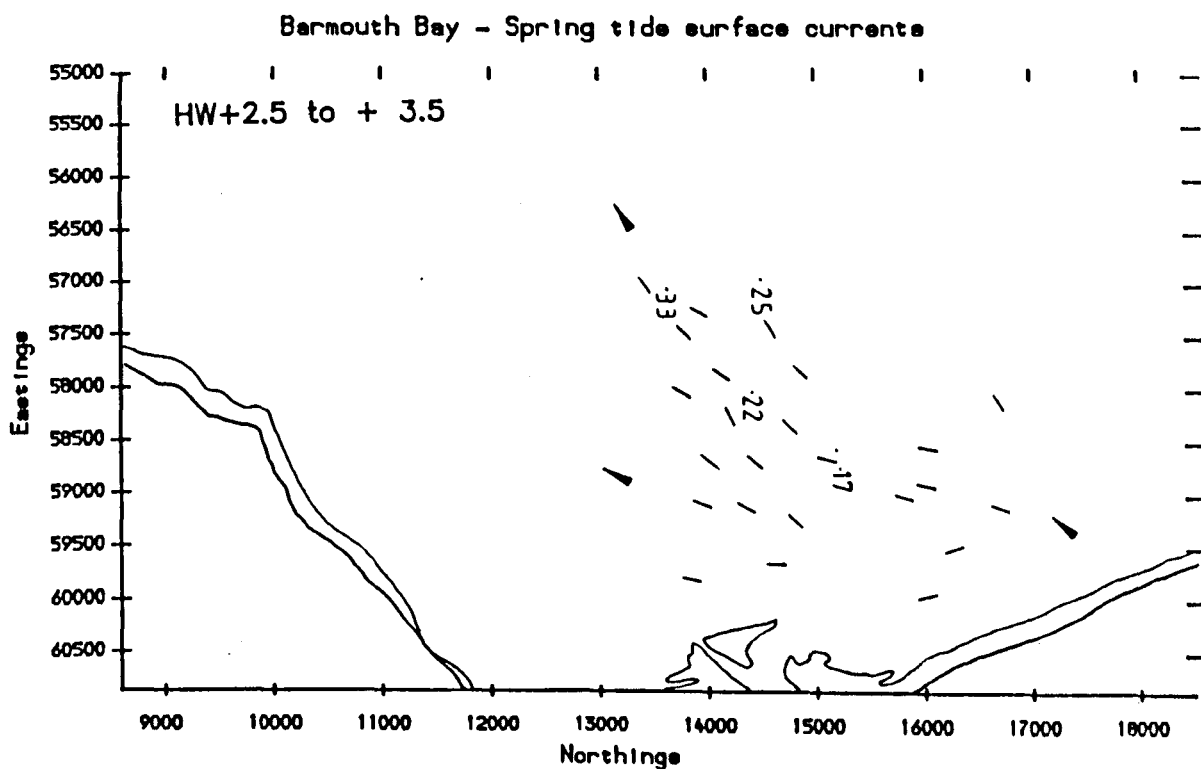
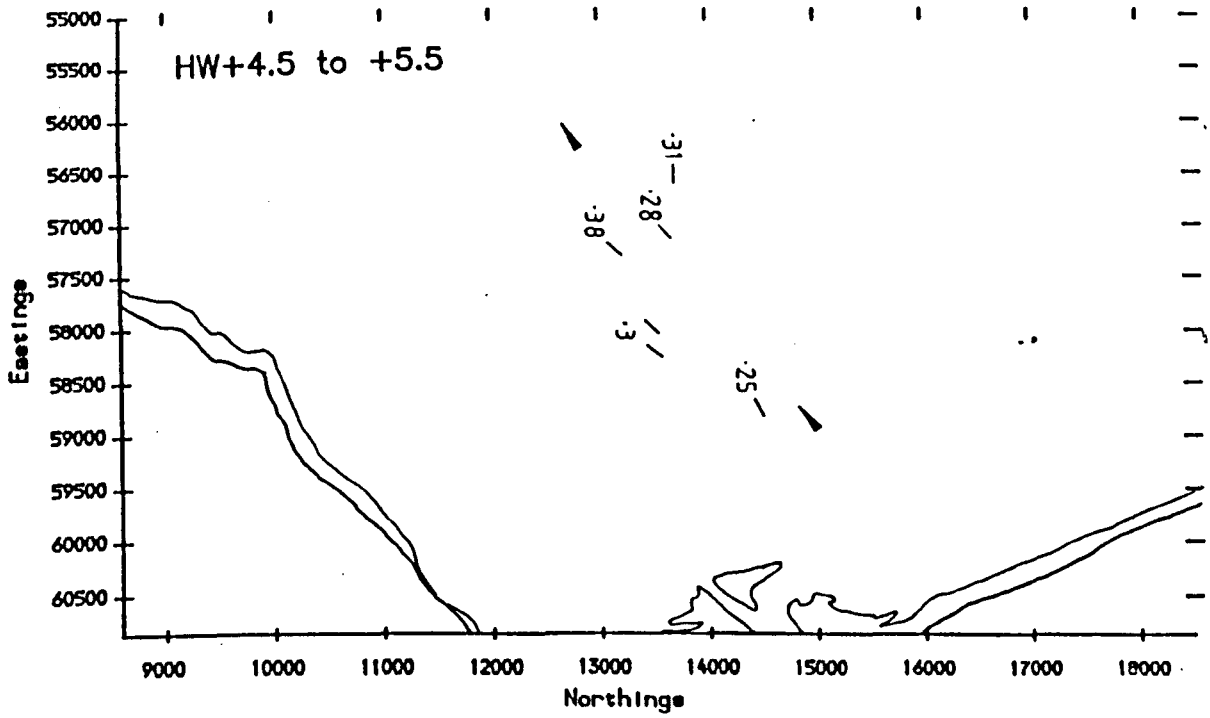


Fig. 1.15.d

Barmouth Bay - Spring tide surface currents



Ebb tide -

-HW + 1.5 to +2.5hrs. In the extreme northeast of the survey area flow is to the SW at $\sim 0.11\text{m/s}$. At 2km NW of the bar, flow is WSW, with faster ($< 0.16\text{m/s}$) and more southerly components west of the bar.

-HW + 2.5 to +3.5hrs. Flow along the Barmouth shoreline is coast parallel, i.e. SSE, but 2km offshore, it is towards the SW. Adjacent to the bar, the ebb is southerly; it has an increased SW component further offshore. Velocities attain $\sim 0.33\text{m/s}$ 3km west of the bar.

-HW + 3.5 to +4.5hrs. As for previous hour.

-HW + 4.5 to +5.5hrs. Data are more limited, but appears similar to the previous hour, except that velocities attain $\sim 0.38\text{m/s}$ at 3km WSW of the bar.

Neap tides - Less data are available for neaps. In general, flow patterns are similar, with the following exceptions:

Flood tide -

- HW-4 to -3hrs. Flow $\sim 3\text{km}$ W of the bar is to the NE.

- HW-2 to -1hrs. Near the bar flow is ENE towards the estuary mouth, and further out water will turn south rather than enter the estuary.

In the light of the above, it is very important to also consider the direct measurements presented in Chapter 2. On the largest tide of the year, of tidal range 5.0m, surface flood currents at G.R. 570120 attained 0.7m/s towards 030-060 degrees (when data collection was discontinued 2.5 hours into the flood tide). The velocity was increasing and maximum currents may have attained 0.8m/s . Clearly, this is much greater than the flow velocities suggested by the mean spring tide data summarised above, and shows that the computed velocities for Cardigan Bay of $< 0.4\text{m/s}$ (B.G.S., 1988) are an over-simplification. Coastal morphology and bathymetry have an effect on local current velocity regimes (Howarth, 1982), and it is likely the coastal projection around Llwyngwriol causes increased local tidal velocities.

In summary, Barmouth Bay experiences a strong tidal current regime. The flood tide flows northwards along the Cardigan Bay coast; locally currents are contour-parallel in inner Barmouth Bay, such as off Ro Wen and Barmouth Beach. Near The Bar, strong currents flow ENE over The Bar and into the Mawddach Estuary. From the limited data available, ebb tidal currents appear more uniform in direction, with a dominant SW trend, although there is also evidence for shore-parallel currents along Barmouth Beach. The evidence on Fig. 1.15 would also suggest that ebb currents are greater than the flood, possibly enhanced by outflow from the estuary mouth. However, if true, it is potentially a phenomenon confined to the region where the effects of estuarine outflow are felt.

1.8 Geophysical Surveying in Barmouth Bay - New Data

1.8.1 Purpose of Surveys

In order to gain more information about the present-day and past sedimentary regimes of the area, a marine geophysical program was undertaken. Its basic purpose was to investigate the bathymetry, bedforms, and sediments of Barmouth Bay, and study the nature of the top layers of the geological sequence in the Bay. The survey was designed to provide information that could be related to the sediments infilling the Mawddach Estuary; firstly, by increasing understanding of the present-day sedimentary controls and depositional patterns; and, secondly, by elucidating the geological expression of both modern and past sedimentary regimes, thereby aiding reconstruction of the late-glacial and post-glacial environments of deposition in the area.

1.8.2 Survey Details

Survey Dates and Vessels Used

Two periods of geophysical surveying were undertaken; the first, on 26-28 May 1987, used the 'Sand Pebbler', an inboard diesel-engined craft borrowed from the Institute of Oceanographic Sciences at Bidston. The surveyed area covered the nearshore zone of the bay, and on the 28th a limited survey of parts of the main channel of the estuary took place.

The second survey was on the 7th and 8th July, 1987, using the U.C.N.W. research vessel Prince Madog; this was designed to overlap the first survey and then extend it westwards into deeper water. Enclosure 2 shows the track lines steamed by the two research vessels.

Brief details of the surveys are given in Table 1.1.. Four basic types of data were collected : water depth, sea-bed information, sub-bottom geological data, and position.

Survey 1, 'Sand Pebbler'

Tidal Curve Construction

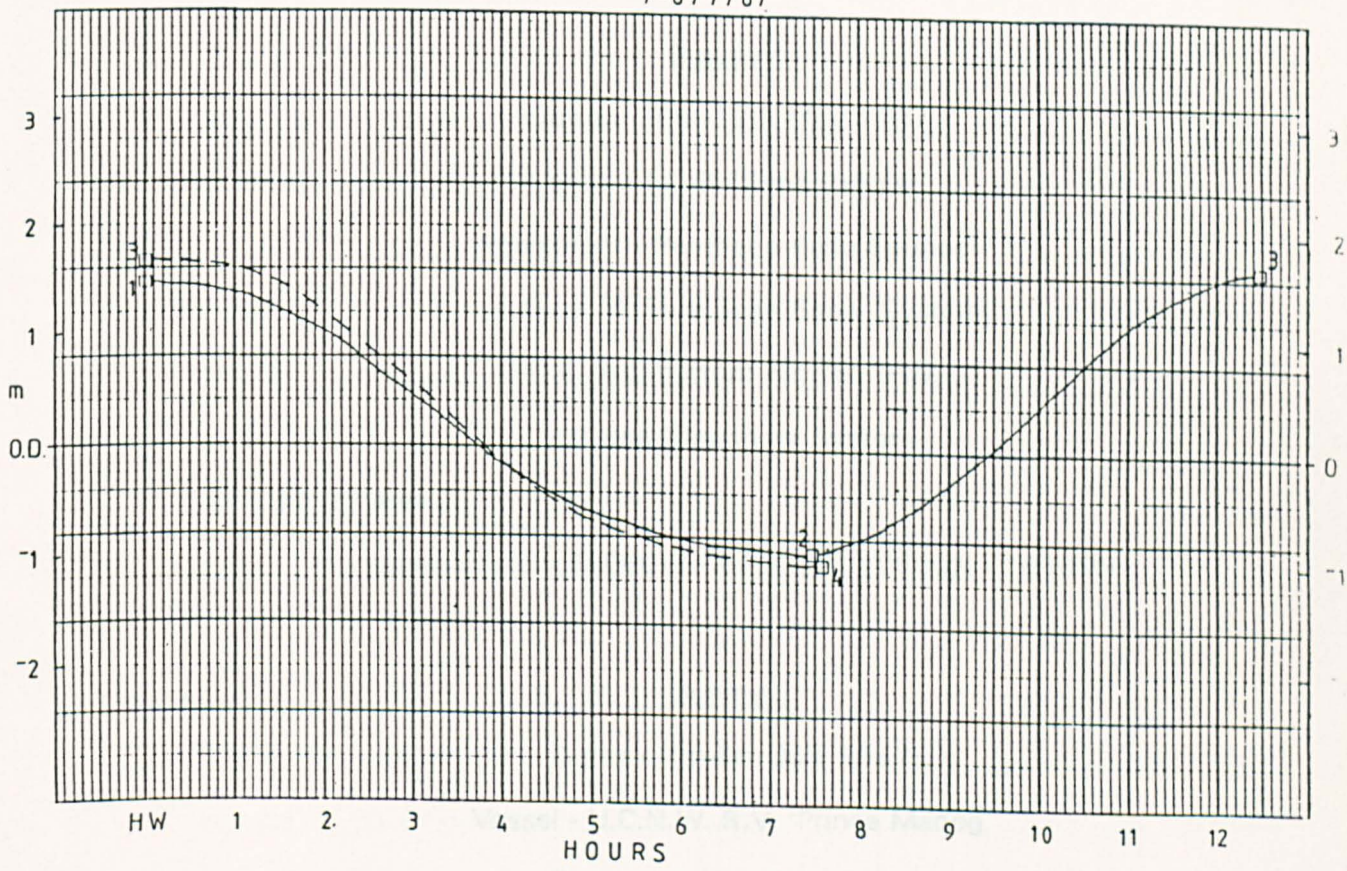
Water level provides the base level from which elevations of the sea-bed are derived. In order to reduce bathymetric data to Chart Datum, it is necessary to obtain a tidal curve for the area of study. Due to a lack of a self recording tide gauge, and limited personnel, no actual readings of tidal height were taken over the study period; therefore the tidal curves were constructed. The tidal predictions for the period provided heights of LW and HW, and the complete tidal curves presented in Chapter 2, were fitted by hand to these predicted tidal heights, to give a shape for the tidal wave in the area. The constructed curve is shown in Fig 1.16. The total errors in height at any particular time on these curves are estimated at $\pm 0.2\text{m}$.

Water Depth Determination

Water depths throughout the survey were continuously measured using the Raytheon echo sounder, with the transducer mounted within the hull. The echo sounder was calibrated each day, by lowering a Secci Disc below the surface on a marked rope to obtain acoustic reflections at known depths. The weather was good and there was only a light swell (maximum amplitude 0.8m), so the water waves recorded on the paper trace as apparent sea-bed undulations were not a major problem (in terms of reading the depth accurately). When combined with the tidal curve construction errors, the maximum error of the calculated sea-bed elevations are estimated at $\pm 0.3\text{m}$.

Fig. 1.16 Assumed tidal curve at Barmouth Bar for 7-8/7/87 and 26-28/5/87.

7-8/7/87



ASSUMED TIDAL CURVE AT BAR

26-28/5/87

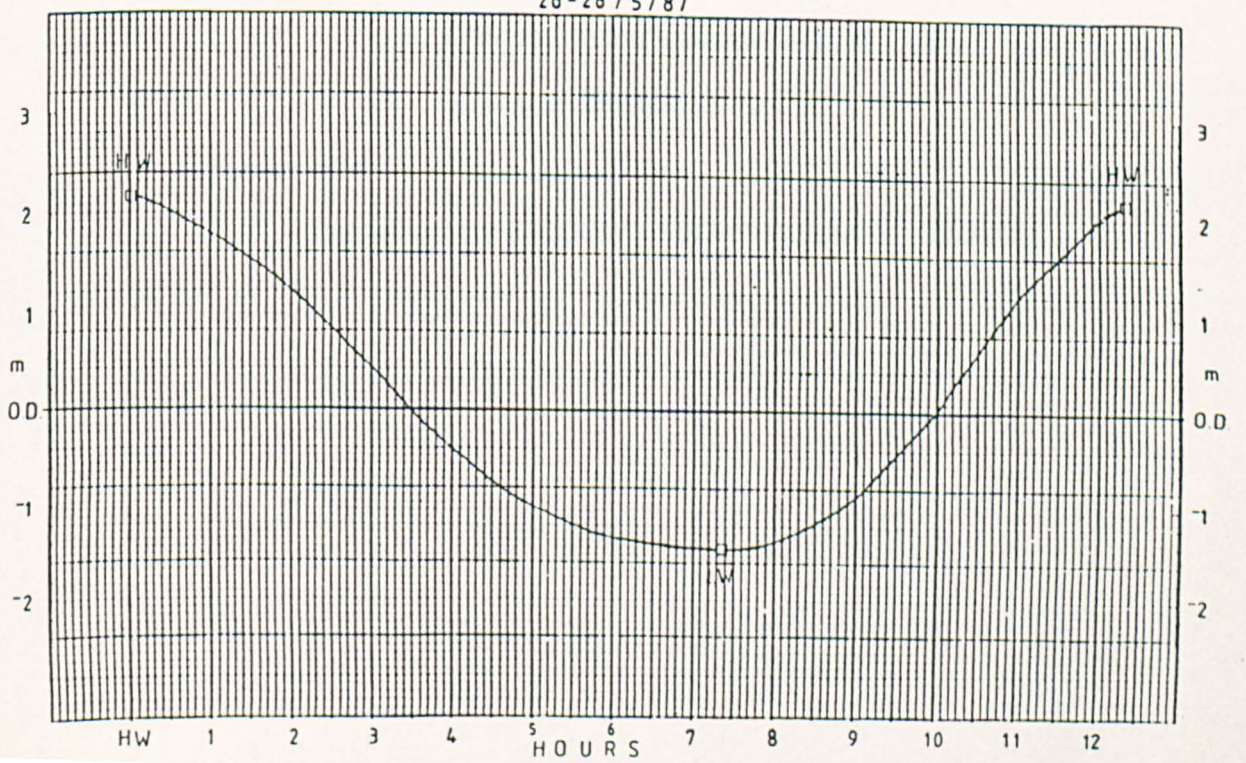


Table 1.1

Details of marine geophysical survey program

Survey 1

Dates - 26th-28th May 1987

Vessel - I.O.S. 'Sand Pebbler'

Equipment - Raytheon Echo Sounder

- E.G. + G. Side Scan Sonar System

- O.R.E. Sub-bottom Profiler, (Pinger)

- Decca Trisponder System

Survey area

- approximately 58000W - 61000W, 10500N - 16500N

Survey 2

Dates - 7th-8th July 1987

Vessel - U.C.N.W. R.V. 'Prince Madog'

Equipment - as above, plus

- E.G. + G. Boomer System

- Prince Madog's Decca System

- 'Shipek' Grab

Survey area

- approximately 53500W - 59000W, 8000N - 17500N

Position Fixing

This survey used the Decca Trisponder system, which consists of a master transceiver aboard the survey vessel, and two or more slave stations onshore at fixed, known positions. The process of position measurement involves a microwave signal being passed between the master station and each of the two slaves, and each travel time is converted internally into a range. Hence, with two ranges from known positions on land, the position of the master station at sea is easily calculated. (A computer program 'FIXPOS.FOR' was written for the purpose). Four different slave positions were used at different times during this survey :

Date	Position	Elevation
26/7th	Barmouth G.R. 61625 15642	37m O.D.
26/7th	Fairbourne " 62011 13124	44m
28th	Coes Faen " 62567 15658	5m
28th	Bod Owen " 63356 17105	10m

The quoted accuracy of the Trisponder system is ± 1 m. The accuracy of surveying the slave station positions was estimated at ± 3 m. It is clear that the system was easily sufficiently accurate for this type of survey, where larger uncertainties derive from such practical aspects as layback of towed geophysical equipment. Such uncertainties may have errors of up to ± 5 m when used from the Prince Madog.

Position fixes were taken approximately 50-300m apart, and a total of 367 fixes were taken for this particular survey. The computer program FIXPLOT.FOR converted the range data into positions on the national grid, and plotted the track chart on to paper.

Survey 2, 'Prince Madog'

Tidal Curve Construction

As with the first cruise, no tidal height data was recorded and so tidal curves for the period were constructed (Fig. 1.16). Estimated errors in this process are $\pm 0.15\text{m}$, less than survey 1, mainly because of the greater size of the survey vessel, and thus decreased effects on the echo sounder data from rolling of the ship etc..

Water Depth Determination

The echo sounder transducer was fixed to the side of the ships hull, at 0.5m below the waterline. The combination of at maximum only a slight swell, and a large survey vessel meant that wave effects on the echo sounder trace were minimal, and it was relatively simple to read depths to $\pm 0.1\text{m}$.

Position Fixing

Position information was obtained from the Decca navigation system installed in the vessel. Navigation errors may be up to approximately $\pm 100\text{m}$ in the Barmouth bay area, around 1/10 of the width of a Decca 'lane'. This survey covered a much greater area than the first, and being done on a much larger vessel it was not necessary or practical to record positions so often. Position fixes were taken at least every 5 minutes, equivalent to $\sim 1000\text{m}$ at a surveying speed of ~ 8 knots.

The position data was in degrees and minutes of Latitude and Longitude; this was converted to national grid co-ordinates, for integration with data from the first cruise. The conversion program 'LATLONG.FOR' was written for the purpose, and is specific to the Barmouth Bay area. A total of 150 position fixes were recorded, of which 38 were grab sample stations (see below).

Grab Samples

To provide information on the nature of the sea-bed, 38 grab samples were taken from Barmouth Bay using a 'Shipek' grab. The positions of the samples are shown on Enclosure 2. Detailed analysis on the grain size distributions, and sedimentary implications from the analyses are presented in Chapter 5. An important use of the data was in 'ground truthing' of the side-scan sonar data, providing for much improved physical interpretations of the sea-bed from the side-scan sonar records (see below).

1.9 Bathymetry of Barmouth Bay

A bathymetric map (Enclosure 3) of the survey area was drawn from the echo-sounder data of surveys 1 and 2. This has contours representing metres below O.D.N.. Chart Datum in this area, equivalent to the lowest astronomical tide (L.A.T.), is at -2.44m O.D.N..

Within 2km of the MHW mark the sea bed dips relatively steeply seawards. At 1km north of Barmouth harbour, between the 4 and 8m contours the sea bed slope is 0.37 degrees, off Llwyngwriil it is 0.57 degrees, and of the southern end of Ro Wen it is just 0.24 degrees. There is a general trend of increasing seaward slope both northwards and southwards along the coast from the southern extent of Ro Wen, and most contours are coast parallel.

From about the 10m contour the slope is markedly lower, at below 0.07 degrees west of Ro Wen and below 0.1 degrees off Llwyngwriil. In the northwest of the area the bed is near horizontal at 11m depth. The deepest water is in the extreme southwest, at up to 15m below O.D.N..

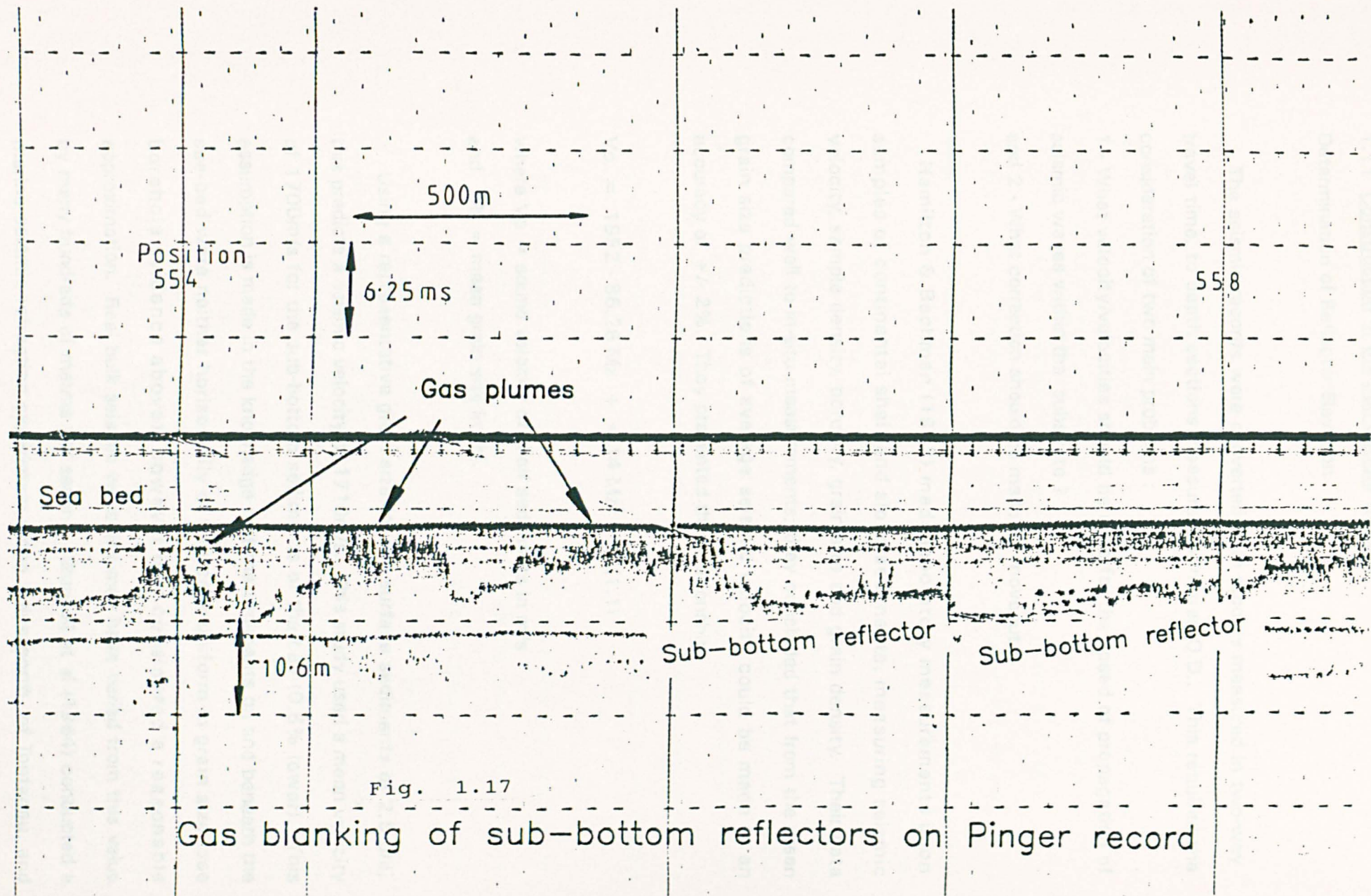
A 4km long perturbation in the contours exists along the 12000N line, with its shoreward extreme approximately 1.5km west of the high water mark. This represents a channel structure up to 0.8m deep and approximately 200m wide. Five hundred metres north and south of this channel there are smaller parallel channel suggested by the contours. The pattern and scale of these features will be discussed later using the side scan sonar data.

1.10 Acoustically Turbid Sediments

The seismic profiling data from both boomer and pinger was of poor quality. Surveys of the Irish Sea by the Geology department at the University of Wales, Aberystwyth had included a few kilometres of seismic data in Barmouth Bay, and these had shown much blanking of sub-bottom reflectors in the sediment column (R. Whittington, pers. comm.). Gas has been widely encountered in the marine environment (Claypool & Kaplan (1974), and is either biogenic, formed more or less in situ (autochthonous) or thermogenic, having migrated upward from deeper in the sediment column (allochthonous) (Mullins & Nagel, 1982).

Gas within sediments causes acoustic turbidity within sedimentary sequences. The high acoustic impedance contrast between gas and liquid, in pore spaces between grains, causes strong reflections of the acoustic wave. Thus reflectors of interest to the geologist may be obscured by strong incoherent reflections, and little energy propagates downwards to be reflected from deeper reflectors. Jones et al (1986) analysed the cause of 'gassy' sediments in Holyhead harbour and the Western Irish Sea, and concluded high concentrations of biogenic methane were responsible.

The distribution of the acoustically turbid layer between 2 and 10m beneath the bed in Tremadoc Bay was reported by Fenemore (1976) and Marine Science Laboratories (1976). This study was not concerned with the distribution of gas; however, the seismic data showed clearly that sediments within Barmouth Bay contain large volumes of gas, which, as in Tremadoc Bay, mask a large proportion of the sub-bottom reflectors (Fig 1.17). The pinger records, having been obtained from higher frequency sound, were most affected by gas blanking; hence the boomer records have been the major source for the data presented here.



1.11 Construction of the Sub-Bottom Geology

Determination of Reflector Elevation

The seismic records were converted from records measured in two-way travel time, to depth sections measured in metres O.D.. This required the consideration of two main problems :

1 - What velocity/velocities should be used for the speed of propagation of seismic waves within the substrate ?

and 2 - What correction should be made for moveout ?

Hamilton & Bachman (1982) made laboratory measurements upon samples of continental shelf and slope sediments, measuring seismic velocity, sample density, porosity, grain size and grain density. Their data compared well to in-situ measurements; they concluded that from the mean grain size predictions of average seismic velocity could be made to an accuracy of +/- 2%. They presented the relationship

$$V_p = 1952 - 86.26 M_z + 4.14 M_z^2 \quad (1.1)$$

where V_p = sound velocity of shelf sediments in m/s

and M_z = mean grain size in phi.

Using a representative grain size for the surface sediments of 2.5 phi, this predicts a seismic velocity of 1710m/s. This study used a mean velocity of 1700m/s for the sub-bottom sediments of the bay (0.5% lower). This assumption is made in the knowledge that the sediments on and beneath the sea-bed were neither horizontally or vertically uniform in grain size (see borehole evidence above), however it is considered a reasonable approximation. Real bulk seismic velocities may have varied from this value by many hundreds of metres per second. Blundell et al (1964) conducted a marine seismic refraction experiment along a line north of Tonfanau, and

deduced a seismic velocity for their assumed Quaternary deposits of 1520m/s, 12% different from the velocity used here.

Correction for 'Moveout'

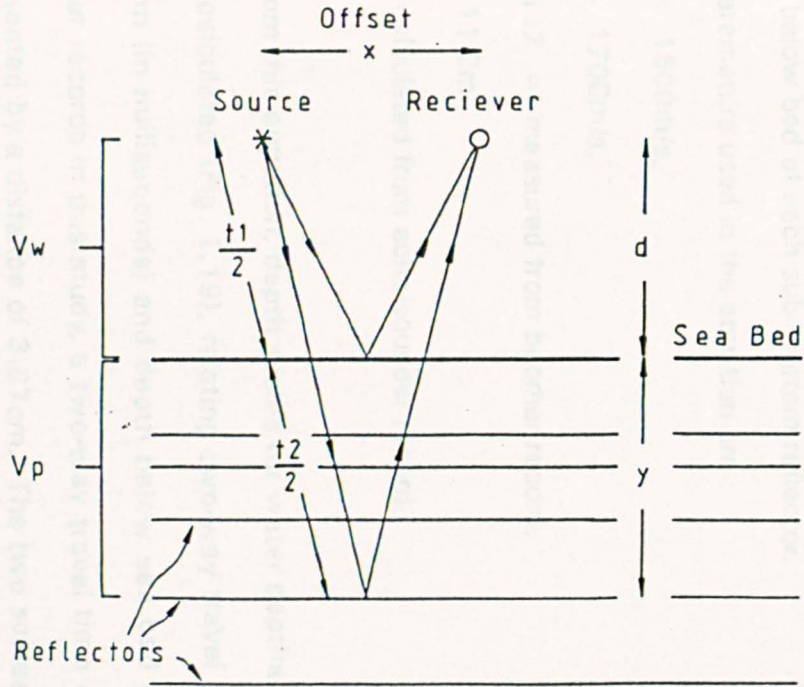
'Moveout' is the term which describes the distortion of the apparent depths and thicknesses of the reflector sequence from their true configuration, caused by the changing geometry of the seismic ray path between source, reflector and receiver when source and receiver are separated by a horizontal offset (Fig. 1.18). This distortion is at a minimum when reflectors are deep and the angle of reflection at the acoustic boundary tends towards zero. In these cases, the direction of wave travel may be considered as being vertical, and two deep reflectors have no difference in the time taken for the wave to travel the horizontal component of the raypath. Distortion is maximum when reflector depth below source and receiver is of the order of their offset, so that a significant proportion of the travel time represents a horizontal component of travel, and there is a difference in time for the horizontal components of travel to two shallow reflectors.

Hence, there is a correction to be applied to the travel time sections for their conversion to depth sections, applicable for the boomer data, but not for the pinger records (because the pinger had zero offset between source and receiver transducers). The correction is a function of both source-receiver offset and reflector depth. Offset was obtained by measuring the time difference on the seismogram, between the pulse and the direct wave, assuming the sound velocity in the water to be 1500m/s. Analysis of the boomer records show that throughout the survey the normal offset varied very little from 11.2m. Depth to seabed during the boomer survey varied between 8m and 13m. Below is a method of constructing a depth scale for use on seismic records, and a consideration of whether the depth variation encountered during the survey was significant in terms of introducing errors

Fig. 1.18

Raypath geometry of seismic reflections

— Boomer system —



Section drawn normal to ships travel

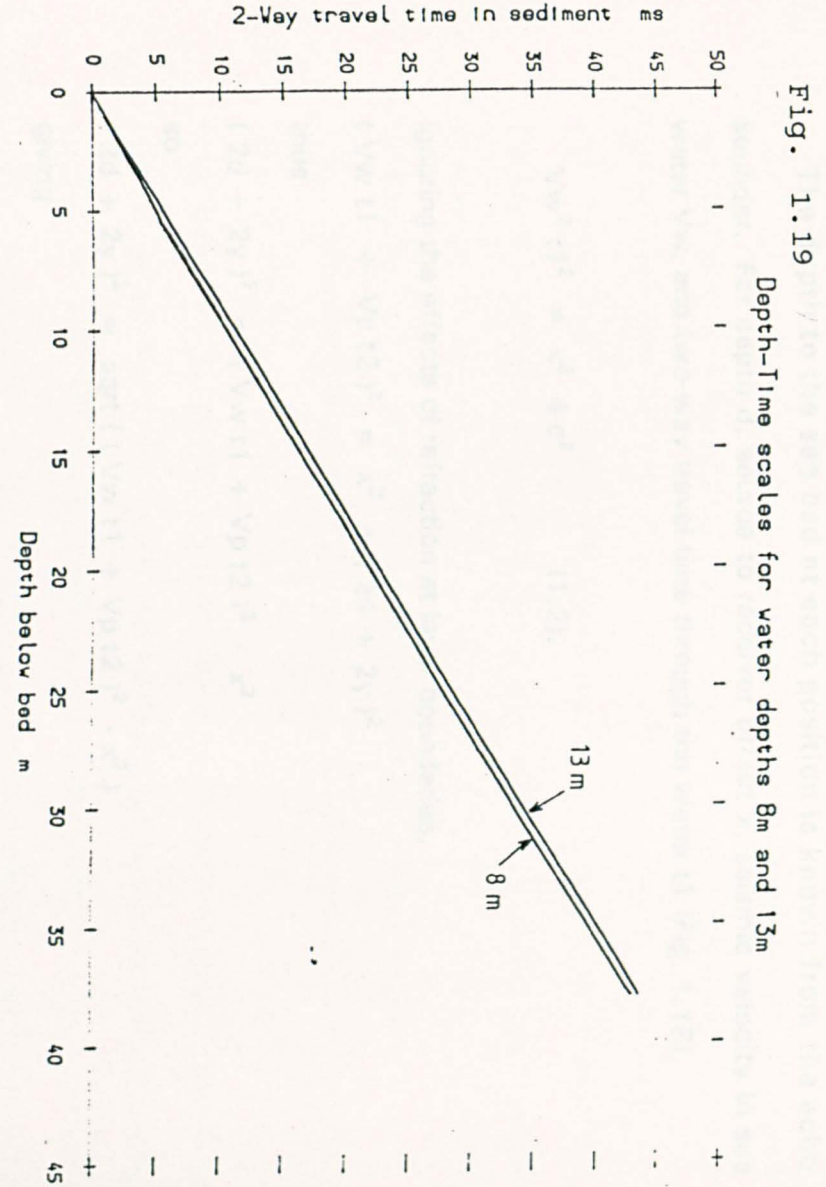


Fig. 1.19

Depth-Time scales for water depths 8m and 13m

into the interpreted absolute elevations of reflectors.

The depth to the sea bed at each position is known from the echo sounder. For depth d , source to receiver offset x , seismic velocity in sea water V_w , and two-way travel time through the water t_1 (Fig. 1.18),

$$V_w^2 t_1^2 = x^2 + 4d^2 \quad (1.2).$$

Ignoring the effects of refraction at layer boundaries,

$$(V_w t_1 + V_p t_2)^2 = x^2 + (2d + 2y)^2$$

thus

$$(2d + 2y)^2 = (V_w t_1 + V_p t_2)^2 - x^2$$

so

$$(2d + 2y)^2 = \text{sqrt}((V_w t_1 + V_p t_2)^2 - x^2)$$

giving

$$y = 0.5(\text{sqrt}((V_w t_1 + V_p t_2)^2 - x^2) - 2d) \quad (1.3).$$

So assuming a constant velocity for all sub-bottom material, y represents depth below bed of each sub-bottom reflector.

The parameters used in the equation are :

$$V_w = 1500\text{m/s},$$

$$V_p = 1700\text{m/s},$$

$$t_1 \text{ and } t_2 = \text{measured from boomer record},$$

$$x = 11.2\text{m},$$

$$d = \text{calculated from echo-sounder record}.$$

From this equation, depth scales for water depths of 8m and 13m have been calculated (Fig. 1.19), relating two-way travel time in the sediment column (in milliseconds) and depth below sea bed (in metres). On the boomer records in this study, a two-way travel time of 10 milliseconds is represented by a distance of 3.87cm. The two scales are very similar, for

example a reflector at 10m below sea bed is represented by 4.05cm and 4.29cm in water depths of 8m and 13m, respectively. This difference of 0.24cm on the record approximates to the practical accuracy of the designation and measurement of sub-bottom reflectors. There are also other variables involved in the determination of reflector elevation, these are :

- the offset (x) fluctuates as the towed source and receiver rise, fall and slew sideways over the water surface, particularly when waves are present or the ship turns;
- the depth (d) varies with bed topography and surface water waves;
- the mean seismic velocity in the water column (V_w) varies with salinity and temperature;
- the mean seismic velocity in the sediment column above each reflector (V_p) may not be 1700m/s, and varies with sediment properties such as grain size, porosity, compaction, pore fluid salinity, and cementation;
- refraction of seismic waves at layer boundaries, which causes the seismic raypath to deviate from the straight line assumed by this equation.

After considering these factors, it was felt justified to convert the boomer records into reflector elevations by use of a depth scale based on a 10m water depth. Using this scale and the known sea bed elevations, absolute elevations of the sub-bottom reflectors were calculated. The results have been presented in a number of interpreted sections (Enclosure 4), which are briefly described below.

1.12 Description of Seismic Sections

1.12.1 Section 1 - positions 522 - 529 - 534

In the north of this section, there are only a few reflectors; these are sub-horizontal, parallel and discontinuous in appearance. Southwards, for 2.7km, there are no internal reflectors. Further SW a major channel structure is present, reaching 3km in width and -30m O.D.N., and with sides sloping at 1.57 and 1.18 degrees. Within the channel, there are a few reflectors at -15 to -18m O.D.N.; these are traceable for > 700m, and indicate (?northerly) dipping cross-stratification, probably produced during the late stages of channel fill. It is unclear whether the northern bank of the channel base material has been eroded to the same extent, as at -19m O.D.N. the layering is no longer traceable.

Where the channel base reflector is near the sea bed, the side-scan sonar records show continuous lack of sand cover. In the extreme SW, there is a slight internal reflector within the basal material, although it is difficult to resolve in any detail. Lack of sand cover, i.e. presumed exposure, also occurs in the 1m deep linear depression in the centre of the bay. Beneath this channel, is some weakly-defined cross- stratification; if the reflector continued southwards, this would match the position of the south bank of the channel (see below). This suggests high relative resistance to erosion of the lower unit.

1.12.2 Section 2 - positions 552 - 542 - 535

Three different types of reflector are also seen in this section, with the same geographical relation as seen in section 1. Only the south side of the buried channel is seen, dipping at an average of 0.87 degrees and traceable to -35m O.D.N.. The reflector is continuous with that seen in section 1, and the side- scan records indicate exposure for 200m between the sections. At -23.5m O.D.N. there is a bench in the channel side, perhaps indicating a

prolonged period of erosion at a particular water level.

The channel fill is ill-defined, with only a few reflectors. These are at similar elevations to those to the SE seen in section 1. North-dipping layers parallel the position of those in section 1, and these give way to flatter relatively continuous undulating layers. Sub-bottom reflectors are absent for 1km at position 542.

In the north of the section, sub-horizontal planar sub-parallel reflectors are found; their southern limit is marked by sea bed surface topography and lack of sand cover, suggesting erosion of underlying units. Reflectors pinch out southwards, inferring the southern boundary of an infilled depression; this is bounded to the south by the more acoustically transparent material. 3km north of this feature is a north-dipping set of layers, interpreted as continuous with the parallel sub-horizontal reflectors to the north and south. The reflectors dip north at 0.46 degrees, on this N-S section for a distance of over 300m.

1.12.3 Section 3 - positions 555 - 566 - 569

This lies approximately 1km west of section 2. The channel margins in the south are not displayed in this section. There is however, one weak northward-dipping reflector between positions 568 and 569, at a depth of -27m O.D.N., traceable for 200m and with an apparent dip of 0.76 degrees. It is a weak feature and considered unlikely to be a continuation of the channel base defined in sections 1 and 2. Above lie a set of sub-parallel sub-horizontal layers, in places showing a cross-bedded appearance; these are considered to be probably equivalent to the reflectors within the channel fill nearer the coast.

The units of the channel fill continue >3km northwards, where they have a strong cross-bedded and more thinly-layered nature. Some units at -20m O.D.N. pinch out northwards. In the lowest identified unit, some unclear north-dipping reflectors occur at an angle of up to 1.31 degrees. At surface, there is a topographic feature, and the side-scan sonograms indicate

exposure. These characteristics are similar to the southern limit of the well-bedded units in sections 1 and 2. The nature of the transition between these units and the gently north-dipping reflectors 1 km to the north is unclear. However, there does appear a clear similarity between the layering in the north of sections 1 - 3.

There is a correlation made between the north-dipping layers of section 2, and the layers beneath positions 523 and 524 (section 1), and beneath positions 556 and 558 (section 3).

1.12.4 Section 4 - positions 586 - 590

At least 12 individual units are distinguished in this section. There are a clear lower set of curved (possibly sigmoidal) easterly-dipping reflectors (apparent dip 1 degree), evident down to -27m O.D.N., and 1-2m thick. In the centre of the section they pass up into more horizontal units; these are interpreted as pinching out beneath position 587 at -15m O.D.N.. Some units suggest an eastwards thickening. The uppermost unit is continuous across the onlap relationship described above, varying between 1 and 3m in thickness.

1.12.5 Section 5 - positions 597 - 603

The main features are easterly-dipping sigmoidal layers in the eastern part of the section; these are evident to a depth of at least -21m O.D.N.. At their base, they form a gentle anticline, with its apex beneath position 600. The folded sequence is truncated by a west-dipping reflector with dip between 0.2 and 0.45 degrees, possibly outcropping (although not exposed) at a 0.6m high plateau east of position 600.

1.12.6 Section 6 - positions 608 - 605

This section displays divergent seismic reflectors. The deepest dips due east, at 1.95 degrees. Above it, two units onlap to the west, and thicken

eastwards, being traceable to a depth of -27m O.D.N.. A second set of onlapping units occur above a reflector of 0.24 degrees easterly dip. At the east of the section, some short reflectors (dipping at up to 1.7 degrees) underlie 300m of surface exposure.

1.12.7 Section 7 - positions 638 - 641 - 644

The SW end shows a channel complex, seen down to -25m O.D.N., and the major part of which is over 1400m wide and 8m deep. At the SW end, a reflector at -22m O.D.N. dips northeast at an apparent angle of 1.6 degrees (the steep dip and position suggest a relation to channel morphology, extending northeast from the coast).

The lower units on the eastern side can be traced to the east, where they are interpreted as being exposed in three positions, each a topographic high. Layer dip remains southeasterly and, in the east, they are underlain at -28m O.D.N. by a reflector with apparent eastwards dip of 0.55 degrees. This may be an expression of morphology related to deeper channelling. At position J, there are reflectors correlated with the cross-bedded units at -18 to -20m O.D.N. of section 3.

1.12.8 Section 8 - positions 570 - 575

The channel complex is also shown in this section, with reflectors forming a syncline with its base beneath position 573. The southwestern margin of the channel dips at up to 2.7 degrees, and the material in which the channel sits contains very few reflectors. The channel fill layers are also synformal, and there is an unclear relationship with the reflectors immediately to the northeast; only one layer suggests continuity. The scarcity of reflectors in the buried channel does not permit correlation with the clearer morphologies seen to the northeast (seismic section 7).

1.13 Sedimentary History, and Correlation with

Boreholes, Exposure and other Seismic Facies Data

Beneath the sedimentary sequence lies a Lower Palaeozoic erosion surface. Although there is no information on its elevation between the estuary head and mouth, the coincidence in elevation (\sim -35m O.D.N.) at Llanelltyd and Barmouth railbridge may represent evidence of a near-horizontal glacially-scoured surface within the valley. Blundell et al (1969) identified an unconformity surface at -40m O.D.N. along the Cardigan Bay coast, with a gentle westwards slope over most of the bay. Within the Dyfi Estuary valley, they identified a reflective horizon at a constant depth of -30m O.D.N., and one at the same depth under Morfa Harlech.

Therefore, there seems to be a common near- horizontal unconformity surface within the estuaries and out into Cardigan Bay, implying a common process of formation. Blundell et al (1969) noted that the surface was near-parallel to the present sea floor, and implies that a sea level still stand at \sim -30m O.D.N. was responsible. This would further imply that the sedimentary nature of the valley fills would change at this level. Unfortunately, the limited borehole data at the railbridge does not allow firm conclusions regarding this. At approximately -28m O.D.N., however, there is an apparent change to fine-grained organic deposition, possibly in a mudflat or saltmarsh environment.

The very low bedrock elevation at the north of the railbridge (\sim -75m O.D.N.) implies overdeepening of this surface, with erosion by one or both of subglacial sediment-laden outwash and pro-glacial outwash from retreating ice masses. These have implications in terms of the age of the erosion surface and sea level. For subaerial erosion to -75m O.D.N., sea level would need to be lower. The global eustatic sea level curve of Jelgersma (1966) shows that a sea level of -75m was attained at \sim 13000years B.P, but data is scarce and the date unreliable. Maximum lowering of Pleistocene sea level was \sim 100-120m below sea level, which is

consistent with the -75m level in the Mawddach, and the -91m level to bedrock in the Dyfi (Blundell et al, 1969). Subaerial erosion is, therefore, not ruled out as a cause for the overdeepening, neither is subglacial activity.

The boreholes along the Barmouth Railbridge do not correlate well with the seismic data. The pinger (see below) obtained very little penetration, and the boomer data further offshore displays great reflector topography. Nearshore reflectors are very coarse, compared to the proven nature of the sediments in the railbridge boreholes (see below), and they appear related to the processes operating on the seaward side of the spit Ro Wen. The B.G.S. boreholes also have little value in terms of correlation with the seismic data; the three dimensional nature of the sedimentary facies in the area precludes their recognition.

However there are some speculative conclusions to be drawn from the data, and four seismic units are identified. It is emphasised that no conclusive proof for these interpretation exists.

1 - Welsh Boulder Clay

Using as a comparison the observations of Fenemore (1976), it is concluded tentatively that the acoustically homogeneous unit occupying the central portion of Barmouth Bay may be a Boulder Clay unit or complex of glacial debris; this is dissected by channels to the north and south (Seismic sections 1 and 2). This is likely to consist of material derived from the Welsh Ice Cap, and have been deposited during the last glacial maximum, i.e. of Devensian age. It is possible that this is part of a terminal moranic complex from the Mawddach Valley glacier. The ~N-S linear exposure of this material, in inner Barmouth Bay, is of unknown origin. It is noted that Boulton (1986) has recently identified moranic ridges ('push moraines') - formed parallel to the ice front of a glacier by successive retreat and advance of an ice front. Thus the explanation for this feature should not exclude a primary cause.

2 - Late- and Post-Glacial Sands and Gravels

The channels which dissect the Welsh moranic unit are cross-stratified in their lower parts (Sections 1 4, 5 and 8). These cross-bedded channel-fill sequences probably reflect relatively rapid deposition in sub- or pro-glacial environments, by meltwaters from the retreating ice sheet. Energy levels of the transporting flows were sufficiently high to erode the substrate, and the grain size of the sediments may be coarse.

3 - Early Holocene Lacustrine and Lagoonal Sediments

These sediments overlie the cross-stratified channel fills and are characteristically sub-horizontal and laterally extensive. Their seismic expression implies low energy conditions of deposition, possibly in a lake or lagoon formed during the continuing sea-level rise of the Early Holocene. The presence of gas implies significant organic content to the original sediments. The dip of the reflectors is generally landward, possibly reflecting a basin of deposition with a border to the west.

4 - A Recent Marine Sand Wedge - The Inner Sand Sheet

The 'Inner Sand Sheet' is described and interpreted more fully later in this chapter. It is probably formed of sand eroded from coastal and sea-bed exposures of glacial material.

All the geophysical records, including the side-scan records presented below, are available for consultation by arrangement with the author. Correspondence should be made in the first instance to Dr C.F. Jago, School of Ocean Sciences, U.C.N.W., Menai Bridge, LL59 5EY, Gwynedd, U.K..

1.14 Side-Scan Sonar

Side-scan sonar has in the last few years become an instrument commonly used in marine geological and sedimentological research. The purpose of its use in this study was to provide information on both the surface sediment distribution and the bedforms of the area, which could be integrated with sub-bottom, echo sounder and grab sample data, and thus to provide a full picture of the Recent geology and sedimentary dynamics. Side-scan sonar, itself a remote sensing device, is able to link together the remotely-sensed geophysical information to the physically known sediment type; it is, thus, invaluable in a survey of this kind - more so because in a relatively short time a very large area of sea-bed may be surveyed.

1.14.1 Description of Equipment

Towed behind the survey ship is a streamlined towfish, which has along its sides piezoelectric transducers. These project a fan-shaped beam of high frequency acoustic energy sideways on to the sea-bed. The beams are very narrow in the horizontal plane, to obtain high along-track resolution; and they are wide enough, in the vertical plane, to give (in this case) a lateral coverage of 100m or 125m either side of the fish.

The acoustic frequency is high (eg. 120 kHz), so that virtually all the seismic energy is either reflected or scattered - with a negligible amount absorbed by the bed sediments. The towfish transducers also receive returning signals, which are then amplified with a time variable gain and displayed on a graphic recorder. For a fuller discussion of side scan sonar systems, the reader is referred to Flemming (1976) and Mazel (1985).

1.14.2 Interpretation of Side-Scan Data

The resulting acoustic 'picture' of the sea-bed is an acoustic equivalent to oblique aerial photographs of the earth's surface, one on each side of the

aircraft. The records were interpreted in conjunction with the bed samples, the sub-bottom records, and published side-scan sonar interpretations. Of particular use in interpreting the records in a geological and sedimentological sense is Belderson et al (1972), and Mazel (1985) was of use in aiding identification of patterns caused by non-sedimentological effects.

1.14.3 Terminology of Shelf Bedforms

In order to gauge the geological, sedimentological and hydrodynamic significance of distributions of shelf bedforms, a descriptive terminology is required. As with intertidal bedforms (Chapter 4), a bedform classification based on a range of morphological and morphometric parameters is needed to adequately describe (and, hence, interpret) bed response to the shelf hydrodynamic regime. Amos & King (1984) compared terminology used in a number of different studies of flow transverse bedforms (their Table I), and presented a synthesis of descriptive terminologies. Their system has the advantage of being based on a range of bedform attributes each of which are likely to be visible from standard echo-sounder and side-scan sonar records (except sand ridges, see below). A summary of their bedform definitions and diagnostic criteria is given below, and is the system adopted in this study.

1.14.4 Amos & King (1984) Shelf Bedform Terminology

Sandwaves - (sensu stricto) are composite, flow transverse, constructive features, formed in medium to coarse (grained) sand or gravel, constructed and transported by the superposition and migration of megaripples.

Their diagnostic features are :

- 1 - flow transverse continuous crestlines;
- 2 - a composite, possibly multicrested, profile, resulting from the coalescence of adjacent sandwaves or the superposition of megaripples;
- 3 - adjacent forms show a weak coherence in spacing, though a moderate coherence in crest orientation;

4 - the bedform as a whole has no slipface.

Within this definition, sandwaves may display a range of morphological types, but in general are 0.5- 12m high, and 12-1000m in wavelength. They normally form at near-bed mean flow velocities of 0.4-1.0m/s. Belderson et al (1972) give a peak spring surface current velocity range, for sandwaves, of 0.5-1.0m/s.

2-D Megaripples - straight, sharp-crested, flow transverse, discrete bedforms composed of medium to coarse sand, and exhibiting a simple ripple-like profile which shows a moderate coherence in crest spacing with adjacent forms.

Their diagnostic features are :

- 1 - a flow transverse, continuous crestline;
- 2 - single-crested, ripple-like profiles often found with ripples superimposed on their flanks;
- 3 - the lee-face is a fully-developed slipface, usually dipping at the angle of repose, the overall profile showing a highly asymmetric form;
- 4 - they can show moderate to strong coherence or can coalesce or overlap with adjacent forms;
- 5 - crestline bifurcation can occur in either crest- parallel direction.

They are generally between 0.1 and 2.0m high, and 0.2 and 50m in wavelength; they form at near-bed velocities of 0.4-0.6m/s. In this study, estuarine intertidal megaripples were active and two-dimensional when peak velocities 1m above bed were 0.6-0.75m/s (see Chapter 3).

3-D Megaripples - short-crested, flow transverse, discrete bedforms composed of medium to coarse sand, and having irregularly scoured troughs and a low coherence in crest spacing. Their diagnostic features are :

- 1 - flow transverse, short arcuate crestline;
- 2 - irregular scour pits in the bedform trough;

- 3 - single crested, single forms, although ripples may be superimposed on the flanks;
- 4 - poorly developed slipface, the form in section being only slightly asymmetric;
- 5 - they occur in irregular fields of forms, being generally consistent in size and spacing within each field.

Belderson et al (1982) do not recognise the distinction between megaripples and sandwaves, considering them members of a size continuum; they state, however, that 'small sandwaves' (megaripples) occur under slightly slower current regimes than large sandwaves.

Sand ridges - composite, flow oblique (or parallel) linear sand accumulations, usually of measurable relief, formed by the superposition and migration of sandwave or megaripple fields. Their diagnostic features are :

- 1 - linear to sinuous crestline in plan view, parallel or slightly oblique to current flow;
- 2 - a length to width ratio of over 40;
- 3 - sandwaves or megaripple fields occur on the flanks (of active forms), which may be partially or wholly degraded.

They have elevations of 1-30m, are 700-8000m wide and up to 60km long. Due to their low relief, they are often only detectable on high resolution seismic sections.

Sand ribbons - current parallel 'streaks' of sand marked laterally by shallow features formed by current scouring. Their diagnostic features are :

- 1 - an orientation parallel to flow with, 'tuning fork' bifurcations predominantly occurring in one direction (Flood, 1983);
- 2 - relief of <0.5m;
- 3 - often poorly developed lateral boundaries, the crest grading gradually to

the inter-ribbon 'windows';

4 - ribbon width varies both laterally and down-current, due to the mechanism of 'window' generation (McLean, 1981).

Sand ribbons can be up to 15km long and up to 200m wide (Kenyon, 1970); they usually have a length to width ratio of over 40, and are often only a few centimetres thick. They are separated by a coarser floor, visible on side scan sonograms as a region of higher acoustic backscattering (i.e. darker record). Sand ribbons are formed where peak surface mean spring currents attain about 1.0m/s (Kenyon, 1970; Belderson et al, 1982); however, at lower speeds of 0.9m/s ribbon-like trains of sinuous or barchanoid megaripples are found. At approximately 0.8m/s, smaller sand ribbons (~10m wide) may be found on a coarse substrate between isolated sand waves (Kenyon, 1970). Amos & King (1984) consider that in view of their small volume, sandribbons may be produced in a short period of intense flow, > 1-3m/s, associated with storms.

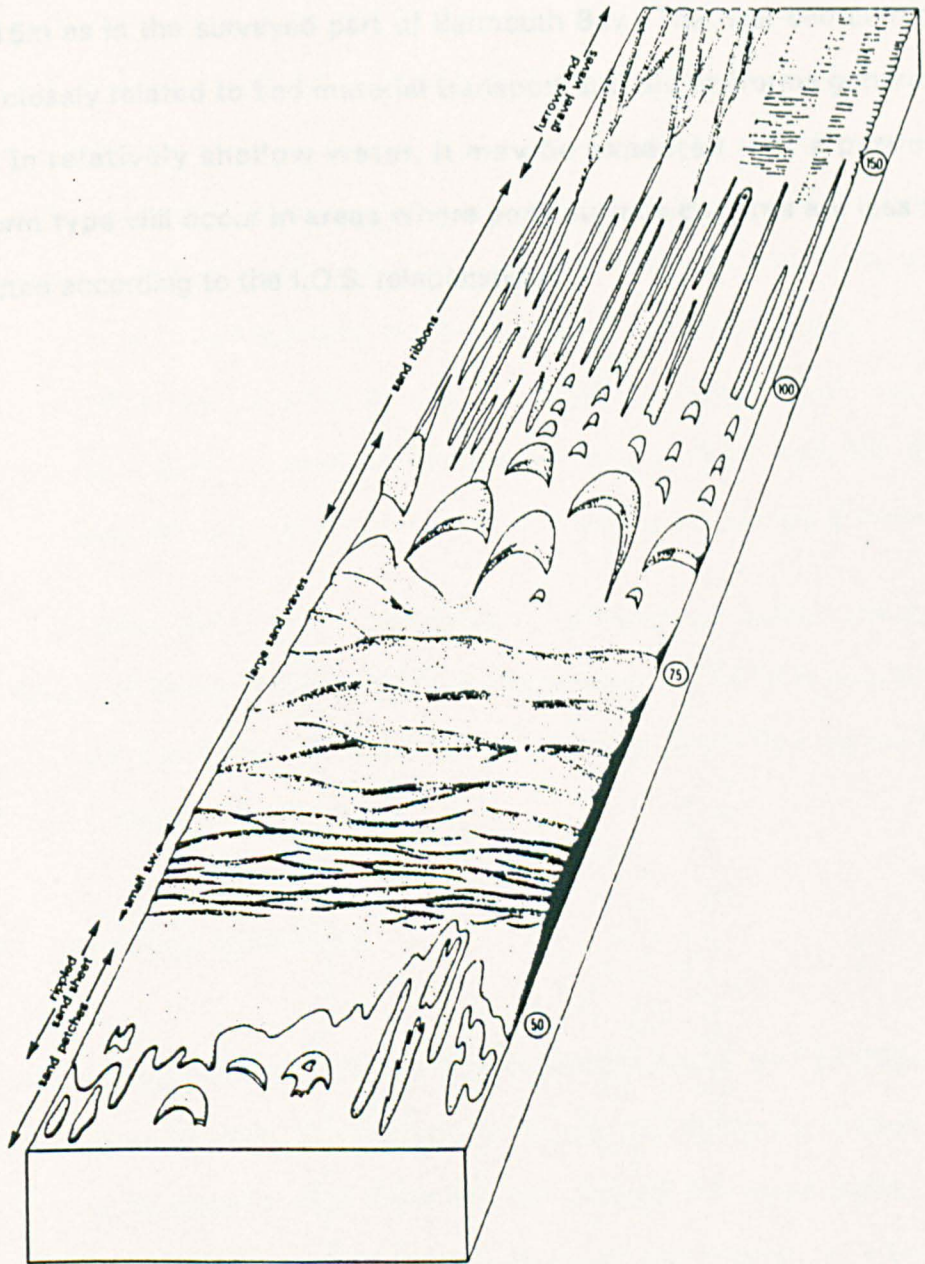
Some comments regarding the above descriptions are necessary to be fully useful for the Barmouth Bay area. A necessary addition to the list of bedforms is :

Sand patches - thinly spread sand bodies, irregular, transverse or longitudinal in broad outline relative to the flow, although their shape may be locally determined by the relief of the underlying material. They are usually less than a few hundred metres across and less than 2m high (Belderson et al, 1972). They are associated with spring peak surface currents of <0.5m/s. Werner & Newton (1975) proposed that sand patches may result from the decay of sand ribbons by reworking by waves and bioturbation. Belderson et al (1982) consider that longitudinal forms, distinct from sand ribbons by having smaller length to width ratios and more ragged edges, may be shown to have the same basic origin.

Belderson et al (1982) note also the possible presence on shelves of 'very low height sandwaves' ($<0.05\text{m}$), observed in flume studies by Guy et al (1966) and Williams (1967) in coarse sands. These have not been recognised in the marine environment and, if present, would be virtually unresolvable with normal sea bed surveying techniques. It would also be very difficult to distinguish them from 'planed-off' coarse-grained ripples. In marine surveys, another difficulty which can arise is in distinguishing 2-D megaripples from sand ribbons, which may appear almost identical on side-scan records. They may be distinguished by using nearby bedforms, or other evidence, to infer whether they feature are flow-normal or flow-parallel, i.e. are 2-D megaripples or sand ribbons, respectively. In this study, it was necessary to use the type and orientation of nearby bedforms, and evidence of tidal currents, to infer the identity of some bedforms.

It is also necessary to note the different ways in which velocity data is specified in quoted bedform stability fields. 'Near-bed' velocity fields are of most value if they are taken at common heights above the bedform (eg 1 or 2m), but it should be remembered that form drag over relatively steep bedforms can produce large velocity gradients (see Chapter 4), so quoted values may be of limited use when comparing values from different studies.

Despite drawbacks regarding the inconsistent relationship between spring peak surface currents and the near-bed hydraulics (eg. bed shear stress), the most successfully used velocity fields are the empirical relationships developed by workers at the Institute of Oceanographic Sciences, England. This uses the velocities of mean spring tide peak near-surface currents, and has been used to infer tidal current strengths and directions and, by implication, net sediment transport paths. Figure 1.20 shows a block diagram of the most common tidal shelf bedforms, together with their mean spring near-surface tidal currents; on the left where there is medium to high sediment supply, and on the right with slightly more limited sediment supply, although still sufficient to form most large-scale bedforms.



Block diagram of the main lower flow regime bedforms made by tidal currents on the continental shelf, with the corresponding mean spring peak near-surface tidal currents in cm/s.

After Belderson, Johnson + Kenyon (1982)

Fig. 1.20

However, an important limitation in the direct use of these velocity fields in Barmouth Bay is water depth. The bedform - velocity relationships were developed from evidence all around the British continental shelf, where water depths are generally from 30 to over 100m. In these depths, for a given surface current the near-bed velocity will be less than in the shallow depths of < 15m as in the surveyed part of Barmouth Bay. The near-bed current is more closely related to bed material transport and the bedforms generated; thus, in relatively shallow water, it may be expected that a particular bedform type will occur in areas where peak surface currents are less than expected according to the I.O.S. relationships.

1.15 Sedimentary Facies of Barmouth Bay

The data collected in this study define three distinct parts of the surveyed area. Enclosure 5 shows the distribution and orientation of various sedimentary features of Barmouth Bay, deduced from the side scan survey, and plotted at a scale of 1:10000. Figure 1.21 illustrates some common sedimentary features found in Barmouth Bay, and common relationships between them.

The flow-parallel sand ribbon has its thin edges shaped into flow transverse bedforms, such as 3-D megaripples, or ripples forming elongate ripple bands. Between the sand ribbons is shown a coarse granular substrate (dark record) underlying the mobile sand bodies (light speckly record). Superimposed upon the sand ribbon are 2-D megaripples, with the darker areas between some megaripples indicative of thin or absent sand cover.

The sedimentary facies identified are discussed below, using the terminology of Amos & King (1984), outlined above. The term sandwave is used throughout in the strict sense. Throughout the following sections, Enclosure 5 should be referred to.

1.15.1 The Outer Sand Sheet

Description

This has approximate southern and eastern limits of ~58000N and 13000W, and occupies the sub-horizontal sea bed in the northwest of the bay. Along its western edge there are well defined 2-D megaripples. There are also NE-SW elongate bedforms, with linear and occasionally branched outlines, commonly having a separation of 20m and height of 0.2-0.3m; they rarely extend up to 0.5m high. The elongate troughs between them are rippled, and the ripples have curvilinear, crestlines 0.9-2.8m apart, orientated normal to the trough, and heights of ~0.1m or less. The bedforms here are interpreted as thin longitudinal sand ribbons, which have ripples of a

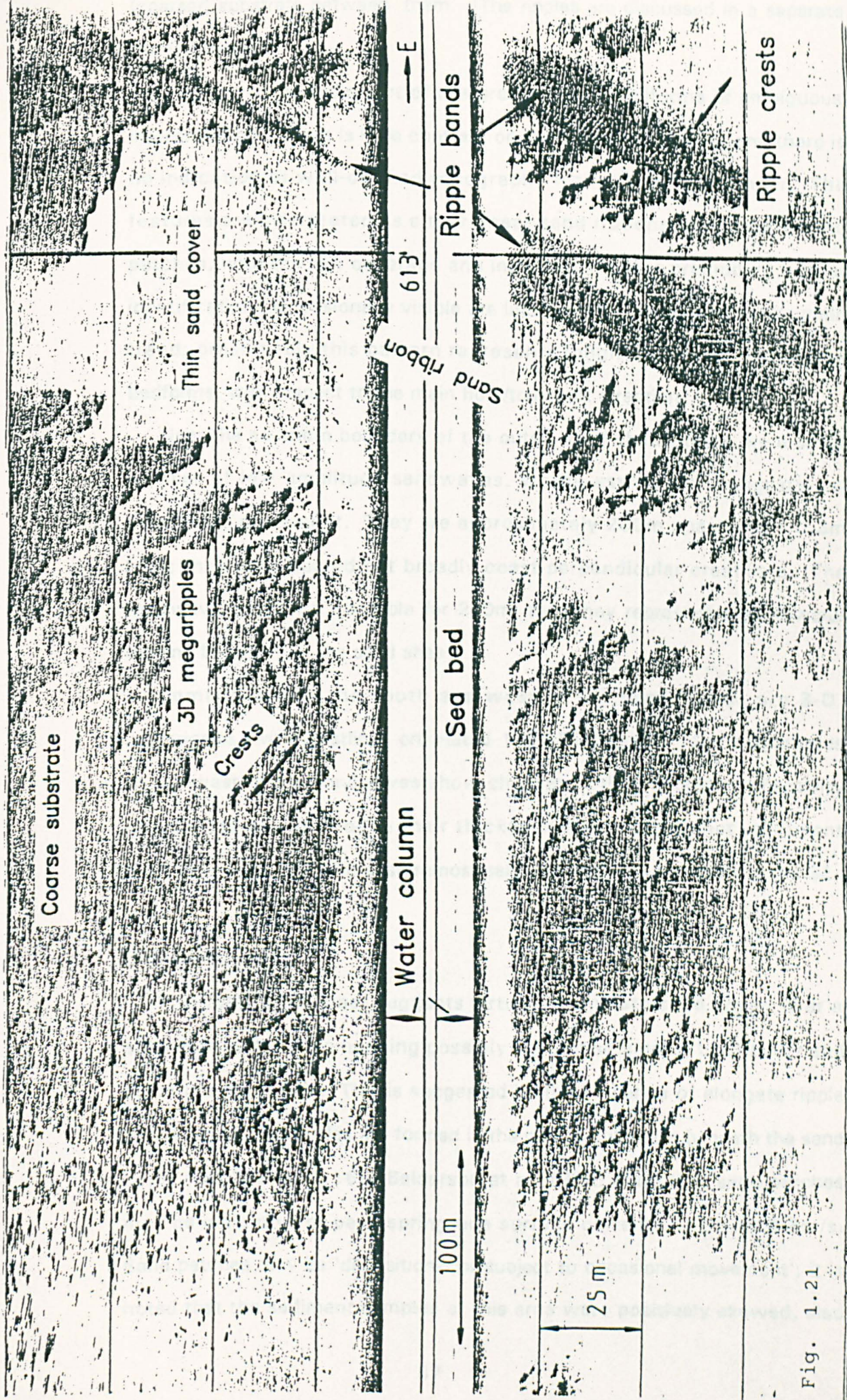


Fig. 1.21

Side scan sonar record showing common sedimentary features

(coarser) substrate between them. (The ripples are discussed in a separate section below).

The central northern part of this area contains bedforms of ambiguous interpretation. There is little contrast on the side scan records and there is no indication of well-defined topography from the echo sounder. The features are interpreted as either linear sand ribbons or elongate sand patches, with the low coverage and indistinct records precluding further identification. Occasionally visible are lineations perpendicular to the main trend; presumably this pattern represents longitudinal and transverse bedforms, with respect to the main flow/transport direction.

Near the southern boundary of the outer sand sheet, there are a small number of low amplitude sandwaves, whose asymmetry suggests net southward movement. They are approximately 200m apart and <0.3m high; they have curved but broadly coast-perpendicular crestlines. The sandwave crests are traceable for 220m; they may represent a southward-moving boundary of the sand sheet.

Immediately to the south and west of the sand waves are 3-D megaripples, with crestlines orientated 130-150 degrees. The megaripples to the west of the sandwaves show changes in their acoustic reflectivity interpreted as variation in their thickness and implying net sediment transport to the NE. The easternmost sandwave implies transport to the SE.

Discussion

The outer sand sheet suggests virtually complete sand cover, over a substrate material comprising possibly coarser sediment; both cover and substrate are mobile. This is suggested by the presence of elongate ripple bands, where the ripples are formed in the coarse substrate beneath the sand cover (see Section 1.16). Belderson et al (1972) state that sand patches may be indicative of peak spring tide surface currents of below 0.5m/s. Sand patches may be 'depositional or subject to occasional movement'; it is noted that the sediment samples of this area were positively skewed, also

implying a depositional regime (Chapter 6). Sand ribbons are formed where surface peak spring currents attain about 1.0m/s. At lower speeds of 0.9m/s, ribbon-like trains of megaripples may occur; at approximately 0.8m/s, smaller sand ribbons (~10m wide) are occasionally found on a gravel floor between isolated sand waves (see above). If the bedforms in the central northern part of the area are sand ribbons, then the bedforms of this facies infer maximum currents of 0.8-1.0m/s; they imply a slight southwards decrease in current speed and/or a southward increase in sand supply (Fig. 1.20). If they are interpreted as elongate sand patches, then the central northern area indicates tidal velocities of <0.5m/s.

The main axis of the tidal ellipse in central Barmouth Bay is aligned broadly SW-NE. The tidal current velocities suggested by the bedforms are probably higher than occur in fair-weather conditions except on the highest tides of the year (see above). It is concluded, therefore, that the bedform array is produced under extreme tidal and/or storm conditions, and that the central northern part of the area may be displaying sandribbons that are presently being reworked. Storm waves would be dominantly from a southwesterly direction, i.e. near-parallel with tidal currents over most of the bay, and these would enhance near-bed shear stress, so potentially producing shelf bedforms indicating apparently high tidal current velocities. These are tentative ideas, due to the lack of current data.

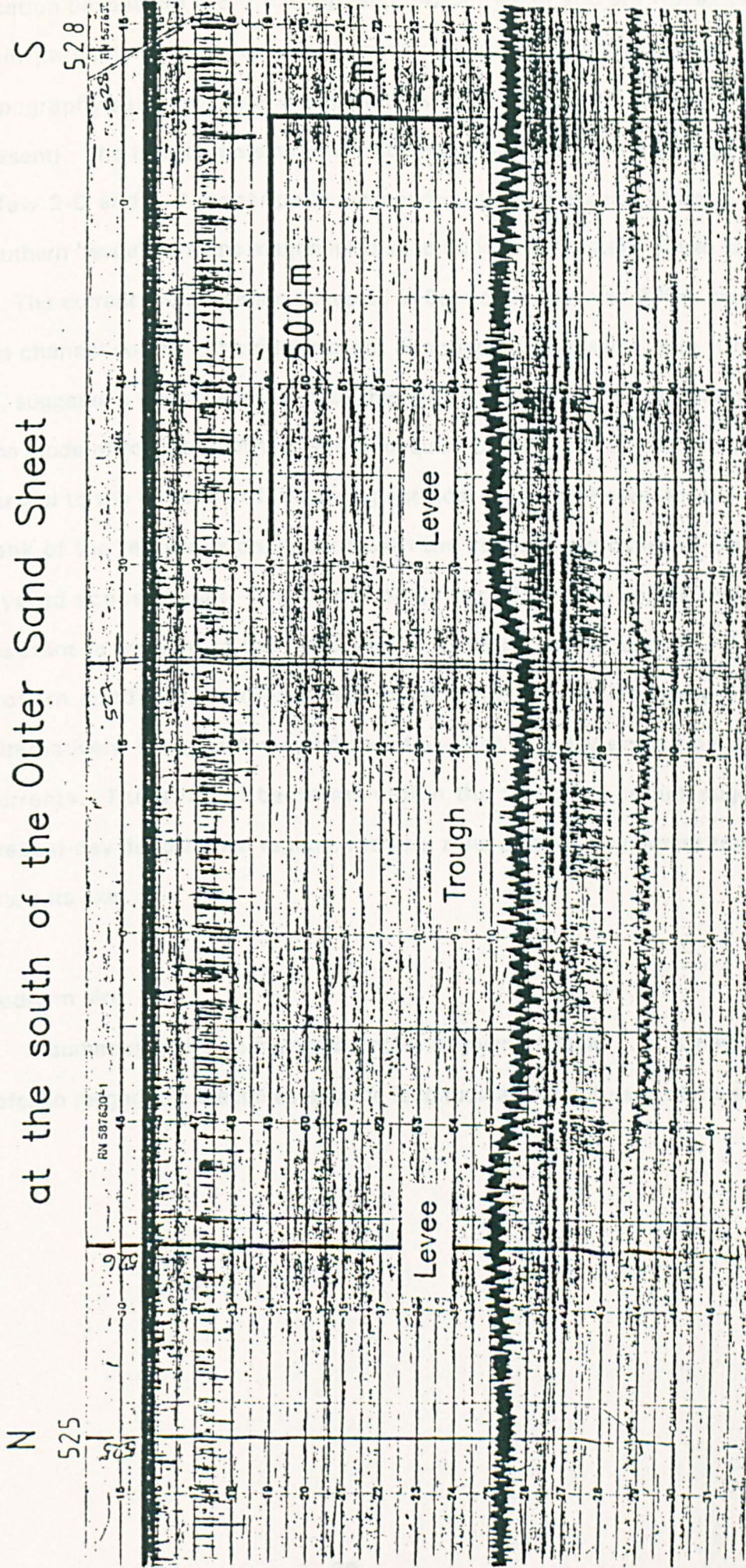
The hydrodynamic generation of the interpatch ripple-like bedforms is less clear. This is discussed later in Section 1.16.

Trough and Levee Feature

The southern limit of the outer sand sheet is marked by a WSW-ENE orientated trough, best seen between fixes 526 and 527 at G.R. 5740013200, where it is approximately 600m wide and 0.6-0.8m below the surrounding sea bed level (Fig. 1.22). Its 'banks' appear 'leveed' at this

Fig. 1.22

Echo sounder trace across trough and levee feature
at the south of the Outer Sand Sheet



location (levees are 0.3-0.6m high and ~400m wide) and are traceable for 2km parallel with the trough, becoming indistinguishable from other topography seawards (and presumably shorewards, but little evidence is present). The trough contains sand ribbons orientated 050-075 degrees, and a few 2-D and 3-D megaripples perpendicular to the sand ribbons. The southern 'levee' contains megarippled sand ribbons and parallel ripple bands.

The current meter station occupied in Barmouth Bay was 600m south of the channel centre. The tidal current directional information here (Chapter 2), suggests a direct causal relationship with the bedforms within the trough. The mode of formation of the feature is questionable. Its long axis is broadly parallel to the direction of the strongest tidal currents; however, the south bank of the feature is coincident with the sea bed exposure of the non-layered acoustic unit. The morphology suggests this unit is relatively resistant to erosion, so the bank may be a relict feature, formed under pre-modern conditions and exploited by the modern sedimentary regime. Alternatively, the trough may be maintained or actively eroded by modern currents. The array of bedforms within the trough does not suggest a present-day depositional regime, rather a zone of active sediment transport along its axis.

Bedform size

A summary of bedform morphologies is given in Table 1.2. Orientations refer to megaripple crestlines and the longitudinal axes of sand ribbons.

 Table 1.2
 Outer Sand Sheet - Summary of Bedform Morphologies

Bedform type	Depth m O.D.	Orientation degrees	Spacing m	Height m
3-D megaripples	-11.2 to -12.4	110-160	5-30 mostly <0.2	<0.5
2-D megaripples	-12.4	130-140	10.4	<0.2
Sand ribbons	-11.3 to -11.8	020-080 plus one	20-55 <100	<0.5
Sandwaves	-10.7	020-070 to -12.1	~200	<0.3

1.15.2 The 'Patchy' Sand Facies

Description

This occurs in the southwest portion of Barmouth Bay, south of 13000N and west of the 10m contour at 58000W. It contains the best developed bedforms within the bay. A variety of bedforms are present, including megaripples, sandribbons, sandwaves, and a few irregular, transverse, and longitudinal sandpatches. The sand cover is intermittent, with exposure of relatively resistant substrates forming topographic highs between sandy areas.

The most numerous bedforms of this area are sand ribbons and 2-D megaripples. The sand ribbons are concentrated in the south; they form small areas of sand between exposures of the substrate. They imply that the mobile sand cover is thin, and often show a darkening towards their edges; these are interpreted as thinning of the surficial sand, forming the ribbon. In general, they are orientated 060-080 degrees, but at the northern limit of their occurrence there are two examples of a more northeasterly orientation.

Many sand ribbons have 2-D superimposed megaripples, with crestlines near-perpendicular to the sand ribbon axes. Some sand ribbons have very diffuse edges, implying a degree of degradation, possibly towards longitudinal sand patches. (Side-scan coverage was often not sufficiently detailed to determine whether the bedform present was a megarippled sand ribbon or a megarippled sand patch. 'Ragged' edges of sand patches would be difficult to distinguish from edges of sand ribbons made irregular by the relief of the underlying substrate). In most cases, since it was known that mean spring peak surface currents attained velocities in excess of the upper limit of 0.5m/s on sand patches, it was not unreasonable to suggest that sand ribbons (rather than patches) were the more likely interpretation. It is likely that the bedforms surveyed were sand ribbons, being actively reworked towards less well-defined longitudinal forms - such as megarippled longitudinal sand patches.

(As a more general point, the 'correctness' of identification here is important in terms of:

- 1 - interpretation of the modern hydrodynamic and sedimentary regime;
- 2 - prediction of the likely form of the sedimentary deposit formed.

If the implications for the interpretation are the same, it is not really useful to the former to declare bedforms as one type or the other, more so because there is possibly a morphological continuum between the two end members).

In contrast, regular arrays of megaripples are found in the north, where there is more complete cover and an implied thicker layer of sand. Where the clarity of the records allowed the asymmetry of the megaripples to be seen, the lee sides always faced towards the NE, implying shorewards net transport of bed sediment. A small number of discrete barchanoid sandwaves, with superposed megaripples, are present towards the western edge of the area. The sandwaves have lee slopes facing the east. The presence of smaller bedforms, superimposed upon the stoss side of the sandwaves, suggests they are mobile features (Terwindt, 1971; Langhorne, 1973).

Discussion

Recalling the points made above regarding the shallow nature of Barmouth Bay, and the implications for the hydrodynamic interpretation of the bedforms, it is only possible to make a first order hydrodynamic interpretation of the bedform distribution pattern suggests faster currents in the south, nearer the shore. However, it is likely to fairly represent the distribution of peak relative velocities in the bay.

According to Belderson et al (1982) megaripples are representative of mean spring peak surface currents of 0.6-0.7m/s. The megarippled sand ribbons in the south suggest velocities of ~0.9m/s. Also inferred is a strong tidal current control on bedform orientation, with sand ribbons orientated parallel and megaripple crests perpendicular to the approximate direction of peak tidal current flow. Measured peak spring peak flood tide surface currents attain >0.7m/s in the north of this area. Together with the presence of megarippled sandwaves, which imply sandwave mobility (Terwindt, 1971), it is suggested that the bedforms in this area are nearer equilibrium than those in the outer sand facies. The nearby presence of the coastline at Llwyngwriil may be a significant factor in the production of high velocities in this area, particularly in the south.

Bedform size

A summary of bedform morphologies is given in Table 1.3. Orientations refer to megaripple crestlines and the longitudinal axes of sand ribbons.

Table 1.3

Patchy Sand Facies - Summary of Bedform Morphologies

Bedform type	Depth m O.D.	Orientation degrees	Spacing m	Height m
2-D megaripples	-11.6 to -14.3	110-180	7-50	<0.4
Sand ribbons	-12.0 to -13.0	055-075	43->50	<0.2
Sandwaves	-13.7 to -14.0	110-135	22-~100	<0.5

1.15.3 The Inner Sand Sheet

Description

This shoreface-attached sand sheet extends westwards from Ro Wen to approximately 59000W, south of the estuary mouth, and to 585000W north of Barmouth. Along Barmouth beach (north of 15000N) it is discontinuous, with an irregular area of gravel ~1km², which at 16000N suggests continuity with the coarse material exposed 1-1.5km further west. The sand sheet is thin, and 'ponded' between the coastline and the offshore sublinear exposure at around the -10m bed contour.

Bedforms seen on side-scan sonar and echo sounder records are only rarely easily identifiable, and bed features have generally poor acoustic definition on side-scan sonograms. This is considered to be due to the effects of shallow survey depths, such as the very low grazing angles of the sound waves reflected back from the edge of the side scan range, and the increased diffusive effects of sediment and other reflectors in the water column.

To the east and south of the estuary mouth bar, small fields of 2-D and 3-D megaripples show well lee- face orientation to the southwest.

Approximately 400m southwest of the seaward face of the bar, there are poorly-defined current lineations over 100m in length, of negligible relief, and orientated at 110 degrees. Similar features are better seen actually on the seaward face of the bar; they are tentatively identified as sand ribbons.

In the north, 2.5km from the estuary mouth, there are large sandwaves (wavelength 160m, height 1m) whose morphology implies coast-parallel net sediment transport southwards towards the mouth. South of the sandwaves are poorly defined 2-D megaripples, with generally coast-perpendicular crestlines. Some lineations cannot be identified; these include those in the extreme south, which are coast-parallel and have topography too small for resolution under the gentle swell conditions in which the survey was conducted. They occur within 200m of the shore, and are parallel to the tidal currents there.

3-D Geometry of the Inner Sand Sheet

Pinger data shows that within 1km of Ro Wen, there is a generally continuous and well-defined sub-bottom reflector at up to 5m below the sea bed. It forms the surface beneath the bar at G.R. 600143 (Fig. 1.23) and continues southwards for >3km. It is not apparent north of the bar. The reflector is exposed at its western edge, where the thickness of the inner sand sheet decreases to zero. Pinger and side-scan sonar records correlate well in showing this relationship. The reflector is also exposed on the shoreward side of Ro Wen (around G.R. 608143). Side-scan and observation at low water confirm the nature of this reflector as a cobble, pebble and gravel layer. At the south end of Ro Wen, the layer is correlated with similar coarse material exposed on the shore (eg. G.R. 600113). It is concluded, therefore, that the whole of the inner sand sheet is underlain by a single, continuous seaward-dipping layer of pebbles and gravel. It's contours are broadly aligned N-S, parallel with the main part of Ro Wen; the dip angle is ~0.3 degrees (Fig. 1.24). However, the surface is depressed along the line of the main channel leading seaward from the present-day

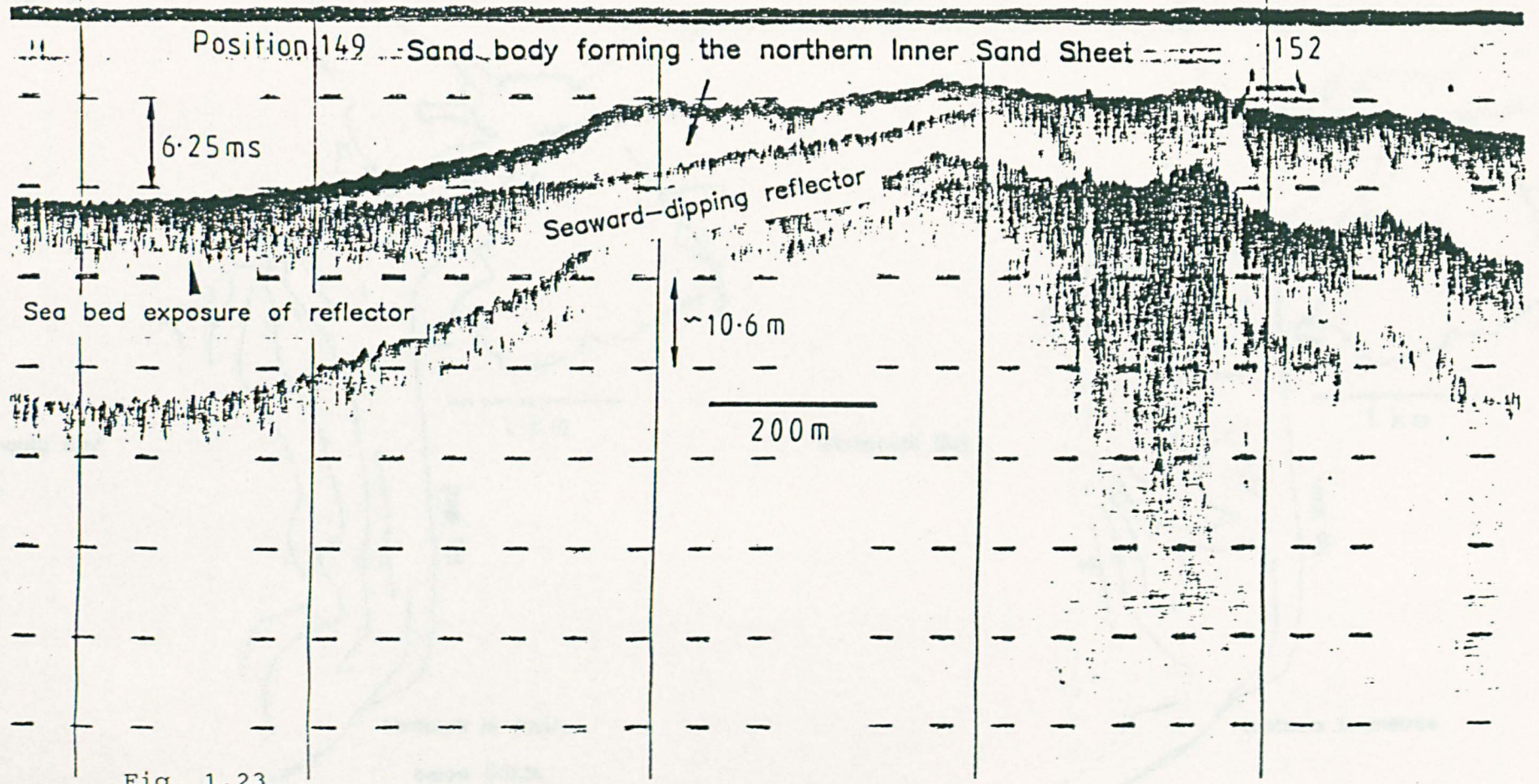


Fig. 1.23

Pinger record across Barmouth Bar, part of the ebb tidal delta

Fig. 1.24 Contours of the base of the Inner Sand Sheet

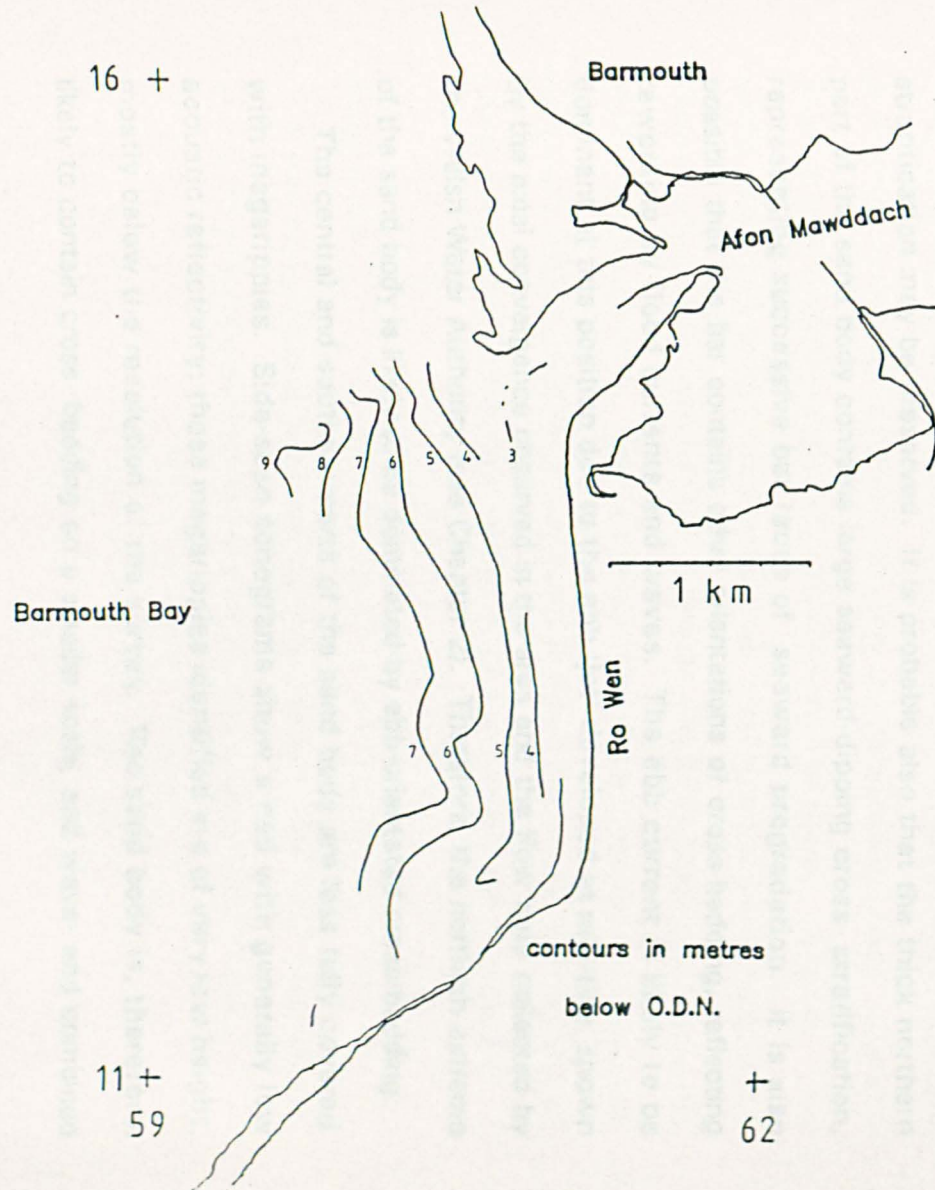
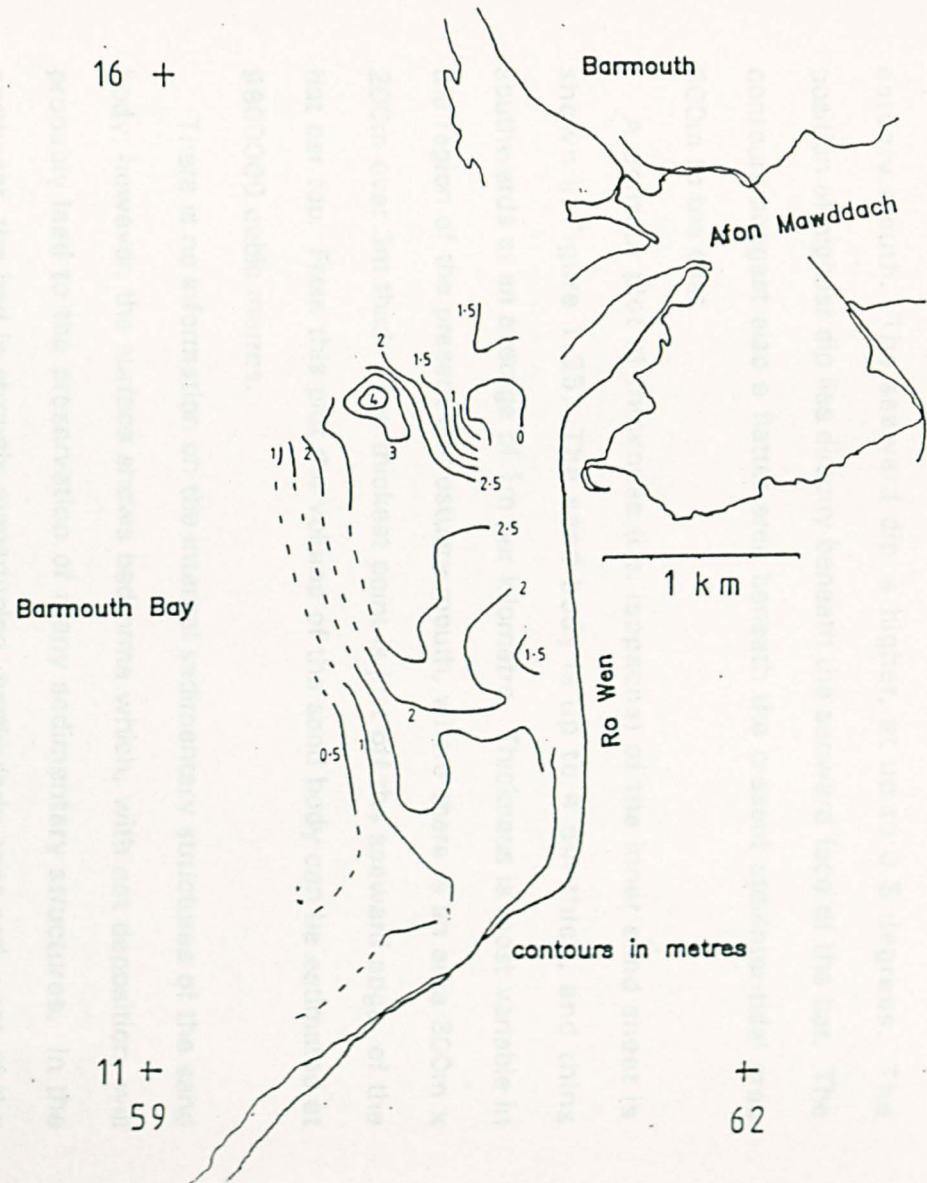


Fig. 1.25 Isopach map of the Inner Sand Sheet



estuary mouth. The seaward dip is higher, at up to 0.5 degrees. The position of highest dip lies directly beneath the seaward face of the bar. The contours suggest also a flatter area beneath the present sub/inter-tidal area 300m to the east.

A contour plot of thickness (i.e. isopachs) of the inner sand sheet is shown in Figure 1.25. The sand body is up to 4.5m thick, and thins southwards at an average of 1m per kilometre. Thickness is most variable in the region of the present-day estuary mouth, where there is an area 300m x 200m over 3m thick. The thickest point is just off the seaward edge of the flat bar top. From this plot the volume of the sand body can be estimated at 9600000 cubic metres.

There is no information on the internal sedimentary structures of the sand body; however, the surface shows bedforms which, with net deposition, will probably lead to the preservation of many sedimentary structures. In the northeast, the bed is strongly megarippled, particularly east and west of the beach exposure of the pebble layer; thus, both planar and trough-cross stratification may be preserved. It is probable also that the thick northern part of the sand body contains large seaward-dipping cross- stratification, representing successive bar faces of seaward progradation. It is also possible that the bar contains other orientations of cross-bedding, reflecting reworking by flood currents and waves. The ebb current is likely to be dominant at this position due to the ebb 'jet' developed at mid-tide, shown by the axial convergence observed in the area and the flow data collected by the Welsh Water Authority (see Chapter 2). Therefore, the northern extreme of the sand body is likely to be dominated by ebb-orientated cross-bedding.

The central and southern parts of the sand body are less fully covered with megaripples. Side-scan sonograms show a bed with generally low acoustic reflectivity; those megaripples identified are of very low height, mostly below the resolution of the survey. The sand body is, therefore, likely to contain cross- bedding on a smaller scale, and wave- and combined

flow ripple cross-laminations may be more prevalent.

Storms have a significant effect on the bedforms present nearshore, through the modification of strength and direction of the normal current regime. A net northwards longshore current will probably result from the most common, southwesterly storms, as shown by the gross morphology of the Ro Wen spit. Coarse sediment may be removed from the surf zone to be deposited onshore as storm beaches, whereas sand will be held in suspension and deposited further offshore, perhaps by rip currents (eg. Morang & McMaster, 1980) or by downwelling shore-parallel currents of the type described by Smith & Hopkins (1972), Swift (1976) and Swift & Freeland (1978).

Discussion

Away from the estuary mouth, most bedforms appear to be orientated transverse to a coast-parallel (i.e. N-S) flow. The flow data summarised in Section 1.7 above, shows that at the western edge of the facies, on spring tides, the flood direction is generally northward; on the ebb tide it is southward, or southwest nearer the line of the estuary mouth. The ebb appears slightly stronger than the flood, and is of greater duration. This would presumably produce a net southward sediment transport vector at the western edge of the sand sheet, agreeing with the observed sandwave asymmetry in the north. Steers (1948, 1969) using coastline morphology, and Moore (1968) using grain size samples taken in the bay, both suggested a local net southward transport vector to the north of the estuary mouth.

Bedform size

A summary of bedform morphologies is given in Table 1.4. Orientations refer to megaripple crestlines and the longitudinal axes of sand ribbons.

Table 1.4

Inner Sand Sheet - Summary of Bedform Morphologies

Bedform type	Depth m O.D.	Orientation degrees	Spacing m	Height m
3-D megaripples	~intertidal, on south side of main estuarine channel		4-8	<0.3
2-D megaripples	-9.0 to -10.0	080-100	12-17	<1.0
Sand ribbons	-3.0	110	7-10-20	<0.2
Sandwaves	-9.0 to -9.3	~045	60-160	0.6-1.0

1.16 Coastal Zone Ripple Bands

Morphology

Ripple bands in the coastal zone are well documented from many different locations (eg. McKinney et al, 1974; Morang & McMaster, 1980; Black & Healy, 1988, Hunter et al, 1988), but there has been considerable debate about their formation. However, their sedimentary morphology is well defined. If relief is apparent, it is negative; i.e. the ripple bands occur in elongate troughs. Trough widths vary between 15m (Swift & Freeland, 1978) and > 250m (Schwab & Molnia, 1987), and the troughs may broaden and shallow in an offshore direction, with the trough- perpendicular ripples gradually disappearing (eg. Morang & McMaster, 1980). Troughs are generally at least 10 times longer than wide, and are less than 1m deep. The ripples may be up to 3m in wavelength, up to 0.35m high, and of near-symmetrical profile.

1.16.1 Hypotheses of Ripple Band Generation

Alternating bands of coarse and fine sediment have been commonly found on tide-dominated shallow shelves, and the bands are near-parallel to the tidal currents (Kenyon, 1970; Stride et al, 1972). Where gravel is subordinate to sand, elongate gravel-floored depressions define the banding (i.e. furrows); where sand is subordinate, the bedform type is known as sand ribbons. However, in some cases it has been difficult to relate the long axis of the trough to the direction of the (assumed) generating flow, which Hunter et al (1988) state may often not be tidal. Swift & Freeland (1978) found that these bedforms tended to be nearly shore-normal on the shoreface and inner shelf, whereas further seawards most ripple bands were shore-parallel. They concluded that the nearshore features were troughs of low amplitude sandwaves produced in the downwelling coast-parallel flows during storms. The offshore features were explained as flow-parallel lineations caused by longitudinal vortices.

Morang & McMaster (1980) studied coast-normal ripple bands within 400m of the shore. They proposed three hypotheses for their generation :

- 1 - rip current action;
- 2 - rip current action and subsequent wave reworking;
- 3 - storm-generated flows (as Swift & Freeland, above).

Cook (1982) & Werner (1982) discussed these hypotheses, and Cook concluded that the formation of wave ripples from plane-bedded sand deposited by rip-currents, was a plausible alternative to storm flow generation. Hunter et al (1988) observed on shore-normal ripple bands that the coarse sand ripples were orbital wave ripples, with spacing proportional to the near-bed orbital diameter, and commonly active rather than storm-produced. However, in their study area shore-parallel bands were dominant, and, having ruled out tidal currents and shore-parallel standing waves as explanations, they could only speculate that explanations for this trend were one of :

- 1 - the bands were longitudinal to a longshore current;
- 2 - transverse to a shore-normal current;
- 3 - transverse to wave-orbital oscillatory currents.

In an attempt to explain ripple bands of the Whangarei Harbour ebb-tidal delta, Black & Healy (1988) undertook a numerical modelling investigation examining wave refraction as a possible causal mechanism. The bands were aligned with the dominant wave orientation, and typical near-bed orbital velocities exceeded threshold values. The symmetrical ripples also increased in wavelength shorewards; thus a wave generation mechanism for the ripples was strongly inferred. The wave refraction study showed that the sea bed morphology concentrated wave energy along a zone coincident with the location of the ripple bands. Furthermore, the localised increased heights and the associated shoreward current could explain the occurrence of the bands

in zones, the coarser grain size, and their presence in topographic lows.

Schwab & Molnia (1987) identified linear depressions, many of them rippled, in water depths of 30-90m on the north Aleutian shelf. They speculated that they were erosional, current-parallel features caused by tidal currents enhanced by storm-induced flows. The ripples were probably wave-induced by the large and frequent storm waves of the area. Leckie (1988) showed that wave-formed coarse-grained ripples form in depths of up to 160m. Crest spacings vary between 0.25 and 3.0m, and heights are 0.05-0.35m. Leckie (1988) calculated that waves which generated such ripples were not large storm events, but had heights of 2-5m and periods of 8-14 seconds. He postulated that coarse-grained ripples are the hydrodynamic equivalents of three-dimensional hummocky cross-stratification. In medium to coarse-grained sand, or pebbly sand, two-dimensional coarse-grained ripples would form under oscillatory or combined flow; in fine sand hummocky ripples would form.

1.16.2 Ripple Bands in Barmouth Bay

Linear bands of ripples were found most in all regions of the bay. In Table 1.5 the details of ripple bands found in Barmouth Bay are presented.

Discussion

The ripple bands encountered in this survey all had negative relief of less than 1m, and usually less than 0.3m. The rippled troughs often merged, (i.e. adjacent troughs became wider and shallower), dominantly seawards (although not exclusively), and where more consistent in width, troughs also bifurcated in both directions.

Table 1.5

Morphology of Ripple Bands in Barmouth Bay

Grid Ref. m	Bed Height ODN	BO degs.	BS m	BW m	BL m	BD m	L m	H m
Outer Sand Sheet								
A	555155	-11	045	21	10	<400	<0.2	1.3 0.15
B	558150	-11	030	55	10	200	0.4	0.9 0.14
C	572174	-11	045	-	5	>140	0.2	? ?
D	560130	-13	040	32	-	>200	<0.5	1.2 0.1
E	571132	-12	060	90	3	<410	0.2	? <0.1
<div style="display: flex; justify-content: space-between;"> -070 -15 -50 -50 -2.8 </div>								
Patchy Sand Facies								
F	535097	-13	075	43	20	>250	<0.2	? <0.1
G	557101	-13	050	65	20	<600	<0.2	? ?
H	565108	-12	060	58	13	>200	<0.2	0.75 <0.03
I	553092	-13	035	-	17	>160	<0.2	0.8 <0.02
J	579129	-10.5	040	70	230	>330	<0.2	1.0 0.15
<div style="display: flex; justify-content: space-between;"> -070 -22 -0.9 -0.55 -0.3 </div>								
Inner Sand Sheet								
K	589169	-9	070	-	99	>160	1.0	0.7 <0.03
L	587147	-9.5	080	130	?	>130	<0.2	1.0 0.07
M	580128	-10.5	070	110	14	>200	0.3	0.66 0.1
N	582117	-10.7	065	80	6	>500	<0.2	0.9 0.07
O	585117	-10.5	060	75	11	>500	<0.3	? ?
<div style="display: flex; justify-content: space-between;"> -090 -080 -70 -0.1 -0.80 </div>								

- Notes :
- BO - Ripple band orientation
 - BS - " " spacing
 - BW - " " width
 - BL - " " length
 - BD - " " depth
 - L - Ripple wavelength
 - H - Ripple height

Trough length to width ratios are mostly greater than 10, and band widths in broad agreement with the limits quoted above, with only a few less than the lower 'limit' of 15m. However, it is often not easy to define

precisely the width of those bands which are very shallow and have no well-defined edges.

There is evidence to suggest a role for tidal currents in the generation or maintenance of the rippled bands. Many of the bands are laterally bounded by 2-D or 3D tidal megaripples, which have crests normal to the long axis of the bands. This could either be a result of coincidence in the direction of the band-forming currents and the tidal flows, or a direct tidal relationship. Certainly, in the outer sand facies, the ripple bands are orientated approximately parallel to the direction of the tide, further suggesting a tidal component in their generation. However it is also possible that during storms the 'overflow' southwards through the Mochras Channel from Tremadoc Bay (Caston, 1965) could combine with the southwesterly flowing ebb tide to greatly increase the currents in the north of Barmouth Bay, and produce the conditions suitable for ripple band generation. That there are no ripple bands in the depositional centre of the outer sand facies may imply that beneath the surface may be ripple bands, infilled by the sediment transport under fair-weather tidal conditions.

Orientations of ripple bands in the patchy sand facies are strongly parallel to the tidal currents, and also to the sand ribbons, evidenced by the fact that megaripples on the sand ribbons have crests orientated normal to the ripple bands (Fig. 1.26). The sand ribbons were above interpreted as being formed under spring tidal currents with or without a significant wave component. There is, thus, the probability that the ripple bands also have a tidal component in their generation, i.e. that they may be generated beneath tidal currents enhanced by storm waves. However, this conclusion must be tempered by the probability that the predominant direction of wave travel from strong southwesterly winds will be parallel to the tidal currents in this area.

Band depths were most consistent and shallow in the patchy sand facies, with deeper troughs in both inner and outer sand facies. This suggests that

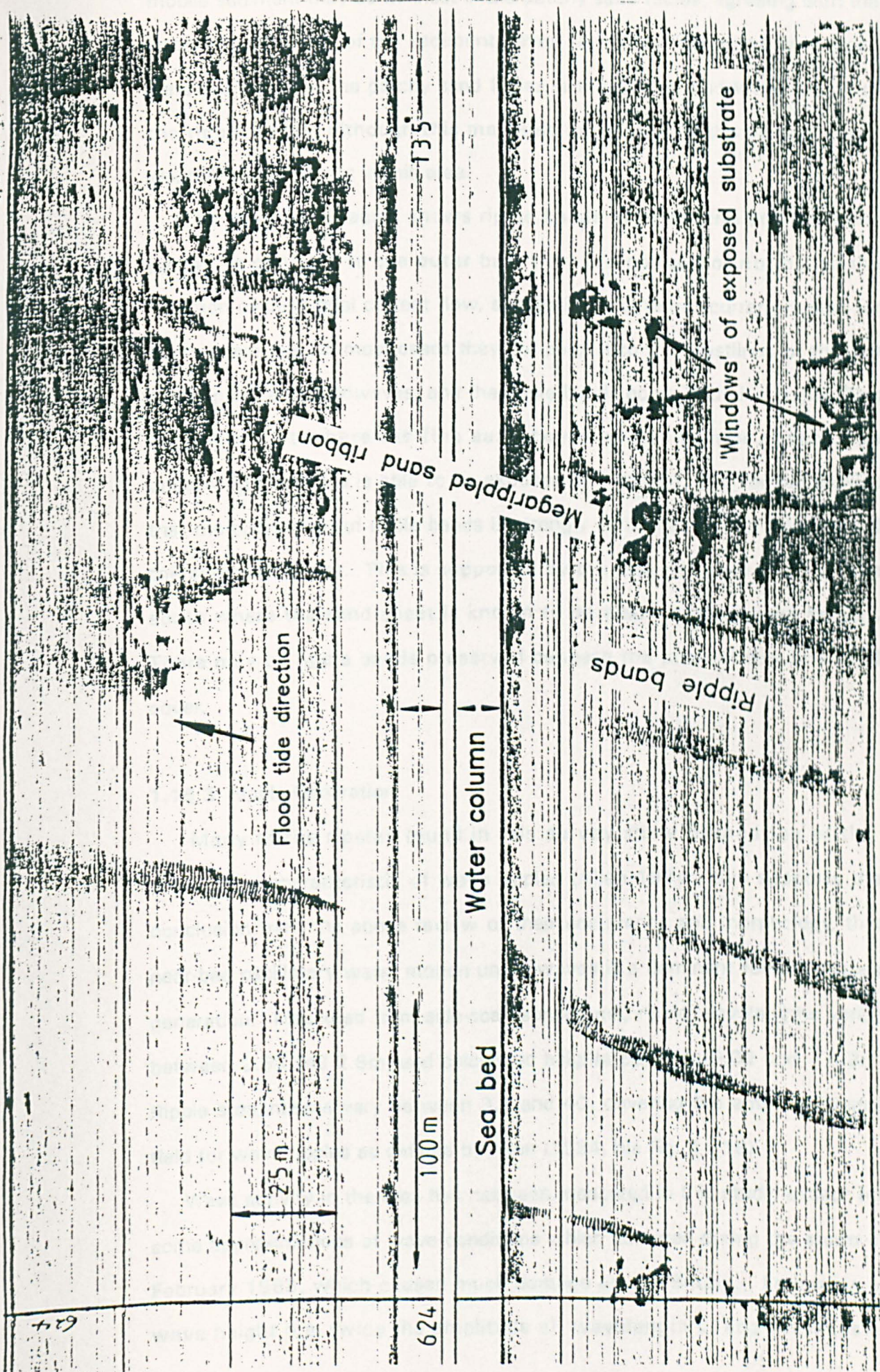


Fig. 1.26 Ripple Bands in the Patchy Sand Facies

mobile sediment may be thinnest in the patchy sand facies, agreeing with the impersistent nature of the sediment cover. A further indication of reduced sand availability in the patchy sand facies is the greater width and length of the ripple bands, although this may also be related to the stronger fair-weather tidal currents in this area.

The inner sand facies shows ripple bands in its central and northern parts. In contrast to the outer bay, they are oblique or normal to the direction of peak tidal current flow, suggesting a different current regime for their generation. In most cases they are parallel to the crestlines of the 2-D megaripples and sandwaves, and the ripple bands occur in their troughs. This suggests that where the fine sand cover is very thin or absent, the underlying substrate is able to be exposed and rippled, and further implies that the distribution of ripple bands is strongly controlled by the thickness of the sediment cover. This is supported by the lack of ripple bands in the south where the sand sheet is known to be over 1m thick (see below). There may be ripple bands preserved beneath the present day fine sand cover.

1.16.3 Ripple Generation

Many of the ripples found in this survey show bifurcation of the crestline, a characteristic of wave ripples (Allen 1984); this supports the conclusion from the above review of their occurrence and morphology, that near-bed oscillatory water motion under waves is a dominant feature in their generation. Measured from side-scan sonograms, ripple wavelengths varied between 0.66 and 2.8m, and calculated heights between 0.02 and ~0.3m. Ripple steepnesses vary between 3.3 and 40, covering the entire existence field for wave ripples as defined by Allen (1984, his Fig. 11-18).

Wave activity in the area has not been measured in this study, except for some approximations of wave conditions which occurred during the storm of February 1988, which caused much damage across Britain. Estimates of wave height (i.e. twice the amplitude a), wavelength L , and averages of

wave period T, were made on 20 waves, at three locations: Barmouth Bay (as viewed from the cliffs to the south), Barmouth Harbour, and half-way along the estuary at Farchynys. These are likely to be near the most extreme wave conditions experienced in the bay and estuary. Data are presented in Table 1.6.

Table 1.6

Wind and Wave Conditions
during the Storm of February 1988

Position	W I N D			W A V E S		
	Direction degrees	Mean m/s	Gusts m/s	Period sec	Wavelength m	Height m
Barmouth Bay	~250	>25	>30	9-10	50-100	<2
Barmouth Harbour	240	25-30	>35	2	11-12	0.5-0.7
Farchynys	240	>25	>30	3.6	~<20	0.5-0.7
Llanelltyd	220	20	>30	-	-	-

The estimated wavelengths are shown to be reasonable by comparison with Newtonian theory for waves. For waves of known period T in known depth D

$$Q^2 = g k \tan(k h) \quad (1.4)$$

where $Q = 2 \pi / T$

$$g = 9.81 \text{m/s}^2$$

and $k = \text{wave number} = 2 \pi / L$

where $L = \text{wavelength}$

$h = \text{water depth.}$

By using water depths of 5-15m for Barmouth Bay, and 2-3m at Farchynys, and solving this equation by iteration for the conditions above, the predicted wavelengths for the bay and Farchynys are 60-95m and 14-16.5m respectively, comparing well to the estimates. The wavelengths in Barmouth Harbour were measured against the Barmouth Lifeboat.

These wave parameters can be used to approximate near-bed orbital diameters and velocities by

$$U_z = \frac{a Q \cosh(kz) \sin(kx - Qt)}{\sinh(kh)} \quad (1.5)$$

where U_z = orbital velocity at height z above bed

a = wave amplitude i.e. 0.5 x height

and $\sin(kx - Qt)$ represents the oscillatory motion.

So the orbital velocity at the bed U_o may be written

$$U_o = \frac{2 \pi a}{T \sinh(2 \pi h / L)} \quad (1.6).$$

The orbital diameter d_o is given by

$$d_o = (2 U_o) / Q \quad (1.7).$$

Results are given below in Table 1.7.

Table 1.7

Calculated Orbital Velocities and Diameters for Storm Conditions
(plus 'normal' conditions for Barmouth Bay)

Position	T sec	L m	a m	h m	U100 m/s	U _o m/s	d _o m
'Barmouth Bay 'Storm'	9	60	0.75	5	0.96	0.95	2.72
	9	81	0.75	10	0.61	0.61	1.75
	9	95	0.75	15	0.45	0.45	1.29
Barmouth Bay 'Normal'	4	22	0.25	5	0.21	0.20	0.25
	4	24.7	0.25	10	0.06	0.06	0.08
	4	25	0.25	15	0.02	0.02	0.02
	4	22	0.5	5	0.42	0.40	0.51
Barmouth Harbour	4	24.7	0.5	10	0.13	0.12	0.15
	4	25	0.5	15	0.07	0.04	0.04
Farchynys	2	11.5	0.3	6	0.08	0.07	0.05
	3.6	14	0.3	2	0.56	0.51	0.58
	3.6	16.5	0.3	3	0.40	0.37	0.42

Note : results given to the nearest 0.01m/s.

The coarsest material sampled in Barmouth Bay is 685um (0.55phi) in modal diameter, being a sample of the substrate taken by divers from beneath the surface rippled fine sands. Under unidirectional flow, the critical threshold velocity at 1m above bed for the substrate is 0.56m/s (Miller et al, 1977). A steady current of this magnitude is probably only exceeded in Barmouth Bay by large spring tides, or possibly by ebb currents enhanced by overflow from Tremadoc Bay (see above). Storm waves create orbital velocities exceeding this value in those parts of the bay shallower than 12-13m (Table 1.7).

Under a purely oscillatory current, movement of the substrate grains will occur when the maximum orbital velocity U_o exceeds 0.17m/s, and plane beds will be formed when U_o > 0.95m/s (Allen, 1984, his Fig. 11-19). Therefore, the storm waves acting alone would create plane beds in those

parts of the bay shallower than ~5m, and wave ripples throughout the bay and shallow parts of the estuary. On abatement of the storm waves, the orbital velocities will decrease, and in Barmouth Bay wave ripples would be formed in the substrate. Under 'normal' wave conditions, the threshold for rippling of the substrate is likely to only be achieved in those parts of the bay less than ~10m deep.

The surface fine sands of Barmouth Bay vary in modal size mostly between 2.4 and 2.7phi (190-154um) (Chapter 6). These sands become rippled at orbital velocities above 0.1m/s, and the transition to plane beds occurs at 0.64-0.68m/s (Allen, 1984, his Fig. 11- 19). This suggests that in 'normal' wave conditions at slack tide, only the fine sands in depths less than ~10m may form wave ripples. The position of the rippling/no motion boundary will be further inshore at high water than at low water. By contrast, storm waves cause oscillatory currents at the bed which exceed the fine sand threshold over the whole of Barmouth Bay. In depths less than ~10m the sand will be formed into plane beds, and only become rippled again as the storm waves die away.

The above suggests that the ripple bands of the Inner Sand Facies are capable of being formed under 'normal' wave conditions, without the enhancement effects of the tidal currents. However, tidal current directions over this facies are strongly oblique to the ripple band orientations, with relatively limited bed shear stress enhancement effects. It is tentatively concluded that, in this facies, the bands represent bedforms generated under waves larger than normal. As concluded above, ripple band orientation is also related to the thickness of the fine sand cover, which is thin in the troughs of the coast-normal megaripples and sandwaves.

The ripple bands of the Outer Sand Facies and Patchy Sand Facies may be formed by storm waves alone or under a wave-current flow regime, possibly under 'normal' wave conditions with spring tides. Conclusions are limited by the lack of data on tidal flow patterns under fair-weather and storm conditions.

The effects of waves upon sediment transport rates is considered below. Fuller discussion of the bedform populations of Barmouth Bay, and the morphology of ripple bands will be presented in a separate publication.

1.17 Sediment Transport Rates

1.17.1 Bedload and Total-Load Sediment Transport Equations

Many workers have devised equations designed to predict a measure of sediment transport under 'equilibrium' conditions in water streams. The measure of sediment transport may be either as suspended load, bedload, or total load, and may be based on a treatment of physical theory, field or flume observations, or a combination. The effects of bedforms is included in some equations, whereas others apply only to plane beds. Some formulae include a grain movement threshold condition, others predict grain movement at all flow stages, which is rather unsatisfactory.

Allen (1984) divided sediment transport equations into five types, where transport is explained in terms of :

- 1 - bed shear stress;
 - 2 - fluid velocity;
 - 3 - a probabilistic view of particle movement;
 - 4 - bedform migration rate;
- and 5 - energetics.

Allen (1984) critically discussed the theoretical rigour of each type of equation, and concluded that the most satisfactory bedload transport formulae are those based on energetics. This type of equation uses the concept that the transporting fluid has a certain available amount of power, which does work by transporting sediment along the bed. All the above types of formulae depend on calibration with data from flume or field studies, which Dyer (1986) points out is both their strength and their weakness. The equations will only be as good as the data used to calibrate them, and their use will be restricted to the range of conditions of the calibration data. All formulae were developed for unidirectional flows, but have been used in the marine environment with little or no modification to account for the influence of waves or tides.

Many different equations have been used in tidal environments, including the equations of Yalin (1963,72), Bagnold (1963,66,73,77, modified by Sternberg [1972], Gadd et al [1978], Vincent et al [1981] and Hardisty [1983] amongst others), Ackers & White (1973), Engelund & Hansen (1967) and Van Rijn (1984). Some of these equations were field tested by Heathershaw (1981) who, in the subtidal environment, compared measured transport rates from tracer dispersion experiments to those from sediment transport equations. He found that the formula of Gadd et al (1978) gave good overall agreement with measured rates, and found the Engelund & Hansen (1967) equation best in depths of ~5m. Lees (1983) calibrated five sediment transport equations in depths of up to 15m in the Sizewell-Dunwich Banks area off the Suffolk coast, also using tracer sand measurements. She found that Yalin's (1963) formula gave best results, and Bagnold's (1963) formula was least comparable with observed transport rates.

Pickrill (1986), using sediment traps, measured sediment transport rates in the tide-dominated entrance of Rangannu Harbour, New Zealand, and found that a modified form of the Yalin (1963) equation produced transport rates similar to the trap over sand beds. Transport rates over shell/gravel lag surfaces appeared independent of near-bed tidal velocity, being more dependent on the passage of pulses of sand moving across the lag surface in 'ribbons', and thus in these cases the sand transport was limited by sand availability rather than flow power.

Use of sediment transport equations in the intertidal environment has been less common, but some examples are the studies of Carling (1981), Collins et al (1981), Jones (1984), Terwindt & Brouwer (1986), and Kohsiek et al (1988). Yang (1986a,b) has recently modified Bagnold's (1963) equation, noting that both the suspended load and total load equation, twice included the energy loss due to bedload transport. On applying the modified equations, sediment transport rates from intertidal megaripple migration were found to be closer to calculated total load (i.e. bedload plus intermittent suspended load) transport rates than those predicted by the bedload

equation. He interpreted this as evidence that megaripple migration involves both bedload and intermittent suspended load transport, which together he termed 'bed material' transport.

1.17.2 Suspended Load Equations

Adams & Weatherly (1981) noted that the 'virtual absence of contemporaneous flow and suspended sediment measurements', forcing a modelling approach to the problem, and Sternberg et al (1988) stated that suspended sediment distributions have not been well tested, thus marine scientists using these relationships have no perspective on the precision or applicability of their results. A heavily used equation to describe the vertical distribution of sediment in a homogeneous boundary layer flow is that of Rouse (1937), often referred to as the Rouse equation

$$\frac{C}{C_a} = \left(\frac{h-z}{z} \cdot \frac{a}{h-a} \right)^{w/kU^*} \quad (7.18)$$

where :

C = sediment concentration at height z above bed

C_a = reference concentration at " a " "

h = water depth

w = particle settling velocity

k = von Karman's constant

and U^* = shear velocity.

Use of this equation requires the measurement or prediction of a reference level concentration, and the equation is solved either for a bulk sediment sample or for each size range if more than one grain size class is in suspension. The reference concentration has been predicted from bed grain size and flow conditions, including work in rivers (Lane & Kalinske, 1939),

and by modelling of marine boundary layers (Smith & McLean, 1977a; Adams & Weatherly, 1981; Shi et al, 1985; Drake & Cacchione, 1989).

The Rouse equation has been modified by some workers to take account of flow stratification induced by high near-bed sediment concentrations (Smith & McLean, 1977a; Adams & Weatherly, 1981; Heathershaw, 1979). The general relationship between the reference concentration and the bed material is given by Sternberg et al (1988) as

$$C_a = \frac{X_o I_b C_b S}{1 + (X_o S)} \quad (7.19)$$

where :

I_b = the proportion of a grain size class in the bed sediment

C_b = bed volume concentration (1 - porosity, i.e. ~0.6 - 0.65)

S = Excess shear stress (i.e. $[T_o - T_c] / T_c$) where T_o = bed shear stress, and T_c = critical shear stress for sediment movement

X_o = an empirical constant, determined variously as :

2.4E-3 by Smith & McLean (1977a);

1.6E-5 by Wiberg & Smith (1988);

and between 2E-5 and 5E-5 by Drake & Cacchione (1989).

Using the Rouse equation with a simplified correction for sediment-induced flow stratification, Sternberg et al (1988) predicted concentrations at 0.2m above the bed within +/-50% of measured concentrations.

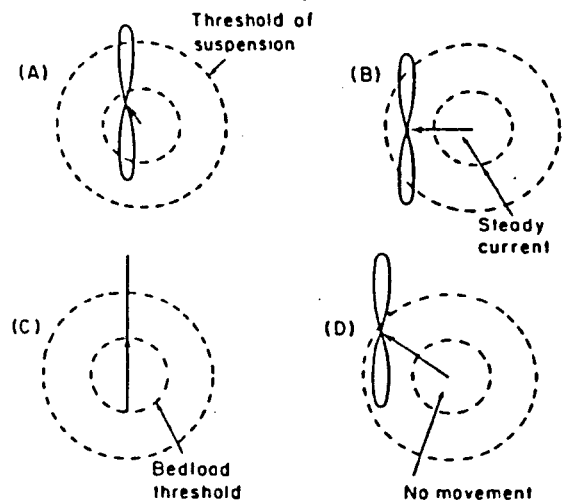
The suspended sediment transport rate is the integral through the water depth of the suspended sediment flux, i.e. the product of velocity and sediment concentration. Some general relationships between velocity and suspended sediment transport rates have been established. Dyer (1980), over an ebb cycle in Start Bay, obtained transport rates proportional to the seventh power of the depth mean velocity, and Owen & Thorn (1978), in the outer Thames Estuary, found a relationship to the fourth power of the flow.

1.17.3 Effects of Waves on Sediment Transport

Under a combined flow of waves and currents, sediment transport rates tend to be greater than under purely unidirectional currents. Of great importance in the angular relationship between near-bed wave- and tide-induced currents. Dyer (1986) presents a neat summary diagram (Fig. 1.27) of the range of possible effects on the entrainment and transport of sediment by the interaction of a steady current with waves from different directions. Wave-induced currents are important in causing periodic enhancements of bed shear stress, and therefore sediment movement, the threshold of which may not be exceeded by the action of the steady flow alone. Grains may be suspended by such interaction, and once in suspension, are able to be transported by relatively slow steady currents, which alone are below transport threshold velocities.

Net sediment transport vectors may be parallel or oblique to the direction of the steady current. It should be noted that there are many complex relationships between waves and tidal currents in the marine environment. Tidal currents vary in speed with time, and may be either rectilinear or rotary in nature. Waves are not consistent in period, direction or height with time, neither is the combination of waves that together constitute the total wave environment at a particular time. The combination of possible tidal and wave conditions in an area are therefore almost infinite, and field studies are forced to simplify, by considering 'representative' conditions of some sort. In flumes, the study of these interactions is restricted to cases where waves are either co-directional or contra-directional to the unidirectional current.

Dyer (1986) states that 'in order to establish a predictive sediment transport formula for combined currents and waves, it is necessary to calculate the fluctuating shear stresses at the bed and to integrate them over a wave cycle'. This mean shear stress could then be used in a unidirectional sediment transport formula. However, this is obviously a simplification of the changing processes of sediment entrainment and transport within each



Diagrammatic representation of the interaction of waves with a steady current. The curves trace the tip of the combined velocity vector during the wave oscillation. (A) Sediment would be moved on the forward stroke much more than on the backstroke, whereas no movement would have been possible for the steady current. (B) Sediment movement equally on either stroke of the wave oscillation. (C) The codirectional case. (D) Suspended sediment movement on the forward stroke. In (A) and (D) Sediment movement would be to the right of the steady current direction. In (B) and (C) movement would be in the direction of the steady current

(After Dyer, 1986)

Fig. 1.27

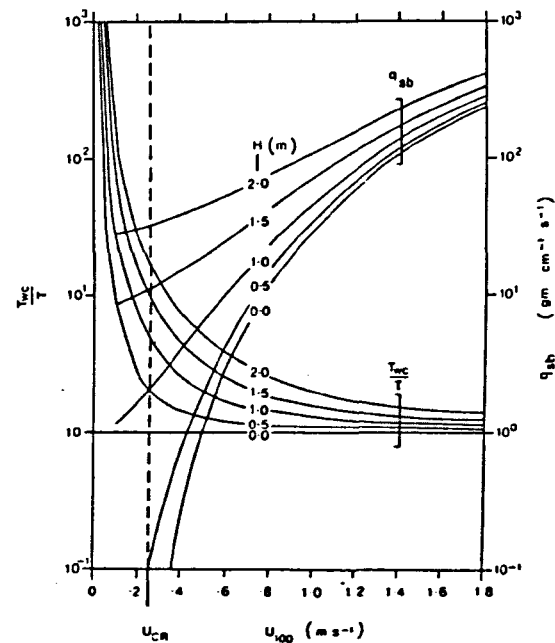


Fig. 1.28

The ratio of the bed shear stress due to waves and currents (τ_{wc}) to the bed shear stress due to currents alone (τ), calculated using Bijker's (1967) equation. The effect of increasing wave height (H) on bedload transport rates (q_{sb}), calculated from Bagnold's (1963) equation, is illustrated in terms of the near-bed current U_{100} . U_{CR} is the steady current threshold. (After Heathershaw and Hammond, 1980a.)

wave cycle, and the integral transport rate may be different to the transport rate calculated from the integral shear stress.

Bijker (1967) presented an equation which assumes that there is a viscous-sublayer in the steady flow, and at the height of this layer the orbital velocity and tidal current vectors are added. The resultant velocity is converted to a bed shear stress via

$$T_{wc} = P l^2 (dU_{wc} / dz)^2 \quad (7.20)$$

where: T_{wc} = bed shear stress due to combined waves and currents

U_{wc} = combined velocity at height z above bed

P = water density

and $l = 0.4z$.

The total resulting shear stress, which can be considered as an enhancement factor, is

$$T_{wc} / T = 1 + 0.5 (N (U_o / U))^2 \quad (7.21)$$

where :

T = bed shear stress

$N = 0.45 \ln ((h / Z_o) - 1)$

and U = depth-mean tidal current.

There is some doubt upon the validity of the constant 0.45 above, as it was empirically determined above stones and rippled sands, above which flows would not form a laminar sublayer except under slow steady velocities (Dyer, 1986). Provided current velocities are known, and a roughness length is assumed, the enhancement factor can be calculated from this equation.

Heathershaw (1981) attributed high transport rates over periods of one year in Swansea Bay partly to the bed response to storm wave activity, but

noted that in general, net sediment transport directions were controlled by the tidal currents. Using Bijker's (1967) formula, and Bagnold's (1963) bedload equation, he calculated that even under moderate wave conditions (wave period 8s, wave height 1m) in 20m of water, with a grain size of 100-200um and roughness length of 0.05cm, sediment transport rates were increased by > 5 for U100 of 0.5m/s (Fig. 1.28).

A problem here is in assuming a bed roughness length. Grant & Masden (1979,82,86), Cacchione & Drake (1982) and Kemp & Simons (1982,83) present experimental data showing that the roughness length can be ~10 times higher than in the same steady current without waves. Additional problems in the choice of a roughness length in tidal shelf areas are the likely Z_0 variations caused by megaripples, sandwaves, and intermittent exposures of coarse substrates (Chapter 4). Grant & Masden (1979,82,86) assume that the waves are dominant compared to the steady velocity, and consider the effect of waves on the flow as an increase in flow roughness length. However, their method of calculating shear stress involves iterative procedures on computers at a number of stages, and is less readily applied than that of Bijker (1967).

1.17.4 The Equation of Engelund & Hansen (1967)

This formula predicts total load transport, and is valid for megarippled beds where the boundary Reynolds number R_b is > 12, and $D_{50} > 150\mu\text{m}$ (Raudkivi, 1976).

$$R_b = (U^* D_{50}) / \nu \quad (7.22)$$

where :

D_{50} = median grain diameter

ν = kinematic viscosity of seawater ($\sim 0.013\text{cm}^2/\text{s}^2$)

The formula is based upon three terms, a friction factor, a dimensionless sediment discharge, and a dimensionless bed shear stress;

$$j_{\text{tot}} = 0.05 P_s U^2 (D50/g((P_s-P)/P))^{0.5} (T/((P_s-P)D50))^{1.5}$$

(7.23)

where :

j_{tot} = total load sediment transport rate (g/cm/s);

T = shear stress;

P_s = sediment density (2.65g/cm³);

P = water density (1.025g/cm³);

U = depth mean velocity;

g = gravitational acceleration (981cm/s²);

and $D50$ = median grain diameter.

Equation applicability

As stated above, this equation is strictly only applicable if megaripples are present, grain size > 150um, and when the boundary Reynolds number is > 12, However, its general use in predicting sediment transport is recommended by A.S.C.E. (1975) and Graf (1971), and it has been used by Collins et al (1981) for a sandflat dominated by ripples.

In all three stations where this equation has been applied (see below) the grain size is above 150um (see Notes in Table 1.8 below), and the bed was megarippled at both Penrhyn Point and Farchynys. There were no megaripples observed at Penmaenpool Tollbridge itself, however at low water, 10-30m downstream on the inside of the channel bend there was exposed a small field (~10mx20m) of ebb-orientated large ripples/small megaripples, with a wavelength of below 2m and heights of a few centimetres. They occurred in a thin fine sand layer above a gravelly surface exposed between bedforms, and appeared limited in size by the low availability of sand. Spring tide depth mean flow velocities at Penmaenpool attained >0.75m/s on the flood tide, well above the threshold for megaripple

formation, and matching that for scour pit formation (Chapter 3). It is thus considered that the sedimentary conditions at Penmaenpool were transitional to being megarippled, and the formula was applicable.

Boundary Reynolds number R_b varied between 0.0 and 41. The largest values occurring at Penrhyn Point on spring tides, when 13 of the 25 half hour velocity conditions gave $R_b < 12$, however these occurred near slack water, and the calculated transport rates give these 13 half hour values a total of only 0.3% of the calculated net tidal sediment transport. On neap tides, this increases to 12%. At Farchynys and Penmaenpool all values of R_b are less than 12 at both spring and neap tide.

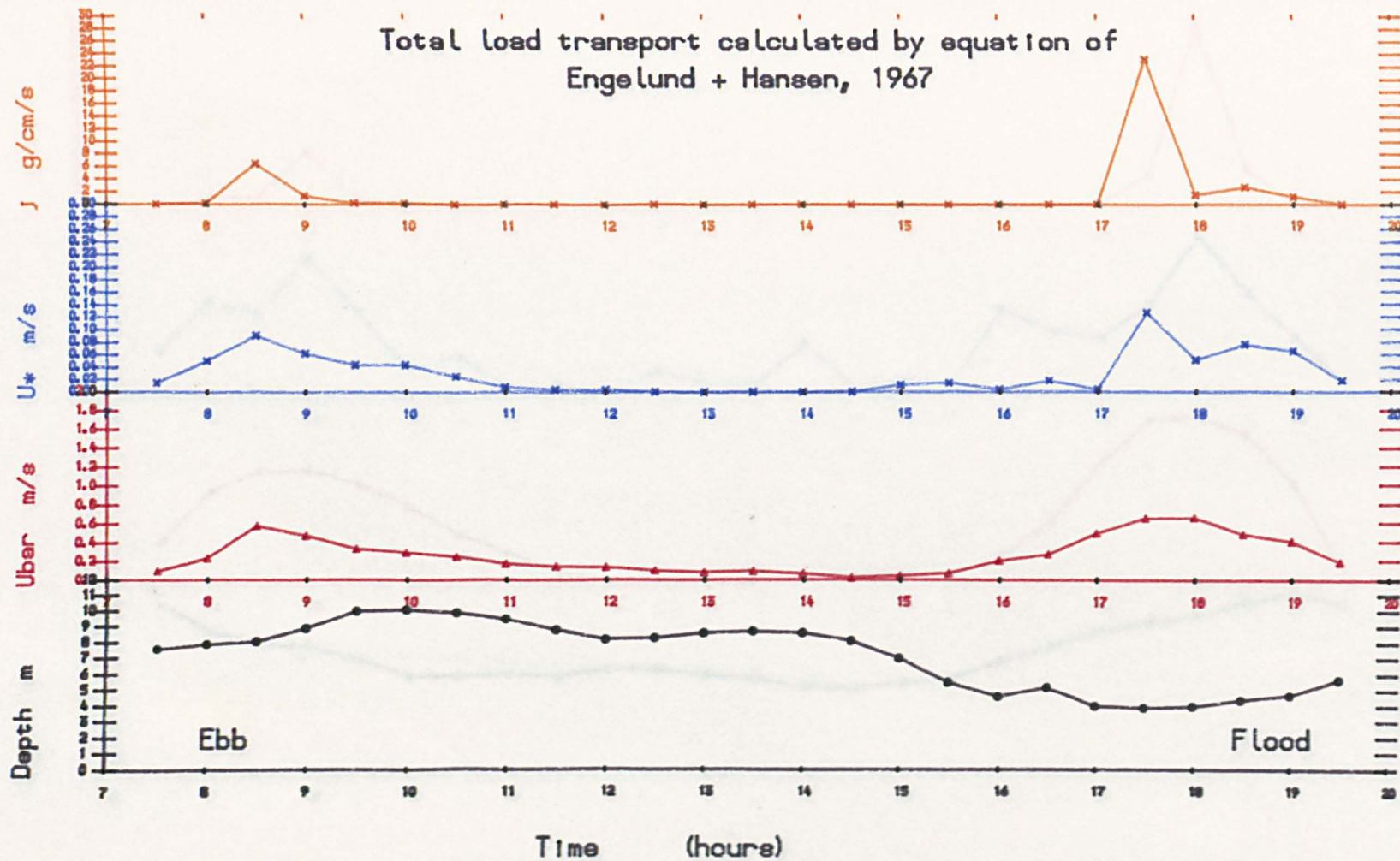
1.17.4.1 The Flow Data Used

In order to estimate sediment transport rates and directions within the estuary, the flow data presented in Chapter 2 has been used to predict sediment transport at spring and neap tides at the estuary mouth (Penrhyn Point), the mid-estuary constriction (Farchynys), and further upstream at Penmaenpool. The importance of sediment fluxes at Penrhyn Point is that all sediment transported by water into the Mawddach from Barmouth Bay passes through the tidal channel at Penrhyn Point. Similarly, all sediment movement between the lower and upper estuary occurs through the narrows at Farchynys. Mean sediment deposition rates within areas of the estuary must be a function of sediment supply, and net sediment transport rates and directions through these conduits will be controlling factors upon sediment supply.

Flow parameters used in the transport formula have been based on velocities at 30 minute intervals at heights above bed of 0.1d, 0.3d, 0.5d, 0.7d, and 0.9d (d = water depth). These depths and velocities were interpolated between measured values (see Chapter 2). Shear velocity U^* has been calculated from the velocities at heights of 0.1d and 0.3d above bed. This is not a fully satisfactory method of obtaining U^* , and errors will

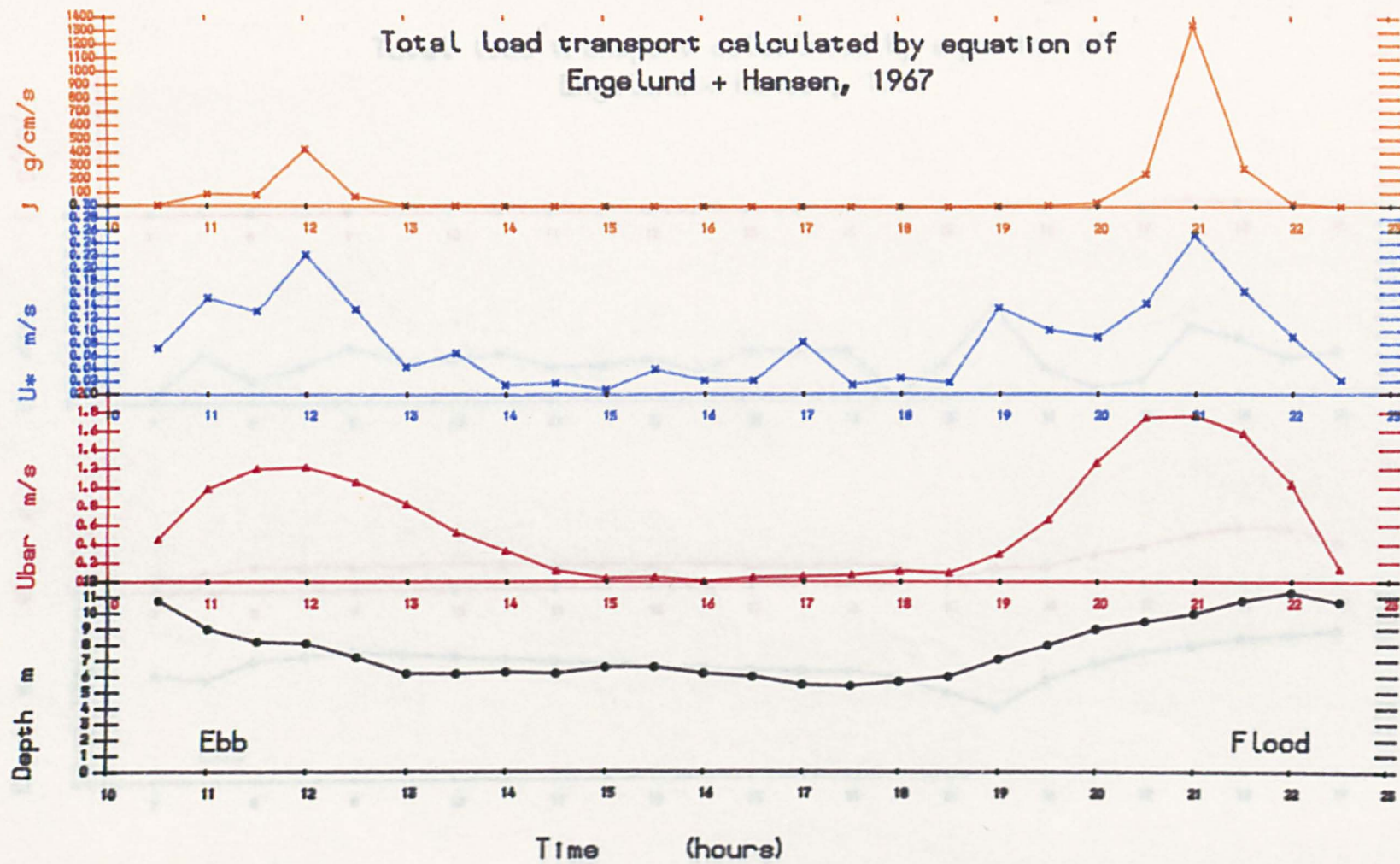
Penrhyn Point - Neap tide

Fig. 1.29



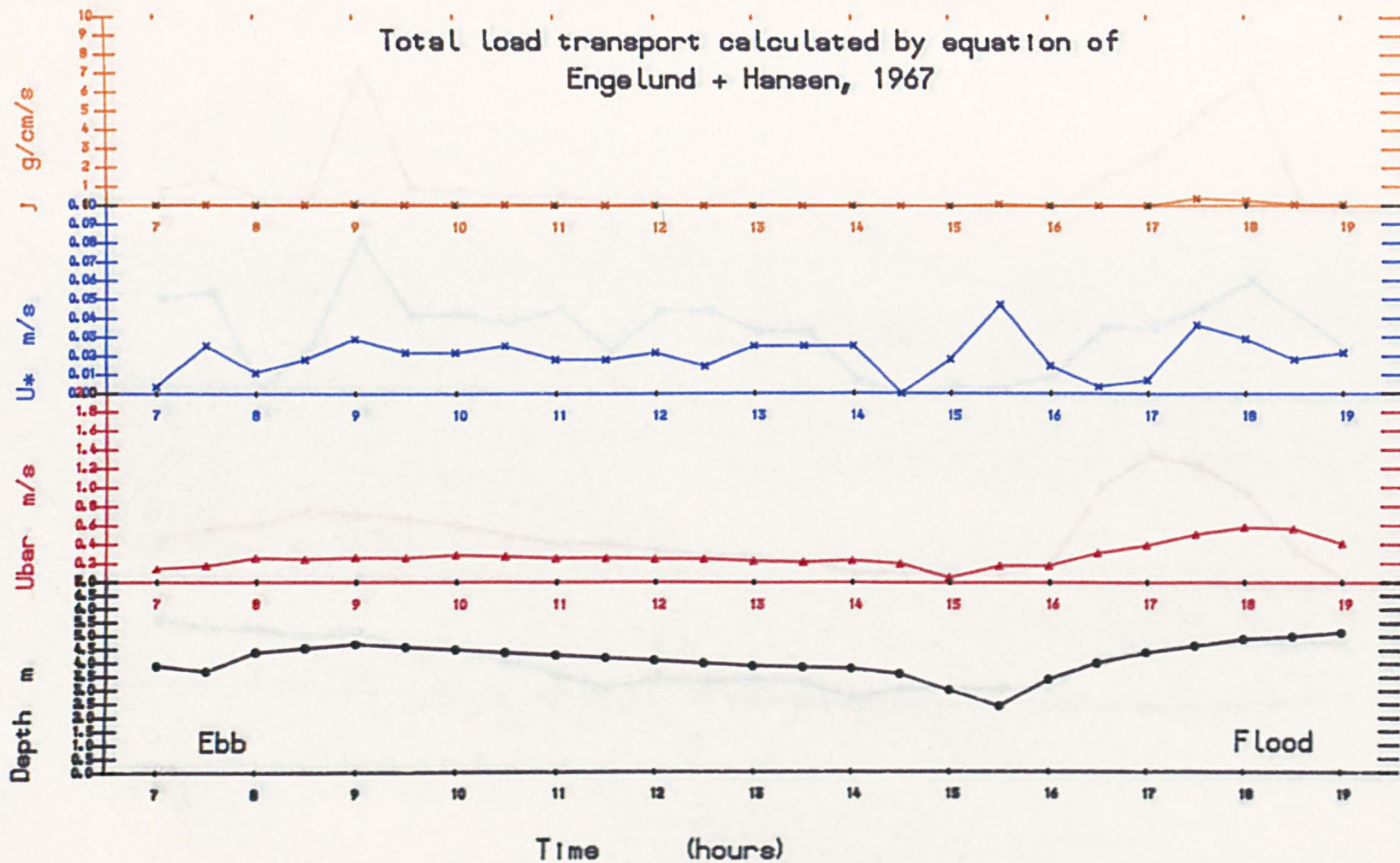
Penrhyn Point - Spring tide

Fig 1.30



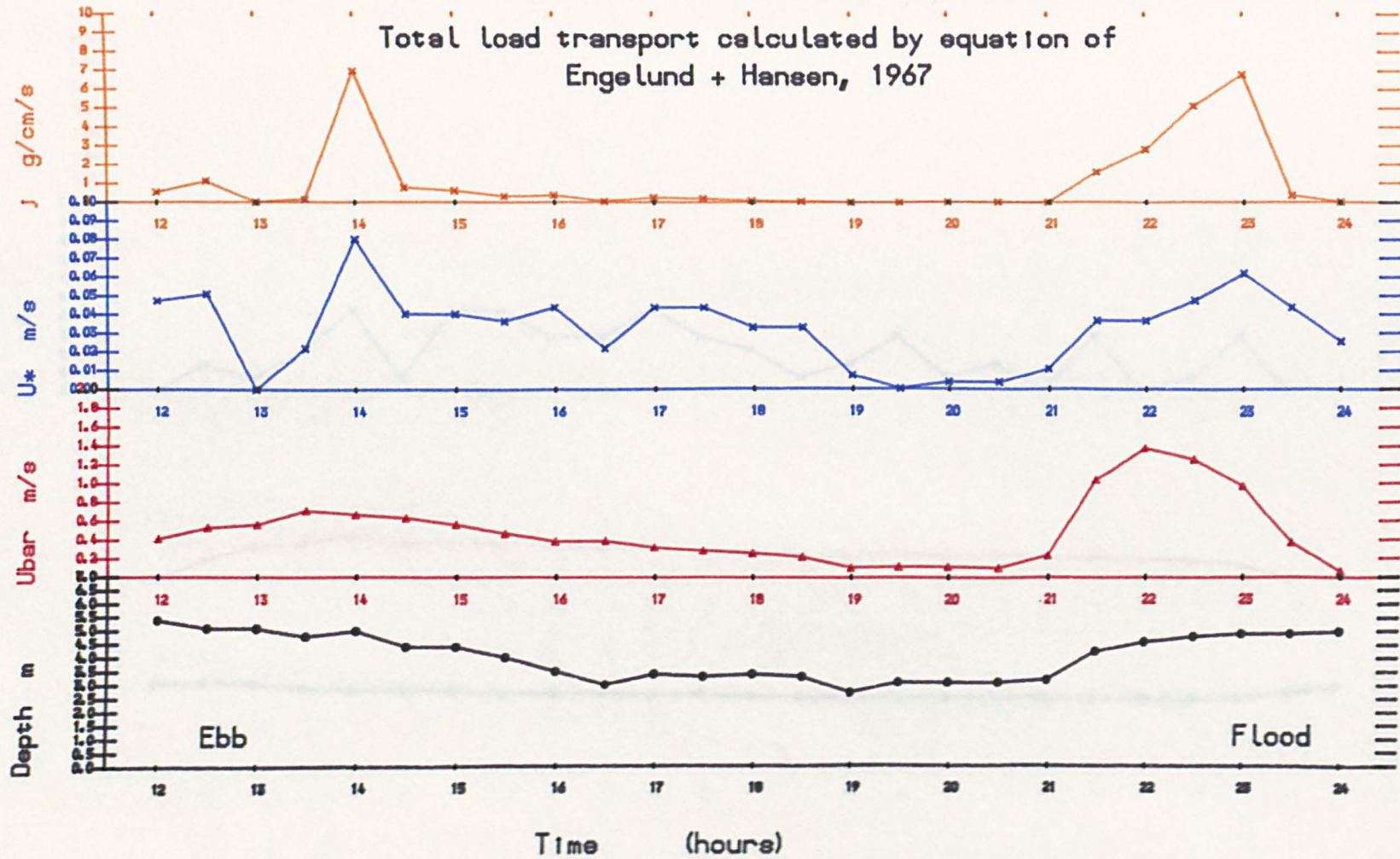
Farchynys - Neap tide

Fig. 1.31



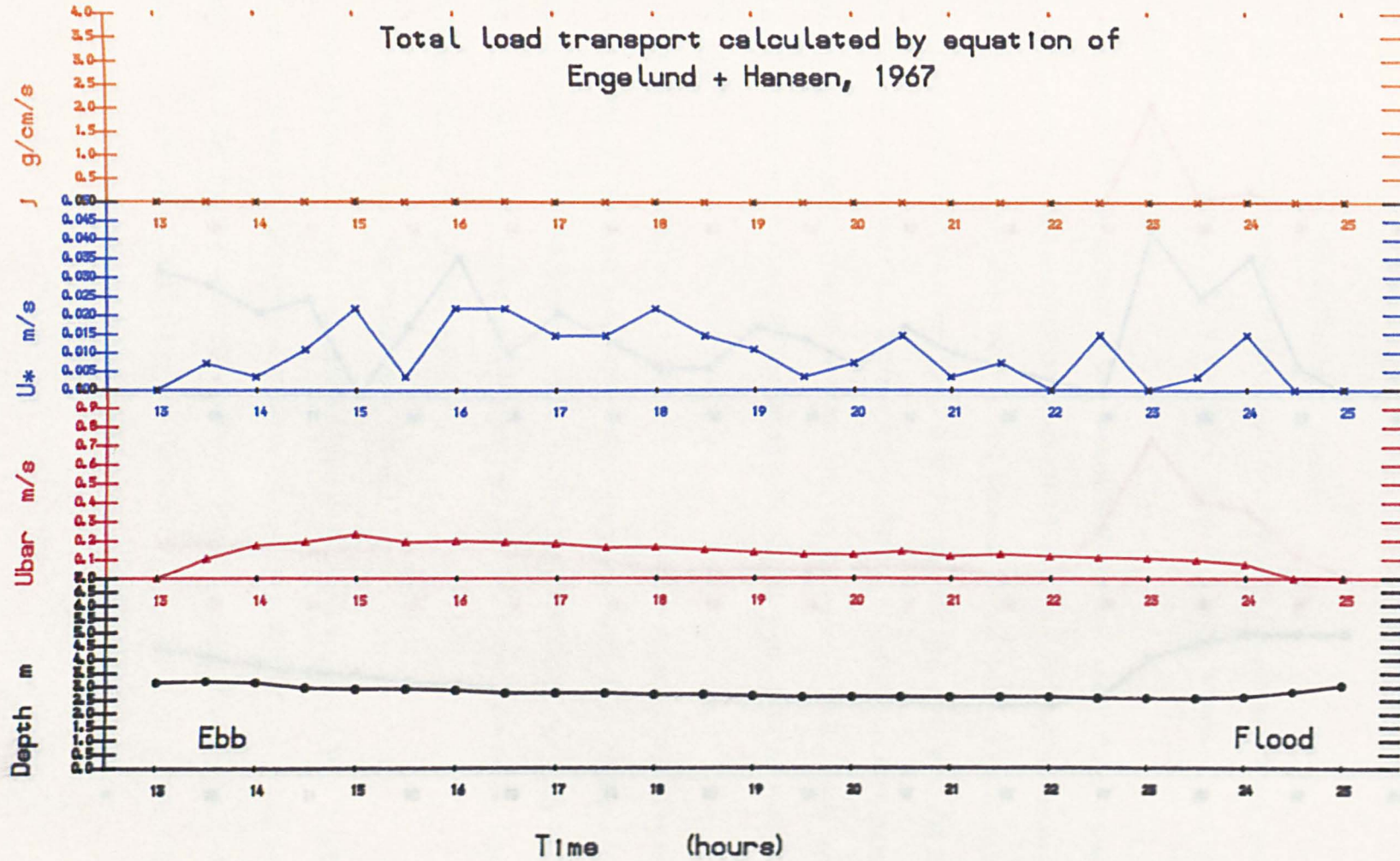
Farchynys - Spring tide

Fig. 1.32



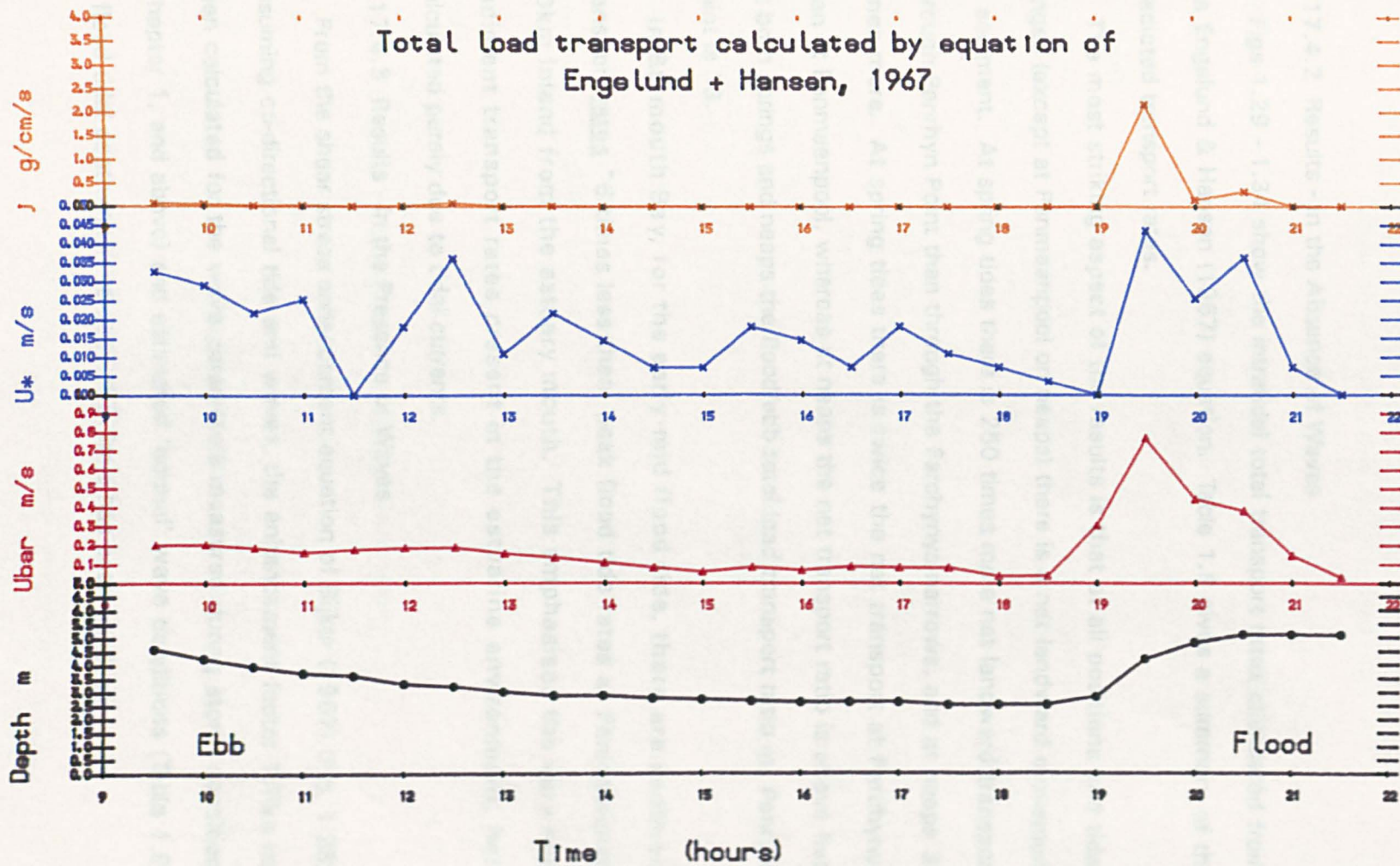
Penmaenpool - Neap tide

Fig. 1.33



Penmaenpool - Spring tide

Fig. 1.34



be present due to the interpolation of values in both time and depth, as well as the errors included in the initial data (see Chapter 2 for discussion).

Also included in Table 1.8 below is a calculated instantaneous sediment transport rate at Station 1 in Barmouth Bay. It uses the final data point, the fastest sampled part of the spring flood tide.

1.17.4.2 Results - In the Absence of Waves

Figs 1.29 - 1.34 show the intratidal total transport rates calculated from the Engelund & Hansen (1967) equation. Table 1.8 gives a summary of the predicted transport rates.

The most striking aspect of the results is that at all positions and tidal ranges (except at Penmaenpool on neaps) there is a net landward movement of sediment. At spring tides there is 250 times more net landward transport through Penrhyn Point than through the Farchynys narrows, and at neaps 37 times more. At spring tides there is twice the net transport at Farchynys than at Penmaenpool, whereas at neaps the net transport ratio is above five. At both springs and neaps the flood/ebb total load transport ratio at Penryhn Point is ~ 3 .

In Barmouth Bay, for the early-mid flood tide, there are sediment transport rates ~ 6 times less than peak flood tide rates at Penmaenpool, 10km inland from the estuary mouth. This emphasises the very high sediment transport rates present in the estuarine environment, here calculated purely due to tidal currents.

1.17.4.3 Results - in the Presence of Waves

From the shear stress enhancement equation of Bijker (1967) (Fig. 1.28), assuming co-directional tide and waves, the enhancement factor T/T_{wc} has been calculated for the wave parameters measured during storm conditions (Chapter 1, and above) and estimated 'normal' wave conditions (Table 1.9). A flood tidal depth-mean velocity of 0.5m/s has been used.

Table 1.8 .

Total Load Sediment Transport Rates at Penrhyn Point, Farchynys, and Penmaenpool, in the Absence of Waves. (Equation of Engelund & Hansen, 1967).

Position	Net flood transport	Net ebb transport	Net tidal transport	
	g/cm/flood	g/cm/ebb	g/cm/tide	m ³ /m/tide
<u>SPRINGS</u>				
Penrhyn Point	3523509	1227596	+2295913	+1.444E-2
Farchynys	30044	20859	+9184	+5.776E-5
Penmaenpool	4734	444	+4289	+2.699E-5
<u>NEAPS</u>				
Penrhyn Point	52589	15266	+36323	+2.284E-4
Farchynys	1511	530	+981	+6.174E-6
Penmaenpool	zero	170	-170	-1.068E-6

Barmouth Bay, Station 1
 (Depth = 13.2m, U = 0.42m/s, U* = 0.04m/s, D50 = 190um)
 19:30 hours, i.e. early flood tide = 0.33 g/cm/s

Peak transport rate:

Penrhyn Point	1352 g/cm/s
Farchynys	6.82 g/cm/s
Penmaenpool	2.18 g/cm/s

Notes :

+ve = flood, -ve = ebb

The median grain diameter used for each position was :

Penrhyn Point	0.021cm (210um);
Farchynys	0.018cm (180um);
Penmaenpool	0.0125cm (125um).

Conversion of dry weight sediment transport rate from g/cm/tide to m³/m/tide used : sediment porosity of 40%; grain density 2.65; giving 1g/cm/tide = 6.289E-9m³/m/tide.

An important point to note in these data is that the waves and tide have been assumed to be co-directional, which is not the case for the inner parts of the bay. However, some useful general conclusions may be drawn from this data. Firstly, bed shear stresses are most enhanced by storm waves in Barmouth Bay, by ~17 times in shallow areas, and by >6 in regions less than 15m deep. Under 'normal' wave conditions, little enhancement of bed shear stress occurs except in depths of <5m, and <10m with waves 1m in height. In the Mawddach Estuary storm waves significantly increase bed shear stresses probably only in shallow water.

An important aspect of wave enhancement of bed shear stress is the potential effects upon sediment transport rates. The sediment transport rates at Station 1, (Barmouth Bay), 2 (Penrhyn Point) and 4 (Farchynys) have been calculated using wave enhanced shear stresses (Table 1.10). The change in sediment transport rates at peak flood velocities provides a good indication of general wave effects on sediment transport. Wave periods and heights used are as above.

These calculations illustrate well that storms enhance sediment transport rates in Barmouth Bay, far more than in the estuary. The increase in peak transport rates at Farchynys indicates that landward propagating storm waves will probably increase the landward sand flux by up to a factor 2, but have negligible effects at the estuary mouth. Sediment transport rates in Barmouth Bay are raised to become comparable to those calculated for the mid-estuary constriction at Farchynys, rather than without wave influence when rates were comparable to a position 4km further inland.

Table 1.9

Calculated Shear Stress Enhancement Factors (T_{wc}/T)
for Storm Conditions
(plus 'Normal' Conditions for Barmouth Bay).

Position	a m	Wave period sec	Depth m	U_o m/s	T_{wc}/T
Barmouth	0.75	9	5	0.95	17.5
Bay	0.75	9	10	0.61	7.3
<u>Storm</u>	0.75	9	15	0.45	6.0
Barmouth	0.25	4	5	0.20	1.73
	0.25	4	10	0.06	1.08
Bay	0.25	4	15	0.02	1.01
	0.5	4	5	0.40	4.23
<u>Normal</u>	0.5	4	10	0.12	1.32
	0.5	4	15	0.04	1.04
Barmouth Harbour	0.3	2	6	0.07	1.06
Farchynys	0.3	3.6	2	0.51	3.22
	0.3	3.6	3	0.37	2.39

Notes :

- T_{wc}/T enhancement factors are for a depth mean tidal current of 0.5/s.
- Z_o used for Barmouth Bay is 0.006m, representative for a rippled sand (Soulsby, 1983).
- Z_o used for Barmouth Harbour and Farchynys is the flood tide mean of 0.02m, measured over intertidal megaripples (Chapter 4).

There are important factors to note concerning the usefulness of these calculations. The shear stress enhancement factors T_{wc}/T are dependent upon estimates of roughness length and the factor 0.45 in equation 7.21. It is unknown how close the Z_o values used are to the actual roughness during storm conditions. If we assume that the roughness length may be increased by an order of magnitude under a current with superimposed waves (Kemp & Simons, 1982,83), the enhancement factor for Barmouth Bay in storm conditions would be reduced from 9.1 to 5.1, and the ratio j_{wc}/j from 29 to 11.5.

Table 1.10

Calculated Total Load Sediment Transport Rates under Peak Flood Tidal Currents and Waves (jwc), for Storm Conditions, plus 'Normal' Wave Conditions for Barmouth Bay.

(Using Equation of Engelund & Hansen, 1967).

	a	Wave period	Depth	Ubar	Uo	Twc	jwc	jwc/j	
	m	sec	m	m/s	m/s	--	g/cm/s	--	
<u>SPRINGS</u>									
<u>STORM CONDITIONS</u>									
Barmouth Bay	0.75	9	13.2	0.42	0.50	9.5	9.6	29	
Barmouth Harbour	0.3	2	10.0	1.77	7.7E-5	1.0	1353	1.0	
Farchynys	0.3	3.6	5.0	0.97	0.20	1.13	8.3	1.21	
<u>NEAPS</u>									
Barmouth Harbour	0.3	2	4.0	0.66	0.03	1.008	23.54	1.01	
Farchynys	0.3	3.6	4.7	0.50	0.22	1.57	0.75	2.02	

Barmouth Bay - Station 1
Instantaneous transport rate = 9.6 g/cm/second

c.f. Peak flood spring transport rate at :
Penrhyn Point 1352 g/cm/s
Farchynys 8.27 g/cm/s

NORMAL WAVE CONDITIONS

Barmouth Bay	0.25	4	13.2	0.42	0.03	1.03	0.34	1.04
	0.5	4	13.2	0.42	0.06	1.11	0.38	1.16

Notes :

- jwc = instantaneous total load sediment transport rate under peak velocity flood tidal currents with superimposed co-directional waves
- j = instantaneous total load sediment transport rate under peak velocity flood tidal currents
- Zo used for Barmouth Bay is 0.006m, representative for rippled sand (Soulsby, 1983). Zo used for Barmouth Harbour and Farchynys is the flood tide mean of 0.02m, measured over intertidal megaripples (Chapter 4).

Other unknowns are storm effects on the net transport rate, through modification of the tidal wave, and the maintenance of fine sediment in suspension. Storms cause orbital velocities above threshold in shallow parts of the estuary (see above).

1.17.4.4 Discussion

The implications of these data are important in determining the source of the sediment in the Mawddach, and the calculated landward net sediment transport directions would certainly support the conclusions of Moore (1968) and McMullen (1964) - that the long-term net sediment transport direction is into the Mawddach Estuary from Barmouth Bay. There is also a strong gradient of net transport rate, with a decrease in the landward direction.

The calculations for transport fluxes, under tidal currents, can also be related to sediment accretion rates in the upper and lower estuary. The cross sectional area of the main channel at Penrhyn Point is greater but of comparable size to Farchynys, and assuming that the two velocity measuring stations both measured the peak velocities (or similar proportions of them) through the sections, then on spring tides it would appear there is a net input of sediment to the lower estuary greater than the net input into the upper estuary. At spring tides this ratio is ~500; at neaps it is ~30. Thus, assuming sediment transport in fairweather conditions, there is a tendency for net sediment deposition in both the upper and lower estuary, but concentrated in the lower estuary. (The bed-level data presented in Chapter 7 shows net accumulation only in the eastern part of the lower estuary, although the data is not considered a reliable indicator of estuarine deposition).

Using the above total load sediment transport rates, some approximations of net sediment accumulation (or erosion) rate can be made. An expression for accumulation rate AR in a given area of estuary is

$$AR = (730 \int W) / \text{area} \quad \text{m/year} \quad (7.24)$$

where :

730 is the number of tides in a year;

j = mean sediment transport rate into the area
($m^3/m/tide$);

W = channel width at flow rate measurement point;

and area = intertidal surface area.

The product of j and W is the net tidal sediment flux through the cross-section of the estuary for which the sediment transport calculation was made. It makes the simple assumption that sediment transport through the whole of the cross-section is the same as that the measurement position.

Pickrill (1986) calculated net tidal sediment transport fluxes at stations across tidal cross-sections, from integrating hourly sand trap measurements of sediment transport. Across sections 500m wide and <8m deep, he found spatial differences in net transport rates of up to 2 orders of magnitude. The grain size of the bed, the presence of megaripples and the tidal current velocities are very similar to those found in the Mawddach, so it may be predicted that similar variation in sediment flux occurs across the Mawddach sections. In this study flow measurements were made as much as possible in the fastest currents of each section, so the calculated sediment fluxes are likely to be systematically overestimated.

Another assumption implicit in this calculation, is that all sediment transported into the estuary is deposited evenly and permanently onto the entire intertidal area. In the same way, erosion is considered to be spatially even. Only the potential sedimentation rates resulting from tidally-induced transport are considered, the effects of waves or very high freshwater runoff is not considered. The value for j used in the equation is the mean of the calculated spring and neap tide values.

In Table 1.11 are tabulated the net volumes of sediment transported through the estuary at stations 2, 4 and 5.

Table 1.11

Calculated Net Total Load Sediment Fluxes
at Stations 2,4 and 5

Station	W m	S e d i m e n t f l u x	
		m ³ /tide	tonnes/tide
2 Penrhyn Point	200	1070.8	2838
4 Farchynys	280	6.53	17.3
5 Penmaenpool	110	0.00104	0.0028

Notes :

- Calculated sediment fluxes are the mean of spring and neap fluxes
- At all three stations the flux was landward.

Calculated rates of sedimentation are :

Whole estuary

(area ~9.5km²) AR = Accumulation of 82 mm/yr.

c.f. Taf Estuary (Jago, 1974) 155 mm/yr.

Dwyrdd Estuary (Mahamod, 1989) 49 mm/yr.

Lower Estuary i.e. between the mouth and Farchynys

(area ~8km²) AR = Accumulation of 97 mm/yr.

Upper Estuary i.e. between Farchynys and Penmaenpool

(area ~1.43km²) AR = Accumulation of 3.3 mm/yr.

Estuary head, i.e. the area inland of Penmaenpool

(area ~0.075km²) AR = Accumulation of 0.01 mm/yr.

These calculations should be viewed with their limitations very much in mind, however, they do emphasise that alone, tidal currents in the Mawddach probably act to cause net sediment accumulation in the estuary,

particularly the lower estuary. The net sediment accumulation rates compare very well with other data from other estuaries on the Welsh coast; the calculated net accumulation rate for the whole estuary is approximately half that measured in the Taf, and nearly twice that for the Dwyryd. Accumulation rates in the Mawddach decrease inland, with sediment accumulating 30 times faster in the lower estuary than the upper estuary, and the estuary head barely accumulating anything. This result agrees with Mahamod's (1989) conclusion for the Dwyryd, which also suggested a landward decrease in net accretion. It is interesting, rather than highly significant, that the accumulation rate measured on the sandflats of Transect 4 (Chapter 7), the equivalent of 102mm/yr., is very similar to the calculated rate from this equation.

This data also tentatively confirms the position (inferred from the grain size survey, Chapter 6) of the landward limit of marine-derived sediment. This data set suggests that at neap tides there is no landward sediment transport, though it should be recalled that the neap data from Penmaenpool was taken 2 days after a period of very heavy rain, so may have had an increased seaward flow component. At spring tides only $2.7E-5 \text{ m}^3/\text{m}/\text{tide}$ (equivalent to a maximum of 8kg) of sediment is transported upstream, and noting the landward decrease in sediment transport rate it is a reasonable suggestion that the position of no net tidal sediment transport is a short distance upstream of Penmaenpool. This position alters with tidal range, moving inland on spring tides.

1.18 Summary and Conclusions

A review of the literature reveals that the Mawddach Estuary is probably situated along a splay of the Bala Fault, which may intersect a southerly extension of the N-S Mochras Fault. The estuary is underlain by Lower Palaeozoic rocks, of Cambrian and Ordovician age.

The Mawddach Estuary occupies a glacially-cut valley, whose base lies at -35m O.D.N. at the estuary head and the mouth; it is overdeepened to below -70m O.D.N. at the mouth. The valley fill includes estuarine, alluvial and probably glaciofluvial sediments, ranging from clays to gravels, but dominated by sands and sandy gravels. At the mouth, the sedimentary sequence above -35m O.D.N. is interpreted tentatively as recording the slow transition from upper-estuarine type saltmarsh silts, through fine sands of tidal flats to the high energy gravelly sands of the present day meso- to macro-tidal estuary. At the estuary head is a sequence dominated by a basal sandy gravel unit proved to be ~30m thick in one borehole; this has been deposited by alluvial or glacially-related flow. Above lies a buried alluvial channel body with related floodplain fines, alternatively explained as glaciofluvial deposition in a postglacial basin, succeeded by a peat unit of up to 1.5m in thickness.

The sea floor in Barmouth Bay within 2km of the shore dips seawards at between 0.24 and 0.57 degrees. Seawards of the -10m O.D.N. depth contour, the slope of the study area varied between zero and 0.07 degrees. Greater than 1.5km offshore, at 12000N north, a 4km long E-W leveed channel structure occurs, <0.8m deep and ~200m wide. It's formation was probably related to a sub-surface outcrop of relatively erosion-resistant glacial drift. Today, the floor of the trough contains mesoscale sandy bedforms, indicative of significant bedload sediment transport.

Marine seismic surveys of Barmouth Bay confirm the findings of other workers that there is extensive masking of sub-bottom reflectors, probably by biogenic gas. After correction of boomer seismic profiles for moveout, and assuming a seismic velocity of the sedimentary succession of 1700m/s, seismic sections have been drawn with reflectors reduced to O.D.N.. A number of different seismic facies have been recognised and tentative geological interpretations proposed. The facies are :

1 - Welsh Boulder Clay : deposited by the Mawddach Valley glacier during the last glaciation. It is heavily dissected by channels of up to > 25m relief, cut by sub- or pro-glacial sediment-laden flow.

2 - Late/Post-Glacial Sands and Gravels : coarse- grained cross-stratified channel infills.

3 - Early Holocene Lacustrine / Lagoonal Sediments : fine-grained sub-horizontal parallel-stratified units, deposited in quiescent conditions possibly behind a barrier of some form.

4 - The Inner Sand Sheet : a Recent marine sand wedge in inner Barmouth Bay (see below).

These interpretations can only be considered tentative, as there are no boreholes within the survey area and there is great lateral and vertical variation in sediment type.

The sea floor off Barmouth can be divided into 3 facies, the Outer Sand Facies (OSF), Inner Sand Sheet (ISS), and Patchy Sand Facies (PSF), occupying respectively the NW, E and SW of the survey area. The OSF and PSF are divided by a major WSW-ENE leveed trough feature. The facies characteristics are related to :

1 - tidal and storm currents;

2 - the thickness of the mobile sand cover;

3 - substrate topography.

Summarised, the facies characteristics are :

OSF : complete sand cover, with 2-D megaripples present in the west. In the centre of the facies there are NE- SW orientated sandribbons or elongate sand patches which have negligible relief. In the south are south-facing sandwaves, with NE-facing 3-D megaripples south and west of them;

Trough and levee feature : the trough is up to 600m wide, and 0.8m deep, in which sand ribbons occur parallel to peak tidal currents. Levees on either side are <0.6m high and ~400m wide, and the southern levee has megarippled sand ribbons;

PSF : generally incomplete sand cover, with well-developed megarippled sand ribbons, some sandwaves, and sand ribbons showing degradation, possibly towards sand patches. There is more complete cover in the north nearer to the OSF, with more regular arrays of 2-D megaripples. In all cases where bedform asymmetry was able to be determined, their steep slopes face the NE;

ISS : complete sand cover in the south, less so north of the estuary mouth. In the north, large (L = 160m) south-facing sandwaves occur, succeeded by 2-D megaripples with shore-normal crests. At, and south of the bar (part of the ebb tidal delta) are 2-D and 3-D megaripples. On the western face of the bar are some low amplitude lineations, possibly sandribbons.

Consideration of bedform types, morphologies and associations, together with tidal current information, have enabled hydrodynamic and sediment transport interpretations of the sedimentary facies to be made. These are :

OSF : the bedforms may be related to storm-enhanced tidal currents, possibly reaching 0.8-1.0m/s and related to a southwesterly directed overflow current from Tremadoc Bay. Reworking by tides, during more normal wave conditions, reduces the height and clarity of the bedforms. The facies may be depositional in nature;

Trough feature : the sand ribbons are probably generated by spring tidal currents. The trough is not likely to have been caused by the modern hydrodynamic regime, but may be maintained by it;

PSF : the bedforms suggest fast currents near the shore to the south, possibly up to 0.9m/s, caused by the projecting coastline. In the north of the facies currents may be 0.6-0.7m/s. Net sediment transport is towards the NE;

ISS : away from the estuary mouth bedforms appear transverse to a shore-parallel current. In the north there is net sediment transport to the south, evidenced by sandwave asymmetry, and this is also suggested for the western edge of the sand sheet.

The work of Dobson et al (1971) leads to the conclusions that in Cardigan Bay there is a nearshore zone of fine-medium sands with net landward transport vector. The sea bed is moulded into sand ribbons and sandwaves, indicating high rates of sediment transport. Wave activity is considered significant in increasing near-bed tidal velocities, by 0.25m/s for 14 days/year, and by up to 0.5m/s for 2 days/year, the latter matching well calculations of orbital velocity at the bed derived from observed storm waves.

Published material relevant to sediment transport in the Barmouth Bay and Mawddach Estuary regions is sparse. However, there is ample morphological evidence suggesting much active coastal and estuarine sediment transport, such as the presence of the shingle spits across many of the estuaries of Cardigan Bay, implying a northward drift of coarse clastic material.

McMullen (1964) from sedimentary and flow observations, and Moore (1968), from a study of the grain size distributions and mineralogy, both concluded that the Mawddach Estuary contained material derived from

Barmouth Bay. Moore identified 2 coastal and 2 shelf sources for the sediment in Barmouth Bay. This study has shown that there are also sediment sources within the bay, i.e. the sea-bed is being actively eroded at the present day. These are implied to be post-glacial deposits, containing fines, a multimodal sand population, and gravel, and are exposed in the southwest of the bay, and in a N-S strip at an easting of ~58500. Localised sources may be related to the incomplete cover of fine sand, allowing supply to the bay of material derived from the underlying glacial substrate.

Elongate ripple bands are present in Barmouth Bay, in all three facies. Their negative relief is up to 1.2m, lengths 140-600m, and trough length to width ratios greater than 10. The ripples within the troughs are up to 0.3m in height and 2.8m in wavelength, and are formed of the coarse sand substrate underlying the more mobile fine sand cover. Their orientations and association with surrounding bedforms suggest that in the the outer parts of the bay, ripple bands have a tidal component in their generation. It is also hydrodynamically possible that they are formed at slack water, under storm waves of period 9 seconds and wave height 1.5m. In the nearshore inner sand sheet, where the ripple bands occur in troughs between sandwaves and 2-D megaripples (i.e. are generally shore-normal), the ripple bands may be generated purely by a 'normal' wave regime. Their control in the nearshore zone by bed topography and sediment thickness is further suggested by their absence in the south, where the sand is consistently over 1m thick.

Total load sediment transport rates have been calculated for three positions along the estuary. At all three stations in the estuary at all tidal ranges the net sediment transport vector is inland. Near the estuary head this may be reversed during periods of high freshwater runoff coincident with neap tides. An average of 2800tonnes/tide enters the estuary from Barmouth Bay. Spring tides cause ~500 times more sediment to enter the estuary mouth on the flood tide than leave with the ebb, and at neap tides

this ratio is reduced to ~ 30 . By assuming equal sediment flux across each estuary cross-section, and even sediment accumulation over the estuary, approximate upper limits of net accumulation rate have been calculated :

- 97 mm/yr for the lower estuary
- 3.3 mm/yr for the upper estuary
- 82 mm/yr for the estuary as a whole.

These compare very well with other published accumulation rates.

The effects of 'normal' and storm waves upon sediment mobility and transport rates have been calculated using the concept of a wave-enhanced bed shear stress. In Barmouth Bay storm waves increase flood tide sediment transport rates, possibly by as much as 30 times, in contrast to the effects of 'normal waves, which enhance transport rates by a factor of ~ 1.15 . Within the Mawddach Estuary storms produce waves which enhance flood tide sediment transport rates by up to a factor 2. These factors are liable to errors due to the necessary assumption of a flow roughness length in calculating the shear stress enhancement factor.

Estuarine Circulation

2.1 Introduction

An essential part of understanding the dynamics of sediment within the Mawddach Estuary is to define its hydrography. This chapter describes the tidal currents and mixing processes, at neap and spring tides; the data was collected at three stations within the estuary, with limited data taken in southern central Barmouth Bay. Also discussed are controls upon the propagation of the tidal wave within the estuary, and effects of high freshwater runoff upon estuarine mixing.

An estuary is defined as :

'A semi-enclosed coastal body of water which has a free connection with the open sea and within which sea water is measurably diluted with fresh water derived from land drainage', (Cameron & Pritchard, 1963).

However, it should be emphasised that in the Mawddach and many other Welsh estuaries, in terms of estuarine circulation, this fresh-saline interaction is a secondary factor to the dominant advection that results from a large tidal range. In these estuaries, salt water is totally flushed out with the ebb tide, and for several hours at a time only river flow may remain. Water depth may vary by 4 or 5 metres over a few hours, i.e. by up to 100% of maximum depths, and it is this variable water depth which is the most important factor in determining estuarine circulation.

Estuaries have been classified in terms of their mixing processes. The classification of Hansen & Rattray (1966) has been used by some authors, e.g. Bowden & Gilligan (1971) in the Mersey; and the classification of Cameron & Pritchard (1963) by others, e.g. Pritchard (1967), Dyer (1973). It is important to note that both these classifications have been based on

estuaries where the tidal fluctuation in depth is fractional, well below the levels attained in many of the strongly tidal estuaries around N.W.Europe.

It should be emphasised that 'estuarine circulation' is variable both spatially and temporally. The influence of the tide varies along the length of estuaries, ultimately to zero at the head, and the relative influence of freshwater is also extremely variable temporally, the most significant factor being the periodic flooding and ebbing of the tide. Some factors have different periodicities; others may be variable on a random basis. It is the shorter-term periodic variations, such as diurnal and fortnightly tidal cycles, that are of most interest and relevance to the circulation study undertaken in this research - in addition to the non-predictable discharges of freshwater into the estuary. The various factors involved in estuarine circulation are introduced below.

2.1.1 Long-Term Variable Factors

2.1.1.1 Morphology

Although not so relevant in terms of day to day processes within the estuary, but nonetheless important in terms of estuarine evolutionary history (i.e. on a timescale of 10000-20000 yrs), are such factors as the physical shape and size of the estuary. Important in the morphology of the present-day Mawddach estuary is the hard rock constriction in the middle reaches at Farchynys, where the outcrop limits the channel width to its' presently achieved maximum (Fig 2.1). This cannot be assumed to have been the case throughout the lifetime of the estuary.

2.1.1.2 Sea-Level Change

Part of the control of tidal characteristics and estuary shape is sea-level, which in this area has risen by around 60m in the last 12000yrs (Haynes et al, 1977). In the past century, mean sea-level in Western Europe has risen by 13cm (Gornitz et al, 1982). Sea-level will affect sediment supply, tidal

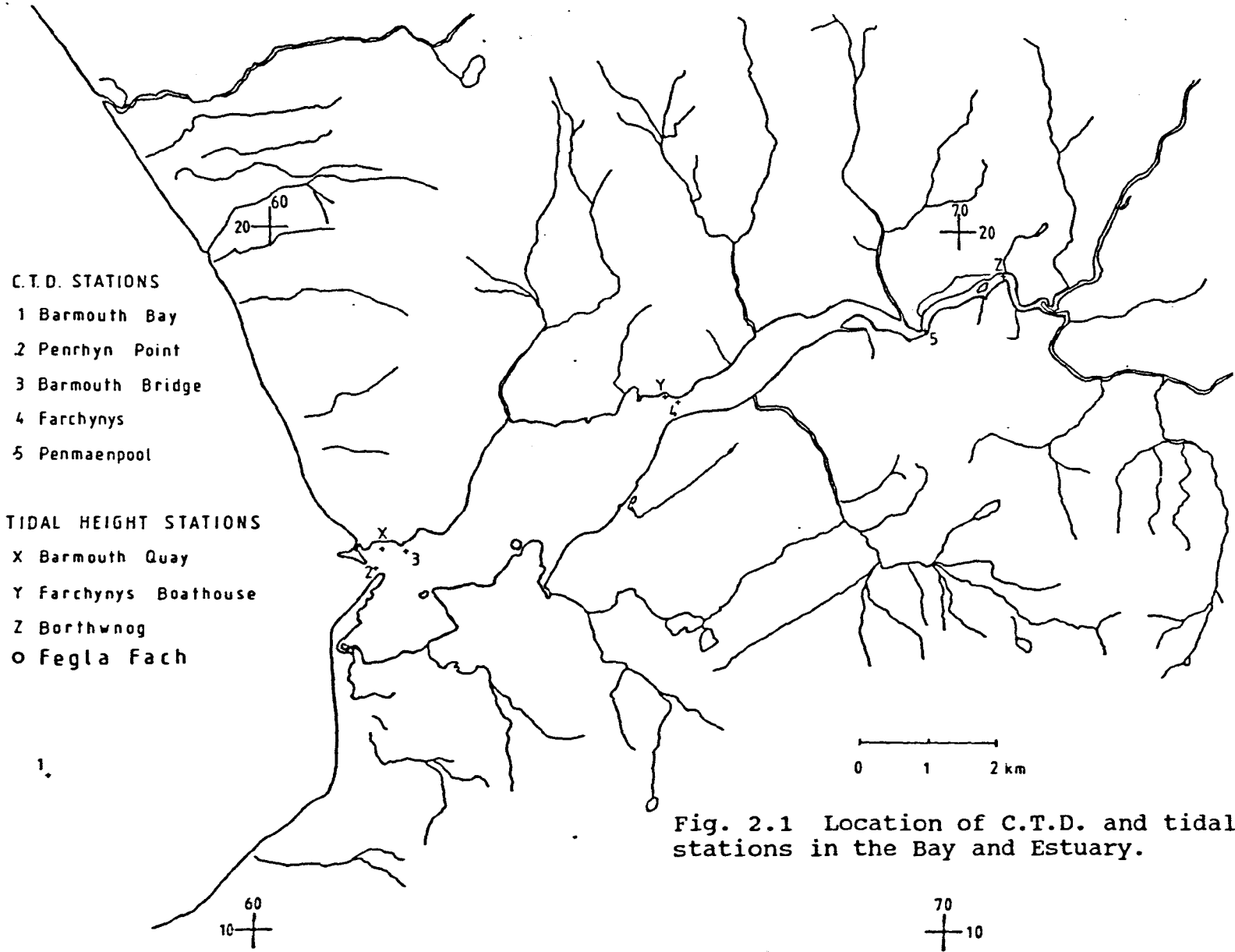


Fig. 2.1 Location of C.T.D. and tidal height stations in the Bay and Estuary.

heights and tidal ranges; thus, modifying coastal and estuarine processes. Wilks (1977) outlines evidence which suggests that in the last 5000yrs a barrier was developed at the mouth of the Dovey estuary, possibly due to a decreased rate of sea-level rise. This barrier became a major influence on saltmarsh development in the estuary and, by implication, on estuarine sedimentation.

2.1.2 Human Intervention

The effect of man is also relevant. When breakwaters are constructed to protect harbours, or large structures are built across estuaries, the effective cross-sectional area through which tidal and river waters flow is decreased, causing increased local erosion and altering the residence time of saline water in the estuary. Net river input may be altered by the diversion of streams or rivers, or decreased by afforestation in their catchments. It may be increased by deforestation or by man-made drainage. The effects, if any, of such man-made changes to an estuary may not be evident for perhaps tens of years later.

2.1.3 Variable Non-Cyclical Factors

In terms of daily processes, these include river flow, wind, waves and the morphologies of the channels, sandflats and saltmarshes. These can all alter over one or several tidal cycles, so that the estuarine system is acted upon by a continuously varying set of energy inputs, processes and limiting conditions.

River discharges vary daily, seasonally and on longer timescales; they are likely to alter stratification and the up-estuary penetration of the saline intrusion. Wind strengths and directions vary continuously with time; they may create a surface wind-driven current. The related waves will increase surface mixing. The combined effect of river flow, wind and waves may be especially significant if extremes occur simultaneously as, for example, during calm dry periods or severe storms. Thus the magnitude and

recurrence interval of such events is important.

In addition to their immediate effects, there are possible resultant morphological changes offshore and within the estuary. These include altered estuary- mouth topography and width, major switching of channels, interchannel bar formation or destruction, or saltmarsh erosion. These different physical factors may then help determine future estuarine circulation.

2.1.4 Variable Cyclical Factors

Most predictable of the process inputs are the tidal heights and ranges achieved by the tidal wave, these cause the greatest circulation changes with time. Twice each day the estuary is virtually emptied of salt water by the ebbing tide, and is then inundated on the flooding tide with saline water to various depths, heights, distances and concentrations. Thus effective channel widths and depths continuously change, as do current velocities.

Tidal parameters in the Mawddach have three dominant periods: semi-diurnal, the fortnightly lunar cycle, and the twice yearly equinoxes. Thus, variations of estuarine circulation are easiest to define in terms of position within these tidal cycles. Without a concentrated long-term data collection programme, the precise distribution of other time- variable processes can only be gauged qualitatively. Due to the interaction of so many variables, no two estuaries are alike, so it is never known if general principles or unique details are being observed (Dyer, 1973).

2.1.5 Spatial Variability

It is important to note that not only are many factors time-variable, they are also spatially variable. The magnitude and range of variation may vary greatly along the length and across the width of estuaries.

The Mawddach displays a form similar to many N.W. European estuaries, with shifting intertidal banks, separating opposed blind channels, or flats where bedforms suggest opposing net bedload transport directions, e.g.

McCave & Geisler (1979), Elliott & Gardiner (1981). This form is both a result and a cause of lateral circulation variations in the estuary, and is an example of one of the most important concepts in estuarine processes, that of a process-response coupling. There is feedback between input variables such as tidal range, river flow, channel depth etc., which control the estuarine circulation, and the response, i.e. sediment transport and deposition.

2.1.6 Welsh Estuaries

Previous studies on circulation within shallow mesotidal (tidal range 2-4m) and macrotidal (range >4m) estuaries are not numerous, possibly due to the practical difficulties involved. Measurements are normally taken in reasonably fair-weather conditions, and by no means cover the full spectrum of possible circulation states, especially in terms of modification by strong winds and large waves. The circulation of most estuaries around the north and west coasts of Wales have been studied in varying degrees of detail, including the Conwy, Seiont, Dwyryd, Mawddach, Dovey, Taf, Towy and Loughor.

The Conwy is partially-mixed (Hansen & Rattray, 1966) along most of its length (Jenkins, 1976), and recently has had particular attention paid to the well-developed frontal systems and their genesis (Lailey, 1980; O'Farrell, 1983; West & Cotton, 1981; Simpson & Turrell, 1986). Lateral velocities at the surface have been measured by Simpson & Turrell (1986) at up to 20% of axial velocities. The Seiont estuary exhibits fine tidal intrusion fronts studied by Nunes (1982), which led Nunes & Simpson (1985) and Simpson & Nunes (1981) to develop models of three-dimensional estuarine flow.

In a study on contemporary sedimentary processes in the Dwyryd, Mahamod (1989) showed it to be partially-mixed (Hansen & Rattray, 1966) in its lower reaches, with increased stratification near the mouth, and on neap tides. In a broad study of the Dovey estuary, Haynes & Dobson (1969) showed increased longitudinal and vertical salinity differences with high river discharges. Stratification was destroyed by spring tides, despite high river

flow. Across-estuary variation was marked during the early flood tide. Haynes & Dobson classified the estuary using the classification of Cameron & Pritchard (1963), and showed that it usually has a vertically homogeneous form with restricted lateral variation, though at times it is a moderately stratified type.

Jago (1974,1980) studied the Taf estuary in Carmarthen Bay, and similarly found that the greatest stratification coincided with neap tides, calm weather, and high runoff. In its upper reaches the Taf is stratified, and is stratified in its main part when neaps coincide with high river flow, but when river flow is low the estuary is well-mixed - whatever the tidal range.

Jonas (1977) compared the Towy estuary with the adjacent Taf, and the James River (Pritchard, 1967), and concluded from the mean salinity profiles that the Towy could be classified as a partially-mixed estuary. Greater than average river discharge produced a marked differential flow between the surface and the rest of the water column. However, in view of seaward net non- tidal velocities and intense mixing generated during the tidal cycle, Jonas (1977) considered that it should be thought of as well-mixed. Studies of the Loughor Estuary, in South Wales, have been done by Moore (1976), and Carling (1981). The estuarine waters are permanently well-mixed and laterally homogenous, and there are only minor inputs of freshwater relative to the tidal prism. The tidal curve becomes more asymmetrical towards the head, and is more asymmetrical at spring tides.

2.1.7 Previous Studies in the Mawddach

The Mawddach estuary has not been given full attention in terms of its circulation. McMullen (1964) gives limited velocity flow velocity data from Barmouth Railbridge. On spring tides, maximum ebb velocities were just greater than the flood, and at 0.15m above the bed most velocities were less than 0.5m/s. However, these data were taken 350m from the north end of Barmouth Bridge, whereas today the channel is only 100m wide at the north

bank, so the data are not directly comparable with more modern data.

The Welsh Water Authority (1978) measured depth profiles of salinity and velocity 100m southwest of the harbour mouth, and found that depth-mean ebb velocities were greater than the flood. On mean and spring tides the depth-mean ebb velocity attained 1.0 and 1.6m/s, respectively; the depth-mean flood velocity reached 0.9 and 1.2m/s. With river flow five times the normal dry weather flow, the top metre of the water column was stratified by 2-3ppt. At HW, depth-mean salinities reached 32.5ppt, at LW spring 18.5ppt and LW mean tides 19ppt.

Pattinson (1979) found that with high freshwater runoff (7.6cumecs) and near neap tides, surface salinities near the mouth dropped to zero for a short time near LW. Lateral surface salinity gradients existed at HW; the salinity was 0.75ppt higher at the south bank at Barmouth Railbridge than the north. In summer, with runoff of only 0.46cumecs, the saline intrusion at HW could extend well beyond the Mawddach- Wnion confluence, ie greater than 12.2km upstream of the bar.

O'Farrell (1983) conducted a qualitative study of axial convergences, and identified a complex system of fronts related to topographically-induced flow separation in the mid-stages of the flood tide. Time-lapse photography showed also that eddies occurred in some fronts, with eddy wavelengths 10-100m, amplitudes <30m and periods >10mins. These eddies occurred at times of maximum velocities, and disappeared as water depth increased. At HW + 1.5hrs, at the estuary mouth, two foam lines formed and stayed coherent for more than 1km seaward.

2.1.8 Summary of Welsh Estuaries

Comparisons between the estuaries mentioned above are not always easy due to their differing size and different type of data. In addition, the data have been interpreted and described using different methods, particularly in terms of estuarine classification schemes. However, the circulation patterns of these Welsh estuaries do have a number of features in common.

Most important is that over a tidal cycle their depths range from a few metres to zero, i.e. they are all very shallow, frictionally-dominated, and experience strong tidal currents with a large tidal range. The effect of river flow, which is often able to act alone in the estuary for periods of hours is, overall, a secondary factor compared to tidal range. Thus, the dynamics are strongly influenced by the cyclical regime of the tides, with more subtle effects superimposed by the non-cyclical river discharge variations.

Wind and waves are also important in determining circulation in these estuaries, with many of them having a wind/wave-built barrier across their mouths, restricting the free connection with the sea; particularly fine examples are the Mawddach, the Dovey, and the Taf. In addition to this long-term role of influencing estuarine circulation, waves can cause mixing of the surface of the water column and the wind may create a surface current. It is notable in this aspect that the three main estuaries of Cardigan Bay are all elongate in the SW-NE prevailing wind direction, and are therefore particularly likely at times to be influenced by wind-driven currents.

The precise way in which these estuaries have developed during the post-glacial sea-level rise is unknown. There are likely to have been differences in their evolution during that time, caused for example by different rates of sediment supply to the estuarine system.

In summary, the Welsh estuaries all show much temporal variation, and it is the short-term cyclical factors, i.e. the tides, with effects superimposed by the non-cyclical factors such as wind and waves, that are of most importance to this chapter. However it is important to note that some of these estuaries have been affected significantly by human intervention; for example, the bridges of the Conwy and Mawddach, or the blocking and reclamation of a major part of the Glaslyn-Dwyrhyd.

Spatial variation of circulation in these estuaries is sometimes a very pronounced and important feature. This will be discussed in more detail below when dealing with estuarine classification.

2.2 Methods

At four locations along the estuary, and at one station in Barmouth Bay (Fig. 2.1), vertical profiles of the water column were sampled over one spring and one neap tidal cycle for current speed, direction, salinity and temperature. Direction was noted either as simply flood or ebb, or sometimes by compass bearing. Depending on total depth, readings were taken at variable depth intervals (i.e. 2m, 1m - or 0.5m if large vertical gradients were found). Using a winch and stainless steel wire, a Braystoke current meter with 5 or 2 inch (12.7 or 5.1mm) diameter impellor and a Valeport Series 600 C.T.D.S. probe, were lowered through the water column, with a streamlined weight below them to ensure as vertical a profile as possible. No depth corrections for wire angle have been made.

At each depth, velocity readings comprised 50secs (or sometimes 10secs) averages, so one profile was completed in about 5 minutes. This was completed every 15, 20, or 30mins as flow conditions merited. Non-availability of equipment dictated that a reliable directional current meter could be used only for the two surveys off Penrhyn Point and the station in Barmouth Bay. However, the limited data collected within the estuary suggests strongly polarised tidal current directions, and unless otherwise stated, data will be treated as if flood and ebb currents were directly opposed.

Equipment accuracy and repeatability was not a major problem with this work. However it should be noted that the current meters used have a manual-stated velocity threshold of 0.015 - 0.04m/s. The quoted accuracy of temperature and salinity data is +/- 0.1 degrees C and +/- 0.3ppt respectively. Depth accuracy was checked occasionally and was found to be limited by water waves or boat-rolling to +/- 0.1m, rather than by the pressure sensor on the CDTs probe. In calm conditions, and used from Penmaenpool Tollbridge, better than +/- 0.05m was obtained.

Most stations were occupied at one spring and one neap tide each, in order to gauge differences in flow characteristics caused by changes in tidal range, but inevitably data includes unquantified influences, such as wind and wave effects.

A summary of the data obtained is shown in Table 2.1. River flow is not gauged on the Mawddach or its tributaries, and the nearest gauging station is at Pont-y-Garth (G.R. SH635071) on the Afon Dysynni, 8km south of Barmouth railbridge, in a separate catchment. The data have been obtained from the Welsh Water Authority (W.W.A.). Monthly mean discharges for the Dysynni vary between 2.3 (June) and 7.1 (December), so it can be seen that the discharge on 27-8-86 (Station 5) was markedly higher than normal in the Dysynni, and almost certainly so in the Mawddach.

Table 2.1

Summary of data

LOCATION + LOCATION NO.	DATE	STATION	PREDICTED TIDAL HEIGHTS (m OD)	DURATION (hours)	RIVER FLOW (cumecs) (Dysynni)
1 Barmouth Bay GR 5694012090	8-9-87	Moored Boat	2.76 -1.94 3.06 ST-3/-2	4	4.82
2 Penrhyn Point	9-9-87	"	2.86 -1.94 3.06 ST-1/ST	11	4.46
2 "	21-8-87	"	1.26 -0.84 1.56 NT+4/+5	11.5	5.71
3 Barmouth Bridge	1-12-86	Railbridge	2.56 -1.64 2.66 ST-3/-2	12	4.96
3 "	28-8-86	"	-0.54 0.96 -0.44 NT-3/-2	8.75	4.88
4 Farchynys	12-8-87	Moored Boat	2.66 -1.84 2.96 ST-1/ST	12.5	5.84
4 "	20-8-87	"	0.96 -0.64 1.26 NT+2/+3	12.5	2.9
5 Penmaenpool	2-12-86	Bridge	2.76 -1.74 2.76 ST-1/ST	11.25	4.35
5 "	27-8-86	"	1.56 -0.64 1.46 NT-5/-4	13.25	7.35

Table 2.2

Maximum currents measured at each station

STATION	(m/s)							
	S P R I N G				N E A P			
	Umax		Umax		Umax		Umax	
	FLOOD	EBB	FLOOD	EBB	FLOOD	EBB	FLOOD	EBB
1	>0.7	>0.33	>0.42	>0.24	no data		no data	
2	2.15	1.37	1.77	1.22	0.77	0.69	0.66	0.57
4	>1.49	0.9	>1.38	0.71	0.63	0.33	0.58	0.29
5	0.94	0.4	0.77	0.21	0.0	0.27	0.0	0.24

recurrence interval of such events is important.

In addition to their immediate effects, there are possible resultant morphological changes offshore and within the estuary. These include altered estuary- mouth topography and width, major switching of channels, interchannel bar formation or destruction, or saltmarsh erosion. These different physical factors may then help determine future estuarine circulation.

2.1.4 Variable Cyclical Factors

Most predictable of the process inputs are the tidal heights and ranges achieved by the tidal wave, these cause the greatest circulation changes with time. Twice each day the estuary is virtually emptied of salt water by the ebbing tide, and is then inundated on the flooding tide with saline water to various depths, heights, distances and concentrations. Thus effective channel widths and depths continuously change, as do current velocities.

Tidal parameters in the Mawddach have three dominant periods: semi-diurnal, the fortnightly lunar cycle, and the twice yearly equinoxes. Thus, variations of estuarine circulation are easiest to define in terms of position within these tidal cycles. Without a concentrated long-term data collection programme, the precise distribution of other time- variable processes can only be gauged qualitatively. Due to the interaction of so many variables, no two estuaries are alike, so it is never known if general principles or unique details are being observed (Dyer, 1973).

2.1.5 Spatial Variability

It is important to note that not only are many factors time-variable, they are also spatially variable. The magnitude and range of variation may vary greatly along the length and across the width of estuaries.

The Mawddach displays a form similar to many N.W. European estuaries, with shifting intertidal banks, separating opposed blind channels, or flats where bedforms suggest opposing net bedload transport directions, e.g.

McCave & Geisler (1979), Elliott & Gardiner (1981). This form is both a result and a cause of lateral circulation variations in the estuary, and is an example of one of the most important concepts in estuarine processes, that of a process-response coupling. There is feedback between input variables such as tidal range, river flow, channel depth etc., which control the estuarine circulation, and the response, i.e. sediment transport and deposition.

2.1.6 Welsh Estuaries

Previous studies on circulation within shallow mesotidal (tidal range 2-4m) and macrotidal (range > 4m) estuaries are not numerous, possibly due to the practical difficulties involved. Measurements are normally taken in reasonably fair-weather conditions, and by no means cover the full spectrum of possible circulation states, especially in terms of modification by strong winds and large waves. The circulation of most estuaries around the north and west coasts of Wales have been studied in varying degrees of detail, including the Conwy, Seiont, Dwyryd, Mawddach, Dovey, Taf, Towy and Loughor.

The Conwy is partially-mixed (Hansen & Rattray, 1966) along most of its length (Jenkins, 1976), and recently has had particular attention paid to the well-developed frontal systems and their genesis (Lailey, 1980; O'Farrell, 1983; West & Cotton, 1981; Simpson & Turrell, 1986). Lateral velocities at the surface have been measured by Simpson & Turrell (1986) at up to 20% of axial velocities. The Seiont estuary exhibits fine tidal intrusion fronts studied by Nunes (1982), which led Nunes & Simpson (1985) and Simpson & Nunes (1981) to develop models of three-dimensional estuarine flow.

In a study on contemporary sedimentary processes in the Dwyryd, Mahamod (1989) showed it to be partially-mixed (Hansen & Rattray, 1966) in its lower reaches, with increased stratification near the mouth, and on neap tides. In a broad study of the Dovey estuary, Haynes & Dobson (1969) showed increased longitudinal and vertical salinity differences with high river discharges. Stratification was destroyed by spring tides, despite high river

flow. Across-estuary variation was marked during the early flood tide. Haynes & Dobson classified the estuary using the classification of Cameron & Pritchard (1963), and showed that it usually has a vertically homogeneous form with restricted lateral variation, though at times it is a moderately stratified type.

Jago (1974,1980) studied the Taf estuary in Carmarthen Bay, and similarly found that the greatest stratification coincided with neap tides, calm weather, and high runoff. In its upper reaches the Taf is stratified, and is stratified in its main part when neaps coincide with high river flow, but when river flow is low the estuary is well-mixed - whatever the tidal range.

Jonas (1977) compared the Towy estuary with the adjacent Taf, and the James River (Pritchard, 1967), and concluded from the mean salinity profiles that the Towy could be classified as a partially-mixed estuary. Greater than average river discharge produced a marked differential flow between the surface and the rest of the water column. However, in view of seaward net non- tidal velocities and intense mixing generated during the tidal cycle, Jonas (1977) considered that it should be thought of as well-mixed. Studies of the Loughor Estuary, in South Wales, have been done by Moore (1976), and Carling (1981). The estuarine waters are permanently well-mixed and laterally homogenous, and there are only minor inputs of freshwater relative to the tidal prism. The tidal curve becomes more asymmetrical towards the head, and is more asymmetrical at spring tides.

2.1.7 Previous Studies in the Mawddach

The Mawddach estuary has not been given full attention in terms of its circulation. McMullen (1964) gives limited velocity flow velocity data from Barmouth Railbridge. On spring tides, maximum ebb velocities were just greater than the flood, and at 0.15m above the bed most velocities were less than 0.5m/s. However, these data were taken 350m from the north end of Barmouth Bridge, whereas today the channel is only 100m wide at the north

bank, so the data are not directly comparable with more modern data.

The Welsh Water Authority (1978) measured depth profiles of salinity and velocity 100m southwest of the harbour mouth, and found that depth-mean ebb velocities were greater than the flood. On mean and spring tides the depth-mean ebb velocity attained 1.0 and 1.6m/s, respectively; the depth-mean flood velocity reached 0.9 and 1.2m/s. With river flow five times the normal dry weather flow, the top metre of the water column was stratified by 2-3ppt. At HW, depth-mean salinities reached 32.5ppt, at LW spring 18.5ppt and LW mean tides 19ppt.

Pattinson (1979) found that with high freshwater runoff (7.6cumecs) and near neap tides, surface salinities near the mouth dropped to zero for a short time near LW. Lateral surface salinity gradients existed at HW; the salinity was 0.75ppt higher at the south bank at Barmouth Railbridge than the north. In summer, with runoff of only 0.46cumecs, the saline intrusion at HW could extend well beyond the Mawddach- Wnion confluence, ie greater than 12.2km upstream of the bar.

O'Farrell (1983) conducted a qualitative study of axial convergences, and identified a complex system of fronts related to topographically-induced flow separation in the mid-stages of the flood tide. Time-lapse photography showed also that eddies occurred in some fronts, with eddy wavelengths 10-100m, amplitudes <30m and periods >10mins. These eddies occurred at times of maximum velocities, and disappeared as water depth increased. At HW + 1.5hrs, at the estuary mouth, two foam lines formed and stayed coherent for more than 1km seaward.

2.1.8 Summary of Welsh Estuaries

Comparisons between the estuaries mentioned above are not always easy due to their differing size and different type of data. In addition, the data have been interpreted and described using different methods, particularly in terms of estuarine classification schemes. However, the circulation patterns of these Welsh estuaries do have a number of features in common.

Most important is that over a tidal cycle their depths range from a few metres to zero, i.e. they are all very shallow, frictionally-dominated, and experience strong tidal currents with a large tidal range. The effect of river flow, which is often able to act alone in the estuary for periods of hours is, overall, a secondary factor compared to tidal range. Thus, the dynamics are strongly influenced by the cyclical regime of the tides, with more subtle effects superimposed by the non-cyclical river discharge variations.

Wind and waves are also important in determining circulation in these estuaries, with many of them having a wind/wave-built barrier across their mouths, restricting the free connection with the sea; particularly fine examples are the Mawddach, the Dovey, and the Taf. In addition to this long-term role of influencing estuarine circulation, waves can cause mixing of the surface of the water column and the wind may create a surface current. It is notable in this aspect that the three main estuaries of Cardigan Bay are all elongate in the SW-NE prevailing wind direction, and are therefore particularly likely at times to be influenced by wind-driven currents.

The precise way in which these estuaries have developed during the post-glacial sea-level rise is unknown. There are likely to have been differences in their evolution during that time, caused for example by different rates of sediment supply to the estuarine system.

In summary, the Welsh estuaries all show much temporal variation, and it is the short-term cyclical factors, i.e. the tides, with effects superimposed by the non-cyclical factors such as wind and waves, that are of most importance to this chapter. However it is important to note that some of these estuaries have been affected significantly by human intervention; for example, the bridges of the Conwy and Mawddach, or the blocking and reclamation of a major part of the Glaslyn-Dwyrdd.

Spatial variation of circulation in these estuaries is sometimes a very pronounced and important feature. This will be discussed in more detail below when dealing with estuarine classification.

2.2 Methods

At four locations along the estuary, and at one station in Barmouth Bay (Fig. 2.1), vertical profiles of the water column were sampled over one spring and one neap tidal cycle for current speed, direction, salinity and temperature. Direction was noted either as simply flood or ebb, or sometimes by compass bearing. Depending on total depth, readings were taken at variable depth intervals (i.e. 2m, 1m - or 0.5m if large vertical gradients were found). Using a winch and stainless steel wire, a Braystoke current meter with 5 or 2 inch (12.7 or 5.1mm) diameter impellor and a Valeport Series 600 C.T.D.S. probe, were lowered through the water column, with a streamlined weight below them to ensure as vertical a profile as possible. No depth corrections for wire angle have been made.

At each depth, velocity readings comprised 50secs (or sometimes 10secs) averages, so one profile was completed in about 5 minutes. This was completed every 15, 20, or 30mins as flow conditions merited. Non-availability of equipment dictated that a reliable directional current meter could be used only for the two surveys off Penrhyn Point and the station in Barmouth Bay. However, the limited data collected within the estuary suggests strongly polarised tidal current directions, and unless otherwise stated, data will be treated as if flood and ebb currents were directly opposed.

Equipment accuracy and repeatability was not a major problem with this work. However it should be noted that the current meters used have a manual-stated velocity threshold of 0.015 - 0.04m/s. The quoted accuracy of temperature and salinity data is +/- 0.1 degrees C and +/- 0.3ppt respectively. Depth accuracy was checked occasionally and was found to be limited by water waves or boat-rolling to +/- 0.1m, rather than by the pressure sensor on the CDTs probe. In calm conditions, and used from Penmaenpool Tollbridge, better than +/- 0.05m was obtained.

Most stations were occupied at one spring and one neap tide each, in order to gauge differences in flow characteristics caused by changes in tidal range, but inevitably data includes unquantified influences, such as wind and wave effects.

A summary of the data obtained is shown in Table 2.1. River flow is not gauged on the Mawddach or its tributaries, and the nearest gauging station is at Pont-y-Garth (G.R. SH635071) on the Afon Dysynni, 8km south of Barmouth railbridge, in a separate catchment. The data have been obtained from the Welsh Water Authority (W.W.A.). Monthly mean discharges for the Dysynni vary between 2.3 (June) and 7.1 (December), so it can be seen that the discharge on 27-8-86 (Station 5) was markedly higher than normal in the Dysynni, and almost certainly so in the Mawddach.

Table 2.1

Summary of data

LOCATION + LOCATION NO.	DATE	STATION	PREDICTED TIDAL HEIGHTS (m OD)	DURATION (hours)	RIVER FLOW (cumeecs) (Dysynni)
1 Barmouth Bay GR 5694012090	8-9-87	Moored Boat	2.76 -1.94 3.06 ST-3/-2	4	4.82
2 Penrhyn Point	9-9-87	"	2.86 -1.94 3.06 ST-1/ST	11	4.46
2 "	21-8-87	"	1.26 -0.84 1.56 NT+4/+5	11.5	5.71
3 Barmouth Bridge	1-12-86	Railbridge	2.56 -1.64 2.66 ST-3/-2	12	4.96
3 "	28-8-86	"	-0.54 0.96 -0.44 NT-3/-2	8.75	4.88
4 Farchynys	12-8-87	Moored Boat	2.66 -1.84 2.96 ST-1/ST	12.5	5.84
4 "	20-8-87	"	0.96 -0.64 1.26 NT+2/+3	12.5	2.9
5 Penmaenpool	2-12-86	Bridge	2.76 -1.74 2.76 ST-1/ST	11.25	4.35
5 "	27-8-86	"	1.56 -0.64 1.46 NT-5/-4	13.25	7.35

Table 2.2

Maximum currents measured at each Station

STATION	(m/s)							
	S P R I N G				N E A P			
	Umax		Umax		Umax		Umax	
FLOOD	EBB	FLOOD	EBB	FLOOD	EBB	FLOOD	EBB	
1	>0.7	>0.33	>0.42	>0.24	no data		no data	
2	2.15	1.37	1.77	1.22	0.77	0.69	0.66	0.57
4	>1.49	0.9	>1.38	0.71	0.65	0.33	0.58	0.29
5	0.94	0.4	0.77	0.21	0.0	0.27	0.0	0.24

2.3 Results

A series of contoured depth-time plots have been produced from the data (Figs. 2.2 - 2.17, and Appendix 2.1). In each case, the x-axis runs approximately from HW to HW. Data points are shown, as it is important to see the spread of data from which the contours were drawn. Note the variable contour intervals, in some plots. Dashed lines on the diagrams show conjectural contours. The data are plotted using the water surface as a datum; the stratification was most strongly developed on the surface of the water column and this form of plot reduces distortion of surface data.

Shown on the diagrams are the calculated times of HW and LW at each station, obtained using the tidal delay curves presented later (Section 2.4.5.3). No measurements of tidal height were taken simultaneously with the C.T.D. data, so these estimated times can be used only as a guide to data interpretation. As can be seen from many of the diagrams, the maximum depth-time curve cannot be used as a tidal elevation curve, for reasons that include the boat swinging in the tide on its mooring and the presence of large bedforms.

2.3.1 Velocity Data (Summary Table 2.2)

(Note that maximum velocities at Station 1 were not measured due to restricted data collection).

2.3.1.1 Barmouth Bay, Station 1 (Fig. 2.2)

This station is 4km SW of the Bar, and was occupied to provide a guide to coastal flow speeds and directions.

Spring tide: - Data were collected in a light swell for 4hrs only (data collection was curtailed due to equipment failure), which included the last 1.5hrs of the ebb and the first 2.5hrs of the flood tide.

Neap tide: - No data were obtained.

2.3.1.2 Penrhyn Point, Station 2 (Figs. 2.3 & 2.4)

Penrhyn Point and the breakwater to the N.W. together constrict the flow of water in and out of the estuary, to a channel less than 180m wide and approximately 7m deep at LW (although depth is very variable over small distances in this area). This small cross-section (1140m² at HWS, 400m² at LWS) is probably a major factor causing the high tidal velocities measured here.

Spring tide:- A notable feature of the velocity profiles at this station is the near vertical velocity contours (isovels) during times of flow acceleration and deceleration, compared to those at neaps.

Neap tide:- Increased stratification occurs (at least in part) causing isovels to be less vertical; this will be discussed in detail later.

2.3.1.3 Barmouth Bridge, Station 3

Data collection on both spring and neap tides was disrupted by equipment failures and forced changes in position. This resulted in the collection of far less useful data than the other station surveys.

2.3.1.4 Farchynys, Station 4 (Figs. 2.5 & 2.6)

This station was situated about 10-20m from the north shore, in what is essentially the river channel at LW. This position was chosen as it is a constriction of only 270m width at its narrowest point; it may act as a significant control upon estuarine dynamics.

Spring tide:- Data collection was disrupted for 50min. during the flood tide. The vertical structure of the flow was not sampled over this period; the instrument cable had become snagged and could not be raised or lowered.

Neap tide:- Peak ebb velocities were maintained constant for 4.5hrs, starting at HW + 1hr.

Fig. 2.3 9-09-87 PENRHYN POINT Velocity (m/s)

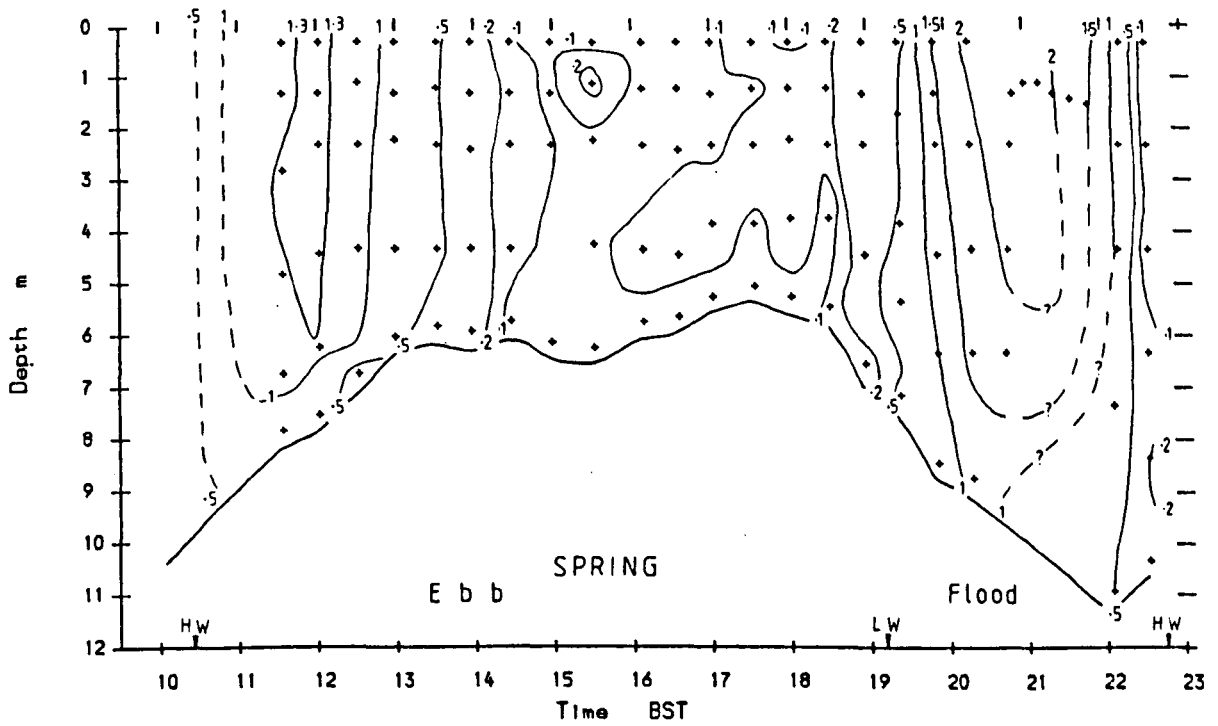


Fig. 2.4 21-08-87 PENRHYN POINT Velocity (m/s)

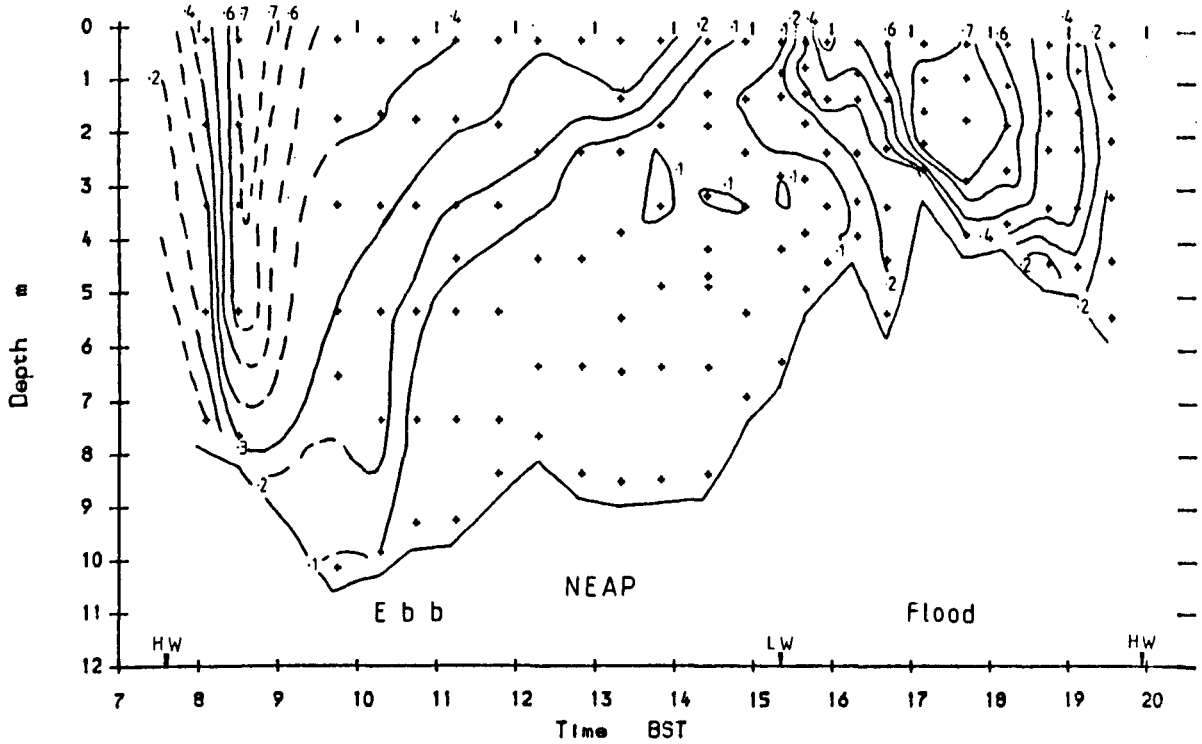


Fig. 2.5 12-08-87 FARCHYNYS Velocity (m/s)

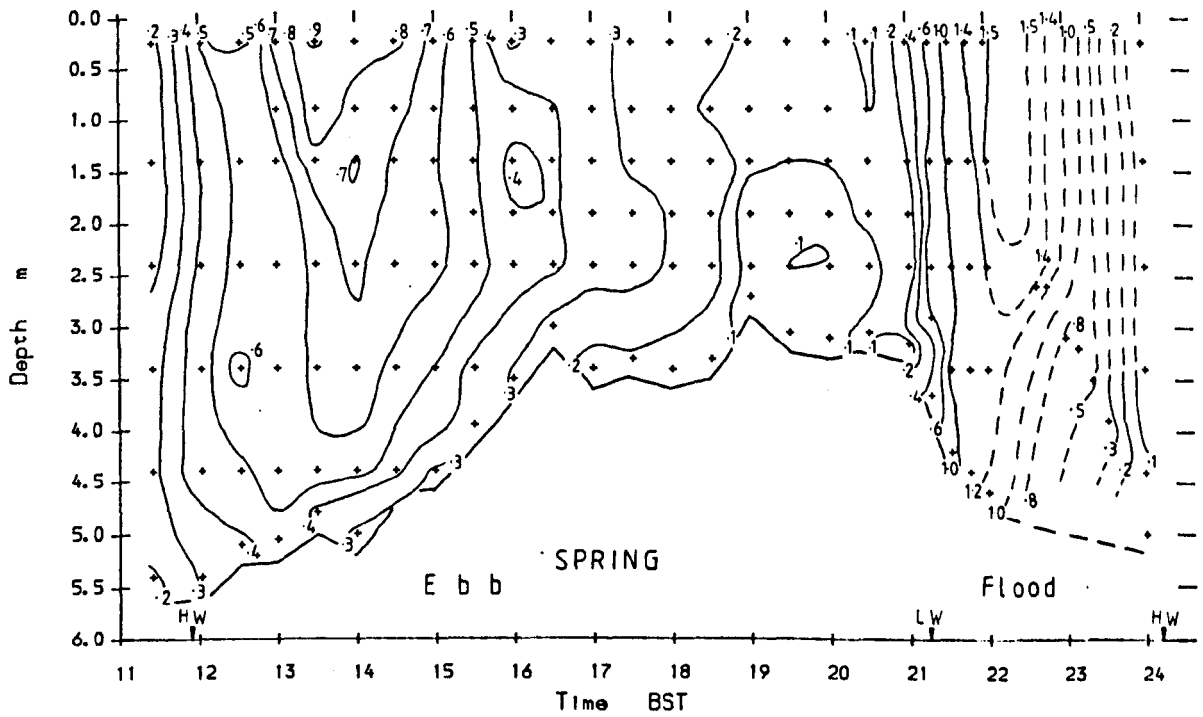
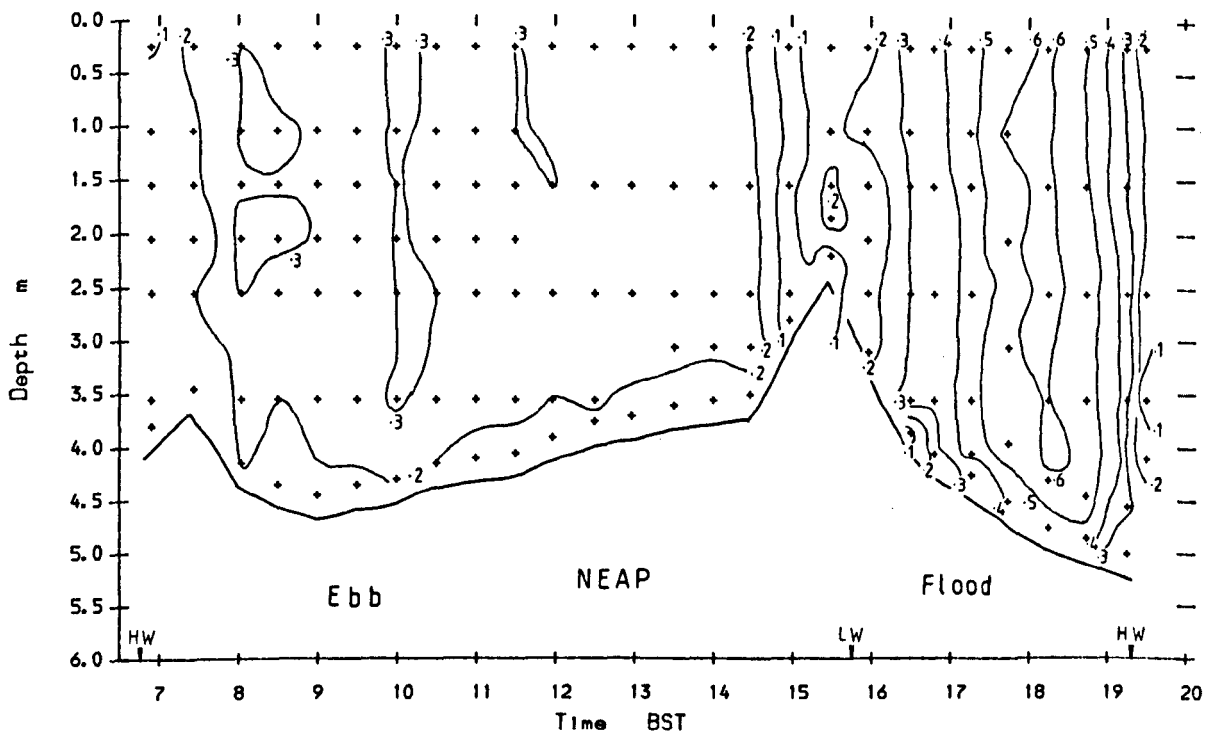


Fig. 2.6 20-08-87 FARCHYNYS Velocity (m/s)



2.3.1.5 Penmaenpool, Station 5 (Figs. 2.7 & 2.8)

Penmaenpool Tollbridge is 11km upstream of the Bar.

Spring tide:- Flood isovels were nearly vertical, but the ebb always had a significant velocity gradient - with near-bed flow velocity always below 0.1m/s.

Neap tide:- Flow velocities were much lower than those of the spring tide, and the neap flood was manifest only as an hour long gradual depth increase - with no measurable inland flow.

2.3.2 Salinity Data (Summary Table 2.3)

2.3.2.1 Barmouth Bay, Station 1 (Fig. 2.9)

Spring tide:- During the late stages of the ebb tide, the surface 4m of the water column was notably warmer and less saline, and had a greater vertical salinity gradient than the underlying water. The boundary between these two layers was at 33.3ppt (parts per thousand), and a maximum gradient of 0.4ppt/m was present near-surface.

2.3.2.2 Penrhyn Point, Station 2 (Figs. 2.10 & 2.11)

Spring tide:- Slight salinity stratification on the ebb tide, with up to 4ppt difference between flow surface and bottom, with a similar degree of stratification in the the early stages of the flood tide.

Neap tide:- This showed the largest salinity range and stratification, with up to 27.7ppt difference surface to bottom in the late stages of the ebb. Stratification remained on the flood, though less pronounced, until peak velocities were attained midway through the flow.

2.3.2.3 Farchynys, Station 4 (Figs. 2.12 & 2.13)

Spring tide:- Up to a 5.3ppt surface to bottom salinity difference was recorded in mid-ebb, with a similar difference persisting for at least the early parts of the flood.

Neap tide:- Zero measurable salinity for at least 5hrs of the tidal cycle.

Table 2.3 SUMMARY OF SALINITY DATA

(ppt)

STATION	S P R I N G				N E A P			
	Max	Min	HW	LW	Max	Min	HW	LW
1	33.54	31.65	--	32.7	--	--	--	--
2	33.2	21.5	33.1	25.1	33.0	3.9	32.9	20.05
3	32.73	7.43	32.34	13.37	--	--	32.53	--
4	32.85	1.62	31.8	1.8	11.0	0.0	18.1	0.0
5	(22)	0.0	(21)	0.0	0.0	0.0	0.0	0.0

(Brackets denote extrapolated figure)

Fig. 2.7 2-12-86 PENMAENPOOL Velocity (m/s)

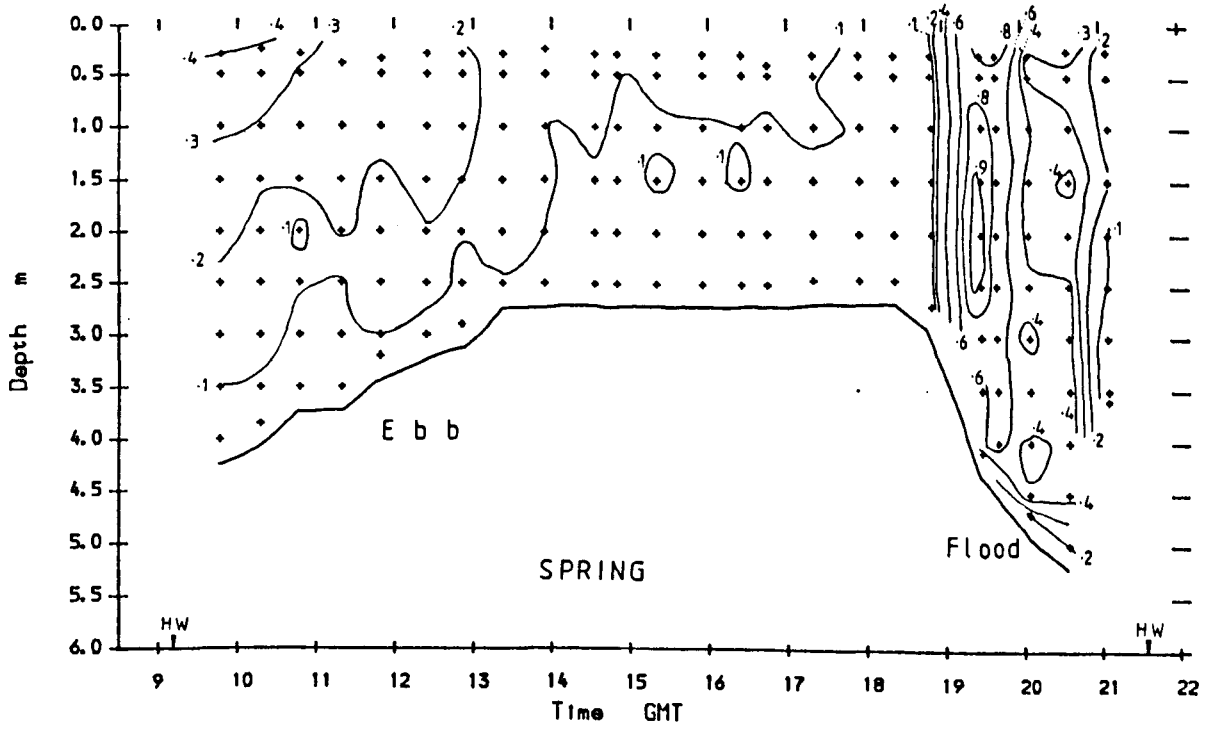
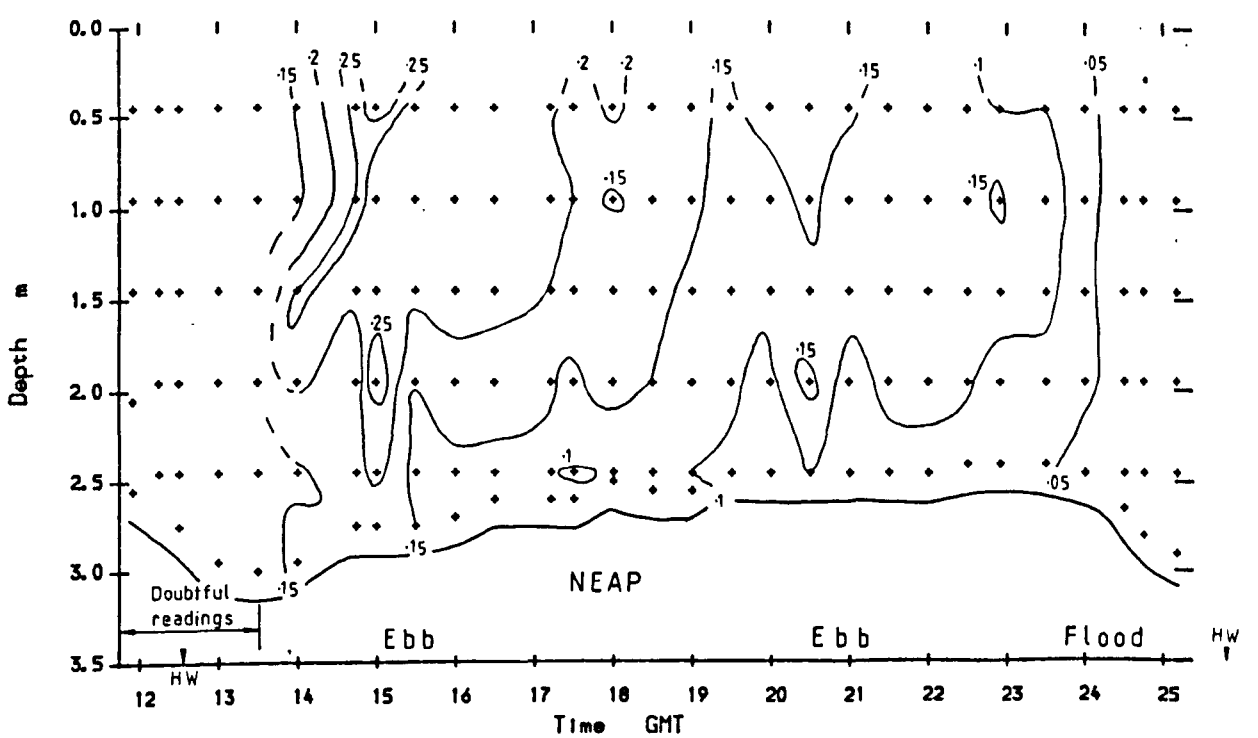
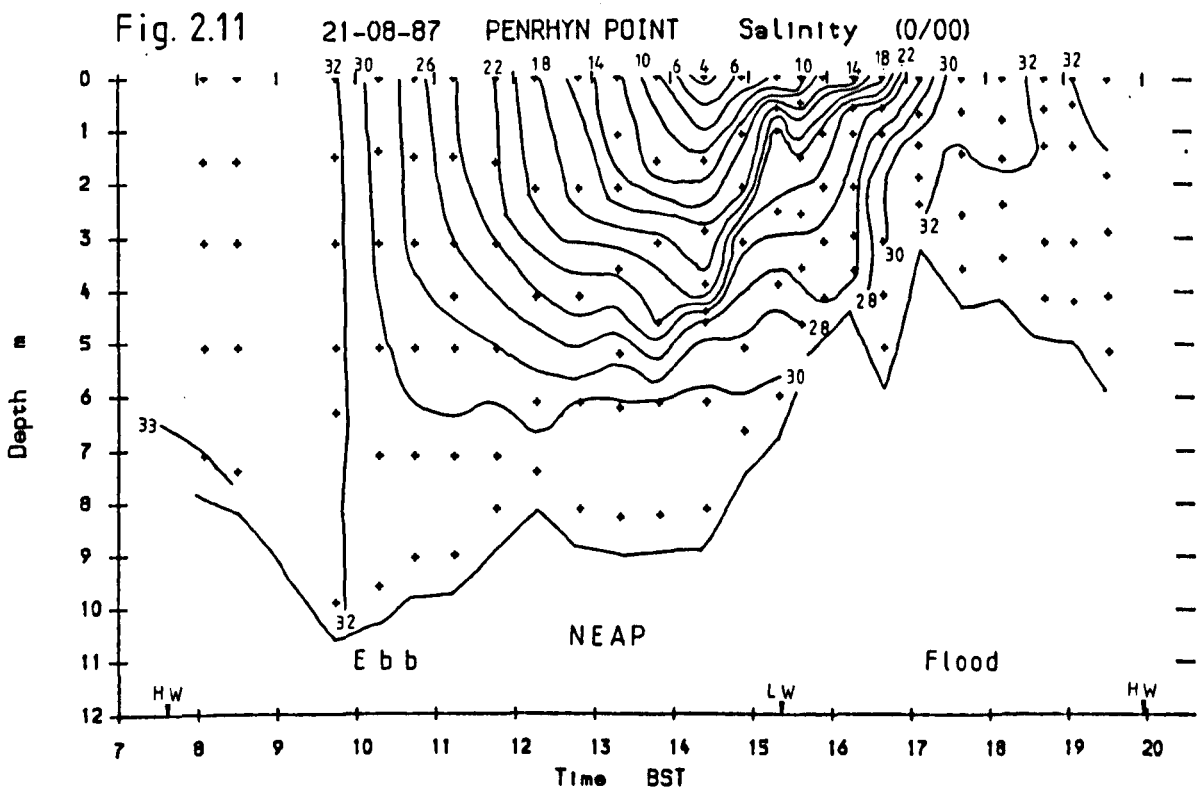
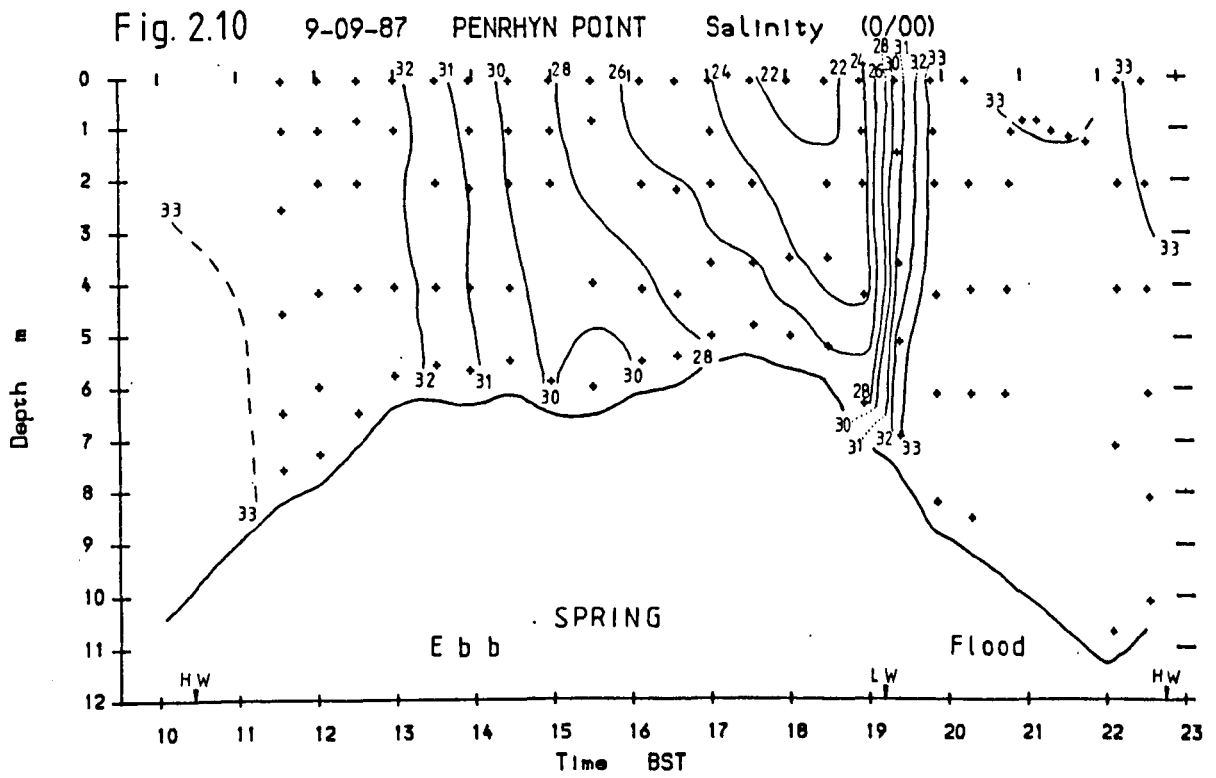
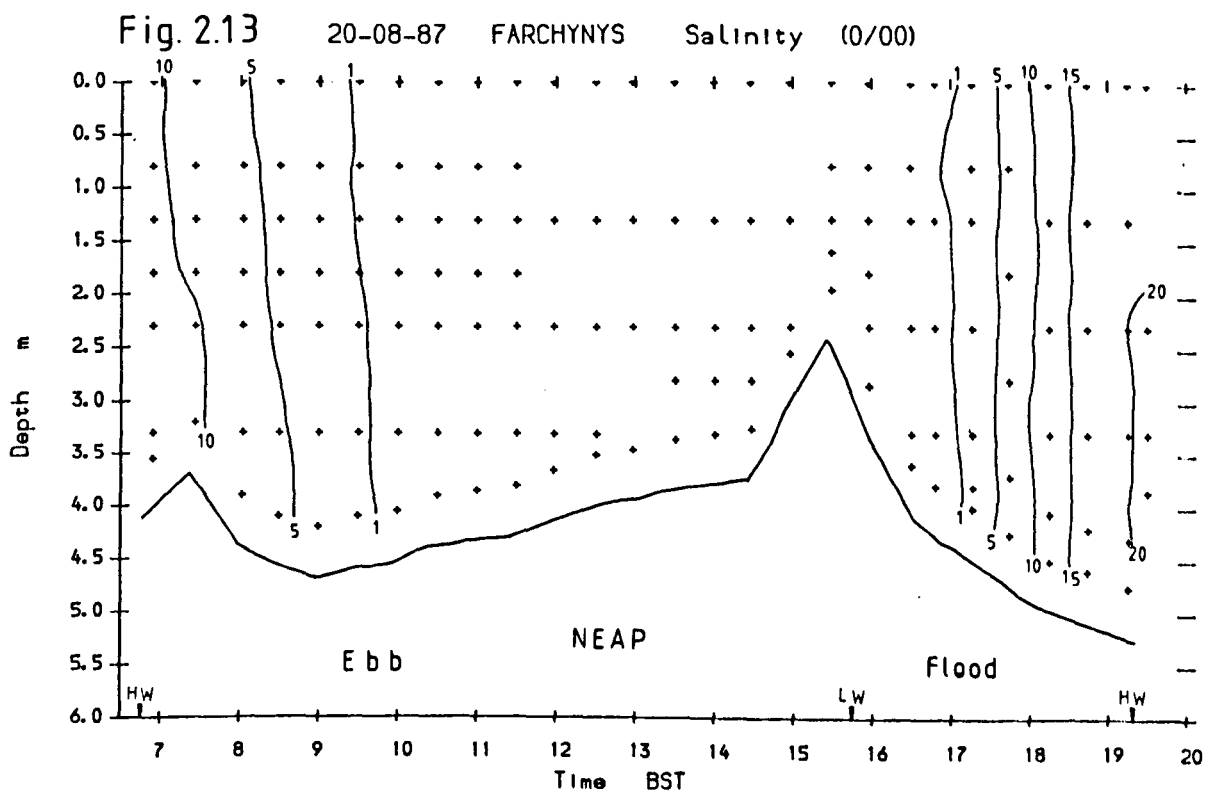
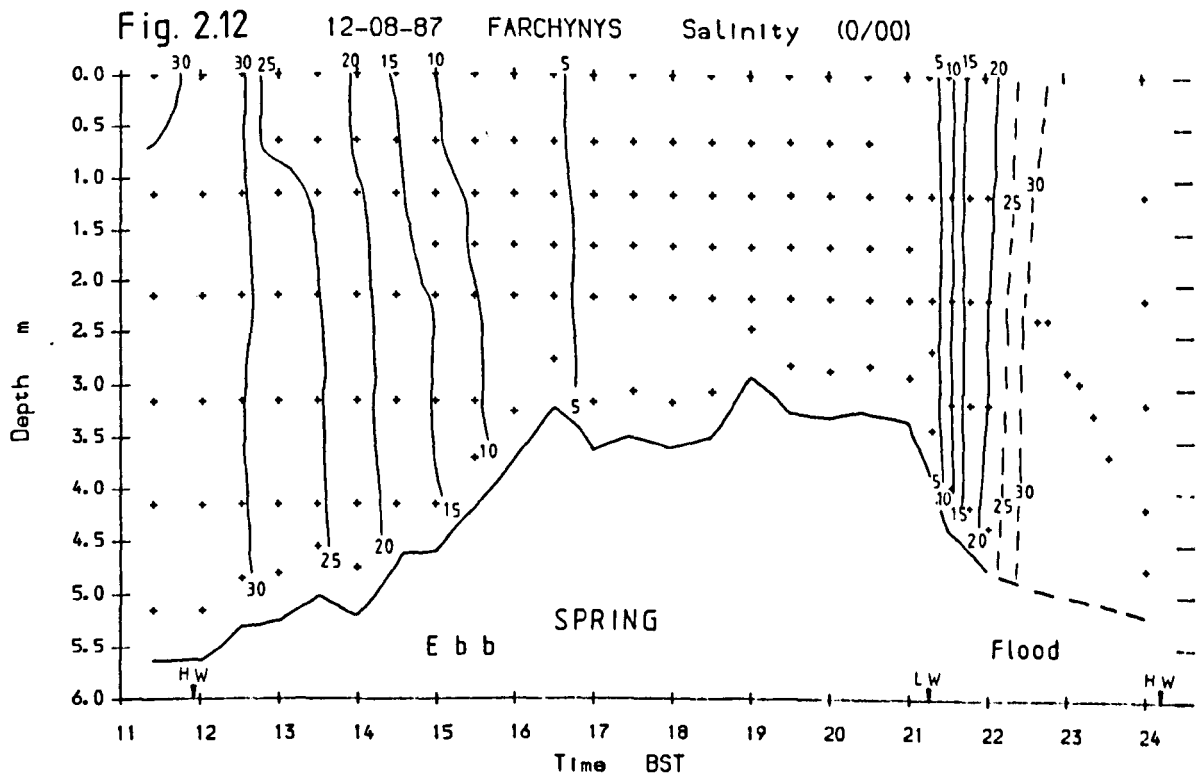


Fig. 2.8 27-08-86 PENMAENPOOL Velocity (m/s)







2.3.2.4 Penmaenpool, Station 5 (Fig. 2.14)

Spring tide:- The early ebb showed stratification, and the early flood showed up to 3.2ppt difference. Salinity was zero for over six hours of the tidal cycle.

Neap tide:- No salinity was measurable throughout the whole tidal cycle, though it is not clear how much this was due to extremely heavy rain two days previously.

2.3.3 Flow Direction Data

Accurate data was obtained only for Stations 1 and 2. The Braystoke current meter gave readings to the nearest 10 degree interval.

2.3.3.1 Barmouth Bay, Station 1 (Fig. 2.15)

Spring tide:- The late stages of the ebb flow varied in direction between 180 and 240 degrees, with mid-depths tending more towards 230-240 degrees. At LW the flow direction turned anticlockwise and the entire water column flowed towards 030-060 degrees.

2.3.3.2 Penrhyn Point, Station 2 (Figs. 2.16 & 2.17)

Spring tide:- The ebb tide flowed towards 240-270 degrees until HW + 4hrs when a complex directional regime was measured, largely because the main ebb flow occurred 60m north of the boat, and an eddy was present. As the flood began, the water column flowed towards 050-100 degrees, later with increased velocities, veering towards 140-180 degrees, though detail here is lacking.

Neap tide:- This had an ebb direction of 220-270 degrees, and the basal 4m of the flow was of negligible velocity. In the first hour of the flood tide, the surface 3m flowed towards 050-070 degrees; later the whole column moved in this direction.

Fig. 2.14 2-12-86 PENMAENPOOL Salinity (0/00)

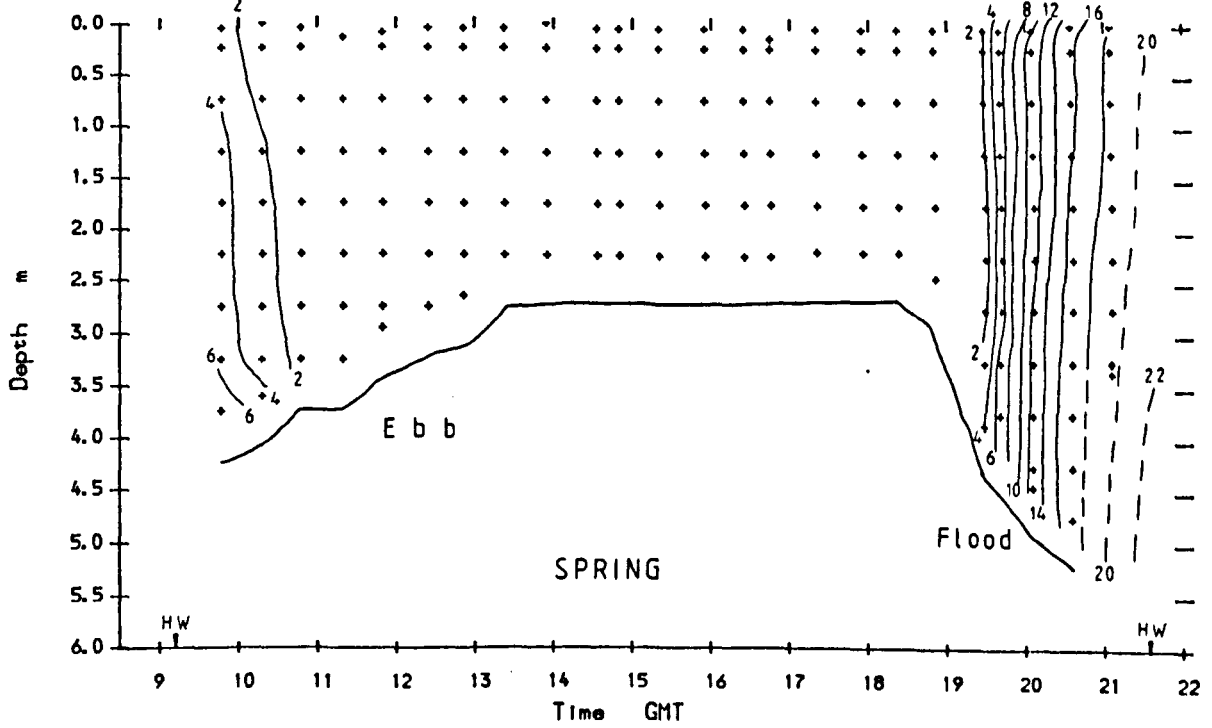
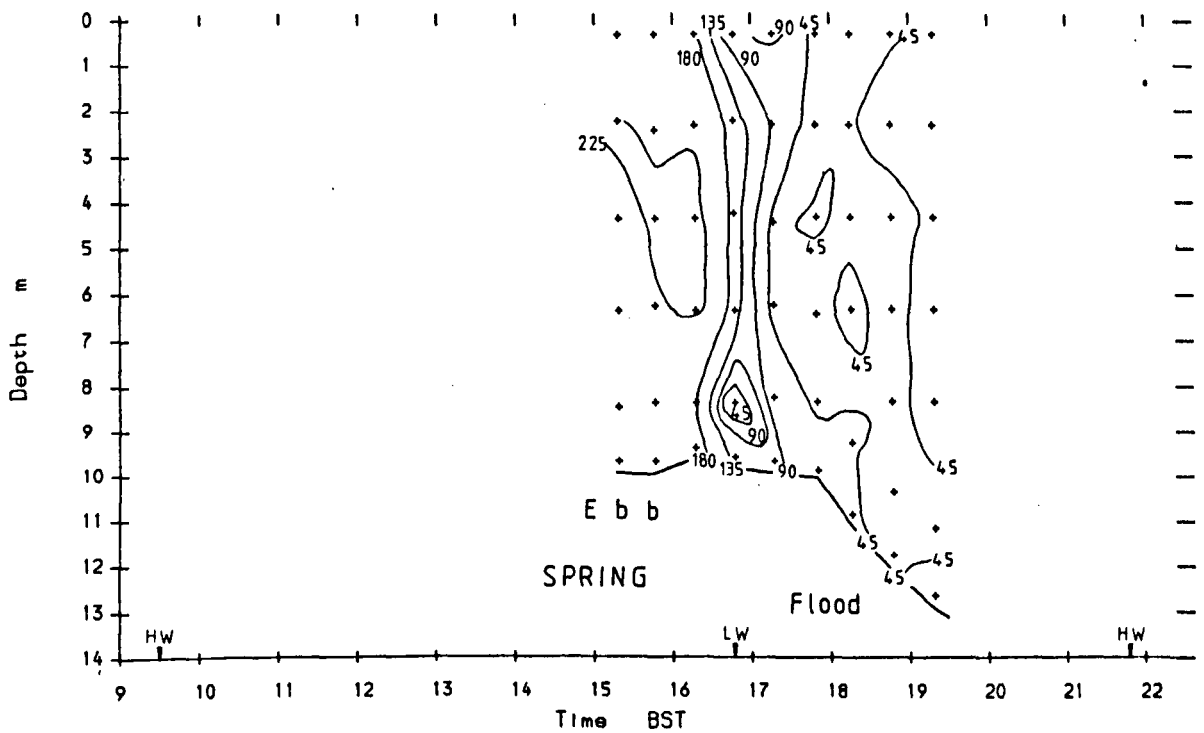
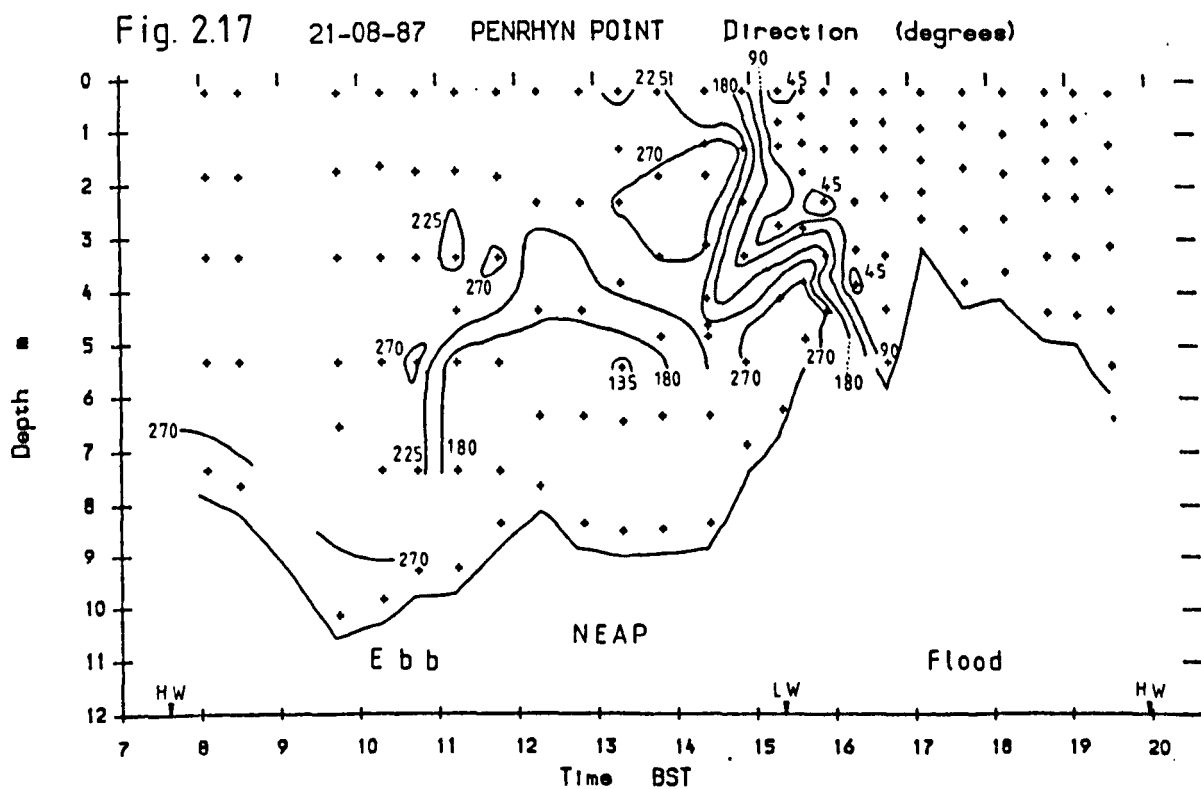
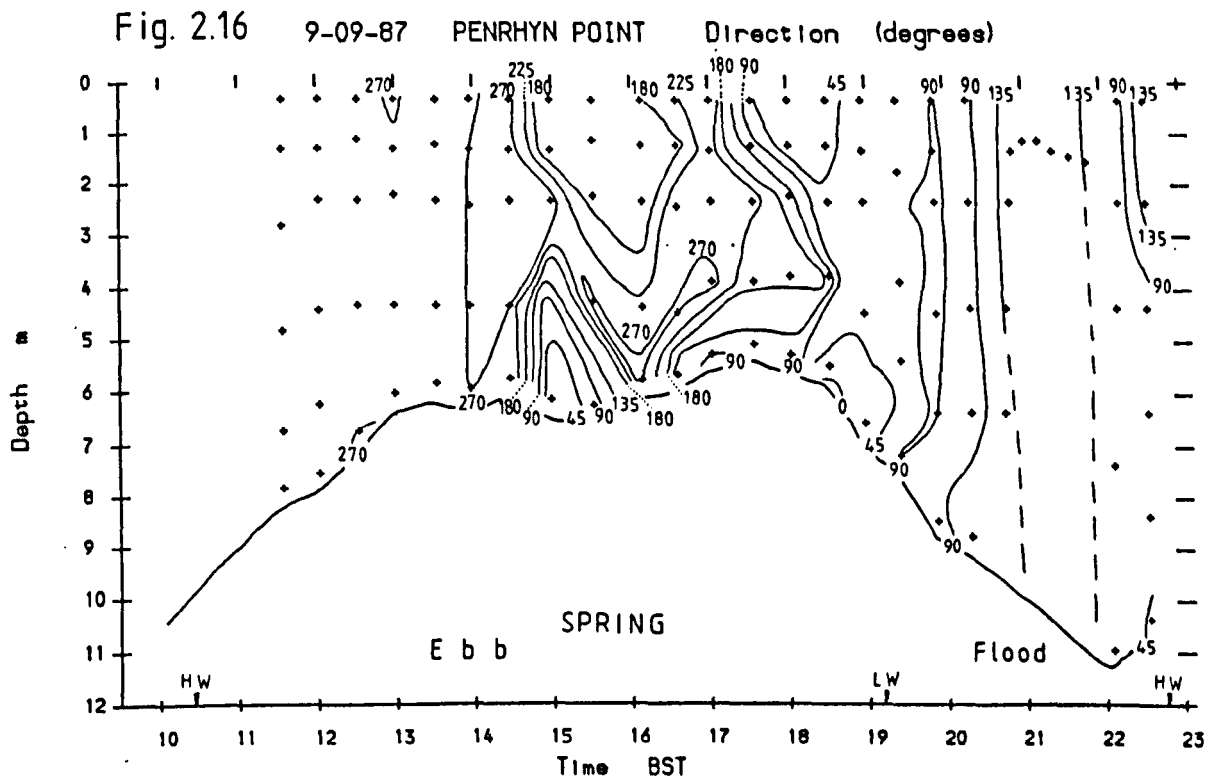


Fig. 2.15 8-09-87 BARMOUTH BAY Direction (degrees)





2.3.3.3 Farchynys, Station 4

A less reliable directional current meter suggested that, as expected, flood and ebb currents at this station were directly opposite in direction. A significant feature shown on both spring and neap tide surveys was that at HW the surface began ebbing while the bottom still flooding.

2.3.4 Summary of Results

There are a number of important points to note :

(1) Velocities experienced in Barmouth Bay are generally weaker than in the estuary; however, landward of the mouth, measured velocities decrease rapidly. Generally, the flood has higher velocities and a shorter duration than the ebb, although there is a less pronounced velocity asymmetry on neap tides. The ebb- flood duration ratio increases progressively up- estuary.

See also other data on tidal durations, Section 2.4.5.3, and Tables 2.6 and 2.7.

(2) On neap tides, saline water reaches between 6.5km and 10.5km upstream of the Bar, though the river flow is halted for one hour and the water level is raised approximately 0.5m. Spring tides result in the saline intrusion reaching 12km upstream (Pattinson, 1979), with peak flood velocities approaching 1m/s 10.5km upstream of the Bar (Station 5).

(3) 6.5km from the Bar at Farchynys (Station 4), neap ebb velocities remain at their maximum for 4-5hrs, implying that a factor additional to the tide is important.

(4) There is a very high salinity range in the lower estuary, approximately 30ppt over a lunar cycle, decreasing upstream to 22ppt at station 5, 10.5km from the Bar. On neap tides and with high runoff, significant stratification occurred at the estuary mouth, with up to 27.7ppt top to bottom difference in the late stages of the ebb.

(5) Even on spring tides, near LW, in Barmouth Bay there may exist a 4m thick surface layer of relatively low salinity and high temperature.

(6) In Barmouth Bay at Station 1, spring tide flood flow is towards 030-060 degrees at over 0.7m/s, and there is an anticlockwise flow rotation over time. At the estuary mouth (Station 2), spring tide current directions are variable, whereas at neaps and further up-estuary they are essentially rectilinear.

2.3.5 Data Interpolation / Extrapolation

In understanding and classifying the hydrography of the estuary, it is desirable to know the direction of net flow of estuarine waters, which also has relevance to the potential transfer of nutrients or pollutants within the estuary. With a time series of flow data, net water velocities are computed by totalling water flux at each relative depth over a full tidal cycle, hence removing the effects of the tide.

Not all of the data sets are 12.5hrs long (Table 2.1), so some data has been extrapolated in order to calculate some time-averaged parameters. Interpolation has been used if data was lost in mid-survey.

Both interpolation and extrapolation have been done by joining or extending contours on the time-depth plots, so that contours represent physically plausible situations consistent with those measured or expected. For example, flow velocities at predicted times of HW at each station have been taken as zero.

2.4 Discussion

2.4.1 Time-Averaged Parameters

The velocity data, and some salinity data, have been manipulated to provide time-averages at relative depths (z/h , where z = depth of reading, h = total depth) of 0.1, 0.3, 0.5, 0.62, 0.7 and 0.9. The velocity data are presented in three diagrams, respectively, averaged over the time of the flood flow, ebb flow, and whole tidal cycle (here taken as 12.5hrs). These are below referred to as flood-averaged, ebb-averaged and tide-averaged data. On the figures, the suffix after each station number indicates whether the data is from a spring or neap tide.

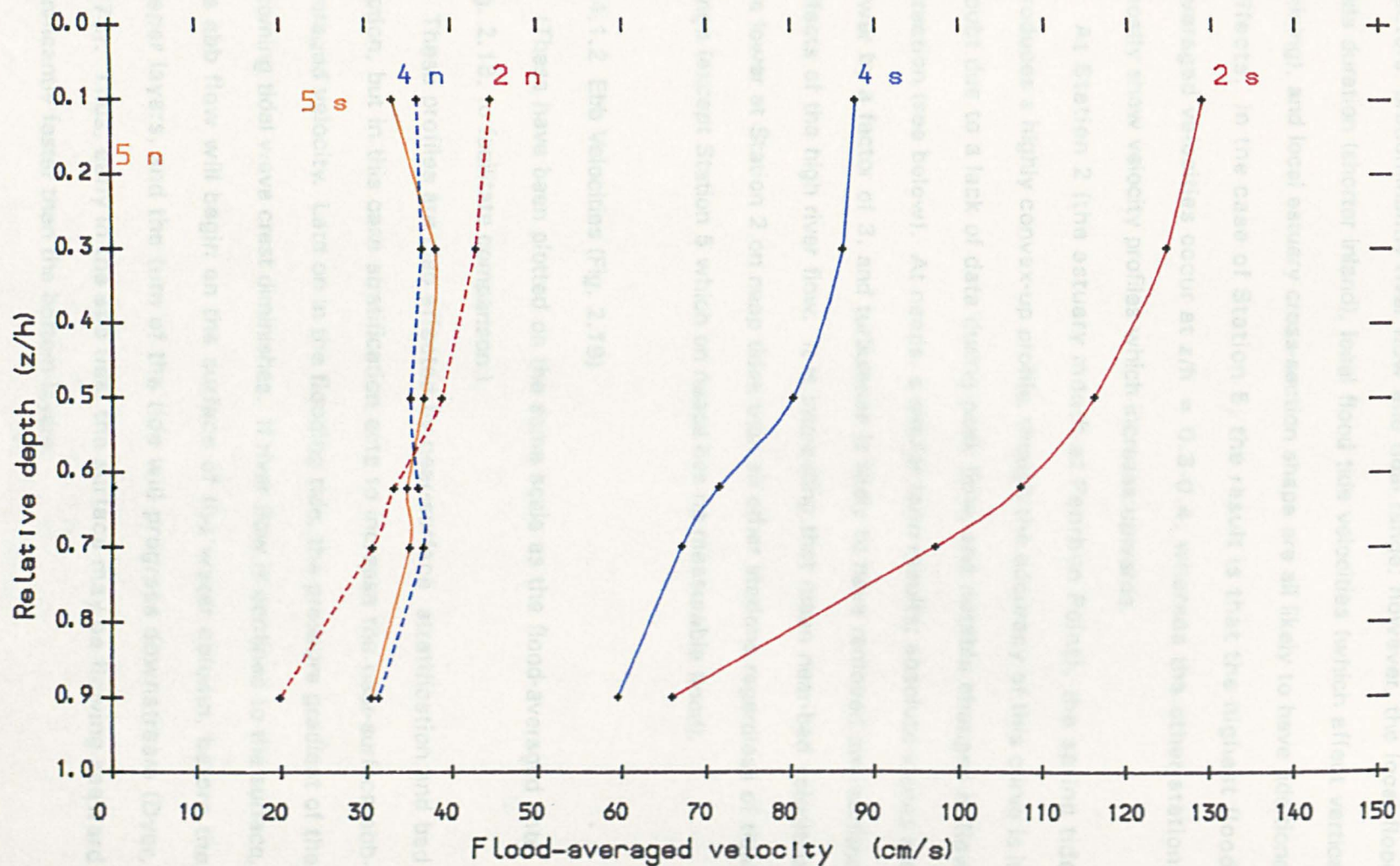
For each data set the times of zero depth-mean velocity near LW and HW formed the limits between 'flooding' and 'ebbing' tides. No account has been taken here of flow direction variations; the tide has been treated as rectilinear. The data sufficiently complete for use here are from Stations 2, 4 and 5, spring and neap tides.

2.4.1.1 Flood Velocities (Fig. 2.18)

The flood-averaged velocity profiles show well the large spatial and temporal variations; for example the different flood current strengths along the estuary, and with tidal range. Jago (1974) showed that the flood-averaged velocity profile is affected by two main factors: firstly, any near-surface stratification, (i.e. river flow), and secondly, bed friction.

Eleven kilometres from the bar, at Station 5, there is no flood current on neap tides, whereas on spring tides the flood-averaged velocities are between 0.3 and 0.4m/s, and the profile showed both a near-surface and a near-bed decrease. This was the only recorded instance of significantly reduced flood tide surface velocities, and may be attributed to stratification. In a stratified (two-layer) flow, the outflowing surface (river) water will not turn until there is a pressure gradient sufficient to reverse it. Thus the bottom floods first, before the surface (Dyer, 1973), and so upstream

Fig. 2.18 Flood-averaged velocity profiles - Stations 2, 4, 5



surface velocities will be decreased.

There is a very slight surface velocity decrease in the neap tide curve of Station 4, suggesting that this phenomenon may occur over many kilometres of the estuary, to a varying extent. It may be dependent upon a number of factors, predominantly river flow and tidal range; however, the local flood tide duration (shorter inland), local flood tide velocities (which affect vertical mixing), and local estuary cross-section shape are all likely to have additional effects. In the case of Station 5, the result is that the highest flood-averaged velocities occur at $z/h = 0.3-0.4$, whereas the other stations mostly show velocity profiles which increase upwards.

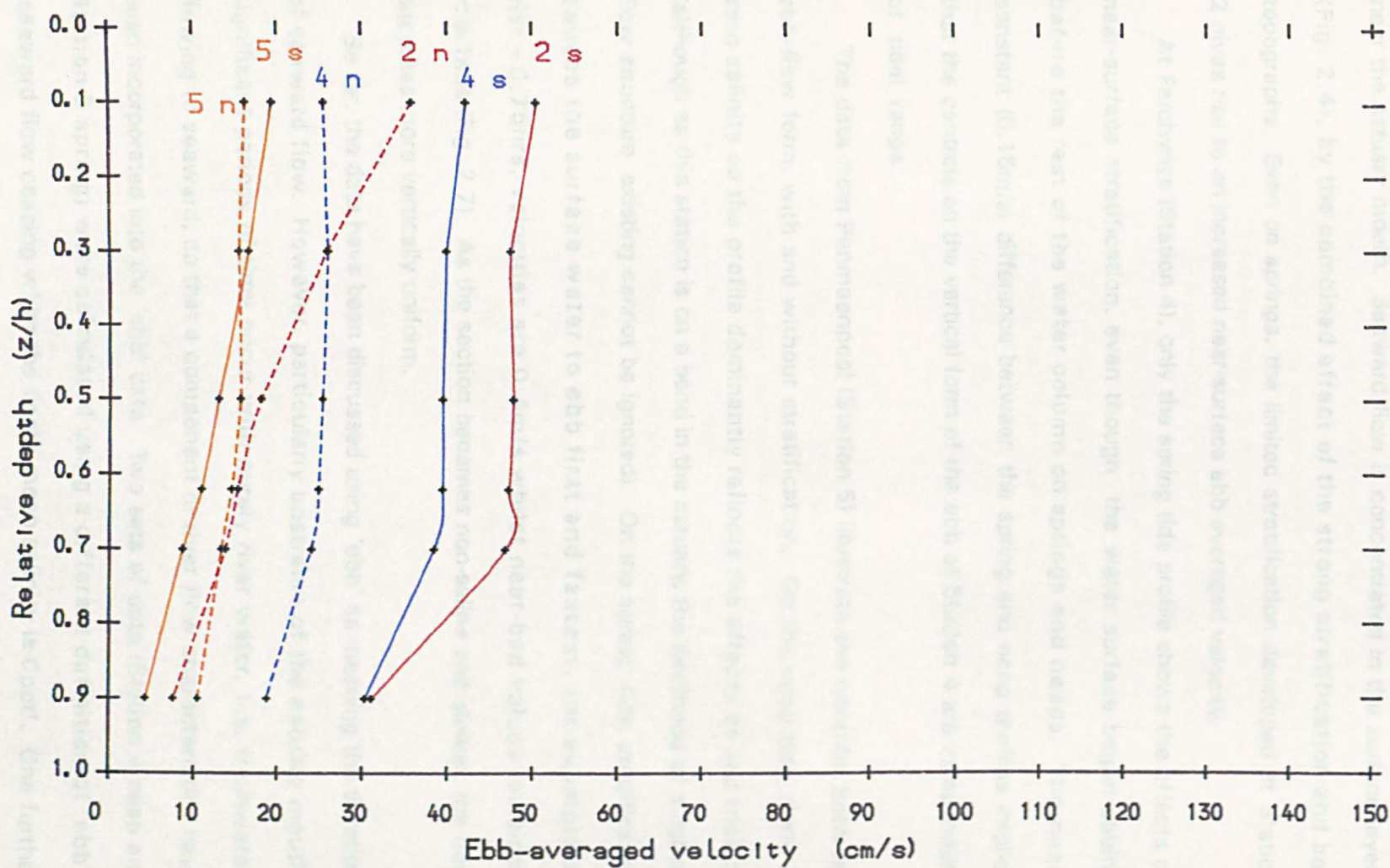
At Station 2 (the estuary mouth at Penrhyn Point), the spring tide produces a highly convex-up profile, though the accuracy of this curve is in doubt due to a lack of data during peak flow, and notable changes in flow direction (see below). At neaps, a similar form results; absolute values are lower by a factor of 3, and turbulence is likely to have removed any surface effects of the high river flow. It is interesting that mean near-bed velocities are lower at Station 2 on neap tides than all other stations regardless of tidal range (except Station 5 which on neaps has no measurable flood).

2.4.1.2 Ebb Velocities (Fig. 2.19)

(These have been plotted on the same scale as the flood-averaged data, Fig. 2.18, to facilitate comparison.)

These profiles are also affected by near-surface stratification and bed friction, but in this case stratification acts to increase the near-surface ebb-averaged velocity. Late on in the flooding tide, the pressure gradient of the incoming tidal wave crest diminishes. If river flow is confined to the surface, the ebb flow will begin on the surface of the water column, before the deeper layers, and the turn of the tide will progress downstream (Dyer, 1973). Thus, early in the ebb tide, the surface may be flowing seaward significantly faster than the bottom layers.

Fig. 2.19 Ebb-averaged velocity profiles - Stations 2, 4, 5



The most obvious candidate for such an interpretation is Station 2 at neap tide, which shows 0.2m/s difference between z/h at 0.1 and 0.5. However, there is insufficient directional evidence for this, and a possible alternative or additional explanation is that near-bed saline water was slowed down when moving through a scour depression, of which there are a number near the estuary mouth. Seaward flow is concentrated in the surface layers (Fig. 2.4), by the combined effect of the strong stratification and bed topography. Even on springs, the limited stratification developed at Station 2 gives rise to an increased near-surface ebb-averaged velocity.

At Farchynys (Station 4), only the spring tide profile shows the effects of near-surface stratification, even though the water surface began ebbing before the rest of the water column on springs and neaps. The near-constant (0.15m/s) difference between the spring and neap profiles implies that the controls on the vertical form of the ebb at Station 4 are independent of tidal range.

The data from Penmaenpool (Station 5) illustrate the contrast between ebb-flow form, with and without stratification. On the neap tide, there is zero salinity so the profile dominantly reflects the effects of bed friction (although as this station is on a bend in the estuary, the likelihood of a helical flow structure existing cannot be ignored). On the spring tide, stratification causes the surface water to ebb first and fastest, for example at HW + 0.75hrs, velocities are 0.4m/s whilst near-bed values remained <0.1m/s (Fig. 2.7). As the section becomes non-saline and slower, the flow becomes more vertically uniform.

So far, the data have been discussed using 'ebb' as meaning the duration of seaward flow. However, particularly upstream of the estuary mouth, significant periods of time occur with purely river water, (i.e. freshwater) flowing to seaward, so that a component of river flow characteristics have been incorporated into the 'ebb' data. Two sets of data (Station 4 neap and Station 5 spring) were calculated using a different definition of 'ebb': 'seaward flow ceasing when the depth-mean salinity is 0ppt'. One further

set (Station 4 spring) was recalculated using ebb as the time when water depth was decreasing, as the salinity when water depth stabilised was 2.2ppt and is considered to be due to runoff of saline water from saltmarshes further upstream.

The recalculated 'ebb'-averaged profiles are presented with the original calculations in Fig. 2.20. The salinity-defined profile at Station 5 has greater velocities at all depths, and an increased overall velocity gradient. The effect of stratification is more clearly seen in the upper half of the flow.

In contrast, the recalculated data of Station 4 shows identical form to the duration-calculated profiles. The neap profiles are also identical in absolute velocities, showing that the river flow and ebb flow are of very similar character. This implies that the flow control is a physical one, which may also explain the identical flow form of the two spring tide 'ebb'-averaged profiles.

2.4.1.3 Flood- and Ebb- Depth-Mean Velocities (Fig. 2.21)

The flood- and ebb-averaged velocity profiles of Figs. 2.18 & 2.19 have been used to compute a depth- mean velocity for each time-averaged velocity profile i.e. a velocity representative of the complete flood- ebb cycle. (It should be noted that these data do not represent the mean flow through a complete cross- section of the estuary, at each section). The numbers beside each point are the the change in predicted height of HW (in metres) from the first HW to the second.

The velocity profiles in these figures are based on 'ebb' as the duration of seaward flow, so flood tide values include the effect of landward-shortening duration (likely to increase flood-averaged velocities), as well as effects of friction, and convergence. The greater the relative influence of bed friction on the tidal wave, the more rapid the upstream decrease in flood-depth-mean velocity. In contrast, tidal wave amplification by convergence will cause tidal speeds to increase upstream towards the estuary head.

Fig. 2.20 'Ebb'-averaged profiles - 2 definitions of 'Ebb'

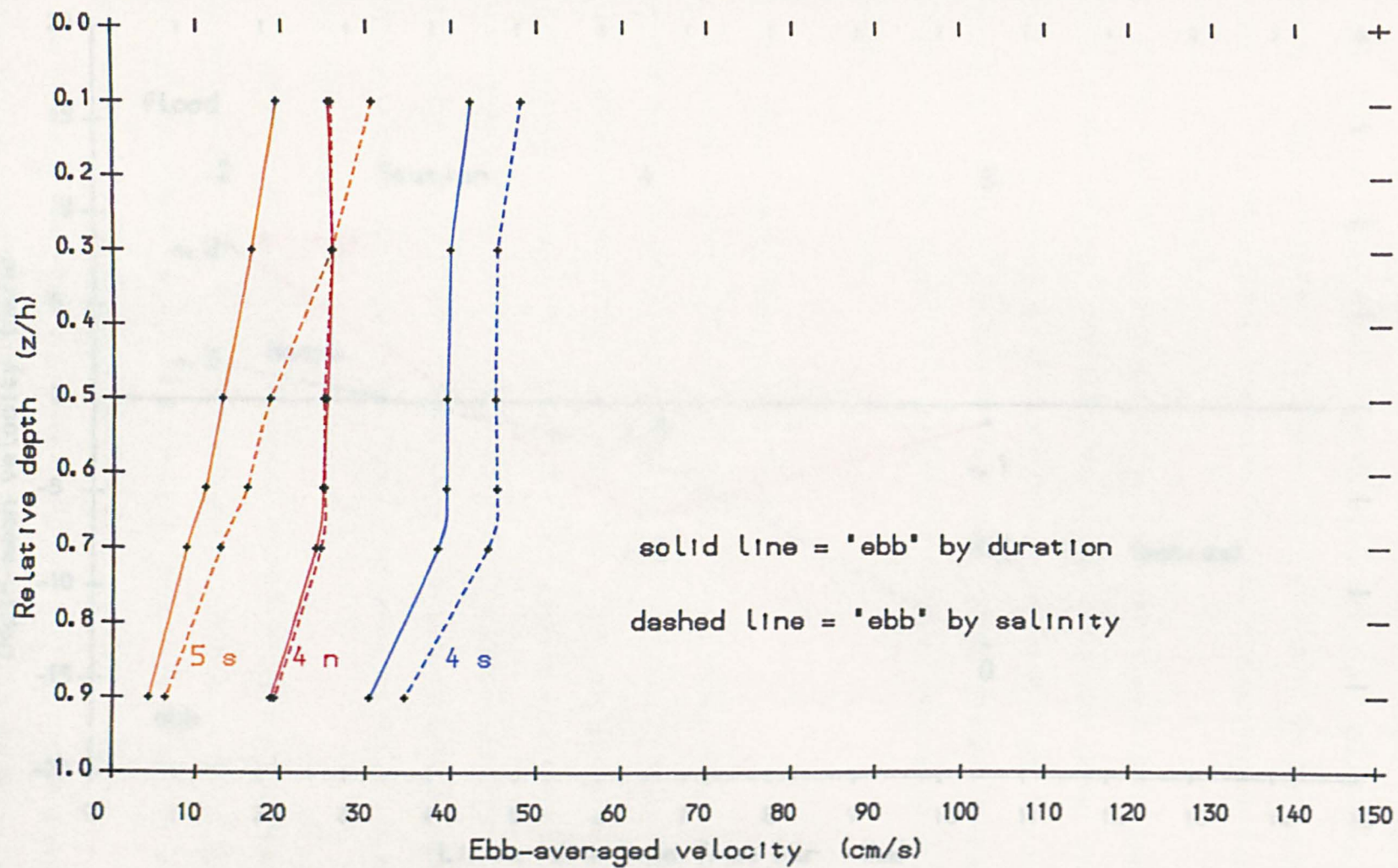
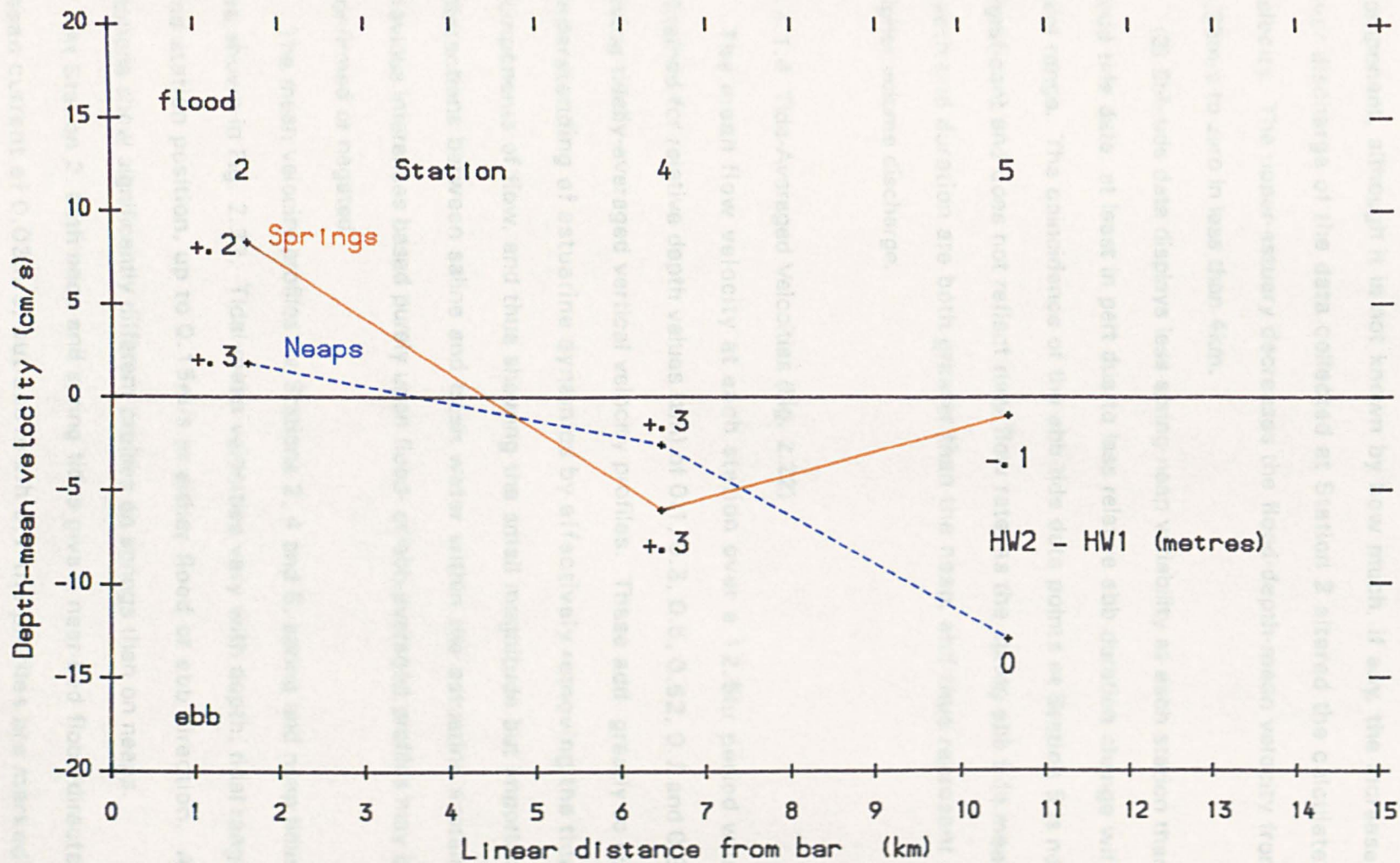


Fig.2.21 Tide-averaged depth-mean velocity - Stations 2,4,5



Some useful general points may be noted:-

(1) The spring flood tide suffers the greatest relative influence of friction (by virtue of having the steepest negative gradient), with apparently increased frictional effect upstream of Station 4.

(2) The neap flood tide also shows an up-estuary- increasing frictional component, although it is not known by how much, if any, the increased river discharge of the data collected at Station 2 altered the calculated velocity. The upper-estuary decreases the flood-depth-mean velocity from 0.35m/s to zero in less than 4km.

(3) Ebb-tide data displays less spring-neap variability at each station than flood tide data, at least in part due to less relative ebb duration change with tidal range. The coincidence of the ebb-tide data points at Station 5 is not significant and does not reflect river flow rate, as the spring ebb tide mean depth and duration are both greater than the neap, and thus represent a higher volume discharge.

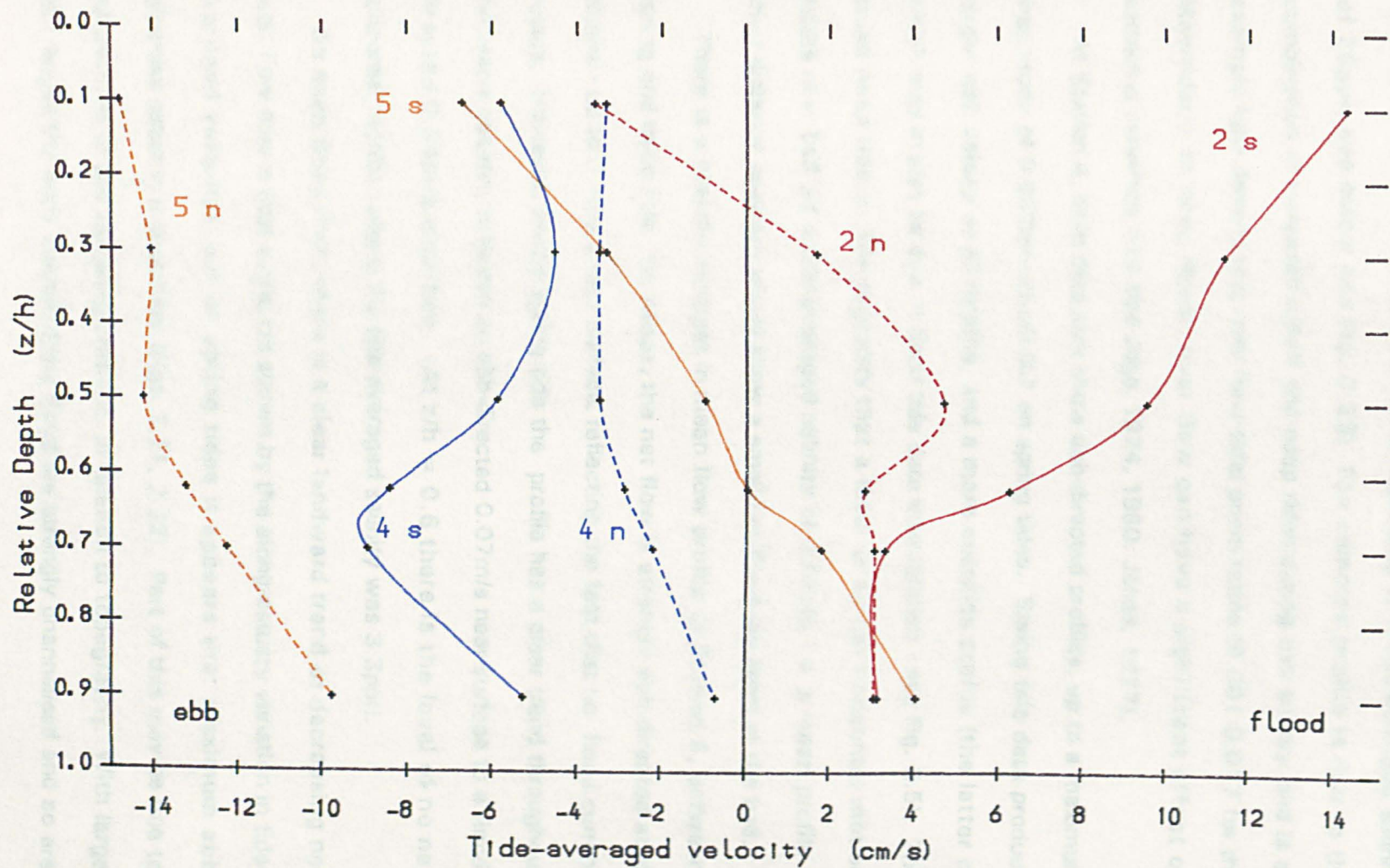
2.4.1.4 Tide-Averaged Velocities (Fig. 2.22)

The mean flow velocity at each station over a 12.5hr period was obtained for relative depth values (z/h) of 0.1, 0.3, 0.5, 0.62, 0.7 and 0.9, giving tidally-averaged vertical velocity profiles. These add greatly to our understanding of estuarine dynamics by effectively removing the tidal components of flow, and thus showing the small magnitude but important interactions between saline and fresh water within the estuarine system. Previous inferences based purely upon flood- or ebb-averaged profiles may be confirmed or negated.

The mean velocity profiles for Stations 2, 4 and 5, spring and neap tides, are shown in Fig. 2.22. Tidal-mean velocities vary with depth, tidal range, and station position, up to 0.15m/s in either flood or ebb direction. All stations show significantly different profiles on springs than on neaps.

At Station 2, both neap and spring tides give a near-bed flood-directed mean current of 0.03m/s, but above z/h 0.7 the profiles are markedly

Fig.2.22 Tide-averaged velocity profiles - Stations 2,4,5



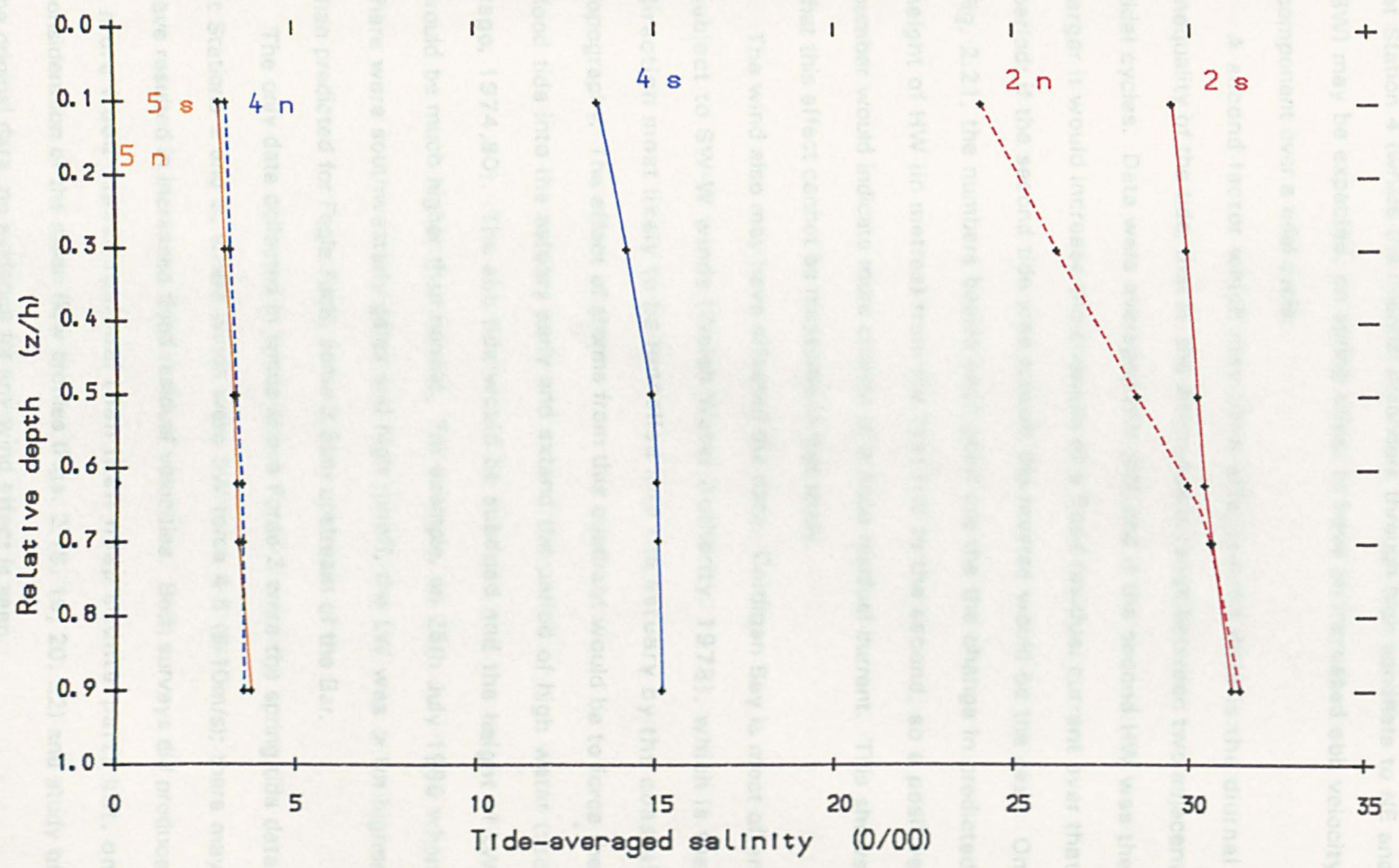
different. On the spring tide the profile shows upwards-increasing flood magnitude, up to 0.14m/s at z/h 0.1, whereas the neap data shows a complex profile changing from a peak flood-directed net velocity of 0.05m/s at z/h 0.5 to a peak ebb-directed net velocity of 0.04m/s at z/h 0.1. (The level of no net flow is at z/h 0.25, corresponding to a tide-averaged salinity of 25ppt, see below and Fig. 2.23) The complex profile is due to the combination of increased runoff and neap tides during this survey, and is an example how despite low river flow-tidal prism ratios (0.001-0.017 for the Mawddach on neap tides), river flow can have a significant effect on estuarine dynamics (see also Jago, 1974, 1980; Jonas, 1977).

At Station 4, both data sets show ebb-directed profiles, up to a maximum magnitude of 0.089m/s at z/h 0.7 on spring tides. Spring tide data produce larger ebb values at all depths, and a more complex profile (the latter of which may in part be due to flood tide data interpolation - see Fig. 2.5). The mean neap tide profile suggests that a level of no net horizontal motion exists near-bed (at a tide-averaged salinity of 3.6ppt), i.e. a mean profile a short distance seaward would show a small net flood resultant at the bed.

There is a notable contrast in mean flow profile at Station 5, between spring and neap tide. On neaps, the net flow is strongly ebb-directed at all depths - up to 0.15m/s near-surface, reflecting the fact that no flood current occurs. However, on the spring tide the profile has a clear trend throughout the water column, between an ebb-directed 0.07m/s near-surface to a flood-directed 0.04m/s near-bed. (At $z/h = 0.6$ there is the level of no net horizontal motion, where the tide-averaged salinity was 3.3ppt).

On neap tides then, there is a clear landward trend of decreasing net flood flow over a tidal cycle, (as shown by the along-estuary variation in tide-averaged velocity), but on spring tides it appears that maximum ebb velocities occur in mid-estuary (Figs. 2.21, 2.22). Part of this may be due to the position of the sampling stations, in relation to topography. With large tidal ranges the early stages of the flood are strongly channelised and so are

Fig.2.23 Tide-averaged salinity profiles - Stations 2,4,5



of relatively high velocities. Towards HW, when the sandflats are fully covered currents, are less topographically restricted and will be relatively slower. A skewed tidal curve produces a relative increase in the net ebb flow in the channels and net flood flow over the banks. Thus the data taken at Station 4 (where the channel meanders through high sandflats to NE and SW) may be expected, on spring tides, to have an increased ebb velocity component over a tidal cycle.

A second factor which may have affected the data is the diurnal inequality of the tide, that is, the difference in range between two adjacent tidal cycles. Data were averaged HW-HW, and if the second HW was the larger it would increase the chances of a flood residual current over that period; if the second tide was smaller the reverse would be the case. On Fig. 2.21, the numbers beside each point are the the change in predicted height of HW (in metres) from the first HW to the second, so a positive number would indicate more chance of a flood residual current. This shows that this effect cannot be measured in this study.

The wind also may have affected the data. Cardigan Bay is most often subject to SW-W winds (Welsh Water Authority, 1978), which is the direction most likely to be funnelled into the estuary by the coastal topography. The effect of storms from this quadrant would be to force the flood tide into the estuary early and extend the period of high water (see Jago, 1974,80). The ebb tide would be subdued and the height of LW would be much higher than normal. For example, on 28th July 1986 when there were southwesterly gales and high runoff, the LW was > 1m higher than predicted for Fegla Fach, some 3.5km upstream of the Bar.

The only data collected in winds above Force 3 were the spring tide data at Stations 2 and 5, where winds were SW force 4-5 (6-10m/s); there may have resulted in increased flood residual velocities. Both surveys did produce a more flood-biased residual than their neap counterparts but, on consideration of the mean flow profiles (Figs. 2.18, 19, 20, 22) and study of the original data, no evidence for any wind effect is seen.

2.4.2 Tidally-Averaged Salinities (Fig. 2.23)

With spatial and spring-neap variations, tide-averaged salinity profiles cover a large salinity range, from zero (Station 5 neap) to 31.45ppt (Station 2 neap). Absolute surface-bed salinity differences decrease up-estuary, and neap tides are always far less saline than spring tides (Fig. 2.24).

The effect of high river flow was evident at Station 2 on neaps, with a 7.35ppt salinity difference between $z/h = 0.1$, and 0.9. In a stratified flow, one process that may operate is termed 'entrainment'. This term describes the upwards-mixing of dense saline water into the seaward-flowing surface freshwater layer. At the boundary between the two layers volumes of saline water are mixed into the fresh layer above i.e. saline water is 'entrained' by the surface layer; thus, the total volume of water flowing seaward is increased. This increased surface seaward flow is compensated by a near-bed landward influx of saline water. It is likely that the high volume of surface freshwater during this survey caused a relatively high near-bed influx of seawater, which could explain why the neap near-bed tidally-averaged salinity at Station 2 was greater than the spring tide value. It is considered that the effect of increased vertical mixing, through stronger turbulence on spring tides, was a lesser factor in explaining the different tidally-averaged vertical salinity gradients at this station.

The different extent of saline penetration was well seen at Farchynys (Station 4). The neap tide produced a near-uniform salinity profile, with less than 0.5ppt between $z/h = 0.1$ and 0.9. The spring tide resulted in a 4-5 fold increase in both the salinity values and surface-bed difference. The upper half of the profile had an increased salinity gradient.

Station 5, on neap tides, had zero salinity; the spring tide profile had significant relative stratification, with 0.9ppt surface-bed difference in a depth-mean salinity of 3.27ppt.

Figure 2.24 shows the depth-mean salinity at HW and LW for Stations 2, 3, 4 and 5, except LW neap tide for Station 3. (Not shown is Station 1, 4km out in Barmouth Bay, where LW spring tide attained 32.7ppt). The

Fig. 2.24 Depth-averaged salinity at HW and LW - Stations 2, 3, 4, 5

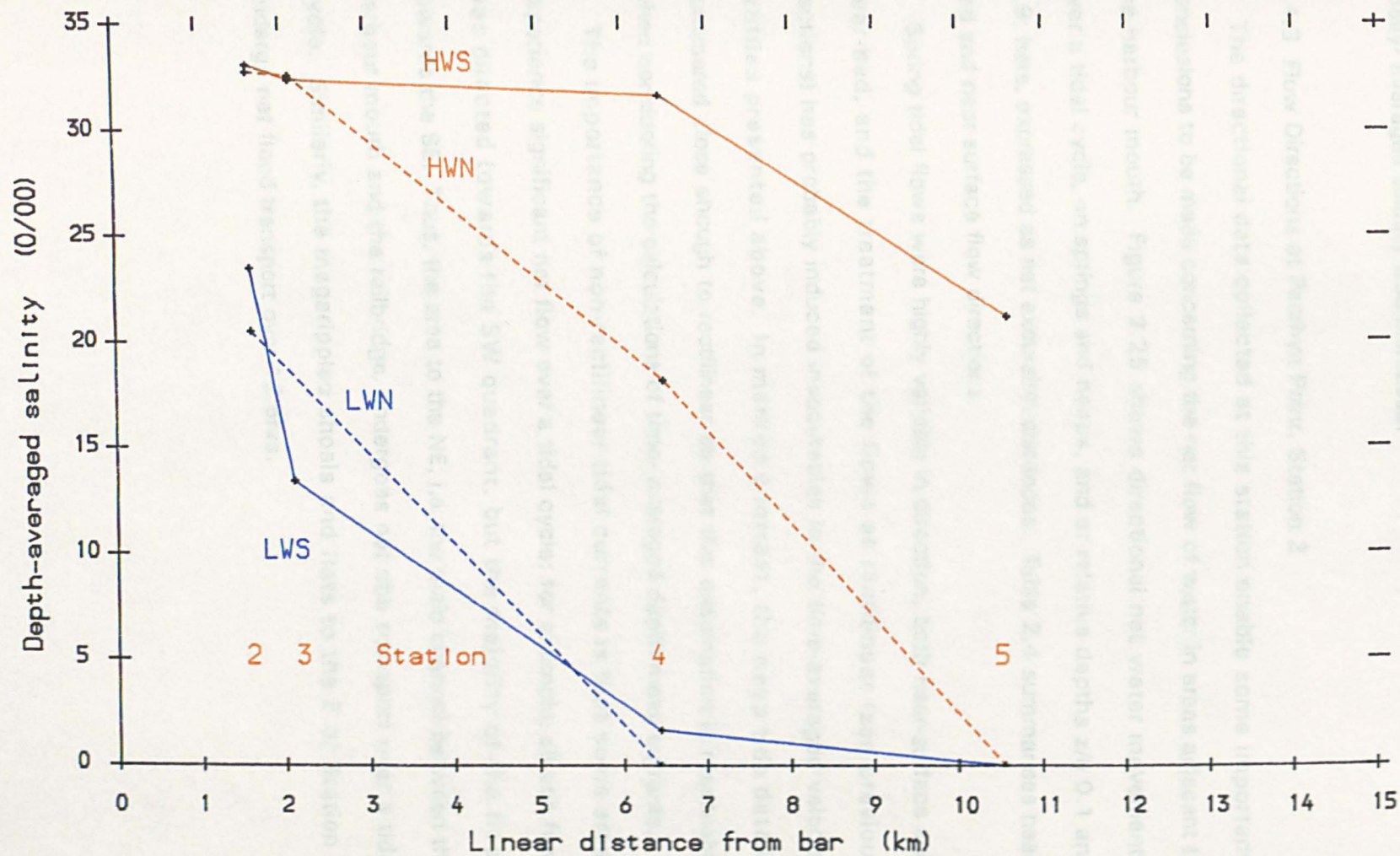


diagram emphasises the spatial variation in salinity extremes and ranges, and shows the largest range of salinities occurs in mid-estuary, particularly on spring tides. For most stations where data was collected, spring tides produced higher depth-mean salinities at both HW and LW, and depth- and tidally- averaged salinity was increased.

2.4.3 Flow Directions at Penrhyn Point, Station 2

The directional data collected at this station enable some important conclusions to be made concerning the net flow of water in areas adjacent to the harbour mouth. Figure 2.25 shows directional net water movements over a tidal cycle, on springs and neaps, and at relative depths z/h 0.1 and 0.9; here, expressed as net excursion distances. Table 2.4 summarises near-bed and near-surface flow directions.

Spring tidal flows were highly variable in direction, both near-surface and near-bed, and the treatment of the flows as rectilinear (see previous sections) has probably induced inaccuracies in the time-averaged velocity profiles presented above. In marked contrast, the neap tide data is considered close enough to rectilinear so that this assumption is reasonable when considering the calculations of time- averaged depth-mean currents.

The importance of non-rectilinear tidal currents is that some areas experience significant net flow over a tidal cycle; for example, all ebb flow was directed towards the SW quadrant, but the majority of the flood towards the SE. Thus, the area to the NE, i.e. the main channel between the harbour mouth and the railbridge, undergoes net ebb transport over a tidal cycle. Similarly, the megarippled shoals and flats to the E of Station 2 undergo net flood transport over 12.5hrs.

Fig. 2.25

Tidal excursion directions over a tidal cycle
at Penrhyn Point (Station 2)

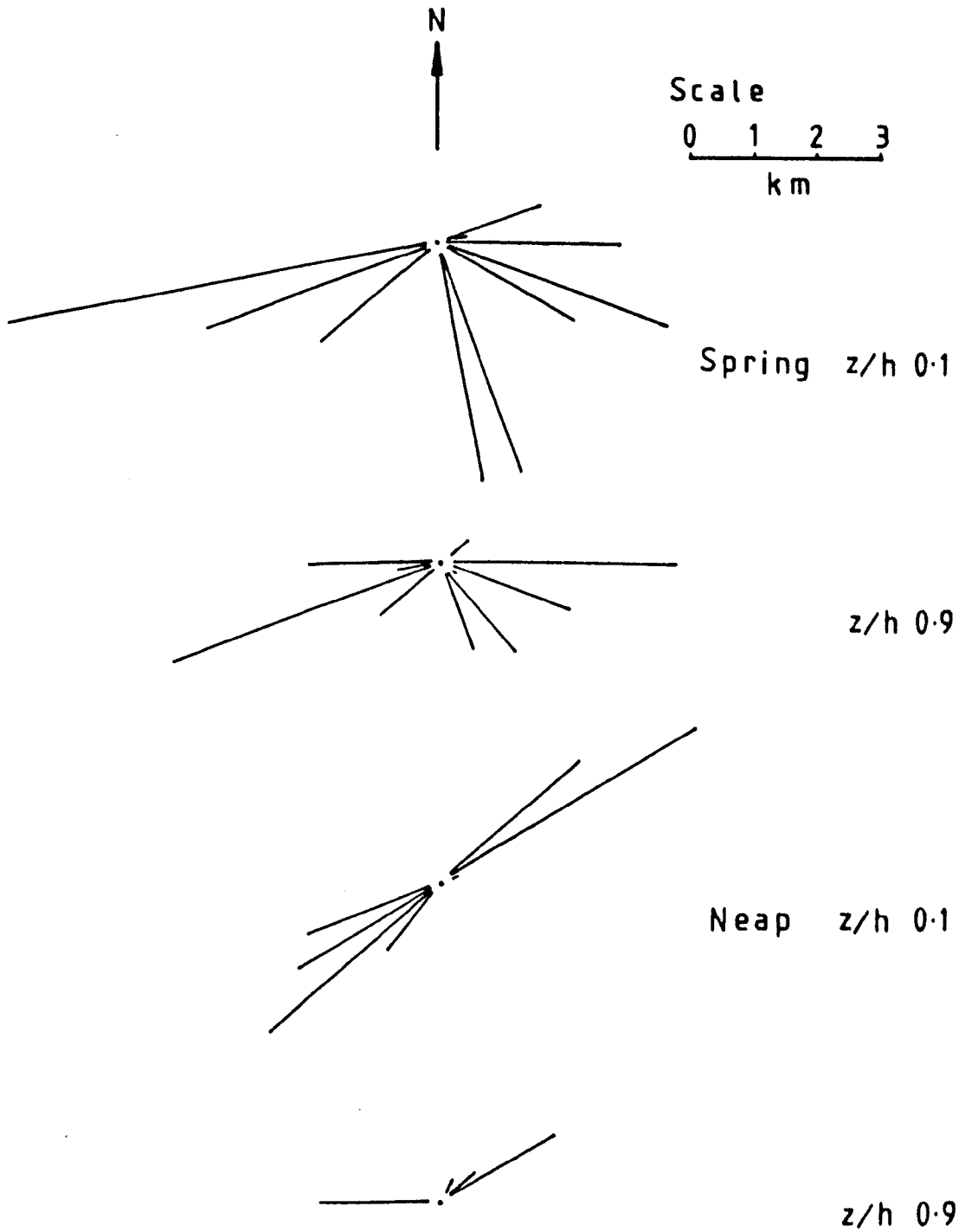


Table 2.4

Near-Surface (S) and Near-Bed (B)
Flow Directions at Station 2 (degrees)

	S P R I N G		N E A P	
	TIME (Hours)	Flow Direction	TIME (Hours)	Flow Direction
E	HW - HW + 4	S 230 - 270	HW - HW + 3.5 B "	S 220 - 270 B 260 - 270
B			+ 3.5-HW + 7	S 220 - 270
B	HW + 4 - LW	S 020 - 260 B 030 - 270		
			HW + 7 - LW	S 200 -> 030 B 270
	LW			LW
F	LW - LW + 1.5	S 060 - 100 B 045 - 100	LW - LW + 1	S 040 - 060 B 270->050
L				
O	LW + 1.5 - LW + 2.5	S 120 - 170 B ditto		
O			LW + 1 - HW	S 050 - 070 B ditto
D	LW + 2.5 - HW	S 060 - 160 B 040 - 070		
	S P R I N G		N E A P	

Notes:

(- = varying between)

(-> = changing to)

These conclusions are backed up by the data of McMullen (1964) and the Welsh Water Authority (1978), who found that the main channel at the railbridge, and 100m seaward of the mouth respectively were ebb-dominated in both duration and velocity. The net flood-dominance to the southeast of Station 2, in the blind flood channel, is the probable cause of the 0.75ppt increase in salinity from the N end of the railbridge to the S end at HW measured by Pattinson (1979).

Further evidence of the flood-dominance in this area is provided by unpublished current meter data of the author, obtained 500m ESE of the harbour mouth. Velocities were averaged over 60 seconds. Both spring and neap tides showed peak velocity ratios flood-ebb of approximately 2, with flood spring tides attaining 0.98m/s at 0.37m above bed. The megaripple field in this area consists of flood-orientated forms exposed at low water, whereas to the N, near the main channel, exposed megaripples are all ebb-orientated.

The control of these different tidal current directions is water depth. On neaps, at virtually all stages of the tide flow is constrained within channels, as are the spring tide currents near LW. With increasing depth, the main channel banks are covered and the flow is more free to spread out to the SE. The breakwater at the north of the harbour mouth may also deflect water in a southwesterly direction.

2.4.4 Classification and Mixing Controls

2.4.4.1 Qualitative Classification

In presenting the classification of Cameron & Pritchard (1963), Dyer (1986) states that one of the characteristics of a 'partially-mixed' estuary is that on spring tides higher turbulence enhances the exchange of fresh and salt water. The extra volumes of salt water from the bottom layer discharged seawards at the surface are replaced by a compensating landward inflow.

This has three results: firstly, decreased stratification; secondly, an enhanced mean circulation (i.e. increased mean surface ebb and bottom flood components); and, thirdly an apparent seaward shift of mean salinity values. The Mawddach actually exhibits a landward movement of mean salinity values at spring tides. In addition, decreased stratification at spring tides is probably due to increased turbulence alone rather than enhanced entrainment of bottom salt water onto seaward-flowing surface freshwater - because entrainment is a minimal factor in the estuary, only locally important with suitable river flow-tidal prism ratios. So the estuary does not exhibit the criteria of a partially-mixed estuary although locally it may approach some.

The description of a 'well-mixed' estuary is also not fully met by the Mawddach; however, to a first-order approximation, it is a good example. Intertidal flats and banks occur and there are topographically distinct ebb- and flood-channels separated by sandbanks. Little vertical circulation is present, although significant lateral salinity gradients occur (Section 2.4.6), evident in some of the fronts generated in the estuary.

The time of HW is delayed up-estuary, on a spring tide by 15mins over 4.8km between Barmouth Harbour (Station 2) and Borthwnog (Station X) (Fig. 2.1), and by 10mins on a neap tide (Fig. 2.31a). Thus, at HW at the harbour, some water is still flowing inward to raise levels upstream - so slackwater should be after HW. No data were taken to confirm this. However, a consequence would be that to ensure removal of all the water, ebb velocities are increased, and in all data collected the peak flood velocity was always greater than the ebb.

The conclusions are that the Mawddach is too short and shallow for these two effects (late slackwater and fast ebb) to be significant, and that frictional effects on the incoming tidal wave are dominant from some way out in Barmouth Bay to the estuary head. Hence according to the qualitative classification in Dyer (1986) the Mawddach is well-mixed, although locally and periodically approaching partially-mixed.

2.4.4.2 Quantitative Classification and Mixing Controls

Hansen & Rattray (1966) proposed a quantitative estuarine classification scheme, which relates estuarine 'type' to its position on a stratification-circulation diagram. Estuaries are characterised using two dimensionless parameters :

(1) a stratification parameter dS/S_o , which is the mean surface-bottom salinity difference divided by the mean cross-sectional salinity;

(2) a circulation parameter U_s/U_f , which is the net surface current divided by the mean cross-sectional velocity, (i.e. the ratio of river flow plus water mixed into it, to the river flow itself).

Before further discussion of the data, or comparison with other estuaries, a number of points should be made regarding how the two parameters were calculated. Firstly, there were no measurements of lateral salinity or velocity variation, so the values of S_o and U_f used are depth-mean averages over a tidal cycle at each station, rather than mean cross-sectional values. This may be important as significant lateral salinity and velocity gradients do occur in the estuary (Pattinson, 1979; O'Farrell, 1983; this study). Secondly, in contrast to Jago (1980) but in common with Mahamod (1989), the circulation parameter has not been derived from a weighted-average cross-sectional area. Finally, 'surface' and 'bottom' values were taken as z/h 0.1 and 0.9 respectively.

In this classification, Type 1 estuaries have net seaward flow at all depths, and any upstream salt flux is by diffusion. In Type 2, the flow reverses at depth and upstream salt flux is by both advection and diffusion. Type 3 estuaries have salt transfer primarily due to advection; Type 4 have intense, salt-wedge type stratification. The suffixes a and b correspond to conditions of slight and appreciable stratification, respectively. Type 1b represents the well-mixed laterally homogeneous estuary, and Type 2 the partially-mixed.

On this diagram, estuaries are characterised by a line rather than a point, due to three factors; river discharge, tidal range, and estuarine cross-section, i.e. position (e.g. Jago, 1980; Uncles et al, 1985; Dyer, 1973). At any one hydrographic station, the estuarine 'type' is also highly dependent on these factors, as the data presented in Fig. 2.26 show.

For ease of comparison, the spring and neap data points for each station have been joined by straight lines. The lines also tentatively suggest the variation in position on the diagram for that station due to the lunar tidal cycle, although, as they do not represent simultaneous datasets, they join points of different river discharge. Of note here is the neap tide of Penrhyn Point (Station 2), where high river flow has led the line to extend to a region of the diagram where stratification is appreciable and the flow reverses at depth.

From the Hansen & Rattray diagram it can be stated that the estuary is generally well-mixed, with moderate to appreciable stratification. On spring tides, the upper-estuary is partially-mixed. However, the use of these statements may be limited when one considers the nature of the estuarine system in many of the mesotidal and macrotidal estuaries around the Welsh coast. For long periods of time, the majority of the estuary bed is subaerial, with some channelised 'river' flow remaining. Thus, the tide is a transient effect periodically turned on and off, rather than having a continuous effect on the estuary as a whole. This is in marked contrast to the deeper estuaries such as the James River, Mississippi River mouth, Columbia River and the Mersey Narrows, on which the Hansen & Rattray classification was conceived and developed, so comparisons with such estuaries and their classification is not applicable.

However, this classification has been used for some of the Welsh estuaries where large areas of sand- or mudflats are exposed at LW, e.g. the Conwy (Jenkins, 1976; Jones, R.E.H., 1981), the Glaslyn-Dwyrdd (Mahamod, 1989), and the Taf (Jago, 1980), Table 2.5.

Table 2.5

HANSEN + RATTRAY (1966) CLASSIFICATION OF SOME WELSH ESTUARIES

ESTUARY	SOURCE OF REFERENCE	LENGTH (km)	FLOW RATIO	CLASSIFICATION
Conwy	Jenkins (1976)	22	0.0002 - 0.02	2a Partially-mixed, slight stratification
Glaslyn-Dwyrdd	Mohammed (1988)	11	?	2a - 2b Partially-mixed in lower reaches (stratification increased near mouth and on mean and neap tides)
Mawddach	This study	11	0.0002 - 0.016	1a / 2b Upper reaches well-mixed, appreciable stratification (-partially-mixed) 1a / 1b Lower reaches well-mixed (-transitional), moderate stratification
Taf	Jago (1974)	15	0.01 - 0.19	1a / 2b Upper reaches well- to partially-mixed appreciable stratification 2a Main part partially-mixed slight stratification

Table 2.6

SOME PARAMETERS DERIVED FROM TIDAL CURVES

LOCATION	FLOOD DURATION (hours)		EBB/FLOOD DURATION RATIO		TIDAL RANGE (m)		DELAY c.f. PREDICTION (mins)			
	S	N	S	N	S	N	HW		LW	
Bar Prediction)	6.25	6.25	0.97	1.01	4.3	1.95	0	0	0	0
X	4.42	5.75	1.71	1.22	4.2	2.25	20	5	100	35
Y	2.92	4.67	3.2	1.69	3.1	1.95	35	15	220	110
Z	2.67	3.3	3.75	2.82	2.4	1.35	50	23	270	200

(S = Spring N = Neap)

Despite the limited comparability of data sets, and varying rigour of calculation, some useful comments and conclusions can be made. Data are available for the Conwy, Dwyryd and Taf. One tendency in these estuaries is for the circulation parameter, U_s/U_f , to gradually decrease upstream. However, the Mawddach on spring tides shows the least value at the mid-estuary constriction (Station 4), suggesting that the physically limited estuarine cross-section at this point is important in controlling mixing processes in the estuary. It may induce relative homogeneity (in terms of currents) in water flowing either way through it, also implying that the specific process of entrainment, the upwards mixing of saltwater into overlying freshwater, is weak here, due to the relative lack of stratification.

This upstream decrease in U_s/U_f is also shown in some deeper estuaries, e.g. the Tamar (Uncles et al, 1985). The Tamar also exhibits another feature common to some of the Welsh estuaries named above. Data from the Dwyryd and Conwy, and less detailed data from the Taf and Dovey, all show decreased stratification with increased tidal range, i.e. points plot lower on the Hansen-Rattray diagram. The Mawddach also exhibits this tendency, although it is significant that at Farchynys the stratification parameter was barely changed, from 0.138 on neap tide to 0.125 on the spring. This suggests that flow structure and mixing processes vary little with tidal range at this station, and when taken in addition to the deductions made above from the variation of the circulation parameter, point to a dominant topographic/cross-sectional control in this area. To the upstream and downstream of this constriction the estuary widens, and it is likely that velocities decrease and more stratified conditions occur. Pritchard (1955) also considered estuary width and depth to be important factors controlling flow structure.

2.4.5 Tidal Wave Propagation and Flow Controls

Some simultaneous tidal elevation measurements at three stations along the estuary, on 5th and 10th December 1985, were taken by a sub-

contractor, as part of a hydrographic survey for the Central Electricity Generating Board. The stations are shown on Fig. 2.1,

Station X	Barmouth Quay	1600m	upstream	of the	Bar
" Y	Farchynys Boathouse	6450m	"	"	" "
" Z	Borthwnog	9550m	"	"	" "

The collected data are shown in Figs. 2.27 & 2.28, with the predictions for the Bar also shown. As part of the megaripple-flow study at Fegla Fach Shoal (1.6km east of Station 3, Fig 2.1) two tidal curves were obtained by measuring water level on a fixed tall mast using a theodolite. This data (Fig. 2.29) did not give complete tidal curves because the shoal was exposed at LW.

The most striking aspect of the data is the up- estuary-increasing asymmetry of the tidal wave, particularly on spring tides. Distortions of the tidal wave arise, especially if currents are high, when the wave enters shallow or constricted water, or when the direction of the tidal current varies with geographical position (Howarth, 1982). When total water depth varies significantly over a tidal cycle the interval from LW to HW becomes shorter than that from HW to LW.

In Cardigan Bay, depths are low enough (< 20m) to cause significant friction at the sea bed; thus distortion of the tidal wave has already occurred before it enters Barmouth Bay, where decreasing depths increase tidal wave asymmetry. Further distortion is caused on entering the estuary, by the tide being forced firstly over the Bar, then through the constriction between Penrhyn Point and the Breakwater.

Some modifications of the tidal wave are tabulated in Table 2.6, where parameters derived from the tidal predictions for the Bar are also included. Spring and Neap tide data are indicated by S or N, respectively. From these, a number of graphs have been plotted to show variation of various tidal parameters along the estuary, namely Limits of Tidal Height, Tidal Range,

Fig. 2.26

Estuary Classification of Hansen + Rattray (1966)

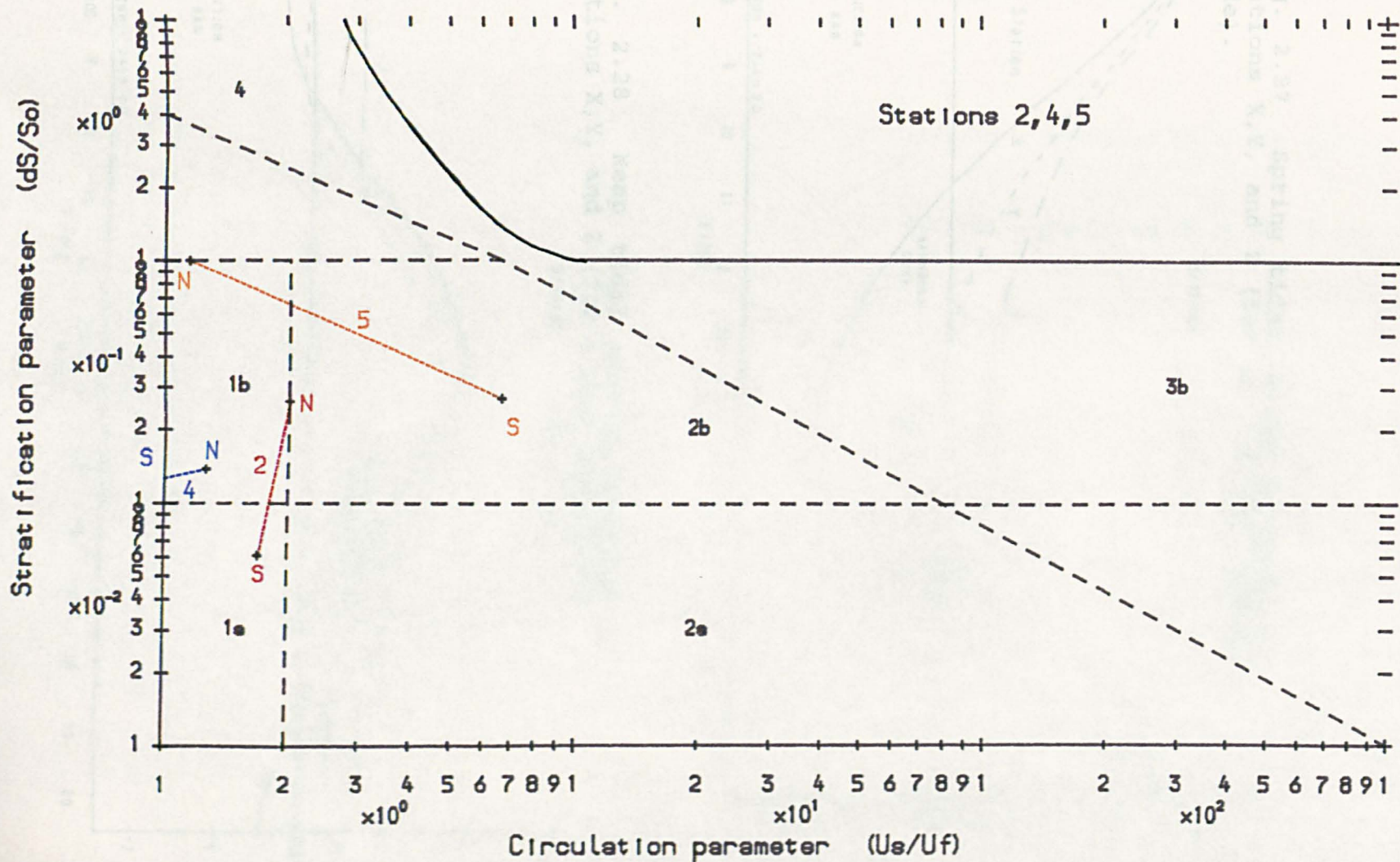


Fig. 2.27 Spring tidal curves measured at Stations X, Y, and Z (for an ordinary Spring Tide).

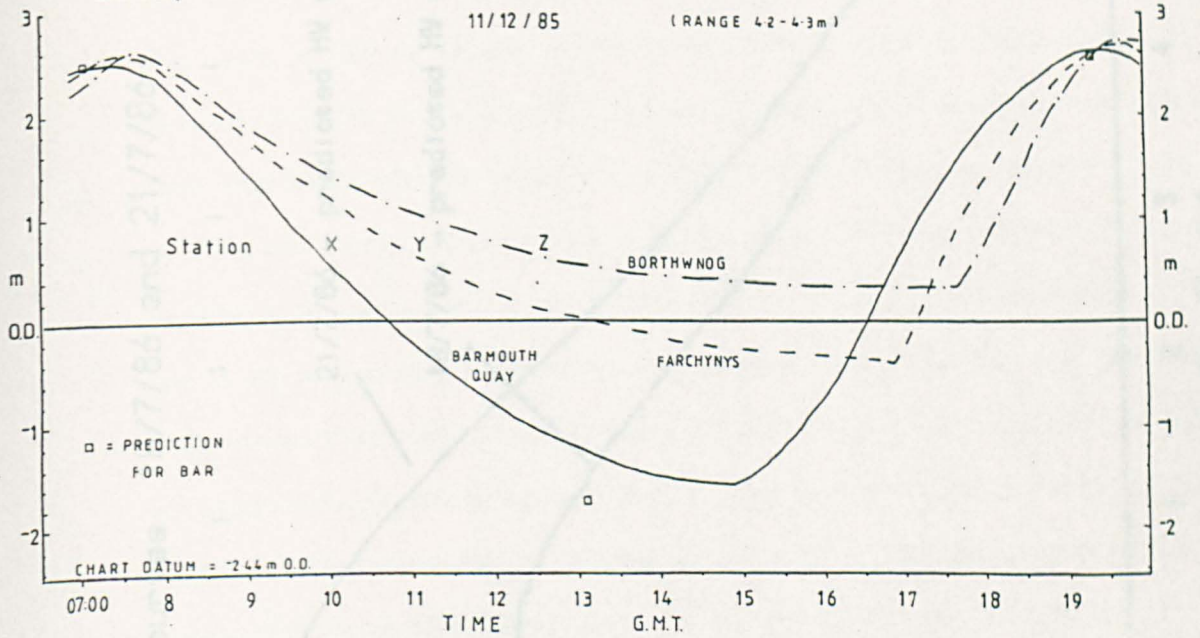


Fig. 2.28 Neap tidal curves measured at Stations X, Y, and Z (for a High Neap Tide).

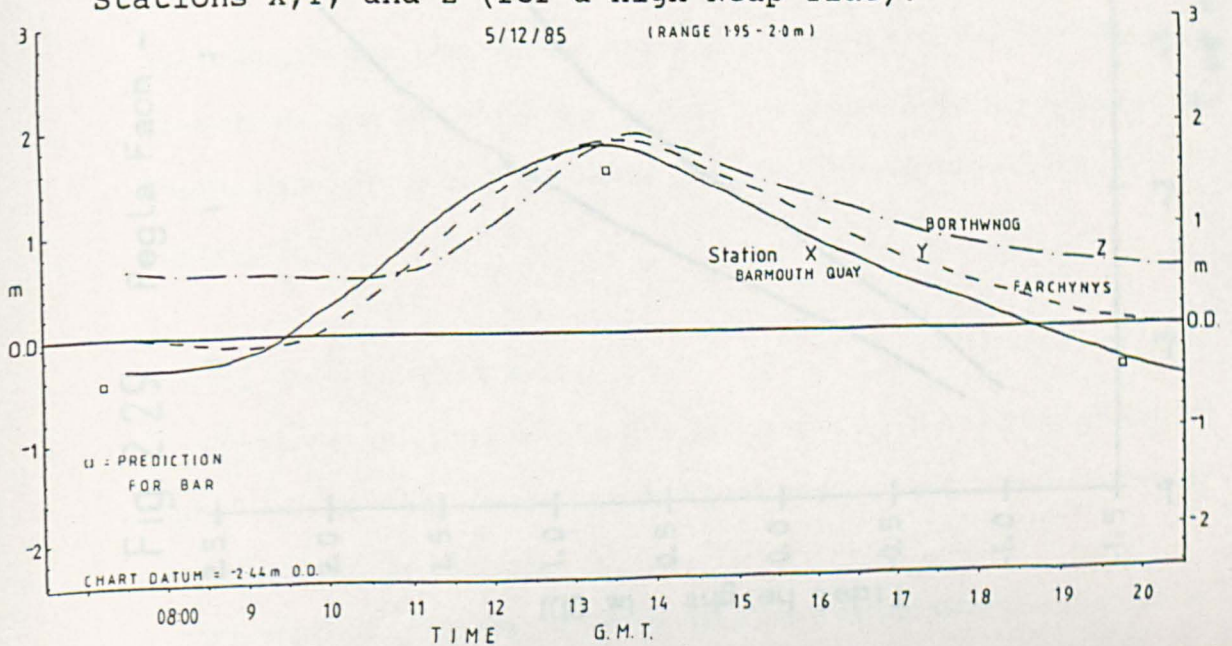
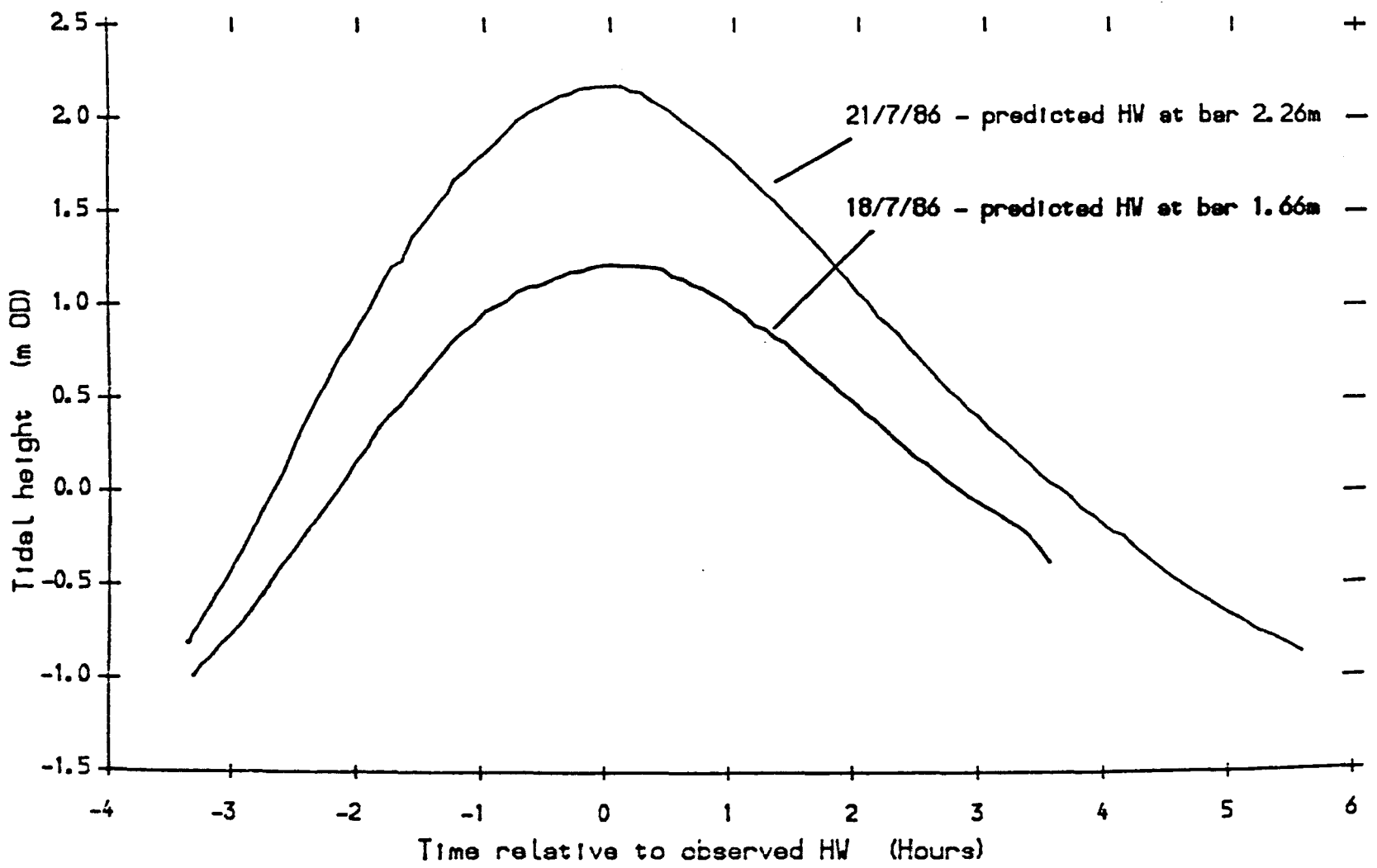


Fig. 2.29 Fegla Fach - Tidal curves 18/7/86 and 21/7/86



Tidal Delay, and Tidal Duration (Figs. 2.30 & 2.31). In each case, the points plotted for the Bar are derived from the tidal predictions and do not indicate actual observations.

2.4.5.1 Tidal Height and Range (Fig. 2.30a & b)

The elevation of HW slightly increases towards the estuary head, by the same amount for both tidal ranges (0.15m between Stations X and Y). This is caused by convergence of the tidal wave as the estuary cross-section decreases landward, this effect overcoming the effect of bed friction (which decreases rapidly as depths increase and currents approach zero near HW). Further towards the heads of estuaries, Dyer (1986) suggests it is more likely that friction becomes more important and the height of HW decreases.

The LW mark is much more affected by tidal range; it is also more variable in its timing along the length of the estuary. Between Stations Y and Z, the similar height difference (i.e. slope on Fig. 2.30a) for the two data sets implies that river control is important in this area (i.e. that river slope is established in the late stages of the ebb (see below)). This is because the level of LW is below that of the estuary bed, thus tidal range is decreased up-estuary (Fig. 2.30b) due to landward increasing 'low water' levels.

For mean spring and neap tides, predicted LW is approximately -1.7m and -0.6m O.D. respectively; this corresponds to bed level in the channel, at approximately 4km from the Bar on springs and 7km from the Bar on neaps. Immediately upstream of these positions, tidal ranges would be expected to sharply decrease, and LW elevations increase. This is broadly in agreement with Fig. 2.30.

2.4.5.2 Water Surface Slopes

Time series of hourly tidal heights at Stations X, Y and Z are shown in Figs. 2.32 and 2.33. These data has been used to calculate mean water slopes between the stations.

It is significant that the maximum ebb slope attained between Stations Y

Fig. 2.30 Limits of (a) tidal height; and (b) tidal range, along the Mawddach.

Fig.2.30a

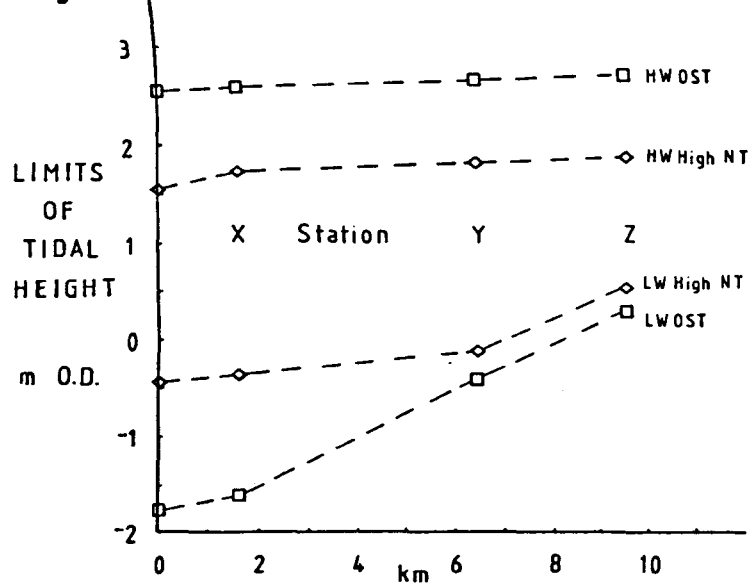


Fig. 2.30b

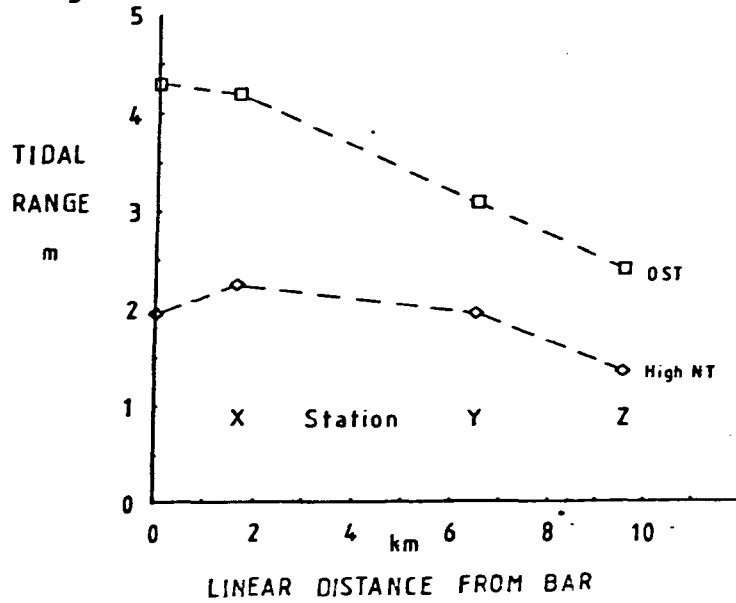


Fig. 2.31 (a) tidal delay; and (b) tidal flow duration, along the Mawddach.

Fig.2.31a

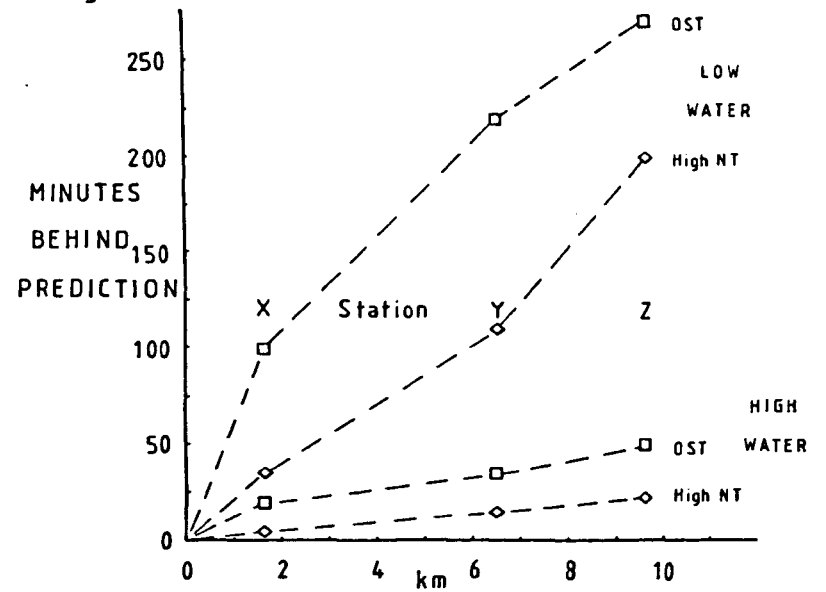


Fig.2.31b

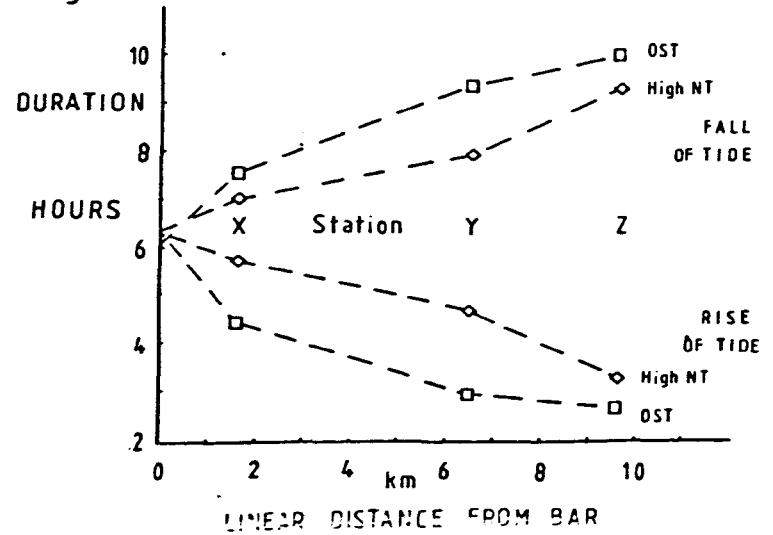


Fig. 2.32 Spring tidal water slopes between Stations X, Y and Z.

TIDAL RANGE

4.2-4.3 m (=OST)

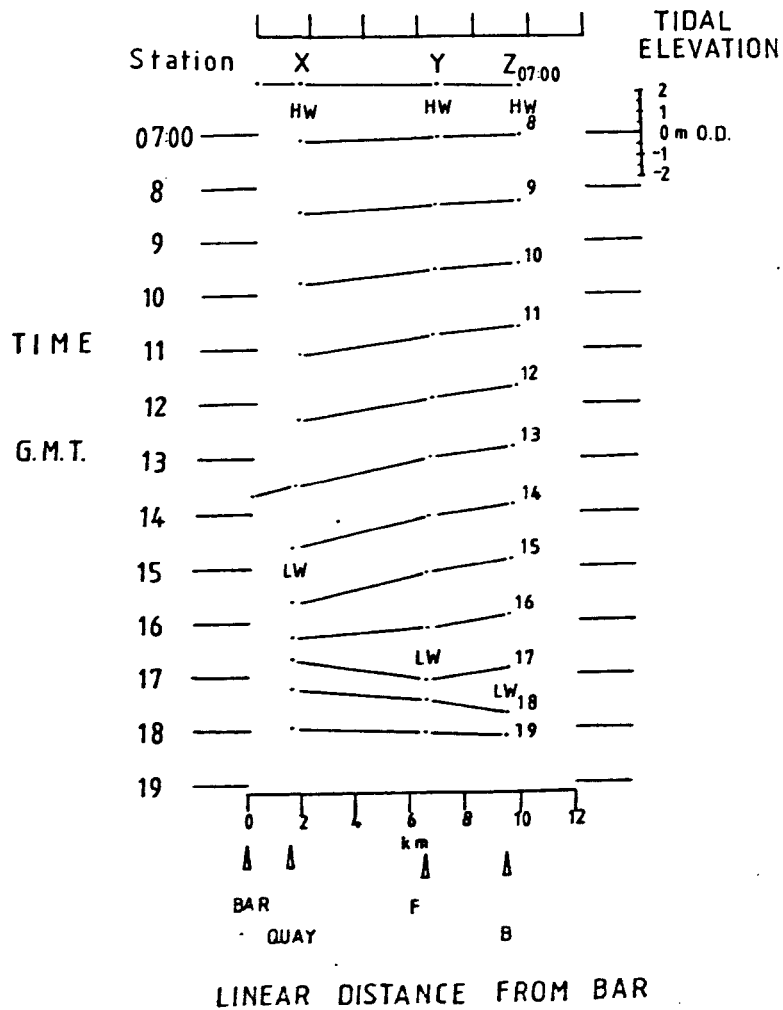
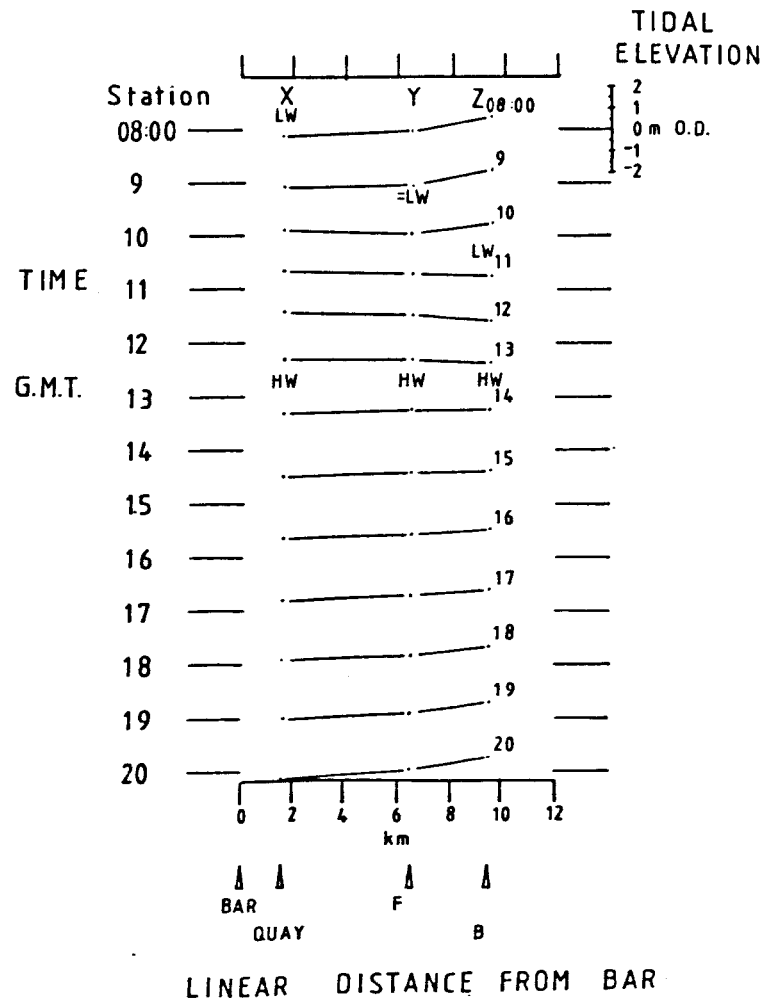


Fig. 2.33 Neap tidal water slopes between Stations X, Y and Z.

TIDAL RANGE

1.95-2.0 m (=High NT)



and Z is the same on springs and neaps, 2.3×10^{-4} , at 16:50 and 09:00 GMT, respectively. This strongly implies that the ebb flow between these stations is limited by frictional effects, agreeing with the conclusion from the tidal range data.

The maximum slope between the same stations attained on a flooding tide was 2.2×10^{-4} on springs (at 18:00 GMT), and 8.1×10^{-5} for neaps (at 12:00 GMT). On both occasions the tidal height at Farchynys (Station Y) was the same, 1.3 - 1.4m O.D. This corresponds with the maximum level of sediment at this station banked up against the vertical rock face on the north bank, and against the stone-faced railway embankment on the south bank. Two things are suggested by this:

1 - that the level of sediment at Farchynys may be controlled by upstream tidal propagation. Over an obstacle in a channel, flow streamlines will be closer together, and, hence, bed shear stress will be increased. In this case, the 'obstacle' is the thin constriction between the upper and lower estuary. If sediment level is high, then the tidal wave will produce higher near-bed velocities, resulting in increased sediment transport at the site, and so reducing bed level. If sediment levels are low, then the tidal velocities at the bed will be low enough to allow sediment accumulation, raising bed level;

2 - that energy dissipation by bed friction, i.e. potential sediment transport, is at a peak here.

Both these relationships involve an interaction between tidal currents and sediment transport.

As seen above, the maximum ebb slopes between Stations Y and Z appear independent of tidal range. It is notable that the maximum attained flood slope on a spring tide is the same as the maximum ebb slope, to within 3cm over 3.1km. The spring and neap maximum flood slopes both occurred when tidal height at Station Y was 1.3 - 1.4m O.D.; this suggests a

local frictional slope control, but the maximum ebb slope occurred when the tidal height at Station Y was -0.1 - -0.3m O.D.; thus this does not appear to be controlled by the same factor.

Seaward of the constriction at Farchynys, water slope exceeded those described above only on the late stages of the spring ebb tide, where a slope of 2.9×10^{-4} was reached at 14:00 GMT. The spring flood tide only achieved 1.9×10^{-4} , less than the ebb because of water being retained in mid-estuary by friction. Similarly on neap tide the maximum ebb slope exceeded the flood, 9.1×10^{-5} for the ebb, 4.1×10^{-5} for the flood.

By noting that the neap maximum flood slope in the upper estuary was twice that attained in the lower estuary (8.1×10^{-5} cf. 4.1×10^{-5}), high frictional effects landward of Farchynys are inferred. The spring tide maxima were much closer (1.9×10^{-4} in lower estuary, 2.2×10^{-4} in upper estuary), suggesting that on spring tides friction is a more uniform factor along the estuary. This agrees with the above conclusion that friction increases significantly landward of Fegla Fach (see Fig. 2.30) on springs, and landward of Farchynys on neaps.

Maximum tidal velocities at Station Y occur at times of maximum slope between X and Z, i.e. the flood current is related to the force driving the water up- estuary. However, this is not the case for the ebb, where maximum velocities occur 2-3hrs after HW, and maximum slopes 4-5hrs later. A qualitative explanation of this time difference can be based on the significance of water depth and bed friction. Friction at Station Y has earlier been implied to be relatively high, particularly on the flooding tide and with shallow water. At HW + 2hrs, both depths and currents are high, although the overall slope between X and Z is only 15-40% of the maximum attained. The fast depth- mean current may be due to the relatively large depth, in that only a small fraction of the water column near the bed is significantly slowed by bed friction. The majority of the flow is able to move relatively freely to seaward. In contrast, near LW, depths are much smaller and bed friction affects a higher proportion of the water column, so that depth-mean

velocities are slower despite the greater water slope. It is hypothesised that slopes near LW approach river slope, and that the structure of the water column will be related to bed friction, and locally, surface stratification.

2.4.5.3 Tidal Wave Delays

Modification of the tidal wave, by bed friction causes the timing of HW and LW to vary along the estuary. Dyer (1986) states that typical estuarine delays are of the order of 1-2mins/km. Mean delay times between Stations X and Z (~7.8km) are tabulated below (Table 2.7) in mins/km, with the mean effective water depth calculated using the equation for a shallow water wave,

$$U = (g h)^{0.5}$$

where,

U = velocity,

g = gravitational acceleration,

and h = water depth.

Table 2.7

HW and LW Delay Times between Barmouth Quay (X) and Borthwnog (Z)

	Delay Times (mins/km)		Calculated water depth (m)	
	SPRING	NEAP	SPRING	NEAP
HW	3.8	2.3	1.96	5.35
LW	22.0	21.0	0.06	0.06

These values emphasise the energy dissipated due to friction, particularly by the trough of the incoming tidal wave. More detail is shown on Fig. 2.30a, which can be thought of as illustrating relative frictional effects in the estuary. The steeper the line between two points, the greater the energy loss by friction. Thus least energy is lost by the neap wave crest; the most by the spring trough. (It must be pointed out that the lines joining 0km to 1.6km do not represent observed data. No data were taken at the Bar, and the lines are only to aid comparison. It is the slopes between observed data points that are most important).

There is an increased delay in HW between Stations Y and Z on a spring tide compared to a neap, where one may perhaps consider that the greater depth in the estuary at HW springs, would lead to a higher velocity of the tidal wave crest, and thus a smaller delay. The observations cannot be explained purely in terms of a depth-related velocity difference. Two other factors may be influential: data quality and estuarine morphology:

1 - Data were read from the tidal height curves to within +/- 1min., and the curves drawn from readings taken every 10-15mins; hence it is considered that the effect is a real one, not due to poor data quality;

2 - In contrast, estuarine morphology is considered important. At HW springs, the higher saltmarshes which border the estuary are flooded to a small depth, not so on HW neaps. When the saltmarshes begin to flood, the cross-sectional area of the estuary is much increased for each increment of water level rise. Thus, if the discharge through the constriction at Farchynys is assumed constant (and velocity profiles were taken too infrequently to confirm or deny this) the rate of tidal rise in the upper estuary would decrease. The result would be that the time of HW would be later than if the upper estuary lacked bordering saltmarshes. On a spring tide, the volume of water required to pass into the upper estuary to bring about HW is far greater than on neaps. Although flood tide velocities on springs are more than twice those of neaps (at Farchynys), it is considered that the increased estuarine cross-sectional area above saltmarsh level is responsible for the

relatively slow rise to HW, up-estuary of Station Y on a spring tide.

The pattern of delay of LW along the estuary (the upper 2 lines of Fig. 2.31a) reinforces the conclusions drawn above that friction affecting the neap flood tide, i.e. the trough, is increased landward of Farchynys, while the spring is slowed much further seaward.

Throughout the period of this research, Fig. 2.31 has been used to estimate times of HW and LW throughout the estuary for different tidal ranges, by interpolation or extrapolation. It has proved surprisingly accurate and has rarely been more than 10 minutes out either way.

2.4.6 Fronts and Convergences

Regions of intense horizontal gradients, termed fronts, occur widely in the estuarine environment (Simpson & Turrell, 1986). Invariably associated with them are foam lines, which are surface accumulations of buoyant material caused by the convergence at the water surface. O'Farrell (1983) studied fronts in the Mawddach, but could only speculate on their causal mechanism.

During various hydrographic and geophysical surveys for this study, some fronts were noted both in the Mawddach Estuary and in Barmouth Bay. Axial fronts (Nunes & Simpson, 1985) were observed commonly in the estuary both on spring and neap tides, including during up-estuary winds of force 7-8 on a particular flood tide. They were seen to extend at least 9.5km upstream of the Bar at HW. At HW + 1hr, on a spring tide, three parallel axial fronts were observed in Barmouth Harbour. These show the presence of lateral currents in the estuary. Simpson & Turrell (1986) measured lateral components of flow in the Conwy estuary of up to 20% of the axial speed.

One axial convergence at Farchynys was observed to have strong lateral salinity gradients associated with it. Immediately to the north of the NE-SW elongate convergence, the salinity was 19ppt; to the south it decreased

rapidly to 10.4ppt - some 14m south of the convergence line. This is evidence that considerable lateral salinity gradients can exist in the estuary. So the data which enabled hydrographic stations 2, 4 and 5 to be placed in the Hansen & Rattray classification diagram (Fig. 2.26) are undoubtedly deficient, in not considering lateral gradients of either velocity or salinity.

On two successive days (26th and 27th July 1987), a plume front was observed and recorded with side-scan sonar, 2km WSW of the harbour mouth. Sea conditions were calm, with the tidal stage LW-1hr on both days. Tidal range was 3.6m, i.e. a small spring tide.

2.4.7 Sources of Error, and Notes on Unused Data

In a study of this kind, where field data is worked up to a high degree, it must be acknowledged that many sources of error were present both in the collection and manipulation of the data. The validity of the conclusions based on those data must, therefore, be considered. Identified sources of error and their importance are discussed briefly here, in no particular order.

(1) Boats swing about their moorings, thus readings will be taken over a different part of the bed on the flood and ebb tides. If the bed elevation is greater in one place, then relative flow depths will be less and velocities may increase. This may have been significant for the neap tide data at Penrhyn Point (Station 2), where flood tide depths were 3-6m, compared to 5-10m on the ebb.

(2) Re-occupation of sites for spring-neap data comparisons was accurate at all sites, except for Penrhyn Point (Station 2). The neap data were taken, for the first hour, 300m to the west of the harbour mouth, then at 100m east of the mouth. The spring tide data were taken precisely at the mouth, but only 40m from the south bank; hence, they may have included both higher current speeds, due to being directly at the constriction, and a flood tide bias by being closer to the 'flood-dominated' area to the southeast.

At Farchynys (Station 4) some 40m of up-estuary movement of the survey vessel occurred on the spring tide at 22:13 BST, due to both bow anchors dragging in the strong current, but the effect on the data is considered negligible.

(3) Data interpolation and/or extrapolation were sometimes necessary, to compute flow- and tidally- averaged parameters.

This was due to :

- data loss by instrument malfunction;
- practical limitations on length of data collection;
- time spent relaying anchors after position changes;
- safety considerations.

The precise shape of some time-averaged depth profiles may have been slightly affected, but it is considered that the overall conclusions regarding the tide or part of tide involved have not been altered by this process.

(4) As directional data were limited, time- averages were computed assuming tidal flow to be rectilinear. At Penrhyn Point, this assumption was only valid for the neap tide. At Farchynys, the data were less reliable, although strongly suggested directly-opposed tidal currents - both on springs and neaps, and although no data are available for Penmaenpool (Station 5), rectilinear tidal currents were considered a reasonable assumption for this area of the estuary.

The use of an invalid assumption at Station 2 on spring tides, means that the flood tide may have been overestimated i.e. the tide-averaged depth-mean velocity of 0.08m/s (Fig. 2.21) is too high. This problem is intimately related to point (1) above, that of sampling slightly different stations for flood and ebb.

(5) The data from Barmouth Bridge (Station 3) have not been presented. On 1-12-86, although lasting 12 hrs the data includes after 4hrs a 40m lateral position change due to initial mislocation directly over an intertidal sand bar. The data of 28-8-86 was not of sufficient length to warrant

working-up without reliable spring tide data for comparison - although use has been made of it at various times (e.g. Fig. 2.24).

(6) It is re-emphasised that the field data collected reflect fairweather conditions. No data exists on the hydrography of the estuary under storm conditions.

2.5. Summary and Conclusions

Of the factors identified in the introduction to this chapter, this study has concentrated upon the effects on estuarine circulation dynamics of the variable cyclical factors, some variable non-cyclical factors, and spatial variation. Namely, these are the tides, river flow, and variation along the estuary length. It has been found that there is a complex inter-relationship between these temporal and spatial parameters, so that the Mawddach Estuary as a whole exhibits a very varied set of circulation patterns. The data reflect fair-weather conditions.

Diurnal tidal ranges at the estuary mouth vary annually between 0.8m and 5.0m (1986 tidal predictions), with extreme water levels of -2.04m and +2.96m O.D. on the equinoctial tides. Tidal ranges vary spatially, with a landward decrease in range on spring tides of up to 0.25m/km, due purely to higher levels of LW caused by frictional effects and river level.

Spatial variation in the relative duration of the flood and ebb tides is also a prominent feature; ebb tide duration exceeds the flood, in all cases and locations in the estuary. Increased friction in the upper-estuary further skews a tidal wave already skewed in Cardigan Bay and at the estuary mouth, measured by highly increased ratios of ebb/flood duration and flood/ebb velocity. Delays in the timing of HW and LW along the estuary show the tidal wave to be a standing wave with an increasing progressive nature up-estuary.

Flood velocities were greater than ebb velocities at most measured stations in this study, but this is reversed in the upper-estuary with neap tides. For example, at Penmaenpool (Station 5) $U_{maxflood}/U_{maxebb}$ equals 3.67 on spring tides, but zero on neaps when no flood current occurs. Tidal asymmetry and energy losses increase most rapidly upstream of the position where LW elevation is equivalent to the estuary bed.

Spatial variations in circulation are also apparent in a lateral sense, i.e. across the axial trend of the estuary. This is evident from the occurrence of strongly-formed axial convergences, some topographically-induced; others show considerable lateral gradients of current speed and salinity. There is also evidence from the main channel, near the mouth, for a large-scale anticlockwise circulation to the east of the mouth, particularly on spring tides.

The penetration of saline water up the estuary varies with tidal range, reaching at least 1.5km further inland on springs than on neaps. The majority of the estuary experiences large salinity variations over a lunar cycle, particularly with variable runoff. Using the classification of Hansen & Rattray (1966), the Mawddach is generally well-mixed with moderate to appreciable stratification. On spring tides, the upper estuary is partially-mixed; this is also approached near the mouth on neap tides with high runoff. Using the qualitative classification in Dyer (1986), the estuary is 'well-mixed', though periodically and locally close to 'partially-mixed'.

Flood tide velocity profiles are affected dominantly by bed friction. Although not measured in this study, vertical components of turbulence must have a thorough mixing effect, especially with large tidal ranges. Large 'boils' were noted at the surface in the lower and mid-estuary, both on flood and ebb tides; these are surface reflections of upward moving packets of water, i.e. large-scale turbulence, and are partly responsible for the mixing of surface freshwater layers into the water column.

Of the variable non-cyclical factors (mentioned in Section 2.1.3), river flow has been shown to be the major control on estuarine circulation; it can also cause stratification in Barmouth Bay. High river flow can reverse the surface net non-tidal flow at the estuary mouth, on neap tides.

No direct evidence of wind- or wave-induced currents or mixing was observed in this study, although they undoubtedly occur during stormy periods. Their general effect would be to increase mixing in the surface

layers of the water column, and to drive a wind-driven surface current, see, for example, Jago (1974), Jonas (1977). The precise effect on estuarine circulation would be highly dependent upon wind direction and the depth of the estuarine waters.

Another non-cyclical variable is the sedimentary morphology of the estuary. Within this context, it is clear that the small estuarine cross-section and high sandbank relief in the mid-reaches (at Farchynys) are today very important features in controlling estuarine circulation. There is evidence that the relative effect of bed-friction on the tidal wave increases upstream of this point; the constriction itself is a site where tidal wave energy loss is at a peak. Moreover, the level of sediment in this area is probably controlled by tidal wave propagation. Finally, salt transfer through the constriction is dominantly by advection, the mechanism is independent of tidal range and there is little spring-neap change in the degree of stratification.